An analysis of the relationship of apparent electrical conductivity to soil moisture in alluvial Recent Soils, lower North Island, New Zealand.

Michael Killick

A thesis presented in partial fulfillment of the requirements for the degree of

Masters of Philosophy (MPhil) in Soil Science

at the Institute of Agriculture and Environment,

MASSEY UNIVERSITY

Palmerston North, New Zealand

April, 2013

‘Unto God would I commit my cause: which doeth great things and unsearchable; marvellous things without number:
Who giveth rain upon the earth, and sendeth waters upon the fields’

Job 5:8-9

Abstract

Electromagnetic induction (EMI) sensors can be used in kinematic systems to provide rapid high-density measurement of apparent soil electrical conductivity (EC_a) over large areas. In non-saline soils EC_a has been used as a surrogate measurement for many soil properties including soil texture and moisture, critical properties in precision agriculture. However, complex interactions between soil properties and the irregular depth profiles of EMI measurements have prevented consistent interpretation of EC_a in terms of soil properties. This study uses kinematic surveys and multi-height spot measurements of EC_a with Geonics EM38 Mk2 and EM31 instruments together with field measurements of soil moisture and investigation of EC_a theory to analyse the relationship of EC_a to soil moisture in alluvial Recent Soils at two locations in the lower North Island, New Zealand. Soil samples from these locations were also analysed for bulk density, porosity, texture and the electrical conductivity (EC) of 1:1 soil pastes and extracts. Intact soil cores from one location were analysed for moisture retention properties. Results raise uncertainty about the function of EMI instruments, particularly the nature of temperature effects and the comparability of measurements by different instruments. Effects of soil solution conductivity on EC_a were found to be significant though the soils studied were non-saline. Correlations of soil moisture with EC_a in this study were varied and not in every case significant. The relationship of EC_a to soil moisture in this study was too complex to allow simple use of EC_a for measurement of soil moisture.

Acknowledgements

The author wishes to thank among others the following people:

My Supervisors: Ranvir Singh, Carolyn Hedley, Ian Yule and Alan Palmer, for patience, encouragement, support and advice.

Mike Hedley and Peter Kemp for supporting my scholarship application.

Mike and Mel Poulton for supporting the project at Wairiri (Burnside block).

Ben Grant for help with access at No.1 Dairy Farm, Massey University.

Ranvir Singh, David Feek, Paul Boyce, Ian Yule and Pip McVeagh for help with fieldwork.

Mike Tuohy, Matt Irwin and Pip McVeagh for help with GIS offset code and calculations.

Matt Irwin for general help with GIS and IT.

David Feek for making and sourcing field and lab equipment.

Bob Toes for help with transport, shopping and invaluable advice: 'Remain calm.'

Mark Osbourne for the use of workshop facilities and equipment.

Ian Furkert for help with lab methods and equipment.

John Dando (Landcare) for use of the lab and equipment.

Chris Rawlingson for help with time domain reflectometry (TDR) gear.

Mike Catalano (Geonics) for responding to my strange queries.

Mark Bebbington and Bethanna Jackson for advice on statistics.

Bob Stewart for XRD analyses and advice.

Anja Moebis for instruction in use of the PSDA and sample preparation.

Lance Currie for open door, open ears and good advice.

Kathy Hamilton for most excellent administrative support.

My wife Josie for indulging in me the strange obsession of a Masters.

Contents

List of Figures

List of Tables

Glossary of Terms

Ωm Ohm.metre: standard unit of electrical resistivity.

Allegro: The Juniper Systems Allegro CX field computer used for datalogging in kinematic systems.

ATV: The all-terrain vehicle or 'quad bike' used for kinematic surveying.

AWC: Available water capacity: the water holding capacity of soil between field capacity (~10 kPa soil matric potential) and permanent wilting point (~1500 kPa). Certain literature referred to uses AWC to mean available water content, otherwise referred to as plant available water (PAW). These instances are noted where they occur.

Burnside: The study location at Burnside Block, Kumeroa.

depth profile resolution: The processing of EC_a data to indicate the depth profile of EC_a measurements.

EC: Electrical conductivity.

EC_a: Apparent conductivity (of soil): the bulk or generalized electrical conductivity of a soil in response to EMI.

EC_b: Bulk liquid phase electrical conductivity of soil according to the 'dual pathway' model of Rhoades et al. (1976).

EC_s: Electrical conductivity of soil solids, mainly associated with soil particle surfaces.

EC_w: Electrical conductivity of the soil solution; salinity.

EM31: The Geonics Ltd. EM31 Mk2 electromagnetic induction meter.

EM38: The Geonics Ltd. EM38 electromagnetic induction meter (similar to the EM38 Mk2 but with only the 1m coil spacing).

EM38 Mk2: The Geonics Ltd. EM38 Mk2 electromagnetic induction meter.

EMI: Electromagnetic induction (in soil).

ER: Electrical resistivity.

GPS: Global Positioning System, receivers of which were used to contribute location data in kinematic surveys.

inversion: The processing of EC_a data to indicate the depth profile of EC_a measurements.

IP The 'in-phase' measurement of Geonics EMI instruments, related to the primary electromagnetic signal emitted by the instrument.

kinematic: A type of surveying in which sensor measurements and GPS location data are linked and logged while moving.

LIN 'Low induction number'. Under LIN conditions the effects of the magnetic fields of EMI at each depth in the soil are de-coupled from effects at adjacent depths above and below, enabling EC_a to be measured via the ratio of the secondary to primary magnetic fields.

location: One of the two study locations, Burnside or No.1 Dairy.

meq/L: Milli-equivalents per litre; a measure of ionic charge corrected for differing valencies of ions in solution.

No.1 Dairy: The study location at Massey No.1 Dairy Farm, Turitea, Palmerston North.

PAW Plant available water: the actual water content extractable from soil by a force <1500 kPa.

proximal sensing in soil: The detection of a soil property by an electronic sensor close to, but not requiring contact with the soil.

QP the 'quad-phase' measurement of Geonics EMI instruments which reads directly as EC_a (mS/m).

RTK: Real time kinematic: a type of GPS system in which corrections to a mobile 'rover' receiver are transmitted by a radio link from a stationary 'base station' receiver.

site: One of the sites of replicate soil sampling and measurements at one of the two study locations.

θ: Theta: the volumetric moisture content of soil.

Chapter 1

Introduction

Precision agriculture is the spatial management of water, nutrients, and other agricultural inputs and processes at a scale responsive to variation in productivity within paddocks or other conventional land management units. By varying, targeting and optimising inputs such as irrigation, fertilisers and pesticides according to crop and soil variability, precision agriculture can improve agricultural productivity and limit pollution from agrichemicals.

An increasing array of technology exists to implement precision agricultural processes such as variable-rate application of water, fertiliser, pesticides or variable sowing density (Winstead, 2010). Such technology requires spatial information of sufficiently high resolution to guide management decisions and to control variable-rate processes at the required scale. This information can be in the form of maps or real-time measurements by sensors.

Crop variability can be assessed by yield mapping or by optical sensing or imaging. This information however, requires further assessment and data collection to indicate the causes of variability which may not be constant across spatial and temporal scales. Furthermore the collection of optical data by aircraft may be too expensive for private landowners; data collection by satellites or aircraft at critical times may also be prevented by cloud cover.

Sub-paddock crop variability follows patterns of variation in the growing environment, most notably the soil and its relationships to the status and availability of water (Sudduth et al., 1996). Soil data can be related to an extensive body of knowledge about soil-water-plant interactions to interpret or predict effects on crop growth (Sudduth et al., 2001). The need for scientific expertise in the lengthy process of conventional soil observation and sampling followed by laboratory analysis and interpretation of results makes this type of soil survey largely too

expensive to be practical at the scale required for precision agriculture (Lund et al., 1999).

Soil sensors provide for more rapid and intensive data collection over large areas. Total coverage of the survey area removes the need for expert location of sample sites and provides data directly without lengthy collection of field samples or subsequent physical analysis of soil. As a means of obtaining soil data of high spatial resolution, non-invasive proximal sensing has advantages as it does not disturb crops (although vehicular transport of sensors may) and it is well suited to rapid mobile deployment in kinematic systems, enabling high resolution coverage of relatively large areas (Lesch et al., 2005). Kinematic or 'on-the-go' surveying involves logging of continuous, mobile sensor measurements linked to precise differential GPS location data, generally using vehicle-mounted sensors and GPS.

Of the non-invasive methods of proximal soil sensing, electromagnetic induction (EMI) is widely used (Hedley, 2009). EMI provides measurements of 'apparent electrical conductivity' (EC_a) of soil: the bulk electrical conduction response of soil to incident electromagnetic radiation. EC_a is generally not a soil property of interest in itself, but is strongly influenced by soil salinity, or in non-saline conditions by soil moisture, texture and cation exchange capacity (CEC) which are important in precision agriculture (Friedman, 2005). Correlations have also been drawn between EC_a and many other soil properties including nutrient concentration, water holding capacity, water infiltration rate, structure, bulk density, organic matter, soil depth, the presence of restrictive soil layers and depth to water table (Sudduth et al., 2001; Siqueira et al., 2012).

The sensitivity of EMI instruments is not even with depth but declines in a non-linear fashion above and below a peak sensitivity, the depth of which depends on instrument specifications (Geonics, 2008). To confirm relationships between EC_a and soil factors in a given survey it is necessary to know the magnitude of EC_a at various depths so that comparisons can be made with complementary soil data. Because EMI sensitivity and soil properties all have irregular depth profiles which together produce an integrated EC_a measurement at the surface, the depth profile of such measurements is unclear. This has been a significant impediment to interpretation

of field-measured EC_a. Quantitative interpretation in terms of soil properties such as soil moisture has been impossible or site-specific only (Farahani and Buchleiter, 2004; McCutcheon et al., 2006).

The ability to vary the sensitivity profile of EMI measurements in specific, predictable ways by using different instruments, instrument orientations or measurement heights means that resolution of the actual depth profile of EMI measurements (often referred to as 'inversion') is theoretically possible. Considerable research has been directed at EC_a depth profile resolution (e.g. Slavich, 1990; Gebbers et. al., 2007; Triantafilis and Santos, 2010). Success in this field reported in the literature has been to varying degrees site-specific or impractical for kinematic surveying, e.g. requiring multiple raised-height measurements at each point; nonetheless improvements have been observed over unresolved measurements.

Quantitative mapping of soil moisture from kinematic survey data would make a vital contribution to precision agriculture research and practice. Soil moisture is a major influence on crop variability and a major determinant of EC_a (Sudduth et al., 2001). EMI methods have the potential to provide real-time estimates of soil moisture profiles (Khakural et al., 1998). This in turn would facilitate more precise interpretation of EC_a for other factors such as soil texture.

Reported correlations of EC_a with soil moisture have varied considerably (e.g. R^2 = 0.5-0.9, Brevik et al., 2006.) Such variability has been associated with variable moisture profiles (contributing to variable EC_a profiles) and unknown contributions to EMI measurements of EC_a below the depth of moisture measurement (Hossain et al., 2010.) Depth resolution of EC_a measurements is therefore necessary for consistent correlation of EC_a with soil moisture, and furthermore could facilitate the application of theoretical models of EC_a to field measurements.

Reflecting the above considerations, the following goal and objectives are identified for this study:

Goal:

To analyse the relationship of EC_a to soil moisture in alluvial Recent Soils in New Zealand.

Specific objectives:

- To characterise the influences of soil moisture, soil solution conductivity and soil solid properties on EC_a at the study locations using experimental data and published theory of EC_a.
- To determine a method for resolving depth profile of EC_a measured by EMI.
- To determine the influences of temperature and other sources of error or 'drift' on EMI measurements.
- To evaluate the potential to use EC_a for soil moisture measurement at the study locations.

This study uses kinematic surveys with two EMI instruments, the Geonics EM38 Mk2 and EM31 Mk2 to enable comparisons between EC_a measurements. Soil moisture and ambient and soil temperature are measured concurrently with kinematic surveys. Soil at the survey locations is analysed for bulk density, porosity, texture properties and electrical conductivity of soil pastes and extracts. Spot measurements of soil moisture and EC_a are made at soil sample sites, including use of EMI at multiple measurement heights. Possible sources of error or drift in EMI measurements are investigated.

This main body of this thesis comprises six chapters: *Introduction, Literature Review, Materials and Methods, Results and Discussion, Summary and Conclusions,* and *Recommendations and Future Work*. The *Literature Review* attempts to identify the factors most necessary to understanding the relationship of soil moisture to EC_a measured by the Geonics EM38 Mk2 and EM31 Mk2, and to inform the experimental methodology of this study. Methods are described in detail in the *Materials and Methods* chapter as some are adaptations of standard methods and others are novel. Explanation of the EC_a depth resolution technique and its development is extensive and has partly been relegated to *Appendix 7,* with a brief

description only in the *Materials and Methods* chapter. *Results and Discussion* will first examine EC_a at soil sample sites and its correlations (or lack thereof) with soil moisture, followed by the contribution of EC_a depth resolution and measurements of other soil properties to understanding or enhancing those correlations. Subsequently the results of kinematic surveys are presented and discussed including EC_a-moisture correlations and their explanation according to the results from soil sample sites, other soil observations and EC_a theory. The *Summary and Conclusions* chapter will briefly review the form and context of the study and present the main findings. *Recommendations and Future Work* will identify some potential subjects for further research and some guidelines for use of EMI indicated by the study

---

Chapter 2

Literature Review

This chapter begins by examining theory relating to electromagnetic induction in soil (EMI) and models of apparent conductivity of soil (EC_a). Subsequently the use of EMI in the field is reviewed in the context of EMI and EC_a theory to identify methods or limitations relevant to the relationship of soil moisture to EC_a. Resolution of EC_a depth profiles and the theoretical relationship of EC_a to soil moisture receive particular consideration.

2.1 Electromagnetic induction in soil

A detailed understanding of the geophysical basis of EMI in soil or of the electronic mechanisms of EMI instruments is beyond the scope of this project. However, a broad appreciation is important and in this and the following section, *Models of Apparent Conductivity*, the theoretical basis of EMI will be explored.

2.1.1 Electromagnetic radiation and electrical conductivity in soil

Electrical conductivity (EC) is a measure of the ease with which an electric current flows through a substance, and is the inverse of resistivity. Mulders (1987) describes electromagnetic radiation (ER) as an advancing interaction between electric and magnetic fields which can travel through substances or voids. In conductors ER causes electrical current flow which generates its own 'secondary' ER.

Unconsolidated earth materials at temperate ambient temperature have EC ranging from about 1 to 1000 millisiemens per metre (mS/m; McNeill, 1980a). In non-saline loams of temperate regions EC is generally in the order of 10 mS/m, higher for clays and less for sandy soils. EC of such soils has been found to increase as approximately

the square of the moisture content (McNeill, 1980 after Smith-Rose, 1934). Blakemore et al. (1987) rate soil EC >80 mS/m as 'high' and >200 mS/m as 'very high' for New Zealand soils.

McNeill (1980b) describes how the 'time-varying magnetic field' i.e. the primary field generated by the alternating current of EMI generates electric currents in the ground which create their own 'secondary' magnetic fields. These magnetic fields (primary or secondary) are components of ER in accordance with the theory described above (Geonics, 2012). McNeill (1980b) considers that materials with conductivities in the 1-1000 mS/m range will exhibit similar conductivity in response to direct or low-frequency alternating current applied by either 'conventional resistivity equipment' (electrodes contacting the ground) or EMI. Soil EC measured by EMI is often referred to as the 'apparent electrical conductivity' of the soil (EC_a). Accordingly in this thesis, EC_a refers to the bulk or generalized electrical conductivity of a soil in response to EMI.

2.1.2 Mechanisms and measurements of EC_a

Flow of electrical current depends on the presence of charged particles (electrons or ions) which are free to move. Soil solution contains mobile dissolved ions which conduct electric current. Clays, mostly secondary silicate minerals of colloidal size with negatively charged surfaces, attract cations from the soil solution. Clays contribute relatively strongly to EC_a because of their very high surface area and their electrochemical structure. Such EC occurs in adsorbed ions as discussed below in *Models of Apparent Conductivity*, however, McNeill (1980) considers the EC of soils mainly electrolytic through the soil solution (EC_w).

Electrical resistivity (the inverse of EC) can be measured directly by installing electrodes in soil. McNeill (1980b) describes how measurements of resistivity made in this way are disproportionately and to an unknown extent affected by inhomogeneities in soil close to the electrodes.

EMI operates by generating a time-varying magnetic field (arising from the ER pulse of an alternating electrical current in the instrument) which induces electrical current in the soil without the instrument contacting the soil. This induced electrical

current in the soil generates a secondary magnetic field which, together with the primary magnetic field generated directly by the instrument, is detected by the instrument. The EC_a measurement is derived from a ratio of the secondary to primary magnetic fields (Geonics, 2008).

2.1.3 Geonics EM38 Mk2 and EM31

In the Geonics EM38 Mk2 and EM31 the induced, secondary magnetic field used to measure EC_a is termed 'quad-phase' because it is offset in time from the primary magnetic field generated by the instrument. There is also a component of the induced magnetic field which is in phase with the primary magnetic field, termed 'in-phase'. The in-phase, induced magnetic field can be used to measure magnetic susceptibility of the ground but is 'nulled' i.e. cancelled out by a nulling signal when the instrument is used to measure EC_a (Geonics, 2008).

The Geonics EM38 Mk2 ground conductivity meter measures EC_a at three 'effective depth ranges': 1.5m, 0.75m and 0.38m (Table 2.01). EMI measurement at the three depth ranges is achieved by simultaneous operation of two alternative receiver coils at different fixed distances (0.5m and 1m) from a transmitter coil. (In EMI, greater coil separation contributes to greater depth of EC_a measurement). In addition there are two alternative orientations of the instrument ('dipole modes'), horizontal and vertical which also alter the effective depth range. The EM31 Mk2 has one coil separation (3.66m) and can also be used in horizontal or vertical modes producing two effective depth ranges: 3m and 6m. To avoid confusion the EM31 Mk2 is hereafter referred to as the 'EM31'.

According to 'relative cumulative response' functions published by Geonics (2008) the effective depth ranges of the above EMI instruments appear to be those which account for ~70% of the depth profiles of instrument sensitivity in each mode, i.e. ~70% of the measured reading is expected to be obtained from the effective depth range with the instrument at ground surface over a profile of EC_a evenly distributed with depth. The remainder of the reading is from greater depths, with instrument sensitivity decreasing with depth.

Table 2.01. Effective depth ranges of the Geonics EM38 Mk2 and EM31 (Geonics 1995; 2008).

Instrument	Coil separation	Effective depth range: vertical mode	Effective depth range: horizontal mode
EM38-Mk2	0.5 m	0.75 m	0.38 m
EM38-Mk2	1.0 m	1.5 m	0.75 m
EM31	3.66 m	6 m	3 m

Slavich (1990) found from modelled data and field observations that the actual depth range of the EM38 (equivalent to the EM38 Mk2, 1m coil spacing) is 3.0-4.5m (vertical mode) and 1.75-3.0m (horizontal mode) depending on EC_a (i.e. when the combination of EC_a and instrument sensitivity at depth is sufficiently low it in practice no longer contributes to the reading). It is not known to what extent the observations of Slavich (1990) are applicable to the full range of field conditions in which EMI might be applied, but they are important in confirming some response of a Geonics EMI instrument below the effective depth range.

The sensitivity profiles of Geonics instruments are irregular with depth; in an even profile of actual EC_a, certain depths contribute more to measured EC_a than others. (In this thesis EC_a is not taken to imply a weighted measurement according to instrument sensitivity, rather it is the actual bulk EC property of soil in response to EMI whether accurately detected or not). The sensitivity depth profiles of Geonics instruments according to their various coil separation-dipole orientation combinations according to response functions given by Geonics (2008) are shown in Figure 2.01.

Despite different profiles and effective depths of measurements in vertical and horizontal modes, the EM31 is described as giving the same EC_a measurement in either mode for an even EC_a profile (Geonics, 1995). Unlike the instrument response functions depicted in Figure 2.01, 'relative cumulative response' functions also given by Geonics (2008), reflecting the greater and lesser sensitivities of each mode to various depths, in each case produce a total sensitivity of 1, which requires

calibration of the instrument to measure mean profile EC_a according to the total sensitivity profile of the instrument. If such a calibration was to the effective measurement depth, the reading would be

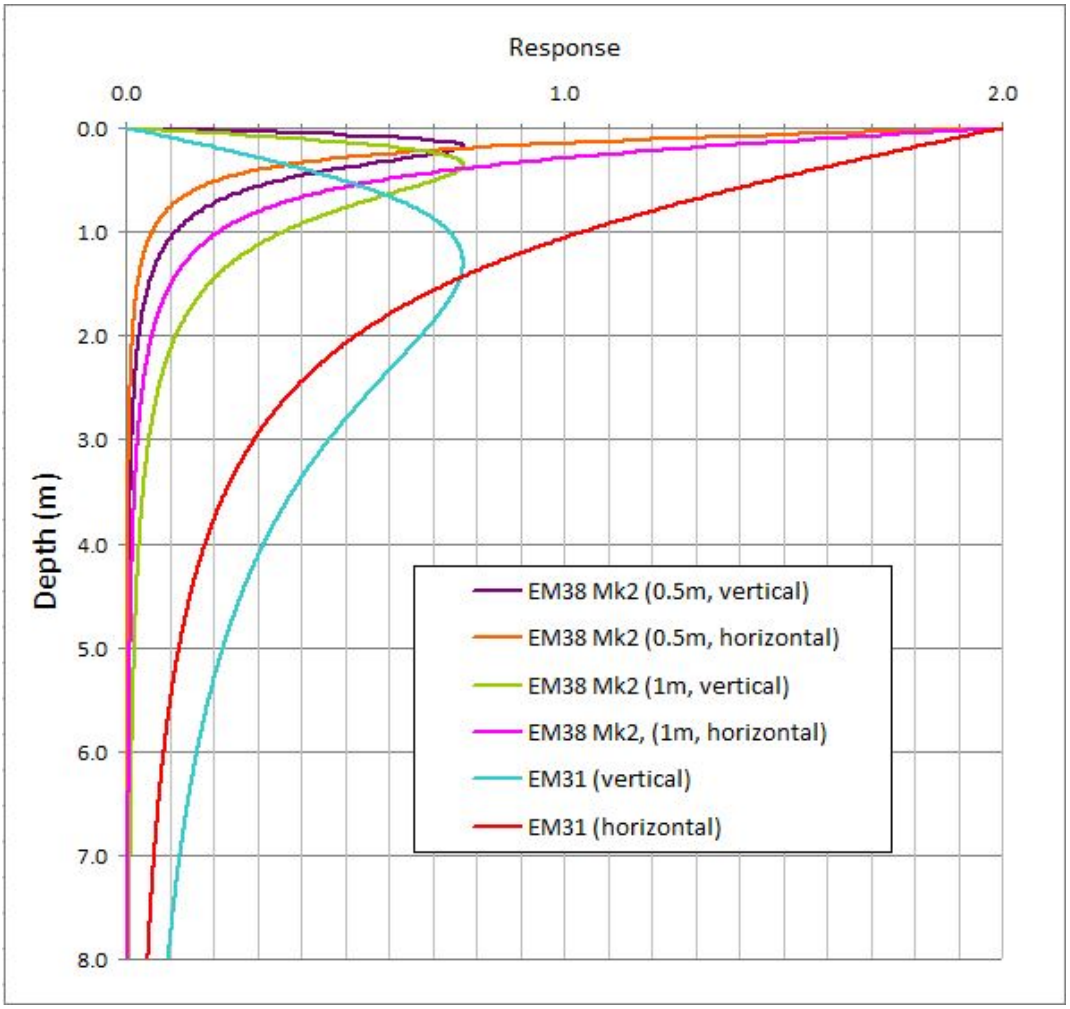

Figure 2.01. Response profiles of the EM38 Mk2 and EM31 for different coil spacings and modes, according to the functions given by Geonics (2008). (The coil spacing of the EM31 is 3.66m).

reduced to compensate for the influence of deeper conductivity; however, where conductivity was actually derived from wholly within the effective measurement depth, e.g. where non-conductive bedrock rose to within the effective depth range, such a calibration would artificially lower the reading.

Geonics (1995) acknowledge that for the EM31 in vertical mode, 34% of the EC_a measurement is derived from depths > 5m. The functions given by Geonics (1995)

indicate that this includes all of the theoretical EM31 response to infinite depth, not just to the effective measurement depth.

Geonics (1995) explains that the EM31 is calibrated to read correctly over an even EC_a profile and that consistent measurements of EC_a are not to be expected where the profile is layered. It appears that no approach to calibration of the EM31 would produce consistent measurements of mean EC_a in response to different EC_a depth profiles. The above observations concerning the EM31 are thought to apply in principle to the EM38 Mk2 according to its shallower effective measurement depths. The lateral extent of the volume of soil for which EC_a is measured by EMI is approximately the same as the vertical extent (Geonics, 2008).

According to Geonics (2012), for a hypothetical even EC_a profile the EM38 Mk2 and EM31 should also give similar measurements of EC_a which are a 'depth-weighted average' of actual EC_a down the profile. This implies a relative scaling down of the EM31 measurement as the total sensitivity of the deeper measurement profile of the EM31 is otherwise greater for an even EC_a profile than that of the EM38 Mk2, as reflected in the greater area of the curve of its sensitivity profile shown in Figure 2.01. The way in which measurements by the different instruments have or have not been scaled by the manufacturer is not entirely clear, but must affect the comparability of readings by different instruments.

Notwithstanding the above, according to Geonics (1995) the EM31 is calibrated so that it reads correct EC_a at hip height or 'about one metre' above ground, where 'it is subject to a reduction in the reading of 12%'. This is consistent with the relative cumulative response functions given by Geonics (2008) which, when applied to the coil separation of the EM31 in vertical mode, put the value of EC_a from the top 1m of the sensitivity profile at approximately 12% of the total reading. In this case the adjusted ground level reading is expected to be approximately 114% of actual EC_a; however, Geonics (1995) instruct that the instrument ground level reading should be adjusted to 112% of actual EC_a where this is known, so it is presumed they have followed the same procedure.

The effect of raising the EM31 instrument is not, however, similar for the vertical and horizontal dipole modes. The horizontal mode derives a little over 40% of the

reading from the top 1m and so loses this amount from the reading when raised to that height. If the ground level reading in vertical mode is adjusted to 112% of actual EC_a, the reading at 1m height in horizontal mode will be approximately 67% of actual EC_a, not 88% as in vertical mode. It appears no adjustment can be made which equally corrects the effects of lifting the instrument on both the vertical and horizontal modes as they use the same transmitter and receiver coils which are affected differently depending on the mode. Geonics (1995) acknowledge this in their instruction that where both horizontal and vertical measurements of EC_a are to be made at the same site the instrument should be at ground level, not the height above ground of 1m for which it is calibrated, and measurements adjusted accordingly.

The 12% adjustment to compensate for raising the instrument also assumes an infinite and even depth profile of EC_a which is not found in practice. If for example the EC_a measurement is derived entirely from the 'effective depth range' of 6m, e.g. due to non-conductive bedrock below that depth, raising the instrument 1m would result in a decrease in the measurement of ~17%, not 12%. Whatever adjustment is used, raising the instrument alters the depth profile of instrument sensitivity, not just the magnitude of the measurement, because the uppermost portion of the sensitivity profile is lost above ground.

The frequencies of the Geonics instruments are 14.5 kHz for the EM38 Mk2 and 9.8 kHz for the EM31 (Geonics 2008, 1995). The combinations of frequency and coil separation used in Geonics EMI instruments are designed to produce operational conditions termed 'low induction number' (LIN). Under LIN conditions the effects of the magnetic fields at each depth in the soil are de-coupled from effects at adjacent depths above and below, enabling EC_a to be measured via the ratio of the secondary to primary magnetic fields. LIN conditions are breached as conductivity increases; for the EM31 that effect begins at about 100 mS/m (McNeill, 1980b).

The 'zeroing' or 'calibration' procedure for the EM38 Mk2 as used in this study in accordance with the method of Geonics (2008) is described in *Appendix 2 – EM38 Mk2 calibration method*. However, it is evident that the procedure concerns relative sensitivities according to coil separation and dipole orientation, and might be

satisfied by any number of absolute values in the correct proportions (for the 1m coil separation at 1.5m above ground, 'zero' is attained when EC_a (vertical mode) = 2 x EC_a (horizontal mode), or V = 2H). Whether the design of the instrument relates these relative proportions to an absolute value or to zero is unclear, especially as the overall sensitivity of the instrument can also be separately adjusted. Geonics (2008), however, state that zero is correctly set when V = 2H. (Setting absolute zero of EMI instruments is problematic because in nearly all situations some EC_a is present and detected; zeroing is done initially by the manufacturer over extremely resistive ground (Geonics 2008)).

Waine (1999) observes additionally that it is necessary when calibrating the EM38 to 'switch off EM38, connect data logger cables and turn on logger, run EM38 program then turn on EM38. The logger will cause a large signal offset if connected with the EM38 switched on.'

Calibration of the EM31 is yet more difficult; due to its greater measurement depth it is inconvenient to raise the instrument to a height at which the equation V = 2H should be satisfied. No such procedure is therefore followed. A range of 'functional checks' are, however, recommended by Geonics (1995); a summary of these methods as used in this study is given in *Appendix 3 – EM31 setup method*.

In illustrating the above principles, Geonics (2008) state that over ground with 'conductivity' of 1000 mS/m, the EM38 Mk2, 1m coil separation, raised to 1.5m above ground should read 100 mS/m in vertical mode and 53 mS/m in horizontal mode (i.e. approximately V = 2H). However, the relative cumulative response functions given by Geonics (2008) for the EM38 Mk2 indicate that approximately 30% of the vertical mode reading is measured from depths >1.5m. Therefore if the correct reading at ground level is 1000 mS/m it would appear the correct reading at 1.5m height should be approximately 300 mS/m. It is not known whether the instrument has been factory calibrated to adjust this value; such a calibration would appear, however, to be of little benefit as it would not limit the penetration depth of the instrument to the supposed 'effective depth range' but only reduce its sensitivity over the same full range, as discussed above for the EM31.

A measurement of 100 mS/m with the instrument raised to 1.5m above ground in any case shows that the actual depth range of the instrument is >1.5m; such a measurement corresponds neither to the 'effective depth range' nor to the published depth profile of instrument sensitivity. The uncertainties created by these apparent contradictions complicate quantitative comparison of EMI data from different instruments which otherwise holds promise for resolution of the EC_a depth profile, in turn enabling better correlation with soil moisture which varies according to its own depth profile. (EC_a depth profile resolution is discussed in section *2.4 - Depth profiles of EC_a*.)

2.2 Theory of apparent electrical conductivity (EC_a)

According to Archie's Law the conductivity of a clay-free mixture of closely packed insulating particles saturated with a solution is largely dependent on solution conductivity, porosity (in this case the fraction of the whole occupied by solution) and to a lesser extent by such properties as particle shape, as expressed in the following equation:

$$EC_a = EC_w\, n^m \qquad [1]$$

where: EC_w = EC of the soil solution

n = porosity = saturated pore volume / total volume

m = empirical constant.

According to this law (and in practice) saturated sands or gravels of similar porosity and EC_w can exhibit similar EC_a (McNeill, 1980b). Archie's Law has been adapted to unsaturated mixtures by replacing porosity with the volumetric moisture content, θ (which applies to both forms of the model as in a saturated mixture: θ = n = saturated pore volume / total volume).

2.2.1 The 'dual pathway' model of EC_a

Rhoades et al. (1976) describe EC_a as arising from two parallel conductors, a bulk liquid-phase conductivity (EC_b) associated with free salts in liquid-filled pores, and a

bulk surface conductivity (EC_s) associated with exchangeable ions at the solid/liquid interface. This has been referred to as the 'dual pathway' model (Lesch and Corwin, 2003). EC_b is the product of EC_w, θ and a transmission coefficient or 'tortuosity factor' (*T*) with its own dependence on θ and other factors including viscosity and tortuosity (of soil pores). The model is a modification of Archie's Law (Zhadnov, 2009; McNeill, 1980b) and is represented by the following equation:

$$EC_a = EC_w \, \theta \, T + EC_s \qquad [2]$$

T is further described by the equation: $T = a\theta + b$. Rhoades et al. (1976) suggest it may be possible to estimate the values of EC_s, a and b from soil texture and mineralogy. Where these are known therefore, EC_w can be determined on the basis of EC_a and θ (which forms the basis of applications in soil salinity appraisal). This raises the possibility that θ can be determined on the basis of EC_w and EC_a, dominated by EC_a in non-saline soils.

In laboratory tests by Rhoades et al. (1976) on undisturbed soil cores, EC_s was found to be larger for finer textured soils. EC_w was found to be zero below a certain threshold of θ because *T* approaches zero. That threshold was also larger for finer textured soils. The description of EC_a by McNeill (1980b) as primarily involving conduction of current through electrolytic solution in an insulating pore matrix is broadly consistent with equation [2].

2.2.2 Electrical conductivity of soil solution

EC_w is proportional to the number and type of ions in solution, according to the following equation for use at 'normal ambient temperatures' (McNeil, 1980b):

$$EC_w = 96500 \, [C_1M_1 + C_2M_2 + ...] = 96500 \, \Sigma \, C_iM_i \qquad [3]$$

where: EC_w = EC of the soil solution

C_i = No. of gram equivalent weights of i^{th} ion per m^3 of water

M_i = Mobility of i^{th} ion in metres per second per volt per metre.

According to Friedman (2005) an EC_w of 100 mS/m approximately equates to 10 milli-equivalents per litre (meq/L) of either cations or anions. The mobility of ions (which enables them to conduct electric current) is affected by the viscosity of the

solution and the size of the ions; for dilute aqueous solutions these values are established (e.g. McNeill, 1980b). Temperature affects EC_w via its effect on viscosity.

Auerswald et al. (2001) found that EC_w was an important component of the EC_a not only of saline but also of non-saline soils, especially insofar as it is influenced by fertiliser application. This calls into question the approximation that EC_a is dominated by water below a certain level of salinity, and by salinity above that level. Mallants (1966) also found an increasing influence of θ on EC_a with increasing salinity (0 – 2000 mS/m) in a sandy loam; Hanson and Kaita (1997) report a similar result from a clay loam with considerable variation in texture.

2.2.3 Electrical conductivity, solids and surfaces in soil

Friedman (2005) observes that θ and EC_w are the dominant factors affecting EC_a of soil, but that EC_s is also a major contributor to the EC_a of medium- and fine-textured soils, especially under conditions of low EC_w (i.e. non-saline soils). According to McNeill (1980b) clays, being a repository of adsorbed ions due to their cation exchange capacity (CEC), contribute to EC_w by releasing ions into solution. Rhoades (1981) presents an 'approximate' calibration method which relates EC_a to EC_w at field capacity simply on the basis of soil texture (represented by θ at field capacity according to the known moisture retention characteristics of various textures of soil, or by measured % clay) which was a major determinant of EC_s.

Bohn et al. (1982), however, found that EC_w was independent of soil solid properties, and that EC_s tends to zero at zero water content. EC_s was also found to be statistically insignificant across the range of salinity considered (200 to 3100 mS/m) even though clay in the soils ranged from 3 to 36%. Therefore EC_a could be derived approximately from EC_w and θ without reference to soil type. However, although Bohn et al. (1982) extrapolated their results to zero salinity, the minimum EC_a for which they measured data, 200 mS/m, is above the maximum encountered in non-saline soils. This may account for the discrepancy between the findings of Bohn et al. (1982) and those of Friedman (2005), McNeil (1980b) and Rhoades (1981) mentioned above who identified significant effects of soil solid properties on EC_a.

Rhoades (1991) considers EC_s constant with θ and 'somewhat dependent on θ'(p.295); therefore EC_s is not a constant independent of θ as in equation [2] above. Nadler (2005) considers EC_s dependent on EC_w, but that at $EC_w > 400$ mS/m such dependency can be ignored, and at $EC_w > 800$ mS/m, EC_s can be ignored altogether. For non-saline soils therefore EC_s remains significant. According to Ewing and Hunt (2006) EC_a may be dominated by EC_s at low EC_w, low θ, or if particulate surface area is high (i.e. high clay content).

McNeill (1980b) relates the effect of clay on EC_a to the CEC of the clay, with higher CEC causing a greater increase in EC_a. This is because the ions adsorbed on clays contribute to EC_s or when released into solution, to EC_w. The presence of charged ions on clays also inhibits the freezing of water immediately adjacent to clay particle surfaces, causing frozen soil, for which EC_a is normally extremely low, to retain some conductivity.

2.2.4 Limitations and extensions of the dual pathway model

Nadler and Frenkel (1980) found that when EC_a is below 400 mS/m the relationship between EC_a and EC_w is curvilinear. Rhoades et al. (1989) found 250 mS/m to be the lower limit of linearity in the EC_a-EC_w relationship, but acknowledges other studies putting that limit at 400 mS/m. Effectively then equation [2] only properly applies to saline soils.

Nadler (1982) considers that EC_s is not constant for a given soil but dependent on other factors including EC_w and *F,* the formation factor (an alternative expression of the tortuosity factor represented by *T* in equation [2]). *F* is determined in soil by the pore structure (Friedman and Seaton, 1998) and is a factor by which the solid matrix reduces EC_w (Nadler, 2005). The model Nadler (1982) describes incorporates these elements and a relative expression of θ to produce the curvilinearity identified by Nadler and Frenkel (1980) in the relationship of EC_a to EC_w at low EC_w.

Rhoades et al. (1989) develop a new model to incorporate supposed phenomena that cause the curvilinearity in the relationship of EC_a to EC_w at low EC_w (as identified by Nadler and Frenkel, 1980). The new model is essentially the dual pathway model plus a third pathway consisting of the other two paths in series. This model is based

on earlier work by Sauer et al. (1955) and Shainberg et al. (1980) and distinguishes between 'mobile water' in large pores (which participates in the series pathway) and water trapped in fine pores (which does not conduct in series with other components, and which Rhoades et al. (1989) suggest may have a different EC_w to mobile water).

Swaid (2010) identifies three layers at particle surfaces which contribute to EC_s: the electrical diffuse layer (or the Gouy layer, which also contributes to EC_w), the Stern Layer (which together with the diffuse layer comprises the EDL), and an additional mechanism operating directly on the particle surface, perhaps involving proton transfer. According to Swaid (2010) the diffuse layer is a path of higher conductivity than pore water outside the double layer due to higher ion concentration.

Mojid et al. (2007) develop a model of EC_a specifically designed around effects of the EDL:

$$EC_a = T(\theta_w E_w + \theta_d E_d) \quad [4]$$

where θ_d and E_d are the volume and conductivity of the electrical double layer, and θ_w and E_w the similar properties of the 'free water' i.e. outside the double layer. Equation [4] appears to be a dual-pathway model in the style of equation [2], but Mojid et al. (2007) describe E_w and E_d as components of EC_w which function in parallel with 'soil solid' conductivity (EC_s).

Mojid et al. (2007) recognize a lower threshold of θ as identified by Rhoades et al. (1976) at which $T = 0$, at which point equation [4] is no longer valid. This is described physically as the point at which clay particles are no longer connected by films of solution.

The above findings and theories of non-linearity in the effects of θ on EC_a are reflected in EC_a theory articulated by Pozdnyakova (1999) and Pozdnaykov (2006). According to Pozdnyakova (1999) effects of soil properties (e.g. EC_w and θ) on EC_a are expected to show an exponential relationship which is generally described as follows:

$$S = \chi \log(EC_a) + \delta \quad [5]$$

where *S* is the relevant soil property and χ and δ are empirical constants.

This is based on the premise that electrical parameters such as resistivity and potential are exponentially related to the volume density of mobile electrical charges (McBratney et al., 2005).

Pozdnyakov et al. (2006) reports that the electrical conductivity of soil pastes is the sum of the exponential functions of θ and EC_w. With regard to θ this function is related to different water content ranges: adsorption, film, film-capillary, capillary, and gravitational water, each of which has a different linear relationship with soil electrical resistivity, and to different mobility states of electrical charges. Taken together these linear functions form the exponential relationship, each representing lower resistivity (or higher EC_a) in the order given below (Figure 2.02).

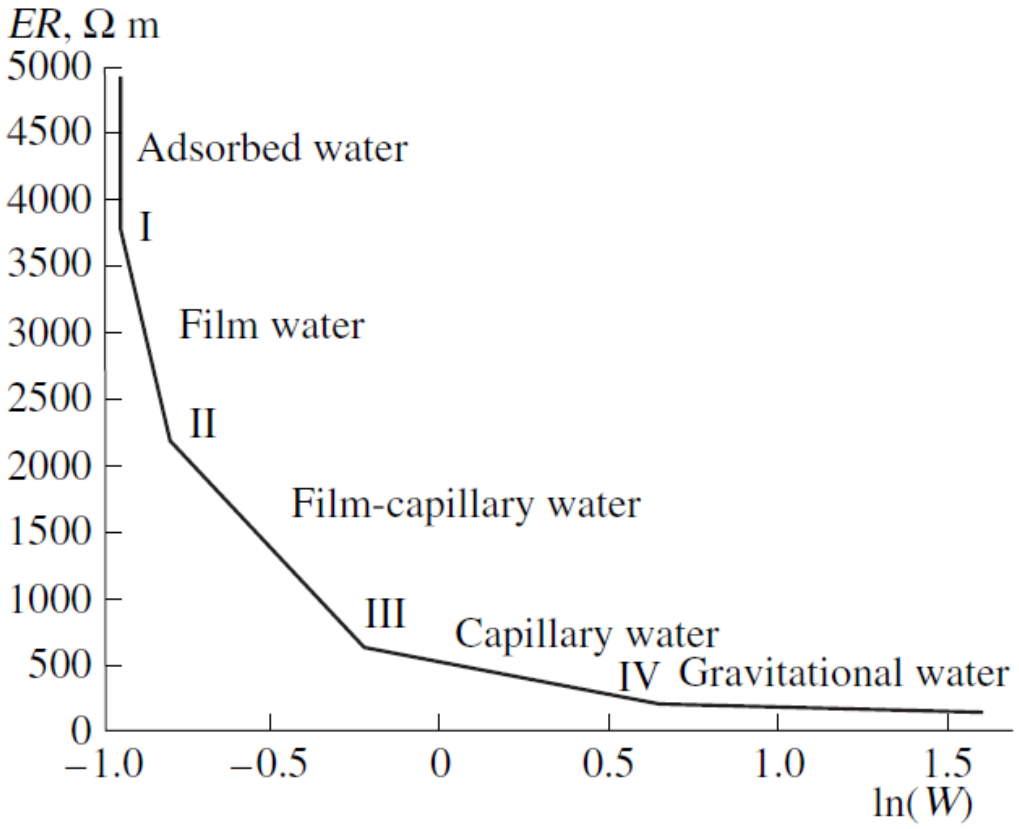

Figure 2.02. Piecewise relationship between water content and resistivity in soil (Pozdnyakov et al., 2006). ER = electrical resistivity. ln(W) = natural logarithm of gravimetric water content.

The above theory then provides a possible explanation for findings of different θ-EC_w relationships, either linear or exponential in various studies, as these could relate to

the different ranges of θ examined, either within one of the linear ranges or spanning two or more such ranges. In agreement with Pozdnyakov, Auerswald et al. (2001) found that in non-saline soils, θ affects EC_a only slightly in the range between field capacity and permanent wilting point (PWP), but more so in conditions drier than PWP.

2.2.5 Empirical models

Rhoades and Corwin (1990) found that EC_w could be approximately determined from EC_a, θ, and % clay (which largely accounts for EC_s) and that particle density, bulk density, and clay mineralogy could be adequately incorporated into calculations by approximations or estimates. This adaptation of the Rhoades et al. (1989) model, designed for practical field use, is a similar approach to Rhoades and Corwin's (1981) approximation of the Rhoades et al. (1976) model. Friedman (2005) questions to what extent the relationships of θ and % clay to parameters of the Rhoades et al. (1989) model (and therefore to EC_a) can be generally applied or whether they are specific to the soils used by Rhoades and Corwin (1990).

Auerswald et al. (2001) reports a strong linear correlation ($R^2 = 0.91$) of EC_a with volumetric clay content at constant θ and presents an empirical model of EC_a based on a multivariate regression of various individual and combined factors measured in a range of non-saline soils. It was found that volumetric clay content, EC_w and logθ influenced EC_a in the proportions 1 **:** 0.8 **:** 0.4 respectively, and provided for an adequate model without any other factors. (EC_w was estimated from EC_e of sequentially concentrated pastes and is represented in equation [6] below as EC_{max}). While this model does not incorporate porosity or bulk density which have been found by others to be significant (e.g. Swaid, 2010; Brevik and Fenton, 2004) those factors are reflected in the use of volumetric measures for both clay and moisture content.

The influence of organic matter was disregarded by Auerswald et al. (2001) because CEC (reflecting the influences of organic matter and clay) was a less significant predictor than volumetric clay alone. Auerswald et al. (2001) found no interaction effects between any factors to be significant, unlike Mojid and Cho (2008) who

found interactions between θ and clay content and between θ and EC_w. The model of Auerswald et al. (2001) is represented by the following equation (R^2 = 0.89):

$$EC_{25} = 348\ clay_{vol} + 0.108\ EC_{max} + 68\ log\theta + 20 \quad [6]$$

where: $EC_{25} = EC_a$ at 25°C.

EC_a in the above model is therefore exponentially related to θ but linearly related to clay and EC_w, in contrast to the theory described by Pozdnyakov et al. (2006) discussed above in which EC_a is exponentially related to all relevant soil factors, in particular EC_w and θ.

Nadler (2002) makes numerous objections to the method, findings, and the above model of Auerswald et al. (2001). Such objections, however, do not account for the reported effectiveness of this simple empirical model. In particular the model of Auerswald et al. (2001) does not directly incorporate any of the complex interactions and tortuosity effects theorised for other models such as those of Nadler (1982) and Rhoades et al. (1989). It may be that the log transformation of θ in equation [7] accounts approximately for complex effects on EC_a via EC_s and/or EC_w at low θ.

Nadler (2005) reports from an analysis of 26 published studies by various authors that it was not possible to establish a consistent, unifying EC_a-EC_w relationship according to texture and θ, and moreover the logically expected order of curves in relation to texture was not observed. It is unclear therefore to what extent the findings and empirical model of Auerswald et al. (2001) might be applied to other soils (as was the case also in relation to the empirical model of Rhoades and Corwin (1990) mentioned above).

2.2.6 Effect of temperature on EC_a

The EC of soils containing moisture increases about 2% per ˚C increase in temperature (Rhoades and Corwin, 1990). Measurements of EC_a are commonly corrected to a standard reference temperature, e.g. 25˚C as in the model of Auerswald et. al (2001) above. Friedman (2005) observes that this is especially

important for finer textured, non-saline soils, for which the effect of temperature on EC_a is liable to be greater than the effect on EC_w alone.

The above relationship between EC and temperature is an approximation based on correction factors published by U.S. Salinity Laboratory Staff (1954) for use in the following equation:

$$EC_{25} = EC_T * f_T \quad [7]$$

where: EC_{25} = electrical conductivity at 25˚C

EC_T = electrical conductivity at measurement temperature

f_T = correction factor.

Equation [7] and the accompanying correction factors were developed using soil extracts, however, subsequent work has confirmed they are appropriate for use with EC_a of soil (Ma et al., 2011).

Ma et al. (2011) review various attempts to model f_T and conclude that the results most consistent with the U.S. Salinity Laboratory Staff (1954) values are produced by the model of Sheets and Hendrickx (1995), corrected by Ma et al. (2011) as follows:

$$f_T = 0.4470 + 1.4034e^{-T/26.815} \quad [8]$$

where T = measurement temperature in ˚C.

However, temperature correction applied according to ambient temperature above ground cannot perfectly represent the temperature profile below ground which it is assumed must affect EMI according to the measurement depth. Measurements of soil temperature might be used to accommodate these effects and might not be onerous if restricted to the near-surface. However, where the soil temperature profile varies strongly, for example due to warming of the soil surface, EMI measurements with sensitivity weighted towards the soil surface such as the EM38 Mk2 in horizontal mode would be affected differently than those weighted towards greater depths.

Reported effects of temperature on field-measured EC_a have not been found adequately explained by the relationships described above, as discussed in section *2.3.5 - EC_a and temperature in the field.*

2.3 EMI in the field

Jaynes (1996) summarises uses of EMI in field mapping of soils according to general categories:

1. Reconnaissance maps to aid in subsequent soil sampling;
2. Refining maps of sparsely sampled soil properties by co-kriging with co-regional EMI data;
3. EMI as a surrogate measurement for difficult or costly soil properties.

Few field studies have focussed on establishing quantitative connections between EC_a theory, such as described in the previous section, and field-measured EC_a. In this review such connections will be made where apparent. A selection of field studies relevant to the description of EC_a in alluvial soils is described below. (Field studies directly relating EC_a to various soil moisture characteristics are examined separately in section *2.5 - EC_a and Soil Moisture).*

2.3.1 Correlation of soil properties with EC_a

Correlations are often examined between EC_a and a variable of interest, e.g. salinity, clay content, depth to clay layer, nutrient status, or moisture content (Lesch and Corwin, 2003). A difficulty with such studies is that due to strong relationships between soil properties, a large proportion of the variation in EC_a can be explained alternatively by different properties according to the focus of research. In particular the soil properties which are thought to most affect EC_a in non-saline soils, soil moisture and texture, are related to almost all other properties of interest and additionally are strongly related to each other.

For example, Eigenberg et al. (2006) found that profile-weighted EC_a differences accounted for 79-98% of the variability due to nitrate-N and only 2-21% of the variability due to water-filled pore space, and concluded for that particular study

that the primary contributor to differences in EC_a between fields with different crop treatments was nitrate level differences. However, nitrate level may have been influenced by soil moisture, temperature and texture through their effects on nitrogen cycling (via aeration, redox potential and CEC) and these are also direct influences on EC_a. While the findings of Eigenberg et al. (2006) are statistically strong it is also important to confirm the mechanism of the effect and whether it is direct or indirect.

Farahani et al. (2005) found that correlations of EC_a with stable soil properties (e.g. clay content) were subject to changes in temporal soil properties (e.g. moisture content or salinity) i.e. there were interaction effects, therefore not only site-specific but survey-specific calibrations were needed to predict soil properties.

The strength of correlation between EC_a and a given soil property can also be highly variable between studies (Lesch and Corwin, 2003; Nadler, 2005). This is to be expected because of the strong relationships and therefore cross-correlations between soil properties; some correlations with EC_a are direct, some indirect or partially indirect through relation to another variable as portrayed in Table 2.02. The mechanism of correlation is not always obvious and may not be the same for different sites or at different times. Where one influence on EC_a is small or unchanging across the area, *variation* in EC_a then relates to whatever other influence is large or variable. This is one reason why one study can explain a large proportion of EC_a by organic matter (Kuehn et al., 2009) while another finds that effect insignificant (Auerswald et al., 2001).

A factor of *relatively* small influence has little effect where stronger factors are present, but in other circumstances where the larger factors are absent, the same small influence can be dominant, producing a highly significant correlation. Likewise, a major determinant of EC_a may have little effect on the correlation if it is constant across the area considered, the correlation being instead determined by a minor but variable factor.

The findings of research such as mentioned above are most useful when the behaviour of a property in the context of the physical system can be explained in

Table 2.02. Possible effects and interactions of some soil properties affecting EC_a. (The effect is of *increase* in the active property where applicable).

Active property	Target property					
	apparent conductivity (EC_a)	water content	salinity	clay content	clay mineralogy	porosity
water content	provides medium of conductivity in solution and across particle surfaces; decreases tortuosity		dissolves salts; enables conductivity of salts; decreases viscosity; decreases electrolyte concentration; increases leaching of salts	enables conductivity across clay surfaces, ion desorption and exchange	influences clay mineralogy during soil development	connects pores; decreases tortuosity
salinity	increases conductivity in solution and across particle surfaces	increases viscosity; increases soil moisture retention		contributes ions for exchange and adsorption on clay surfaces	influences clay mineralogy during soil development	decreased by precipitated salts
clay content	increases conductivity in solution and across particle surfaces	increases soil moisture retention; slows drainage	increases salinity by slowing leaching			increases fine pores
clay mineralogy	influences magnitude of clay effects	different particle sizes of clays affect moisture retention differently	affects solution composition by ion exchange	affects volumetric clay content and charge density		affects pore size
porosity	increases EC_a when saturated, decreases EC_a when dry	increases moisture content at saturation	increases leaching where drainage occurs	decreases volumetric clay content		

accordance with the data (McBratney et al., 2005; Brevik and Fenton, 2002). McNeill (1980) concurs that in every case EMI measurements must be confirmed against known geological conditions and are most useful for extrapolation or interpolation between other data sources (e.g. point measurements of soil moisture). Consideration of 'geological conditions' in this study is mainly confined to pedological conditions which are considered most relevant.

2.3.2 Multiple regression models of EC_a

Better correlations of field soil properties with EC_a may be obtained when a number of factors are considered in a multiple regression (e.g. Brevik and Fenton, 2002; Bronson et al., 2005). These studies however, are subject to the same ambiguity as those examining single factors unless the interaction effects are recognized and some attempt made to quantify them. For example, Bronson et al. (2005) found that clay content was positively correlated with EC_a at most sites (as has been widely reported in various literature e.g. Auerswald et al., 2001) but negatively correlated at one site, possibly because the more clay-rich soils at that site also had lower bulk density. Similarly Brevik and Fenton (2002) found that carbonate mineral content was negatively correlated with EC_a in a multiple regression including other soil factors, despite that salt content is generally recognized to increase EC_a.

The reasons for anomalous results can be difficult to identify. In the study of Brevik and Fenton (2002) the accumulation of carbonates may have been associated with a calcic horizon, a feature of semi-arid soils; therefore soil with more carbonates may have had lower EC_a simply because it was drier, or because being more often dry it had accumulated less organic matter. Salts in any case will not increase EC_a if they are not dissolved, as was alluded to by Brevik and Fenton (2002).

2.3.3 EC_a as a covariate

An example of how EC_a can be used as a general indicator of soil spatial variation alongside measurements of a correlated soil property of interest is given by Lund et al. (1999) regarding depth to claypan. Lund et al. (1999) state that for such uses it is the *relative* variation of EC_a which is important, not its absolute range, as the property of interest will in any case be measured directly; EMI is simply to guide interpolation between those measurements. The relative pattern of EC_a measured by Lund et al. (1999) in the field was found to be temporally stable in conditions of changing moisture content, temperature, or physical conditions affected by tillage (the observed change in moisture was a reduction of 5.8%).

Using discriminant analysis, Kravchenko et al. (2002) determined the significance of various topographical measures (e.g. slope, areas of surface flow accumulation

potential) and EC_a to the drainage class of soil cores from a 20 ha field. The effect of EC_a was found to be significant and improved prediction of drainage class by co-kriging with the class of sampled cores.

2.3.4 EC_a and soil type mapping

James et al. (2003) acknowledge that not only soil texture and moisture but also bulk density and organic matter influence EC_a in the field. However, they relate EC_a directly to soil type zones without quantifying the influence of various soil properties other than by selecting survey conditions in which the soil was estimated to be at field capacity. The field capacity condition was confirmed by comparing a plot of moisture measurements (neutron probe) vs. 'soil fineness class' with a plot of theoretical soil moisture-texture relationships at field capacity. ('Soil fineness class' is a continuous numerical scale of soil texture which facilitates quantitative analysis of the data by linear regression and other techniques; see section *3.5.4 Laboratory analyses – Soil texture*).

There is an assumption in the above method that the relative influences of soil texture and moisture were equivalent across the site; the possibility that soils of similar texture simultaneously had different moisture contents, or that soils of different texture had the same moisture content, for example due to topography-related drainage differences, or the effect of aspect on evapotranspiration, or of the different times required for different soil textures or texture profiles to reach field capacity, was not accounted for in the method. However, the relation of EC_a to soil type contributes the 'soil knowledge' element to interpretation of EC_a patterns as advocated by McBratney et al. (2005) and others by harnessing often considerable existing knowledge about the soils in question.

In the case of soil moisture, understanding whether or not its correlation with EC_a is a function of soil type may suggest to what extent the correlation is likely to be stable, as soil type is, under different conditions.

2.3.5 EC_a and temperature in the field

For most purposes it is the spatial rather than temporal variability of EC_a which is of most interest. However, soil moisture is a notable exception for which both spatial and temporal variability are important. Soil moisture and temperature are both variables which, according to theory discussed in section *2.2 - Theory of Apparent Electrical Conductivity (EC_a)*, could produce temporal variation in spatial patterns of EC_a.

Brevik et al. (2004) examine the effect of daily temperature fluctuations on measurement of EC_a using a Geonics EM38 in the field. Temperature was measured in air and at various depths in soil to 60cm and the greatest temperature fluctuation, about 15°C (from 23 to 38°C) was observed in soil at 5cm depth. No effect of temperature fluctuation on EC_a was observed with the EM38 in either horizontal or vertical modes. This was attributed to correction by nulling of the 'in-phase' (IP) signal of the EM38 immediately prior to each EC_a measurement. (Nulling of the IP signal is a regular part of instrument calibration usually done at the beginning of a survey session and at any other instance of recalibration; see *Appendix 2 – EM38 Mk2 calibration method).*

Also using an EM38, Sudduth et al. (2001) measured an increase in EC_a of ~0.84 mS/m per °C at a fixed location during 8 hours in which ambient temperature rose from 23°C to 35°C. During the same period the IP reading decreased from 0.2 to -101.2 mS/m. In a separate test, manually changing IP by ±150 mS/m from its zero position caused a total variation in EC_a of about 30 mS/m, i.e. 0.1 mS/m increase in EC_a per unit decrease in IP, the same as in the fixed location experiment (the EC_a-IP relationship was however, non-linear in both cases with changes in IP close to its zero value having less effect on EC_a). The effect of ambient temperature change on EC_a could therefore be fully associated with change in IP. However, in other field experiments by Sudduth et al. (2001) EC_a was negatively correlated to soil temperature.

In the fixed location experiment of Sudduth et al. (2001) the EM38 was positioned in vertical dipole mode, 43cm above the ground, where instrument sensitivity would

be maximised at the soil surface and decline with depth. Sudduth et al. (2001) concluded that effects on IP were complex and might not be temperature-induced.

Also using an EM38, Waine (1999) observed an increase in EC_a of 0.4 mS/m per °C at a field reference station during an hour in which ambient temperature rose from 13°C to 23°C. This relationship was used to correct values of EC_a measured in a concurrent survey. The total change in EC_a was ~4 mS/m, i.e. from ~1 mS/m to ~5 mS/m. The percentage change per °C therefore was ~8%, substantially higher than the 2% per °C approximation given by Rhoades and Corwin (1990; see section *2.2.6 - Effect of temperature on EC_a*). In the experiment of Sudduth et al. (2001) described above, the percentage change in EC_a per °C (ambient) was about 2%, in agreement with Rhoades and Corwin (1990).

The above findings highlight some questions about the operation of the EM38. In horizontal dipole mode the EM38 is most sensitive to the soil surface region, with about 18% of its sensitivity applied to the top 10cm of soil. Some increase in measured EC_a might then be expected with a substantial warming of the soil surface as described by Brevik et al. (2004). However, the EM38 in horizontal mode showed slightly declining EC_a during the period of most soil warming, in agreement with the soil temperature experiments of Sudduth et al. (2001). The apparent temperature effect was removed by nulling the instrument IP, which agrees with the results of Sudduth et al. (2001) in which supposed temperature effects were entirely consistent with changes in IP.

EC_a is measured by the EM38 as a ratio of secondary to primary magnetic fields with both measures potentially affected, possibly in different ways, by temperature (either via soil properties such as soil solution viscosity, or by effects on instrument circuitry, or some other mechanism). Repeated zeroing of instrument IP by Brevik et al. (2004) was associated with apparently distorted EC_a measurements i.e. decline rather than increase in EC_a with increasing temperature. No theoretical explanation or justification for addressing temperature effects on EMI by nulling the IP was given.

If the change in EC_a with temperature observed by Waine (1999) was also due to drift in IP, in keeping with the findings of Brevik et al. (2004) and Sudduth et al.

(2001), that drift was unlikely to have been caused by change in soil temperature during only one hour of observations, but if related to temperature at all was more probably related to ambient temperature, as Waine (1999) also concluded. Robinson et al. (2004) likewise found that changes in EC_a measured by repeat surveying (EM38) of a field transect on one day exceeded that which could be explained by changes in soil temperature.

The correction of EC_a for temperature change by Waine (1999) using an empirical function was effective, but as with Brevik et al. (2004) the mechanism of the temperature effect was unexplained. Actual change in soil EC_a caused by temperature was not differentiated from any direct effect of temperature on the instrument as observed by Robinson et al. (2004). EMI may also be affected in other ways by ambient temperature. For example, if the primary electromagnetic pulse travels not only through ground but also above ground it might be affected by ambient temperature, in keeping with some of the findings discussed above.

The approximation by Rhoades and Corwin (1990) of 2% change in EC_a per °C is based on the work of the U.S. Salinity Laboratory (1954) and relates to effects on soil EC via viscosity of the soil solution. The review of EC_a temperature correction models by Ma et al. (2011; see section *2.2.6 - Effect of temperature on EC_a*) also uses the U.S. Salinity Laboratory (1954) data as a reference standard. However, the literature discussed above suggests that if temperature affects EMI field measurements of EC_a at all, it is largely in relation to ambient and/or instrument temperature rather than soil temperature, and appears related to the IP signal.

2.4 Depth profiles of EC_a

Failure to discern the relative contributions to EC_a from different depths is thought to contribute to inconclusiveness of studies correlating EC_a with soil properties, disagreements between such studies, or the site specificity of their findings (Farahani and Buchleiter, 2004; McCutcheon et al., 2006). An example of all the above types of results despite extensive analysis with an array of statistical methods, but without EC_a depth profile information, can be found in Carroll and Oliver (2005). Such results can be anticipated from the irregular, depth-dependent sensitivity

functions of EMI instruments discussed above (see section *2.1 – Electromagnetic induction in soil*).

For example according to the sensitivity function of the EM38 Mk2, 1m coil separation, vertical mode, the contribution of soil moisture to EC_a at 20-40cm depth should be 34% greater than for the same moisture content at 60-80cm depth (Figure 2.01). Correlations of depth-integrated EC_a with moisture content to 1m depth are then expected to be obscured by interaction of irregular depth profiles of moisture distribution with that of instrument sensitivity. Hossain et al. (2010) concur, finding that:

'the shape of the vertical moisture profile proved highly influential in determining the ability of the calibration equations to infer underlying average moisture content, especially where the depth profile shapes differed between sensor calibration and subsequent field validation (for example following rainfall or irrigation).' *(p. 100)*

It is impossible from the simple, depth-integrated measurement of EC_a alone to know whether a higher reading results from an increase in a soil property to which EC_a is positively correlated, e.g. soil moisture, or the presence of the same or even a lesser quantity of the same property at a depth to which the EMI instrument is more sensitive. This situation exists for multiple soil properties, further complicating interpretation of data and supporting the need to ground-truth EC_a maps. As EC_a measured by EMI is determined by soil properties at each depth independently of other depths, knowledge of the EC_a depth profile is a prerequisite to application of the various models of EC_a discussed in section *2.2 – Theory of apparent electrical conductivity*. Mean values of soil properties such as soil moisture cannot be used accurately with EC_a in such models because EC_a measured by EMI is not mean EC_a, except in the case of Geonics instruments where the EC_a profile is even with depth, as discussed in section *2.1.3 - Geonics EM38 Mk2 and EM31*.

When an EMI instrument is raised above the ground its sensitivity profile remains similar but the position of that profile relative to the soil EC_a profile is changed, i.e. the upper portion of the instrument sensitivity profile is lost, the EC of air being

close to zero (Geonics, 1995). EMI readings from different measurement heights at the same site and time will therefore differ and can be analysed according to the known sensitivity profile of the instrument to indicate the EC_a depth profile being measured. A similar approach can be taken with different coil separations or instrument orientations which also exhibit different sensitivity profiles. Such comparisons form the basis of several EC_a depth profile resolution methods discussed below. (EC_a depth profile here refers to the *actual* EC_a profile in the field, not the theoretical profile of instrument sensitivity which is known and described by McNeill (1980b) and discussed in section *2.1 – Electromagnetic induction in soil*).

2.4.1 Empirical methods

Corwin and Rhoades (1982) describe the 'established coefficient method' to determine EC_a depth profile, following from the earlier 'multiple regression method' of Rhoades and Corwin (1981). The latter applied complex simultaneous equations to measurements by a 4-electrode probe at multiple depths in the soil and by EMI at multiple heights above the soil. The established coefficient method exploits the difference between EM38 measurements in vertical and horizontal modes to calculate the EC_a of layers at various depths by linear equations, e.g. for the 0-30cm depth layer:

$$EC_{a,0\text{-}30cm} = 0.2982\ EC_{aH(adj)} - 1.982\ EC_{aV} \qquad [9]$$

Similar equations are calculated for a range of layers, e.g. 30-60cm, 60-90cm, together providing a model of the EC_a depth profile. Note, however, in equation [9] that $EC_{aH(adj)}$ is an adjusted value; this adjustment is considered necessary by Corwin and Rhoades (1982) because EC_{aH} does not 'measure the same soil volume' as EC_{aV} for depths >30cm, whereas in the 0-30cm depth range it is held that the soil volume measured by both orientations is similar. Adjustment values for various depth ranges are determined by Corwin and Rhoades (1982) from EC field measurements using a four-electrode probe.

Whereas the earlier multiple regression method was site specific, according to Corwin and Rhoades (1982) the established coefficient method can be applied to a

range of sites albeit less accurately, which can be explained according to the following observation by Corwin and Rhoades (1990):

'a limitation of the EM38 calibration technique is that it requires prior knowledge of the general EC_a distribution ... and/or the textural layering. Theoretically, a calibration is necessary for every profile shape, but since there are an infinite number of potential shapes this is completely impractical.' *(p.890)*

Determining the 'general EC_a distribution' (i.e. EC_a depth profile) is presumably an objective of the method; if it cannot achieve this it appears the method has limited potential for more precise EC_a profiling. Corwin and Rhoades (1990) propose classification of sites according to the approximate type of EC_a profile: inverted, regular, etc. However, extensive empirical calibration and characterisation of sites to fit main 'classes' of profile would be required.

Like the multiple regression method, the established coefficient method is therefore site-specific to a significant degree. In the New Zealand context EC_a profiles may be yet less predictable as they are not dominated by salinity (the main focus of Corwin and Rhoades' 1982 and 1990 work). Alluvial soils such as those examined in this study are frequently characterised by contrasting heterogeneous textural bands down the profile.

2.4.2 Theoretical methods

Cook and Walker (1992) combined EC_a measurements from different EMI instruments, modes of operation or measurement heights in linear equations with coefficients designed to focus the combined reading on a depth range of interest. Several linear combinations of measurements were used for a test site where EC_a was independently measured, and provided more information about EC_a depth profile than could be determined from uncombined surface measurements.

The method of Cook and Walker (1992) might also improve the relation of EC_a to soil moisture either by statistical correlation or via the models discussed in *2.2 – Models of apparent electrical conductivity*, by enabling more direct comparison of EC_a with soil moisture and other properties at specific depths or depth ranges . However,

despite the altered depth profiles of combined EC_a measurements produced by the method of Cook and Walker (1992), the relationship of the combined measurement to the actual EC_a mean remains unclear because no simple combination of measurements, even with coefficients applied, produces an even EMI sensitivity profile. Different EC_a profiles will still give different responses for the same mean EC_a.

2.4.3 Iterative methods

The difference between measured EC_a data and expected EC_a (the product of coefficients representing the instrument sensitivity and possible EC_a of various depth layers) can be expressed as a matrix and solved iteratively as a linear least squares minimisation problem using various software packages. This type of method is the one most often referred to by the term 'inversion' and is subject to two problems: different EC_a profiles can account for the same set of surface-measured EC_a data (i.e. solutions are not unique) and small errors in the data can cause large errors in the solution (in mathematical terms, an 'ill-posed problem'; Gebbers et al., 2007).

Borchers et al. (1997) use a mathematical method, Tikhonov regularization (TR) to reduce the effect of data error in inversion models of EC_a depth profile. The data used is from EM38 readings in vertical and horizontal modes at the ground surface and at 11 heights above ground: 10cm intervals to 100cm height, and at 120cm. Following EMI measurement the actual EC_a profile was measured using TDR at 10cm depth intervals while excavating a pit at the site.

Inversion with TR requires complex calculation but is facilitated by appropriate software. Borchers et al. (1997) report superior results to Cook and Walker (1992) and Corwin and Rhoades (1990) whose methods were also applied to the data (indeed it could be observed that the latter methods estimated some profiles that appeared markedly dissimilar to the measured profiles). The TR model was insensitive to large fluctuations in EC_a over small changes in depth as it produced a smoothed profile, but there was broad agreement with profiles of TDR-measured EC_a. However, McBratney et al. (2000) show that profiles modelled using TR can be

surprisingly unlike the actual EC_a profiles they represent (indeed some profiles appear as mirror images i.e. opposite to the measured profile).

Inversion such as that used by Borchers et al. (1997) is unlikely to be used for kinematic or other extensive surveys as it requires many different height measurements at each site. However, it could be used to provide intensive data from a limited number of sites to accompany extensive kinematic measurements as suggested by Gebbers et al. (2007), who also sees potential for a multi-coil EMI instrument capable of simultaneously measuring EC_a to different depths. The Geonics EM38 Mk2 is designed to meet the latter specification.

Gebbers et al. (2007) tested several inversion and regularization methods using simulated and actual soil EC_a profiles with accompanying resistivity measurements at various depths. Some models were well matched with measured or simulated EC_a profiles but no method produced consistently accurate results. Some profiles, e.g. a 'ramped' profile of EC_a steadily declining with depth, were especially problematic. Among non-saline New Zealand soils such a profile might not be uncommon. Predictions for a limited number of broad layers were not better than more detailed profile models.

Triantafilis and Monteiro Santos (2010) applied an inversion method based on earlier work by Monteiro Santos (2004) to EM31 and EM38 measurements of a transect in a cotton field. Horizontal and vertical mode measurements were made with both the EM31 and EM38, the former at a height of 1m and the latter at 0.2, 0.4 and 0.6m. Samples were also taken from the transect and analysed for various properties including the EC of soil pastes and paste extracts.

Correlations of inverted EC_a with EC and other soil properties were not strong; best results were obtained with combinations of EM31 and EM38 measurements. Inversion helped identify physiographic features such as drainage channels in the field. Inverted EC_a profiles did not reflect the expected 'duplex' nature of the soil, but indicated more gradational profiles. This was not necessarily an artefact; McBratney et al. (2000) makes the general observation that soil properties have been found more often to vary continuously with depth rather than stepwise in accordance with horizons.

A requirement of any method which compares EMI measurements according to their sensitivity depth profiles in various modes and measurement heights is the avoidance of any interference or other effects which might alter those profiles. Triantafilis and Monteiro Santos (2010) note the flexing of the EM38 mount used in their method as one example, this effectively causing some fluctuation in measurement height. The EM31 and EM38 data used by Triantafilis and Monteiro Santos (2010) was measured using a 'mobile electromagnetic sensing system (MESS)' as described by Triantafilis et al. (2003).

In the MESS, the EM31 was mounted 1.65m in front of and perpendicular to a small tractor and the EM38 mounted 1.5m behind, in line with the tractor. It is difficult to see in this arrangement how interference from the tractor, or of the instruments with each other, was avoided. While the EM38 was separated from the tractor beyond the 'effective depth range' of the instrument in horizontal or vertical modes (0.75m and 1.5m respectively) it is suggested by the data of Geonics (1995) that 30% of the sensitivity of the instrument is to greater depths (or in this case distances).

In addition the EM31 on the MESS was mounted at little more than half the effective depth range (3m) from the tractor, or a quarter for vertical mode (6m; apparently measurements in both orientations were made using the MESS). An additional complication is that the primary EM pulse from the EM31 would be expected to induce current in the ground beneath the EM38 at the distance involved, in addition to that induced by the EM38 itself, and so could affect EM38 measurements. Some direct physical interaction might also occur between the EM pulses of the two instruments. In summary there is some question whether the sensitivity profiles of the instruments in the MESS were unaffected by interference. (In practical research for this thesis, interference of an electric fence with the EM31 was found to begin at 15m distance, or 2.5x the vertical mode effective depth range of the instrument; see section *4.1 - EMI instrument functional tests* and *Appendix 6 - EMI instrument functional tests.*

2.4.4 Simulation methods

Simulation methods of resolving EC_a depth profile are founded on analysis not of data from actual EC_a profiles but from hypothetical or simulated profiles, for which the theoretical response of EMI instruments can be calculated and described in models or formulas; these models are then applied to field measurements.

Geonics (1995) present equations predicting EC_a (EM31) measurements of ground formed of two layers of known EC_a according to the depths of the layers. Applications of this method are obviously limited to the above scenario - profiles consisting of two homogenous layers of known EC_a – but apparently would be useful in such cases, i.e. to calculate the thickness of the upper layer.

Further equations are presented by Geonics (1995) for the two-layer scenario to calculate EC_a of one layer by comparison of EM31 measurements from vertical and horizontal modes. These equations introduce the concept of relative response: the total horizontal mode response for a given layer as a proportion of the total vertical mode response. This method also applies to a particular scenario, a two-layered profile where the EC_a of one layer is known, but still might find useful application there.

The final method for depth profile resolution given by Geonics (1995) is to determine whether a profile fits the two-layer category and if so, what are the depths and EC_a of the layers. This is done by plotting vertical and horizontal mode measurements from the EM31 at different measurement heights according to specific charts provided by Geonics (1995) showing a range of existing plots of two-layer scenarios (field data is to be plotted on 'transparent paper' to enable a direct visual comparison with the charts). If a match is discovered the profile is confirmed as two-layered and the EC_a and depths of the layers may be calculated from further equations.

Apart from the seemingly inconvenient approach given for the above method, which could be relieved by its adaptation to modern technology, a difficulty which is noted by Geonics (1995) is that some curves for different two-layer profiles are not dissimilar. Presumably if the layers concerned are variable or poorly defined with

regard to EC_a, comparisons with expected curves could be yet more problematic, as indeed is suggested by Geonics (1995).

Slavich (1990) modelled expected EM38 measurements for 66 simulated EC_a profiles of contrasting shapes according to the sensitivity depth profiles of the instrument in vertical and horizontal modes. For each of the simulated profiles to a depth of 1m, the contribution of EC_a in each 5cm layer was related by multiple linear regression to the expected vertical and horizontal mode measurements of the whole EC_a profile. This method is termed the 'modelled coefficient approach'.

The equations derived from the above regressions were applied to field soils for which vertical and horizontal mode measurements were made; the EC_a profile was also measured using a four-electrode probe. The established coefficient method of Corwin and Rhoades (1982) was used for comparison. The field soils included a range of profile shapes. Profiles estimated by the modelled coefficient approach showed closer resemblance to measured profiles than those estimated by the established coefficient method of Corwin and Rhoades (1982). The modelled coefficient approach also performed better when applied to the field data of Corwin and Rhoades (1982).

2.5 EC_a and soil moisture

This section reviews selected literature in two broad categories: that which relates EC_a to soil moisture indirectly though the relationship of moisture to other soil properties (section *2.5.1- Moisture-related characteristics of soil*) and that which examines the direct relationship between EC_a and soil moisture (section *2.5.2 - Direct relation of EC_a to soil moisture*). It will be seen, however, that these categories at times overlap.

2.5.1 Moisture-related characteristics of soil

Soil can be thought of as progressing through a range of moisture states following addition of water. According to this model, soil 1-2 days after heavy rain or irrigation is considered to be at field capacity, those pores which drain under gravity having been emptied, while smaller pores with sufficiently strong suction or 'matric

potential' remain filled. Other states such as 'stress point' or 'permanent wilting capacity' (PWP) are attained as the soil dries and water is extracted from increasingly finer pores (Maclaren and Cameron, 1990).

A number of researchers have used the relationship between soil texture and water-holding capacity to simplify interpretation of field-measured EC_a, e.g. James et al. (2003), Domsch and Giebel (2004) and McBratney et al. (2005). According to this method, EC_a surveys are done when the soil is judged to be at field capacity, at which time differences in moisture content reflect the known moisture retention characteristics of different soil textures, giving consistency to the combined effects of texture and moisture which commonly dominate EC_a in non-saline soils. Waine (1999) facilitates this approach by the establishment of a continuous scale of soil texture (the 'fineness class') linked by functions to soil moisture at field capacity or PWP (see section *3.5.4 - Laboratory analyses – Soil texture*).

Waine (1999) explores the use of EC_a as a proxy for soil moisture and also to indicate available water capacity. In the former case, similar linear correlations were found between moisture content and EC_a on all of three occasions. However, Waine (1999) also refers to the Rhoades et al. (1976) finding that the relationship between soil moisture and EC_a is a second order, curvilinear relationship and is texture specific. In keeping with that relationship, a loam with θ of 20% may have the same EC_a as a sandy loam with θ of 35%; yet greater differences occur between more dissimilar soil textures.

The three occasions on which EC_a was measured by Waine (1999) in the moisture-proxy study were all within a two week period, for the first week of which the soils were considered to have remained at field capacity in cool, dry, cloudy conditions. The two occasions for which soil moisture was mapped using date-specific calibration curves relate to that week. As expected soil moisture was closely related to soil texture.

While the above findings may be valid for the conditions in which the work was done, the accompanying description by Waine (1999) of texture-moisture-EC_a relationships suggests that very different results might arise from EMI measurements in drier conditions; it is such conditions in which moisture

measurement using EMI is likely to be most useful. EC_a-moisture relationships could also be derived for such conditions but this raises further questions about the method.

As with the work of James et al. (2003; see section *2.3.4 - EC_a and soil type mapping*) there is an assumption by Waine (1999) that soil moisture is related consistently to soil texture across the whole site. The positions of neutron probe access tubes, by which data for the EC_a-moisture relationships was obtained, were in the first place determined by EC_a. The possibility that similar EC_a in different areas might arise from different soil texture-moisture associations is not accommodated by the method. Such differences in response to factors such as discussed above in section *2.3.4 - EC_a and soil type mapping* are most likely to emerge as soil dries.

Waine (1999) estimates available water capacity (AWC, or in the terminology of Waine (1999), total available water capacity, TAWC) as the difference between soil texture-moisture curves of field capacity and dry conditions, the former from neutron probe measurements, the latter from soil pit data. No EMI measurements are presented for the dry conditions. The assumption is that soils of similar EC_a at field capacity will show similarly changed EC_a in dry conditions. This depends on the earlier assumption that soils of similar EC_a at field capacity have similar texture. However, as already noted, if there are exceptions to the latter assumption, in dry conditions the extent of exceptions might be increased. Without EC_a from dry conditions both assumptions are untested.

Finally, Waine (1999) presents a logarithmic relationship between EC_a and plant available water (PAW, or in the terminology of Waine (1999), available water content (AWC)). This relationship is held to apply across the widely variable texture of the study site; however the material presented by Rhoades (1976), referred to earlier, holds that the EC_a-θ relationship is texture specific. The EC_a-PAW relationship as presented appears unconvincing (Figure 2.03).

Kachanoski et al. (1988) also report a good quadratic relationship between EC_a and θ across a wide range of θ and soil textures at one location. However, as with the data of Waine (1999) when a quadratic relationship is obtained, the upper part of the curve is flattish and the highest values of EC_a are associated with declining PAW. This

is less than satisfactory in practice as it means two different measured EC_a values can be associated with the same value of PAW. It is, however, consistent with Mojid and Cho (2008) who found that in non-saline soils at high θ, EC_a is expected to decline with increasing θ. The finding of Waine (1999) is then, together with Kachanoski et al. (1988) and Mojid and Cho (2008), a third finding of decreasing EC_a with increasing θ at high θ in non-saline soils. This again highlights the need for ground-truthing at an intensity appropriate to the required application of the data.

The work of Waine (1999) demonstrates how useful information can be derived from moisture and EC_a measurements together with established reference data. No effective differentiation is made, however, between the effects of texture and moisture on EC_a. Results are presented variously in terms of either soil texture or moisture but the underlying methods assume these to be covariant for the purposes of the work.

McNeill (1980) presents a model in which various moisture states can be present together in the soil, with greater saturation at greater depth or in zones with greater moisture retention, lower hydraulic conductivity, or above horizons of lower hydraulic conductivity, or at lesser depth soon after rain or irrigation. The concept of a soil moisture profile is particularly relevant as it means θ and therefore EC_a can vary with depth even in homogenous soil, which could also cause inconsistencies in the moisture- texture relationships assumed at field capacity for some methods. For example, where soil is at field capacity below 40cm but increasingly dry above that depth, EC_a would not be expected to correspond to a standard value according to the texture of that soil with moisture content at field capacity.

Luck et al. (2009) found that field mapping of EC_a did not produce reliable soil texture maps without complementary spatial information, e.g. soil moisture and nutrient transport models. Luck et al. (2009) suggest that the missing step to achieve this aim might be to develop multi-sensor systems that allow adjusting the EC_a measurement according to the influence of different soil water contents. This is complex however, as the influence of moisture on EC_a also varies with soil texture.

Frogbrook et al. (2003) found that coregionalization (a form of spatial correlation) of EC_a with soil moisture was greater in drier conditions. Auerswald et al. (2001) agrees

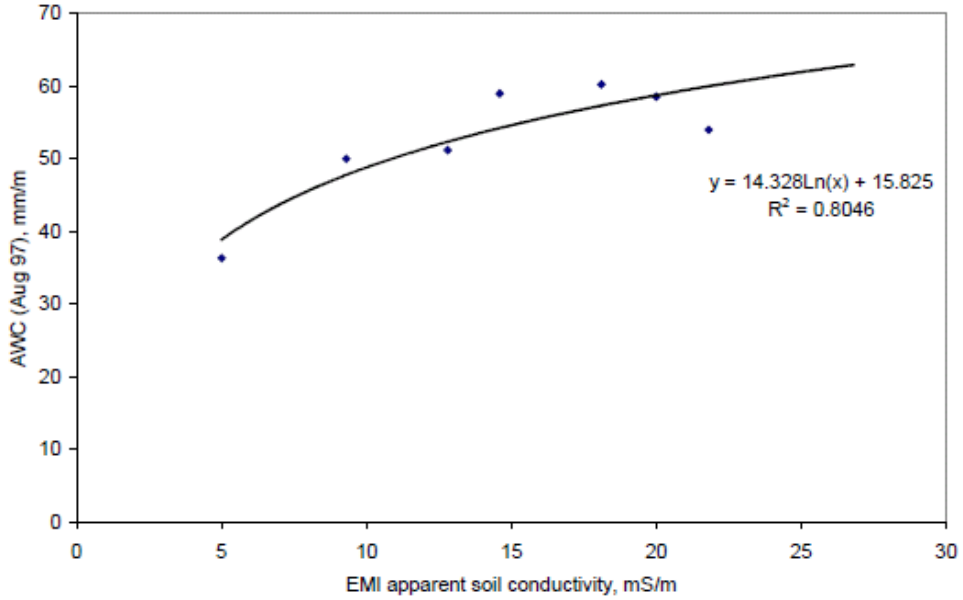

Figure 2.03. 'Available water calibration for EMI' (Waine, 1999). 'EMI apparent soil conductivity' = EC_a as measured by EMI. In the terminology of Waine (1999), AWC = available water content, or plant available water (PAW), not 'available water capacity' as elsewhere in this thesis.

A better fit of the above data is obtained using a quadratic relationship (Figure 2.04).

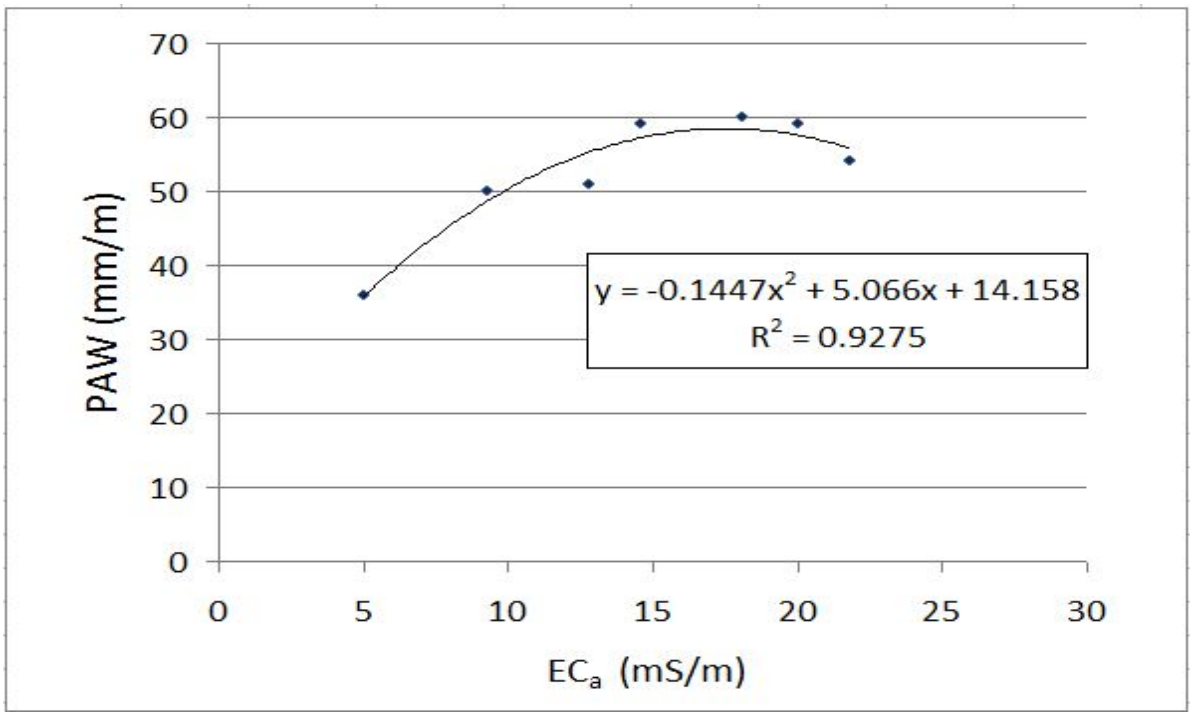

Figure 2.04. Quadratic relationship in the data of Waine (1999). 'EMI apparent soil conductivity' = EC_a as measured by EMI. PAW = plant available water, or in the terminology of Waine (1999), 'available water content' (not 'available water capacity').

that changes in θ have their most pronounced effect on EC_a at PWP and drier. Pozdnyakov et al. (2006) and Mojid and Cho (2008) provide support for these observations in terms of electrical double-layer theory (see section *2.2.4 Limitations and extensions of the dual pathway).* Therefore EC_a at low θ, or % change in EC_a as soil dries, may have a diagnostic value (e.g. indication of soil horizon depths and/or texture) in the same way that EC_a at field capacity is used to indicate soil texture, albeit interpretation would be more complex. Less potential is suggested for the detection of soil saturation (i.e. water table depth) in wet soils, the change in EC_a from field capacity to saturation being expected to be minor.

Hedley (2009) adapts the methods of Waine (1999) for application to an irrigated maize field of silty and sandy soils in Manawatu, New Zealand. Gravimetric analysis of soil samples from field capacity, dry, and intermediate conditions revealed similar AWC (<2% difference) despite the fact that the soils ranged in texture from loamy sands to silt loams; differences in AWC from 50-100% might be expected for such soils according to other published data (Waine, 1999). Soil moisture measured by TDR varied by 12.7-13.1% across the field at any one time.

It is suggested by Hedley (2009) that the above variation in soil moisture might result from soil profile differences: texture, structure and depth to gravels, and from topographic position, as it cannot be accounted for by AWC. This finding agrees with the observations of Kachanoski et al. (1990) regarding topography and variable recharge (see section 2.*5.2 - Direct interpretation of EC_a as soil moisture proxy*). Hedley (2009) relates ln(EC_a) to AWC (R^2=0.8) but this does not entirely relate EC_a to soil moisture as variation in AWC and its relationship to soil moisture in the study are both limited.

2.5.2 Direct relation of EC_a to soil moisture

In areas with low salinity, spatial variation in soil moisture content is often a major factor determining variation in EC_a (Sudduth et al., 1999). Many researchers have explored this effect and its potential to support direct measurement of θ using EMI.

Kachanoski et al. (1990) compared EC_a measured by EM38 and EM31 with soil moisture measured by neutron probe at 10m intervals along a 660m transect. A

statistical method ('coherency analysis') was used to establish the strength and spatial scale of correlations between variables. EC_a measured adjacent to the neutron probe locations was correlated with moisture measured concurrently and on two prior and one subsequent occasions. (All moisture measurements were within two months of the EC_a measurements). In this sense EC_a was not used to measure moisture specifically but rather the general moisture storage characteristics of the soil which dried throughout the study period.

EC_a was found to explain 50-60% of the spatial distribution of soil moisture across all measurement sites, but this increased to 80% at spatial scales greater than 40m. Kachanoski et al. (1990) associates the decrease in correlation of EC_a with moisture over small distances with the effect of topography on moisture recharge. This implies that EC_a and moisture were not similarly affected by variable recharge; therefore EC_a was correlated not with moisture only but also with other factors, e.g. some effect of texture other than simply the effect of texture on moisture. Such effects would in many cases be covariant and appear as one, but were distinguished where topography caused varying quantities of water to infiltrate areas of uniform soil texture. In such cases the effect on EC_a was less than the direct effect on soil moisture, disrupting the EC_a-moisture correlation.

The transect studied by Kachanoski et al. (1990) was of a single non-saline soil type (EC of extracts was not correlated with EC_a). Repeated correlation of once-measured EC_a with soil moisture over time depended on similar moisture retention behaviour across the transect which is not expected where textural variation occurs.

Reedy and Scanlon (2003) compared EC_a (EM38) and moisture measurements (neutron probe) at a $578m^2$ 'engineered barrier soil profile' designed for waste containment. Measurements were made on seven occasions over three years. Linear correlations were established between EC_a and θ. Better correlations were found with EM38 horizontal mode measurements than with vertical mode measurements; when both were used, the improvement in correlation provided by the vertical mode measurements was insignificant. This is explained by the fact that the EM38 vertical mode has a deeper weighted sensitivity profile while the horizontal mode has greatest sensitivity where moisture is most variable i.e. near

the surface, and it is this variation rather than the total measurement which is reflected in statistical regression.

Reedy and Scanlon (2003) also found better correlations between site averages of EC_a and θ (from measurements on repeated occasions) than between point measurements of EC_a and moisture at the neutron probe sites (these had PVC access tubes to avoid interference with EMI). This echoes Kachanoski's (1990) identification of a minimum spatial scale at which better EC_a-θ correlations were found, and Allred et al. (2005) who found that point measurements of EC_a were not strongly correlated with soil moisture or other properties, perhaps because of small scale variation in soil properties compared with the spatially averaged nature of EC_a. Linear calibrations of EC_a to represent θ were significantly different for each depth at each site.

EC_a measured by Allred et al. (2005) when sites were very dry (θ = 12.4%) was about half that measured when the sites were very wet (water table at the surface). According to theory explained by Pozdnyakov et al. (2006) most of that decrease in EC_a would occur in the moderately to very dry range with relatively little change in EC_a from saturation to field capacity.

McCutcheon et al. (2006) measured EC_a in repeated surveys of dryland fields of wheat planted in strips alternating with fallow. Spatial and temporal variation in EC_a was dominated by the effect of θ so that patterns of soil type or texture inferred by EC_a were not stable with time. This is consistent with theory presented by Pozdnaykov et al. (2006) whereby different and stronger relationships exist between EC_a and θ in various moisture states of soils drier than permanent wilting point (see Figure 2.02 and section 2.2.4 – *Limitations and extensions of the dual pathway model*). Therefore in the dryland fields studied by McCutcheon et al. (2006) a variety of different ECa-θ relationships may have been present at the same time and changed their respective locations and extents both spatially and between soil horizons over time as soils dried at different rates.

Unlike the delineation of soil texture or type in field capacity conditions, the above situation was too complex to be represented by EC_a- θ correlations across the whole site. This is in keeping also with the field observations of Frogbrook et al. (2003) and

Auerswald et al. (2001) regarding EC_a of dry soils, discussed in section *2.5.1 – Moisture-related characteristics of soil*.

McCutcheon et al. (2006) found potential in the above finding for direct measurement of θ by EC_a but that this would require better understanding of the complex interactions of soil factors affecting EC_a. The fallow and planted strips were strongly represented in the pattern of EC_a due to their influence on θ, which ranged from about 5-25% across the survey dates with some moisture deficit present at all times.

Huth and Poulton (2007) measured EC_a as an indicator of moisture content in an agroforestry system. EMI measurements in horizontal and vertical modes were combined with coefficients according to the method of Cook and Walker (1992; see section *2.4.2 – Simple theoretical methods*). Further adjustments were made according to calendar day to account for expected seasonal fluctuation in temperature, and a calibration for volumetric soil moisture was made by linear correlation of EC_a with soil core moisture data ($R^2 = 0.93$).

The method of Huth and Poulton (2007) provided temporal and spatial resolution of soil moisture measurement which would have been impractical with other methods such as gravimetric or neutron probe measurements. The detailed calibration work was justified by the ongoing programme of measurement at the site but could not be transferred to other sites.

In the study of θ across a hillslope by Tromp-van Meerveld and McDonnell (2009) EC_a was linearly related to soil moisture measured by capacitance sensors but showed less variation than soil moisture, apparently because of the spatially averaged nature of EMI measurements compared to the point measurements of the capacitance sensors. Average soil depth over bedrock at the study site was 0.63m and ranged from 0 to 1.8m; θ was the mean of measurements by capacitance sensors at 5 or 10cm depth intervals to bedrock at each site; the measurement depth(s) of the EMI instrument, a GEM-300, was not specified but 'exceeded soil profile depth' and was more sensitive to surface and upper profile EC_a.

Unlike Reedy and Scanlon (2003), Kachanoski et al. (1990) and Allred et al. (2005), correlation between EC_a and soil moisture at points in the study of Tromp-van Meerveld and McDonnell (2009) was better than for site averages over time. This is possibly because of the stronger influence of bedrock depth in the shallow hill soils, as suggested by the observation of strong variation in EC_a across the site at moisture contents higher than field capacity when variation in EC_a due to moisture is expected to be limited.

Tromp-van Meerveld and McDonnell (2009) found that correlation of EC_a with soil moisture was weaker when rainfall events caused greater saturation of surface soil. As discussed in section *2.4 - Depth Profiles of EC_a*, relation of EMI measurements to any soil property with variable depth profile requires characterisation of, and adjustment to the depth profile due to the irregular depth response of EMI. To accomplish this Tromp-van Meerveld and McDonnell (2009) used an EMI instrument with simultaneous measurements at multiple frequencies but depth profile resolution was hindered by correlation of the different frequency responses.

Like Tromp-van Meerveld and McDonnell (2009), Hossain et al. (2010) found that changes in depth profile of soil moisture e.g. following rainfall, limited the accuracy of EC_a-θ calibrations over time despite the fact that the deep vertisol soils used for the study were chosen for their relatively uniform texture and ion content (non-saline) with depth. Further uncertainty arose from the unknown contribution of EC_a from below the depths to which calibrations were established (0.8 or 1.2m). EMI measurements in horizontal mode, with their shallower depth-response function, were less affected in this latter way than measurements in vertical mode.

Zhu et al. (2010) found that EC_a was correlated with soil moisture flow paths (i.e. where topography causes water to accumulate) and in contrast to the findings of Frogbrook et al. (2003), McCutcheon et al. (2006) and Auerswald et al. (2001), that this relationship was stronger in wetter regions and conditions. It may be that a certain threshold of precipitation or irrigation intensity is required to realise the effect of topography on moisture runoff and associated variable soil moisture recharge.

EC_a was measured by Zhu et al. (2010) as relative differences within repeated surveys for which the pattern was found to be stable. An exception was the isolated fertilisation of one paddock, in which instance EC_a was dominated by the effect of fertiliser and did not conform to the otherwise time-stable pattern across the site (this result agrees with Auerswald et al. (2001)). The effect in this case was to 'offset' the EC_a pattern in the fertilised paddock from other paddocks across the site, which otherwise were subject to broadly similar temperature and moisture influences on the same occasions. It was also found that in drier conditions the effect of soil moisture was masked by other soil and landscape attributes.

2.6 Conclusions from the literature

Despite widespread use of EMI instruments in agriculture and research, uncertainty persists about some aspects of instrument function and behaviour:

- the precise nature of the manufacturer's calibration of EMI instruments, and the assumptions on which it is based;
- the effect of temperature on EC_a, which has been observed in the field to behave differently than would be expected according to theory.

Given the complexity of EC_a interpretation it appears unwise to disregard the above uncertainties. The significance of these limitations depends on the expected use of the data. For example, if the EMI survey is undertaken to identify broad soil differences, these limitations are less important than for accurate, quantitative predictions of soil moisture.

Similarly, resolution of EC_a depth profiles from EMI data has been extensively investigated and practiced according to a number of methods; software is commercially available for inversion. However, no method has been found to be consistently accurate. Resolution of depth profiles is essential to quantitative interpretation of EC_a for estimation of soil moisture.

Lack of consistency in EC_a measurement (at least partly due to the above issues) has limited application of the various theoretical models to interpretation of field-measured EC_a. Effects of the ionic strength of soil solution are reasonably well

quantified, especially at higher (saline) concentrations. Effects of soil moisture are best explained according to theory expounded by Pozdnyakov et al. (2006). Effects of soil particle surfaces and surface area (soil texture) are less understood. Whether the effects of differences in non-saline soil solute concentration or soil texture may interfere with EC_a-moisture correlations in alluvial Recent Soils will be tested in this study.

Field studies in non-saline soils reveal that EC_a can be dominated by numerous alternative soil properties or combinations of properties in different environmental scenarios. Most results then are at least site-specific and often time-specific as well. 'Relative difference' representation of EC_a can reveal temporal stability of spatial patterns in moist soils. EC_a theory has not yet provided for explicit quantitative interpretation of absolute field-measured EC_a values in terms of contributing factors. The effect of soil moisture on EC_a which is the subject of this study has not been fully distinguished from the effect of soil texture in other field studies.

EC_a is expected to be most sensitive to changes in soil moisture content in conditions drier than field capacity. Methods which determine soil texture and related properties or soil type by EC_a measurement at field capacity are then unlikely to be strongly influenced by minor deviations from field capacity. Neither however do such methods make use of the greater sensitivity of EC_a to drier soil moisture conditions, for which interpretation is hampered by complexity, with soils and soil horizons of different textures exhibiting different linear and/or non-linear EC_a responses to moisture.

EC_a theory does not suggest good potential for direct determination of water table depth in moist, non-saline soils, as the expected change in EC_a from field capacity to saturation is relatively small, and either positive or at times negative.

Chapter 3

Materials and Methods

3.1 Introduction to the experimental programme

The experimental programme was applied to each of two locations ('Burnside' and 'No.1 Dairy'; see section *3.2 – Field locations*). To avoid confusion, field sites consisting of whole areas surveyed are referred to as 'locations' while point sites of measurements or samples are referred to as 'sites'. Kinematic surveys and associated measurements were designed to focus on EC_a and soil moisture across the whole of each study location. In addition, detailed information was obtained from a small number of sites to assist interpretation of the kinematic survey data in terms of soil moisture.

Two elements of the programme were applied to the No.1 Dairy location only: analysis for moisture release characteristics of intact soil cores, and measurements of depth to a subsurface sand horizon which was suspected to have a significant effect on EC_a. The remainder of the programme was applied to both locations and is described in detail in the remainder of this chapter.

In addition to the main programme of field experiments, the following instrument tests were also conducted to verify the performance and function of the EMI instruments and to establish sound procedures for using them in the field:

- Observation of the effects of the following on EMI readings:
  - instrument battery depletion
  - removal and replacement of batteries and attachment and detachment of cables
  - change in ambient temperature
  - proximity of EMI instruments to the ATV and to fences.

- calculation of position error in GPS-linked data from kinematic surveys, and design of procedures to correct that error.

3.2 Field locations

The study was conducted on alluvial Recent Soils in the Manawatu River catchment in the lower part of North Island, New Zealand (Figure 3.01). Two locations as follows were selected, being low terrace or river flat lands of the Manawatu River. Both locations were subject to moderately intensive agricultural use.

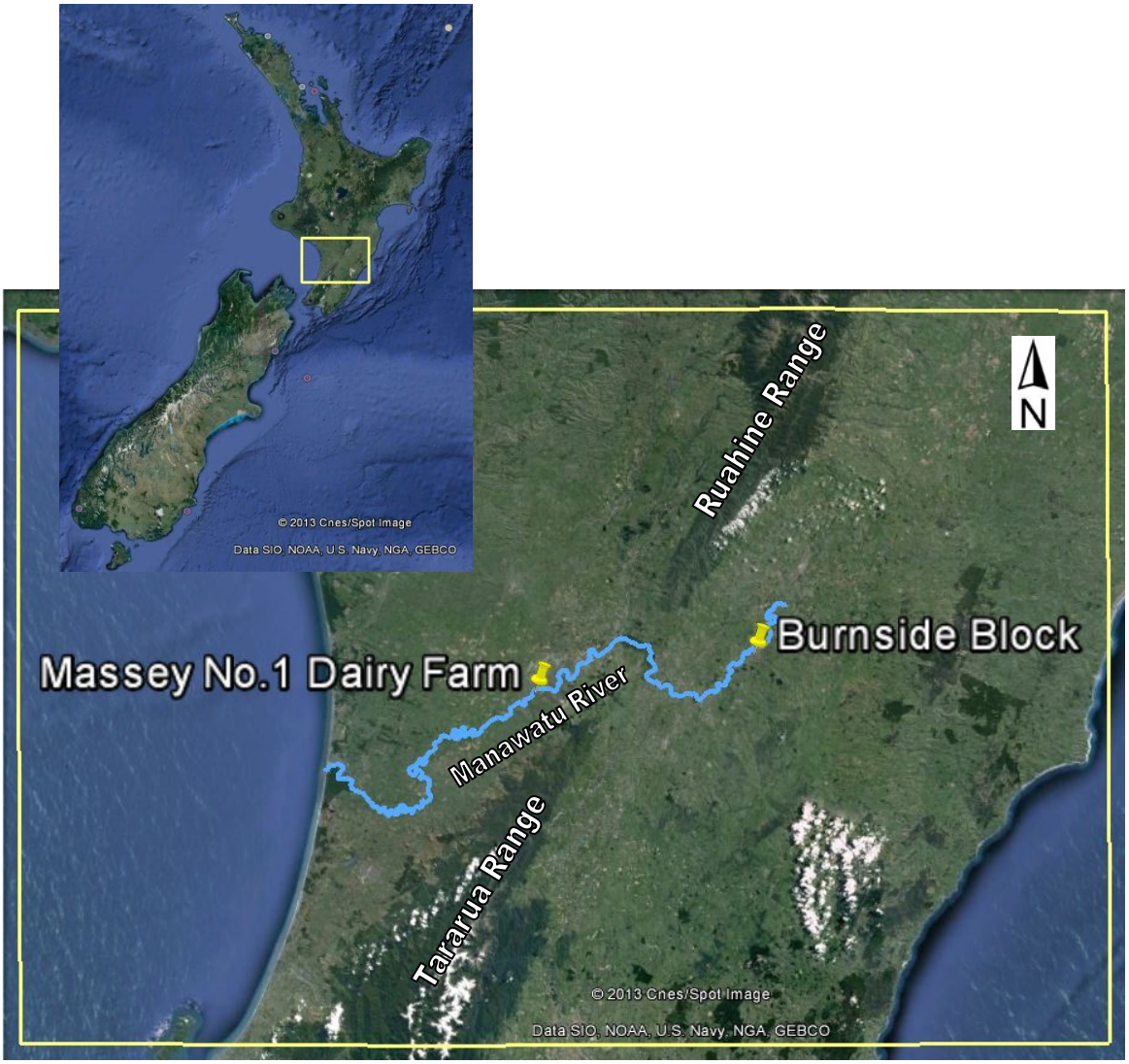

Figure 3.01. Locations in New Zealand of Massey No.1 Dairy Farm and Burnside Block. The rectangle in the upper image contains the same area as that in the lower image. Both locations are east of the Manawatu River. Images: Google Earth.

3.2.1 Massey No.1 Dairy Farm, Palmerston North

Immediately south of Palmerston North city on the east bank of the Manawatu River, the research location comprised three paddocks at the far south end of the farm, 4.9 ha in total, bounded by the riparian margins of the Manawatu River and Turitea Stream on the west and south sides of the location respectively (Figure 3.02). The location was 25-70m from the Manawatu riverbed on the closest (west) side and is recorded as having received 12-13cm of sediment in the Manawatu River flood of 2004 (NZCPA, 2005). The south side of the location was 5-23m from the bed of Turitea Stream which

Figure 3.02. Study location at Massey No.1 Dairy Farm. Turitea Stream is below the location (outlined in red), Manawatu River to the left.

entered the Manawatu River approximately 100m from the edge of the study location. All the adjoining riparian land was planted in willows and alders. To the

east the location was bounded by a farm raceway atop a terrace riser. The riser, approximately 1.5m high, extended into the edge of the surveyed paddocks but was not included in the study location. South of the location across Turitea Stream a bluff some 10m high confined the flow of the stream in that direction.

Soil at the No.1 Dairy location ('No.1 Dairy') is mapped as entirely Rangitikei silt loam over sand by Pollock et al. (2003; see section *3.3 – Soils*). Elevation of the location was approximately 37-39m above sea level, flattish over much of the area, sloping to the southwest and dissected by two swales which combined at the south end close to Turitea Stream. Surface water was observed in these swales which ran approximately parallel to the Manawatu River and perpendicular to Turitea Stream. The location was planted in clover-ryegrass pasture and used for dairying.

3.2.2 Burnside Block, Kumeroa

Approximately 16 km southwest of Dannevirke at Kumeroa, Burnside block occupied alluvial terraces southeast of the Manawatu River (the study location was approximately 650m from the river at the closest point; Figure 3.03). The location comprised three paddocks in the southwest corner of the block, approximately 5.6 ha in total. The block was dissected by Totara Stream which flowed to the west of the study location, between 22 and 120m distant, but did not cross it. Only a small area in the northeast corner of the location included an obvious recent terrace of Totara Stream, which entered the Manawatu River where the latter flowed closest to the study location. The block (including the location) did, however, slope away from Totara Stream on both sides of the stream, suggesting past deposition of sediment from the stream. The location was not inundated by the 2004 flood of the Manawatu River (Poulton, 2013).

Soil at the Burnside block location ('Burnside') is mapped as entirely Manawatu silt loam by Horizons (2008; see section *3.3 - Soils*). The topography was flat, gently sloping to the west, elevation approximately 110-114m above sea level. Surface water was observed on occasions in many parts of the location, especially near the south end (Figure 3.04). Maize was grown at the location in the 2010-2011 season after which clover-ryegrass pasture was sown. At the time of the study the location

was used as grazing for sheep and beef cattle. Adjoining land of other farms was used for dairying (see Figure 3.05).

Figure 3.03. Study location at Burnside Block, Kumeroa. Totara Stream is adjacent to the location (outlined in red), Manawatu River top left.

3.3 Soils

The soils encountered at Burnside and No.1 Dairy are formed in alluvium from the Manawatu River and probably also the tributaries present at each location. The source rocks of the alluvium are Jurassic greywacke and Tertiary sandstones, mudstones and limestones (Cowie, 1978). The soils are accreting, receiving occasional fresh contributions of flood sediment. Topdown processes of soil formation, e.g. leaching, weathering, and melanisation, are curtailed by further accumulation of sediment, burying the previous topsoil before mature features have developed. The main soil-forming factors governing soil properties are therefore soil

Figure 3.04. Standing water at Burnside near site B1. Photo taken on the day of the reconnaissance survey, 22 August 2011.

Figure 3.05. Mixed stock at Burnside, 25 November 2011.

texture, rate of deposition, and drainage. Soil texture is mainly derived from the parent sediment; little in-situ clay formation has occurred (Cowie, 1978).

Texture, age, elevation and drainage are related in these soils: coarser sediments are deposited closer to rivers on lower surfaces (which may however, slope down away from the river) which are also younger and more active and drain better (due to higher sand content). The soils of each phase of maturity are classified according to drainage. The soils of No.1 Dairy are the youngest of these alluvial Recent Soils: the Rangitikei (well to excessively drained) and Parewanui (imperfectly to poorly drained) series. The soils of Burnside are more mature, described as slowly accumulating (i.e. rarely flooded): the well-drained Manawatu and imperfectly to poorly drained Kairanga series (Cowie, 1978).

The topsoils are generally low and subsoils very low in organic matter. Cation exchange capacity (CEC) is medium in topsoils and low in subsoils; the poorly drained Kairanga silt loam however, has medium values also in the subsoil (the above ratings are from data in Cowie (1978) according to standard ratings of Blakemore et al. (1987); no data is given by Cowie (1978) for any subsoils of the Parewanui series). Detailed description of the soil series mentioned above is given in *Appendix 8 - Descriptions of soil series.*

3.4 Climate

Climate at the two locations, No.1 Dairy and Burnside, is somewhat similar as described below. Historical averages are from the previous 10 years.

3.4.1 No.1 Dairy

Climate at Palmerston North airport, taken as indicative of climate at No.1 Dairy, is shown in Figure 3.06. Rainfall in the study year of March 2011-February 2012 year was 1208mm compared with the historical average of 874mm. The autumn and late spring/early summer periods were especially wetter than average. Higher rainfall is

also expected at No.1 Dairy being closer to the ranges compared with the airport farther west on the plains.

Temperature was in keeping with historical records except for higher average minimums in spring and lower average maximums in summer. Historically the warmest month is January with an average maximum of 28.5°C, the coolest month is July with an average minimum of -2.3°C.

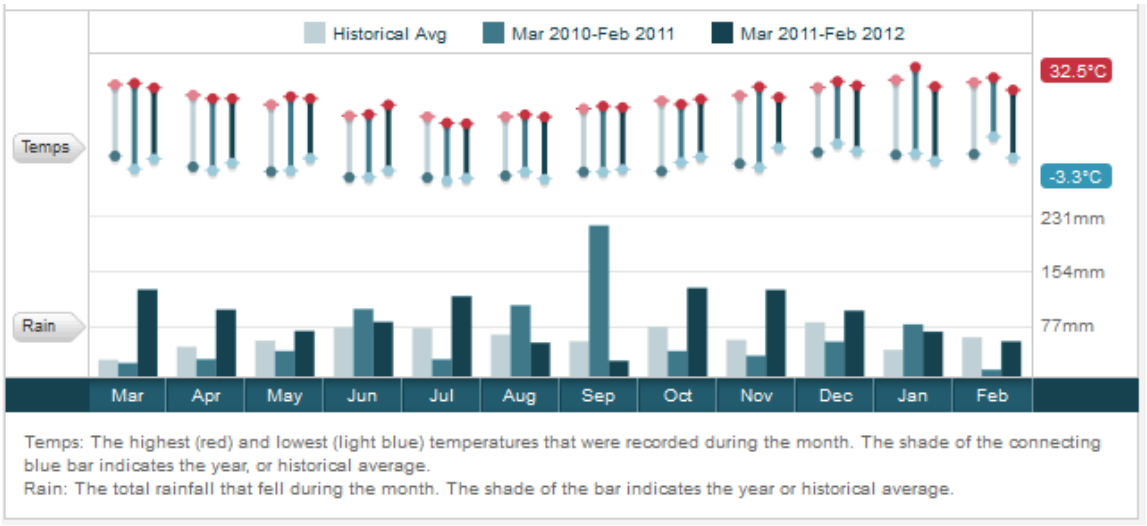

Figure 3.06. Temperature and rainfall at Palmerston North Airport. (MetService, 2012).

3.4.2 Burnside

Climate on the Takapau Plains, taken as indicative of Burnside, is shown in Figure 3.07. Rainfall for the study year of March 2011-February 2012 year was 1105mm, slightly higher than the historical average of 996mm. However, this region experiences both droughts and wet years (which is not evident from the 10 year average), 2010 and 2011 being wet. This has been attributed to the La Nina weather pattern prevalent over this time bringing wet frontal systems from the east (NIWA, 2012). Burnside is expected to have somewhat higher rainfall than Takapau Plains for which the data below is given, being farther south towards the wetter regions of northern Wairarapa.

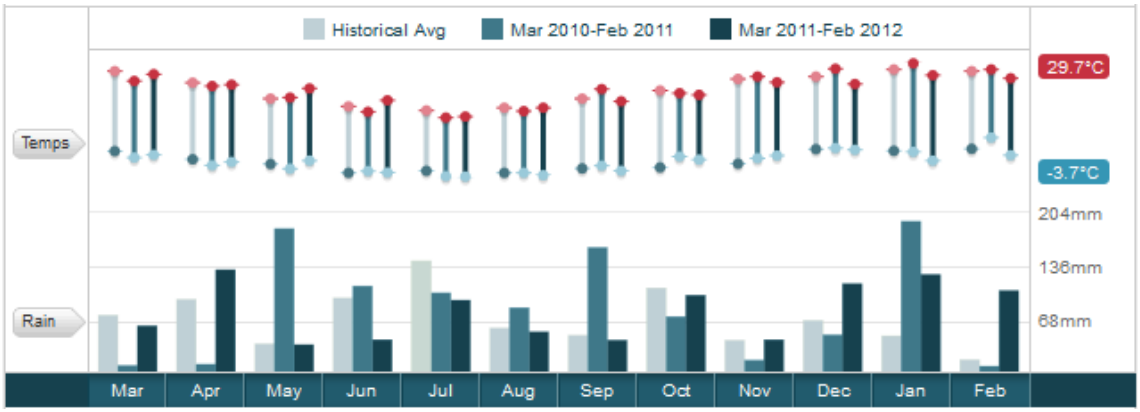

Figure 3.07. Temperature and rainfall on the Takapau Plains. (MetService, 2012).

Historically, June, July and August are the coolest months in this region with monthly average lows between -2.0 and -2.6°C, January the warmest month with an average high of 27.9°C. Temperatures throughout March 2011-February 2012 were cooler than average with the exception of May-June 2011.

3.5 Soil and moisture measurements

3.5.1 Selection of soil sample sites

Three sample sites were selected for replicate sampling at each of the locations, Burnside and No.1 Dairy. Selection of sites was by a visual assessment of mapped survey data (kriged – see section *3.7.2 – Mapping and Spatial Analysis*) to represent a range of values of the following patterns of variation:

- EC_a
- topography
- the spatial extent of each location.

In particular, sites were located to explore the range of conditions from an EC_a perspective (different soil texture and moisture combinations). See Figures 3.08, 3.09 and 3.10.

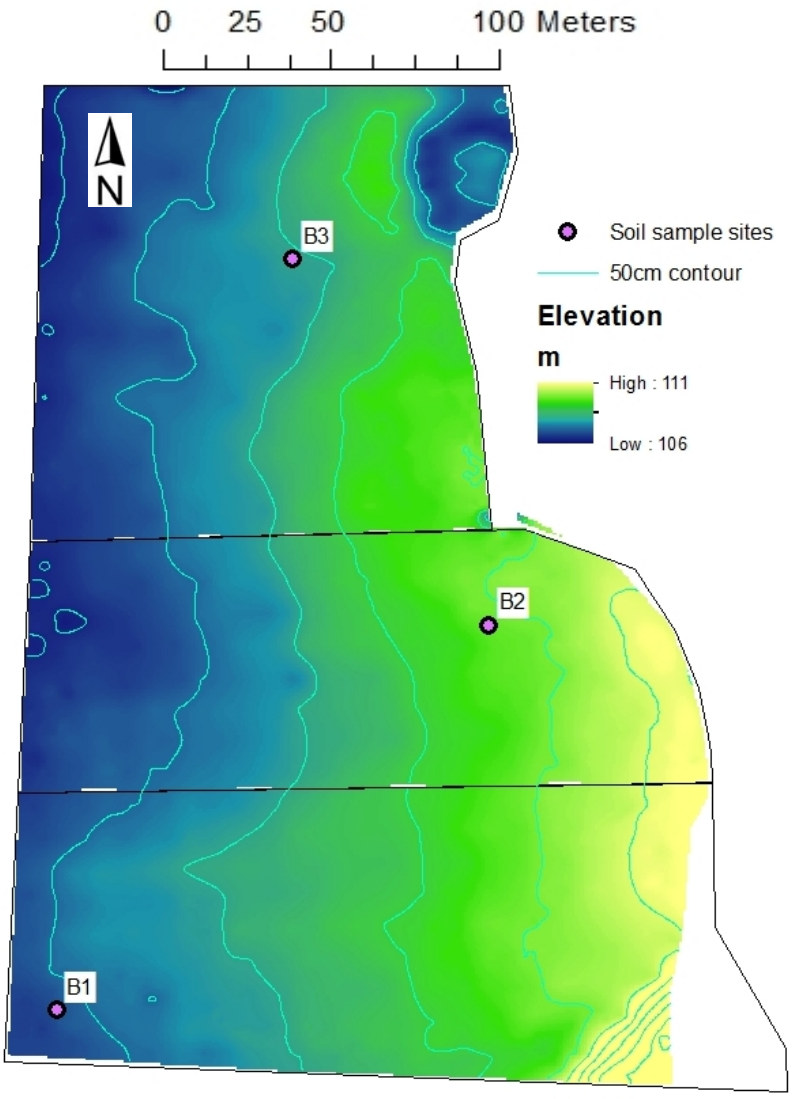

Figure 3.08. Soil sample sites with elevation at Burnside. Black lines indicated fenced paddock boundaries.

3.5.2 Soil sampling and field observations

At each site, 3 holes were made as replicates, each between 0.5 and 1m from the sample site GPS position, to enable repeated TDR and EMI measurements of the undisturbed soil. Intact cores were collected at 4 depths from each replicate hole: 4, 28, 42 and 64cm.

Soil moisture was measured at 4, 28 and 64cm depths by gravimetric methods at six sites for the first kinematic survey after reconnaissance at Burnside. In subsequent kinematic surveys at both locations soil moisture was measured by TDR to 45cm

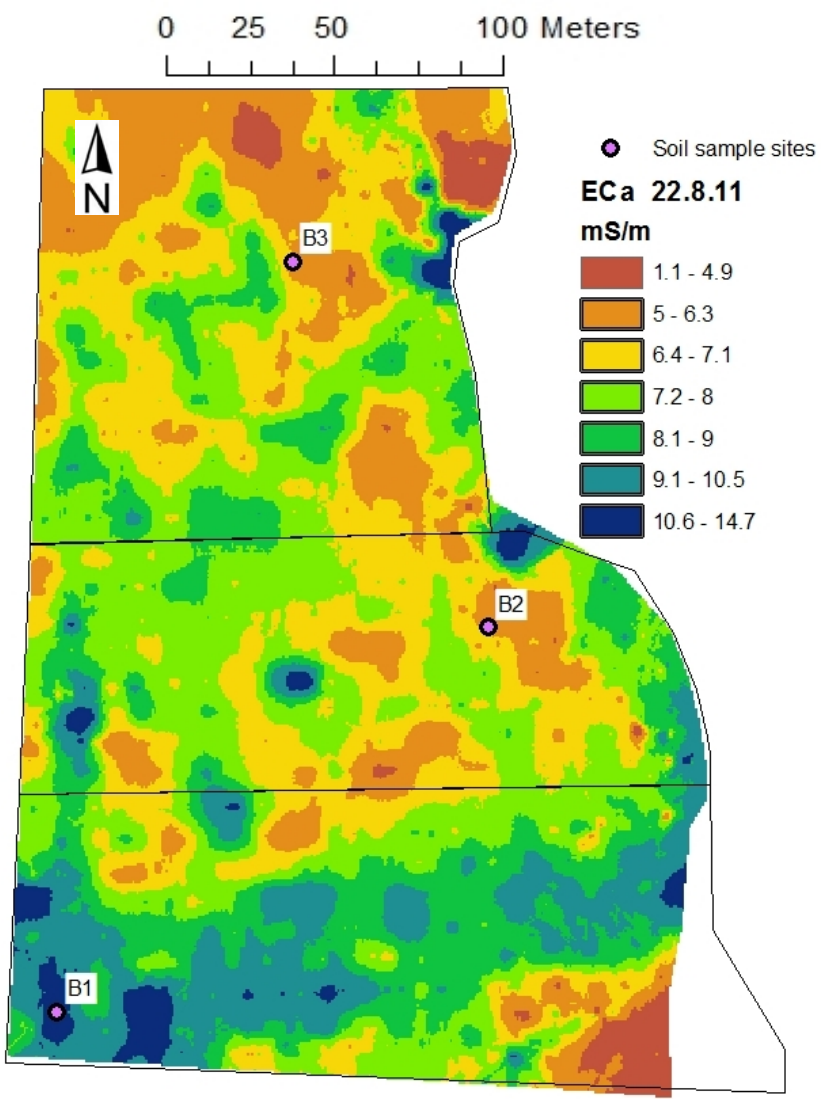

Figure 3.09. Soil sample sites with EC_a at Burnside. EC_a measured by EM38 (1m, vertical) on 22.8.11. Black lines indicated fenced paddock boundaries.

depth as this provided for more soil moisture measurements concurrent with the surveys.

The core tubes used at Burnside were polycarbonate, approximately $10cm^3$ in volume, and were extracted from augured holes (Figure 3.11). At No.1 Dairy the tubes were steel, approximately $50cm^3$, and were extracted from holes dug with a spade. This was a more lengthy procedure but facilitated the use of the cores from No.1 Dairy for soil moisture release analysis. Soil immediately adjacent and at similar

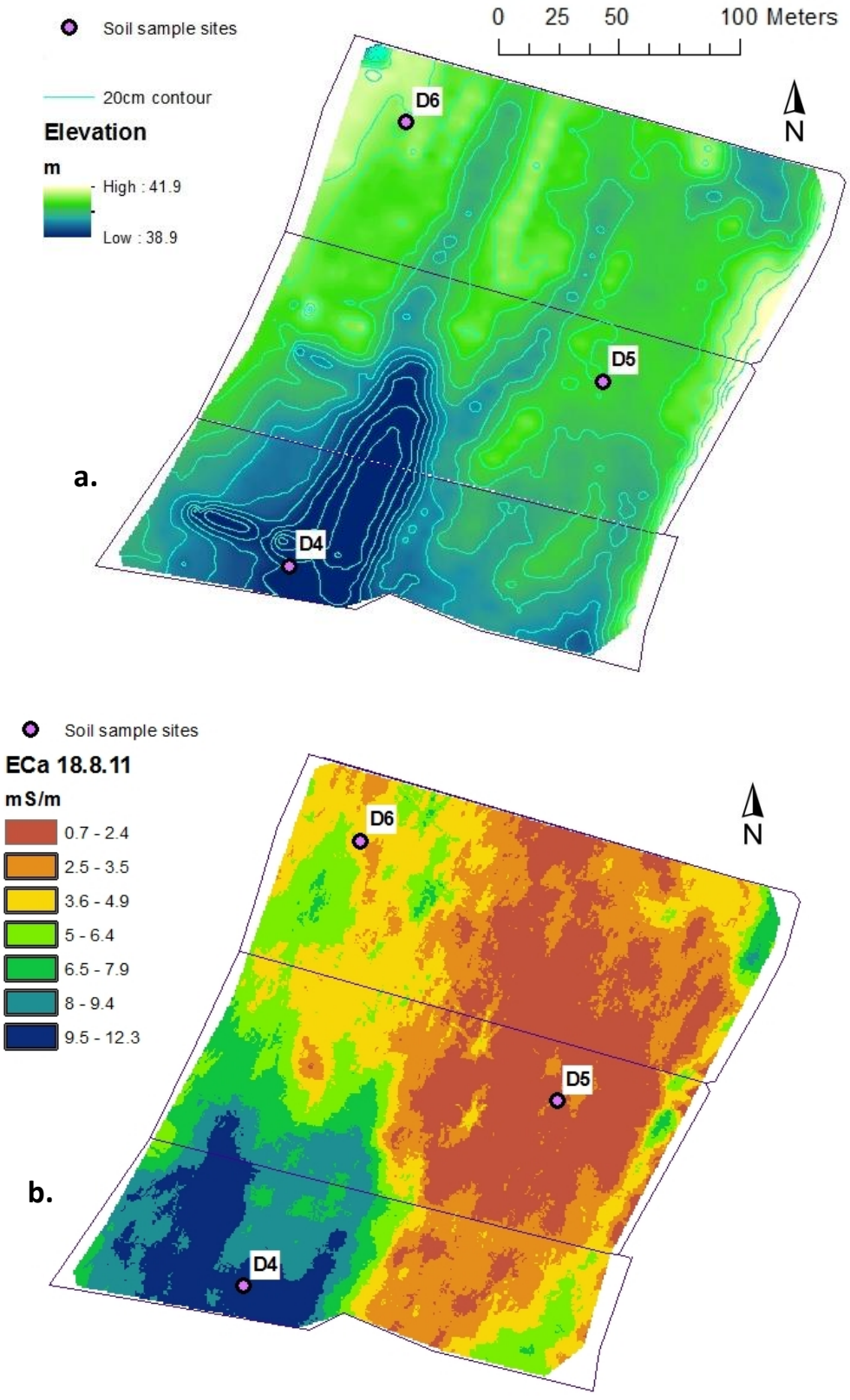

Figure 3.10. Soil sample sites at No.1 Dairy: a) with elevation; b) with EC_a (EM38 Mk2, 1m, vertical on 18.8.11). Black lines indicated fenced paddock boundaries.

Figure 3.11. Soil sampling at Burnside.

depths to the cores was also collected and regarded as similar for analytical purposes.

Depths and descriptions of soil horizons observed during sampling were recorded according to the New Zealand Soil Classification as summarized by Landcare Research (2013). For example, a Bg horizon was defined as a 'B horizon with mottled grey and yellow/orange colours indicative of reduction (gleying)' rather than according to percentages of specific soil colour ranges. Holes were augered or dug below sampling to depths of 1m or more to facilitate soil profile description. Soil sampling was carried out over three days at each location (Table 3.01).

Table 3.01. Schedule of fieldwork. 'Multi hit' = measurements with the EMI instrument at various raised heights above ground.

Burnside			**No.1 Dairy**		
Reconnaissance	EM38 Mk2 (kinematic)	22.8.11	Reconnaissance	EM38 Mk2 (kinematic)	17-18.8.11
	GPS (kinematic)			GPS (kinematic)	
EMI Survey 1	EM38 Mk2 (kinematic)	29.9.11	EMI Survey 1	EM38 Mk2 (kinematic)	8.11.11
	EM31 (kinematic)			EM31 (kinematic)	
	GPS (kinematic)			GPS (kinematic)	
	Soil cores (moisture)			TDR	
EMI Survey 2	EM38 Mk2 (kinematic)	4.1.12	EMI Survey 2	EM38 Mk2 (kinematic)	25.1.12
	EM31 (kinematic)			EM31 (kinematic)	
	GPS (kinematic)			GPS (kinematic)	
	TDR			TDR	
Soil sampling and site measure 1	EM38 Mk2 (multi ht)	22.11.11, 23.11.11, 25.11.11	Soil sampling and site measure 1	EM38 Mk2 (multi ht)	27.12.11, 29.12.11, 6.1.12
	TDR			TDR	
	Soil cores			Soil cores	
Site measure 2	EM38 Mk2 (multi ht)	15.3.12	Site measure 2	EM38 Mk2 (multi ht)	24.2.12
	TDR			TDR	
			Site measure 3	EM38 Mk2 (multi ht)	4.3.12
				TDR	
			Auger sampling	field visual	27.12.11-5.7.12

3.5.3 Supplementary profile observations

Further soil profile observations were made at No.1 Dairy via holes made with a screw auger or a Dutch auger. The major purpose of these observations was to gather information about the depth of a subsurface sand horizon in relation to two broad zones of EC_a apparent in survey data. Nine holes were made in a transect across these zones, and at six other locations in areas chosen to complement the sample site data. Locations of the auger holes were logged using a Trimble Juno handheld GPS. Samples were not collected from these holes.

Three piezometers were also installed at Burnside and four at No.1 Dairy to monitor water table depth. This was done to investigate whether the saturated state of soil moisture could be discerned using EC_a and accompanying measurements. This element of the programme is not described in detail because it was not retained in the programme, but is mentioned here because certain qualitative observations about the soil profiles, made during the piezometer installation process, are mentioned in the discussion of results.

3.5.4 Laboratory analyses

EC of 1:1 soil pastes and extracts

For each sample, 20g of air dry, <2mm sieved soil was weighed into a 50mL polycarbonate centrifuge tube. 20mL of deionised water was added and the tube was initially shaken vigorously by hand to break up dry patches, then using a rotary, end-over-end type mixer for 30 minutes.

The contents were then decanted into a 50mL measuring cylinder and EC of the 1:1 mixture measured using a Hanna 8633 handheld conductivity meter, the probe of which was moved up and down in the cylinder during measurement to agitate the mixture. (The meter was calibrated using one KCl standard at 1412 µS according to the Technician's advice. The temperature setting of the meter was also set to the temperature of the standard during calibration, and subsequently adjusted to sample temperature where this differed from the standard).

Following the above measurement, the 1:1 mixture was returned to the centrifuge tube and centrifuged at 8000 rpm for 7 minutes. Small amounts of mixture were decanted from some tubes before centrifuging, in order to balance the tube weights. Occasionally tubes were further centrifuged at 10,000 rpm where separation of supernatant was incomplete.

The supernatant was then decanted into a 50mL measuring cylinder and diluted 1:2, or occasionally 1:3, with deionised water. EC was measured as for the mixtures. EC of the deionised water was also measured and incorporated into dilution calculations. (EC of extracts was found to decrease in proportion to dilution; EC of mixtures and extracts was also observed to be stable during measurement).

The above described method for EC of soil pastes and extracts was adapted from Blakemore et al. (1987).

Moisture content of soil samples

Cores collected in polycarbonate tubes at Burnside were trimmed and capped with close-fitting polythene caps at the time of collection. In the lab the contents were decanted into pre-weighed aluminium dishes, weighed, dried for 48 hours at 105°C, then reweighed after briefly cooling in a desiccator.

Cores collected in steel tubes at No.1 Dairy were initially left with excess soil protruding past the tube ends, covered with plastic film and placed in ziplock plastic bags in the field. In the lab the cores were trimmed flush with the tubes and weighed in the tubes. The individual weights of the tubes were known from reference data. The cores were dried for 72 hours at 105°C (some cores were weighed after 48 hours before returning to the oven to confirm that no further weight loss occurred) then weighed in the steel tubes after briefly cooling in a desiccator.

Moisture retention characteristics of soil samples

Intact soil cores collected in steel tubes from No.1 Dairy were placed in water overnight to achieve saturation, then on filter papers on porous plates, part of a standard arrangement of laboratory equipment for soil moisture adjustment at

Landcare Research, Palmerston North. Suction was applied to the plates using a water siphon. The plates had a calibrated suction potential of -10 kPa, an approximation of field capacity conditions in soil. When equilibrium was reached with the soil, the cores were removed from the plates and weighed on the filter papers. (A sample paper was used to tare the balance).

A similar adjustment was then made to -100 kPa, and finally to -1500 kPa (an approximation of permanent wilting point – PWP). For the -1500 kPa adjustment, instead of the suction arrangement the plates and cores were placed inside steel pressure chambers into which compressed air was piped at the required pressure.

Soil dry bulk density

Dry bulk density was calculated from the weights of the cores dried at 105°C as described above (*Moisture content of soil samples*), and the known volumes of the core tubes, as follows:

(Dry core (g) – tube weight (g)) / core volume (cm^3) = dry bulk density (g/cm^3)

For cores decanted from polycarbonate tubes, dish weight was substituted for tube weight in the above calculation.

Soil particle density

The volumes of a set of 50mL specific gravity bottles were determined by weighing then filling them with deionised water and re-weighing, following which the temperature of the water contents was measured. The volumes were calculated according to the density of water at the measured temperature.

For each sample, 10-15g of the oven dry soil was added to a specific gravity bottle and the weight recorded. Deionised water was added to cover the soil by about 10mm, and the soil and water mixed by revolving the bottle rapidly by hand. Bubbles were removed by placing the bottle containing water and sample, with stopper removed, in a vacuum desiccator for at least 1 hour. The bottle with sample was then topped up with deionised water, the stopper inserted, and the weight recorded. After weighing, the temperature of the contents was measured.

Particle density was calculated as follows:

Volume of water in bottle with soil =

(weight of filled bottle with soil – weight of bottle with dry soil) / density of water

Volume of dry soil in bottle = volume of bottle – volume of water

Mass of dry soil = weight of bottle with dry soil – weight of bottle

Particle density = mass of dry soil / volume of dry soil

Method adapted from Gradwell (1971).

Soil porosity

Total porosity of soil samples was calculated from the particle density, the mass of soil solids and the volume of intact soil cores as follows:

Volume of soil solids in core = weight of oven dry soil / particle density

Total porosity (%) = ((volume of core – volume of soil solids) / volume of core) * 100

Soil texture

Soil was analysed for fine particle size distribution using a Horiba Partica laser scattering particle size distribution analyser (PSDA) LA-950V2. (No samples contained significant quantities of particles or clasts >2mm).

For each sample approximately 50g of field-moist soil was placed in a 400mL beaker. Due to the number of samples and limitations of equipment and facilities, portions from each site/hole/depth replicate sample were combined to produce a composite sample for each site/depth, rather than separate analyses for every replicate hole at every depth.

On the advice of the Technician no treatment was considered necessary for the removal of iron or aluminium oxides. To remove organic matter from the samples prior to analysis, 10mL of 36% hydrogen peroxide was mixed with each sample and the samples left at ambient temperature in a fume cupboard. When some samples began to dry out a further 10mL hydrogen peroxide was mixed with all samples and the beakers were covered (not sealed). After two weeks, effervescence of the samples was observed to have ceased.

To remove residual hydrogen peroxide after completion of the digestion, the samples were mixed with deionised water and centrifuged for 8 minutes at 7000 rpm. Occasionally centrifugation was repeated where fine particles remained suspended. The clear supernatant was then discarded and samples re-suspended in water and centrifuged again, the supernatant again discarded. The samples were then resuspended in approximately 50mL deionised water in 100mL beakers. (Concentration was not required to be known for PSDA analysis which gives results as %).

To determine an appropriate refractive index or indices for the PSDA analyses a selection of samples from both locations was analysed by X-ray diffraction (XRD) to indicate mineralogy. Two samples were chosen for bulk analysis and a further 7 for analysis of clays. The samples were chosen to be representative of the two locations; the clay samples also were from those that were additional to the regular sampling programme or had sufficient extra material to use for extraction. Clays were extracted by dispersion of the soil in deionised water and pouring off of supernatant (containing the suspended clays) after settling for 8 hours. At the advice of the Technician, deflocculant was not used as flocculation was not apparent. The samples analysed are presented in Table 3.02.

Table 3.02. Soil samples analysed by XRD.

Location	Site(s)	Depth (cm)	Horizon type	Analysis type
Burnside	B1a	110	Bg	clays
Burnside	B2a	110	Bw	clays
Burnside	B3a, B3c	18-24	AB	bulk
Burnside	B3b	110	Bw	clays
No.1 Dairy	D4c	64	Bg	clays
No.1 Dairy	D5b, D5c	28	Bw	clays
No.1 Dairy	D5c	11-21	AB	bulk
No.1 Dairy	D6a	64	Bw	clays
No.1 Dairy	D6c	86	C	clays

The major minerals present in both the bulk and clay analyses were quartz, mica, feldspar and chlorite, i.e. primary minerals rather than pedogenic secondary clay minerals, in keeping with the young ages of the soils. The mineralogy of all samples was broadly similar. A refractive index of 1.54, determined previously for analysis of Manawatu flood sediments, was in keeping with the XRD results in this study and was adopted for all PSDA analyses.

To achieve an appropriate sediment concentration for the PSDA, a 10mL portion was taken by pipette from each sample while the sample was rapidly stirred using a magnetic stirrer. This was added to approximately 50mL of deionised water from which was taken a 1mL sample (also with rapid stirring) for introduction to the PSDA. Some samples were further diluted using the functions of the PSDA after introduction of the sample to the instrument, or in some cases two 1mL portions were used for a single analysis where the initial concentration was insufficient. The suspension volume in the instrument at the commencement of each analysis (after dilutions, additions etc.) was approximately 157mL. The analysis was repeated with a further 1mL sample from the same 10/60 suspension, and where noticeable variation was observed, a third 1mL sample was analysed. Reported results are the average of the 2 or 3 analyses of each site/depth sample.

In other respects the PSDA was operated according to standard methods for the instrument, with de-bubbling of the suspension water and alignment and zeroing of the lasers prior to each analysis, and repeated rinsing of the suspension container between analyses. The particle size limit for the PSDA was set at 2000µm. No particles were detected >1000µm, and only one analysis detected particles >500µm.

Proportions of sand (>62.5 µm), silt (<62.5µm) and clay (<0.98µm) were calculated for each sample depth at each site. In addition, soil texture 'fineness' was calculated according to the method of Waine (1999) applied to New Zealand soils by Hedley (2009):

$$\text{Fineness} = -0.91*T_w^2 + 3.8*T_w + 1.97 \qquad [10]$$

where texture weighting (T_w) = (% clay)*0.03 – (% sand)*0.004

The term 'fineness' has been adopted in this thesis instead of 'fineness class' as used by Waine (1999) because fineness as calculated above is a continuous measure unlike the discrete 'texture classes' from which it is derived. Those classes as defined by Milne et al. (1995) for New Zealand soils are shown in Figure 3.12.

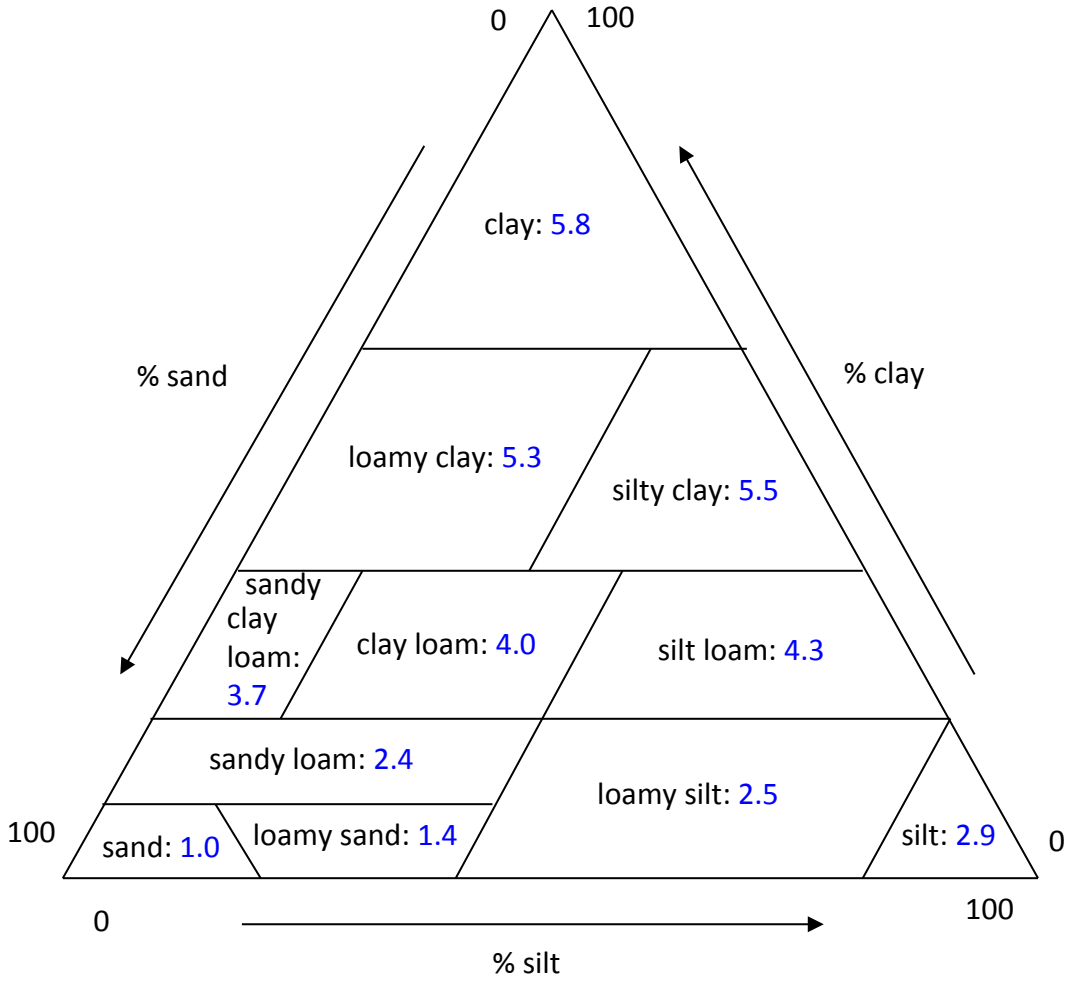

Figure 3.12. The New Zealand soil texture triangle (Milne et al., 1995). Texture fineness calculated for approximately the middle of each class is shown in blue.

3.5.5 Accessory field measurements

Temperature and general observations

Weather, ambient temperature at 1.5m above ground and at ground level, and soil temperature to 15cm depth were recorded at the EMI calibration site at the beginning and end of kinematic surveys. Accompanying soil sampling and spot EMI

measurements at soil sample sites, a single measurement of soil temperature to 15cm depth at the sites was recorded immediately prior to EMI measurement.

Soil moisture

Accompanying soil sampling and spot EMI measurements at soil sample sites, TDR measurements of soil moisture were made to 45cm depth.

Accompanying kinematic EM surveys, TDR measurements of soil moisture to 45cm depth were made at 30-50 points across the location. Use of pre-positioned TDR sites via GPS was found to be time consuming; to maximise the number of measurements, sites were instead selected spontaneously across the spatial extent of the location and the positions logged with GPS (Trimble Juno handheld) at the time of measurement. Some TDR measurements were later excluded from statistical analyses because they were outside the extent of EM31 survey data after the latter was trimmed to exclude measurements <12m from fencelines (see section 3.6.3 Functional tests – ATV interference, section *4.1 EMI instrument functional tests* and *Appendix 6 – EMI instrument functional tests*).

For the first kinematic survey at Burnside, before TDR was adopted for field soil moisture measurement, intact cores were collected from 7 sites across the extent of the location on the survey day and the following day (over which time conditions were mild with no rain) and the moisture content of these cores determined gravimetrically (see section *3.5.4 - Laboratory analyses – Field moisture content of soil samples*). On this occasion cores were collected from 4, 28 and 64cm depths at each site. Results from one of these sites were later discarded because the site was outside the extent of EM31 data as described above.

3.6 EMI

Two EMI instruments were used: a Geonics Ltd. EM38 Mk2 and a Geonics Ltd. EM31 Mk2 ('EM31'). Both instruments can be used in vertical or horizontal modes (the latter mode with the instrument on its side). The EM38 Mk2 makes simultaneous measurements from 1m and 0.5m coil spacings, corresponding to 1.5m and 0.75 'effective depth ranges' in vertical mode (Geonics, 2008). The effective depth range

of the EM31 (vertical mode) is given as 6m (Geonics, 1995). Specifications and performance of the instruments are discussed in more detail in section *2.1.3 - Geonics EM38 Mk2 and EM31*.

3.6.1 EM38 Mk2

Setup and calibration

The EM38 Mk2 was calibrated according the method of Geonics (2008). For a description of the method as used in this study see: *Appendix 2 – EM38 Mk2 calibration method*. The instrument was powered by an alkaline 9V battery, either Energizer brand or Dick Smith Electronics (DSE). It was placed on top of a 1.5m length of 65mm diameter PVC pipe to provide the elevated position for calibration. The 'sensitivity check' described in Geonics (2008) was also performed occasionally.

In kinematic surveys, the Allegro field computer used to log EMI data was attached after calibration when the instrument was put in survey position in the sled (described below in *Kinematic surveys*). The instrument was also switched off after calibration prior to installation in the sled. The above practices were later identified as probable sources of error in the EM38 Mk2 (0.5m) data (see *Appendix 6 - EMI instrument functional tests – Cable and connection effects*). Final zeroing of the 'inphase' reading was done with the instrument in the sled attached to the all-terrain vehicle (ATV).

Kinematic surveys

The EM38 Mk2 was towed on a sled behind a four wheel drive ATV. The instrument was secured by soft plastic foam mouldings inside a PVC cylinder (260mm diameter 'culvert pipe') strapped to a rubber mat which together formed the sled (Figure 3.13). An opening in the top of the cylinder enabled access to the instrument. Wooden brackets fixed to the underside of the cylinder stabilised it against rubber fixtures on the upper side of the mat. A rope was attached to the sled via a crosswise piece of PVC pipe fixed to the front of the mat. The other end of this rope was attached to the tow bar of the ATV and used to tow the sled.

Data was collected continuously during survey by means of a Juniper Systems Allegro CX field computer (the 'Allegro') on the ATV. Real-time kinematic (RTK) GPS locations were obtained from a Trimble AgGPS 332 receiver on the ATV linked to a Trimble Base 900 base station at a fixed point at the survey location. The Allegro recorded continuous EC_a data linked to GPS location from the EM38 Mk2 and mobile GPS via serial cable connections to each.

The rate of data collection was 5 Hz. Locations were surveyed in 6m swaths using a Trimble Ag170 guidance system. Kinematic surveys were done with EM38 Mk2 and EM31 consecutively on the same day, except for the initial reconnaissance survey of each location in which only the EM38 Mk2 was used. Batteries were not changed during the course of kinematic surveys except for the reconnaissance survey of Burnside.

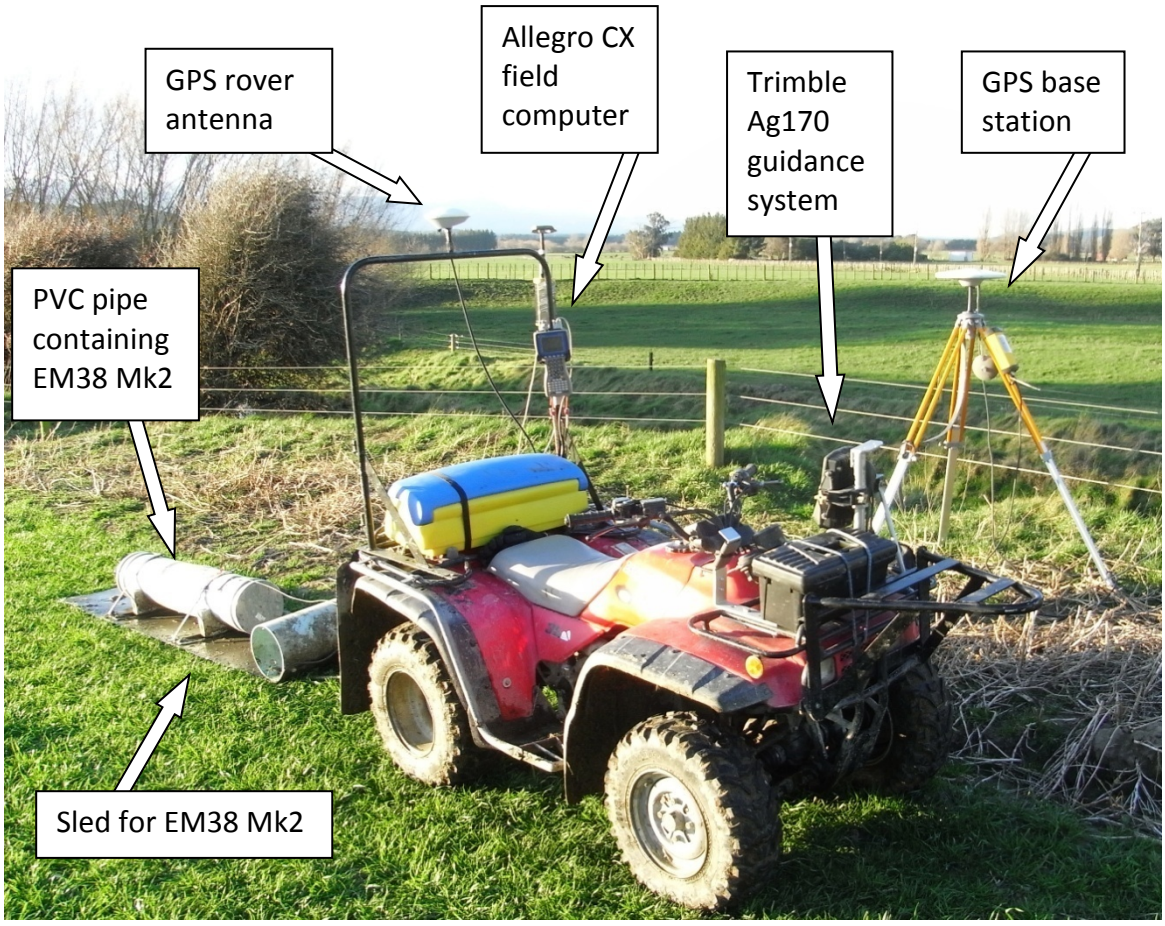

Figure 3.13. Kinematic surveying system for the EM38 Mk2.

Spot EMI measurements

Spot EMI measurements were made at soil sample sites at the time of sampling and on subsequent occasions when sites were located using a Trimble Juno handheld GPS. EM38 Mk2 readings were recorded by hand with the instrument in horizontal and vertical modes, and in raised positions above the ground. The instrument was calibrated once before all spot measurements made at one location on the same day, and usually switched off between sites.

When making horizontal mode measurements (all of which were at ground level) the IP reading deviated noticeably from the zero position set during calibration, as described by Geonics (2008). (IP also varied to a lesser extent between sites for both horizontal and vertical modes). No adjustment of IP was made after the original zeroing procedure. (It was found that zeroing the IP when it had deviated >30 mS/m produced no change in the EC_a reading and therefore the procedure was considered unnecessary.)

When making vertical mode 'ground level' spot measurements the instrument was placed on short lengths of 60mm (outside diameter) PVC pressure pipe to simulate the height above ground of the instrument in the sled during kinematic surveys. This was to enable direct comparison of spot EMI measurements with kinematic survey measurements.

Other readings in raised positions were made using a tripod constructed with no metal components as follows. The tripod legs were of 60mm PVC pressure pipe, 167cm long. Extensions (50cm) of the same material were attached to the ends of the legs using a split sleeve of PVC 'waste' pipe. The tripod head piece was made from nylon block and the legs attached by nylon inserts and bolts. The EM38 Mk2 was raised by means of a polyester strap attached to the instrument which extended upwards through a hole in the tripod head, from where it was pulled through and down and secured to one of the tripod legs, raising the instrument. The strap was centred on the EM38 Mk2 to ensure that it hung horizontally. The height of the instrument was measured against a marked bamboo pole inserted into the ground and initially checked in position with a measuring tape (Figure 3.14).

Readings were recorded by hand from the EM38 Mk2 in vertical mode raised to 44, 87 and 194cm above ground. These heights were chosen to correspond to theoretical reductions in EC_a measured by the 1m coil spacing to 75%, 50% and 25% respectively of the ground level reading in the case of an even EC_a profile.

Figure 3.14. The tripod with EM38 Mk2 in use at No.1 Dairy.

3.6.2 EM31

The EM31 was used only for kinematic surveys and functional tests, not for spot measurements at soil sample sites. The instrument was set up on site before attachment to the mobile rig according to the procedure and 'equipment functional checks' described in Geonics (1995). A description of this procedure as used in this study is given in *Appendix 3 – EM31 setup method*. The instrument was powered by 8 x Arlec nickel-cadmium rechargeable 'C' size batteries.

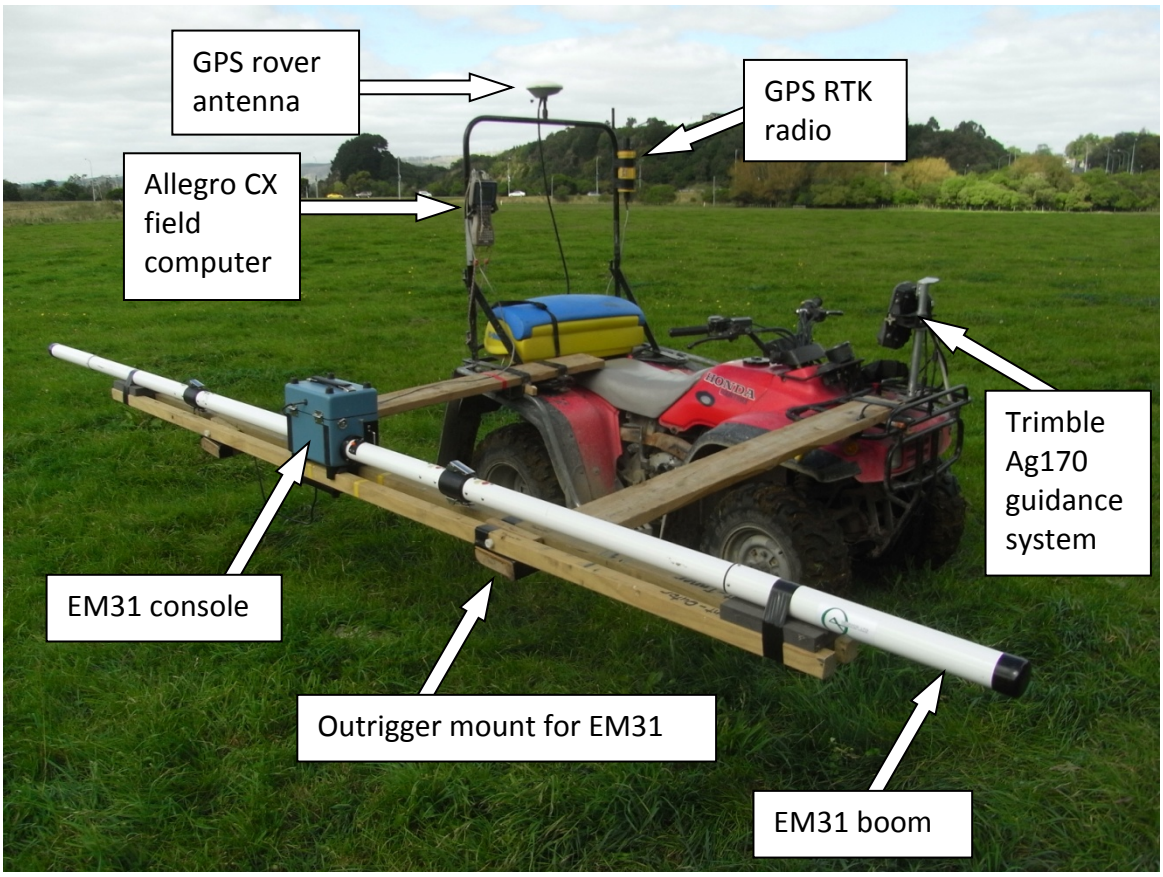

Figure 3.15. The kinematic surveying system used with the EM31.

The EM31 was mounted on the ATV by an outrigger arrangement (Figure 3.15). Two 150mm x 30mm wooden planks ('outriggers') were attached perpendicular to the front and rear of the ATV using metal brackets and bolts. Two 40mm x 40mm wooden rails, 3.5m long, were attached to the EM31 parallel to each other and to the EM31 booms by means of the boom holder bracket on the underside of the instrument console. These rails rested on the outriggers and were fixed to wooden attachments on the ends of the outriggers by nylon bolts. The EM31 booms were attached to the rails using closed-cell foam mouldings and PVC tape.

The EM31 was therefore suspended parallel to the ATV, approximately 80cm above the ground and 170cm from the centreline of the ATV. Data was collected as described above for the EM38 Mk2 using the Allegro linked to RTK GPS and to the EM31 by means of serial cables, also with 5 Hz data collection rate and 6m survey swaths guided by the Ag170.

3.6.3 Functional tests

In light of the intention in this study to extend the use of EC_a data to quantitative methods, where absolute and not just relative values or patterns are required, it was necessary to eliminate or correct any detected sources of error. The following tests were carried out to explore possible sources of error in EMI measurements or 'drift' between surveys or measurements, and to inform procedures for field use of EMI instruments.

Battery effects

EM38 Mk2:

The voltage of a new Energizer 9V battery was measured with a handheld voltmeter. The battery was then installed in the instrument and the instrument calibrated according to the standard procedure. The instrument was placed in vertical mode on the ground at the calibration site and shaded with a piece of plywood (Figure 3.16). In-phase and quad-phase (EC_a) readings from both coil spacings and battery level were recorded manually from the instrument panel over approximately 4 hours. Ambient and soil temperature were also recorded.

Immediately following the above test, with the instrument remaining in the test position, the battery was replaced with another Energizer 9V and further readings taken. The instrument was then recalibrated, replaced in the test position, and readings taken again. On a further occasion at the same site the instrument was calibrated and readings taken before and after substitution of various batteries with and without recalibration.

EM31:

Tests were done with the EM31 to investigate whether EC_a measurements were stable during declining battery voltage and whether the instrument functioned effectively using rechargeable batteries. The voltages of 8 x freshly recharged Arlec 1.25V 'C' size rechargeable batteries were measured with a handheld voltmeter. The batteries were installed in the battery carriage of the EM31 and the combined voltage measured from the carriage connection socket. The carriage was installed in the instrument and the standard functional tests completed. The instrument was

placed on the ground in vertical mode. No shading was provided; instead the test was done in cloudy conditions to avoid solar heating of the instrument. Occasional light rain showers occurred during the test. Ambient and soil temperatures were recorded at intervals throughout.

Figure 3.16. EM38 test for battery depletion effects.

In-phase and EC_a readings were taken at intervals using the Allegro attached by a serial cable to the EM31. After 3½ hours the instrument was switched off, the battery carriage removed and voltage measured from the carriage socket and from the individual batteries. Following these measurements the carriage was restored, the instrument switched on and the test continued for a further hour, then further measurements from the battery carriage and batteries were recorded.
Finally the Arlec batteries were replaced with new Energizer 1.5V 'C' size batteries, the voltages from the battery carriage and individual batteries recorded, the carriage installed in the EM31 and in-phase and EC_a readings taken.

Temperature effects

Tests for the effect of ambient temperature were done only with the EM38 Mk2.

The EM38 Mk2 was calibrated using the standard procedure inside a nylon tent of hexagonal shape measuring 2.25m from corner to corner and 2m high in the centre. The tent poles were fibreglass, however, some interference was noted from the metal ferrules of the poles. The EM38 Mk2 was calibrated in the centre of the tent (at 1.5m height) where interference could not be detected.

The EM38 Mk2 was placed on the ground towards one side of the tent, sufficiently far from pegs and poles that interference could not be detected. An electric fan heater was placed towards the opposite side of the tent. No interference was detected from the heater.

A thermometer was placed on the EM38 Mk2 to measure ambient temperature. Soil temperature (to 15cm depth) under the tent was measured close to the position of the EM38 Mk2 at the beginning and end of the experiment.

The EM38 Mk2 was left operating for 20 minutes to check for any drift unrelated to temperature. Temperature was then raised from 25 to 38˚C using the fan heater, with readings taken at intervals of ambient temperature, in-phase and quad-phase (1m and 0.5m coil spacings) and battery (from the EMI panel). The heater was then turned off and ambient temperature allowed to drop for 70 minutes. The final ambient temperature recorded was 24.5˚C.

The objective of the above procedure was to determine if ambient temperature had any effect on EC_a as was suggested by some results reported in the literature (see section *2.3.5 - EC_a and temperature in the field*). It is noted that the above procedure was contrary to the instructions of Geonics (2008) which are to equilibrate the EM38 Mk2 with ambient temperature prior to calibration and recalibrate if temperature should change markedly, but it was in this case used for experimental purposes.

ATV interference

EM31:

3 x 90m swaths were surveyed with the EM31 using the kinematic system after the standard instrument checks (see section *3.6.2- EM31* and *Appendix 3 – EM31 setup method).* The swaths were then immediately re-surveyed using the EM31 shoulder-carried, suspended at a similar height to that used in the kinematic system. For the carried survey, GPS location was provided by a Garmin Etrex handheld GPS attached to the shoulder of the surveyor who wore clothing and footwear without metal components. Data was logged using the Allegro connected to the Garmin and the EM31 by serial cables. This arrangement was to avoid carrying too much GPS hardware which might contribute its own interference to the EM31. The carried survey followed the path of the kinematic survey by following the ATV tyre tracks with an offset to approximate the position of the EM31 on the boom.

To obtain values from the kinematic survey at the exact points of the carried survey, data from the kinematic survey was interpolated (ordinary kriging) using ArcGIS and values were extracted from the resulting raster to the point features of the carried survey. This dataset was then analysed by linear regression and by plotting of simple offset calculations in Microsoft Excel.

EM38 Mk2:

The EM38 Mk2 was calibrated and installed in the sled according to the standard kinematic survey procedure (see section *3.6.1- EM38 Mk2* and *Appendix 2 – EM38 Mk2 calibration method).* The tow rope of the sled was then disconnected from the ATV which was driven forward to a distance of 7m from the sled. Readings of in-phase and quad-phase were recorded by hand from the EM38 Mk2 for 1m and 0.5m coil spacings (vertical mode in the sled). The ATV was then progressively backed towards the sled with readings taken at intervals from the EM38 Mk2 until contact was made with the sled.

Fence interference

Following regular functional checks the EM31 was mounted on the ATV in the usual system for kinematic surveys (see section *3.6.2 - EM31* and *Appendix 3 – EM31 setup method).* No tests for fence interference were done using the EM38 Mk2.

A short survey was conducted in swaths parallel to a 4-wire fence which ran along the boundary of a paddock. The top and middle wires of the fence were electrified with pulses of current at approximately 1 Hz frequency. Swaths were driven increasingly close to the fence, beginning at 40m distant and continuing until the EM31 was within 0.5m of the fence.

Distances from the fence were assigned to the survey data points in ArcGIS using the 'Near' function. The logged EC_a values and the instrument sensitivity depth profiles (horizontal and vertical modes) were plotted against distance from the fence using Microsoft Excel.

GPS location error

The position of EMI instruments at the time of logging was calculated relative to the position of the GPS antenna at that time using applications of trigonometry according to Figure 3.17. To do this for each logged data point a direction of travel was assigned, either NE, SE, SW or NW (N, S, E and W were included within those four categories). Because the angle of tow in the flexible EM38 Mk2 sled system exhibited lag when the ATV changed direction i.e. the sled was not always directly behind the ATV, a point 2 seconds earlier than the point being adjusted was used to calculate direction of travel. The rigid EM31 outrigger system required no such lag adjustment.

Distance behind the ATV was calculated as the tow length plus the distance travelled during electronic system delay. This also necessitated calculation of travel speed, in turn requiring calculation of travel distance and time elapsed between points. EC_a data was logged using the EM38 Mk2 in a transect towed in both directions at various speeds across and perpendicular to a known buried pipeline which produced distinctive EC_a values as described below. Various values of tow distance and system delay were explored in calculations to see which most tightly aggregated the

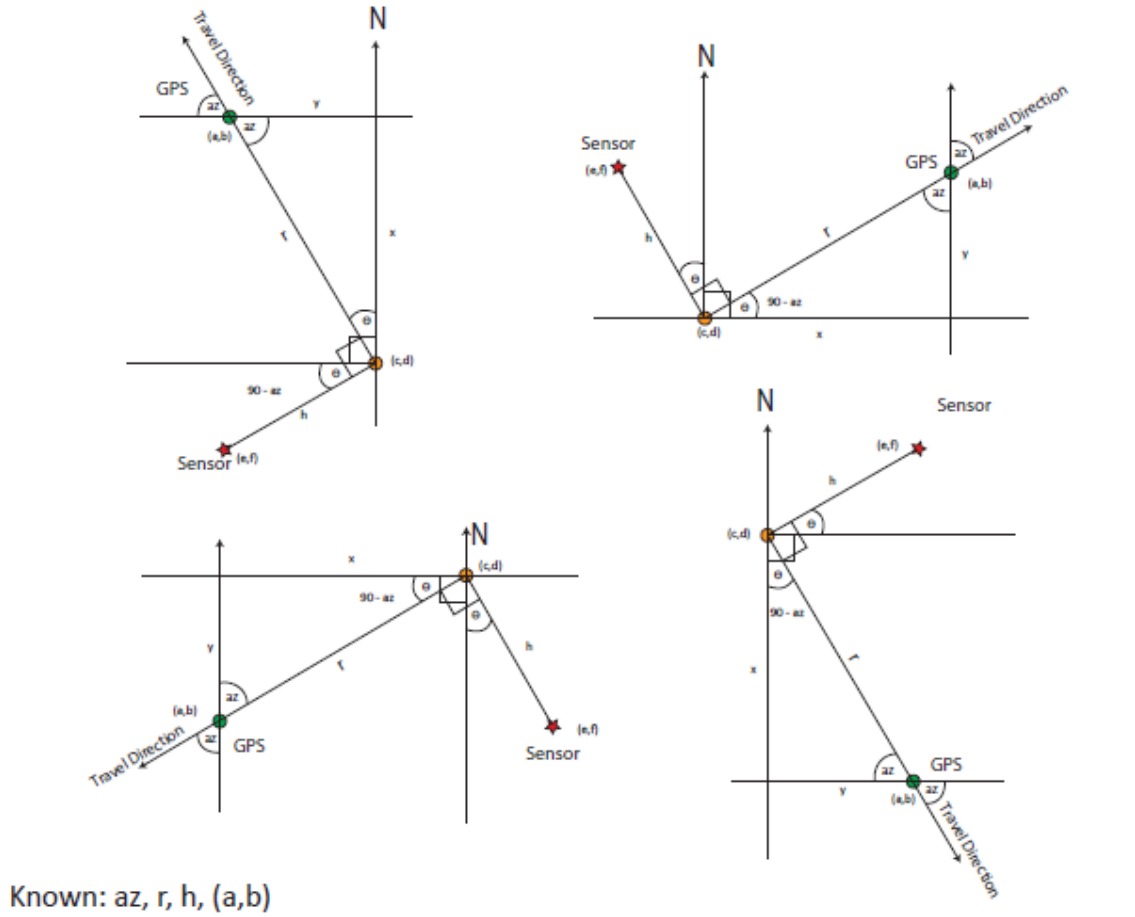

Figure 3.17. Trigonometric relations between GPS antenna and sensor in a kinematic system. (NZCPA, 2011).

pipeline-influenced points when the data was projected in ArcMap (tow distance was known but not to what extent it was related in logged data to the middle of the EMI instrument or to coil positions at either end).

Statistical methods were not used to relate GPS offset to travel speed as the EC_a signature of the buried pipe was quite broad (~15m) and complex, comprising a central zone of low EC_a between two adjacent zones of high EC_a as described by Geonics (1995), whereby simple GPS offsets for all affected points could not easily be measured. Best results were given by a tow distance of 2.13m and system delay of 0.2s as described in section *4.1 – EMI instrument functional tests*. Distance of EC_a data points behind associated GPS locations was therefore 2.13m + 0.2 * travel speed (m/s). The determination that system delay was a positive value suggests that sensor data was obtained fractionally before GPS location in relation to each point logged by the field computer.

No separate test was performed for the EM31. Tow distance was calculated from the position of the instrument console forward from the GPS antenna (-0.9m) and system delay which was taken to be the published 'time constant' of the instrument i.e. 1 second (Geonics, 1995). Distance to the side of the antenna was the fixed distance to the rails supporting the EM31 console: 1.7m.

The various calculations required to calculate sensor position were accomplished by user-defined functions in Microsoft Excel written with Visual Basic for Applications (VBA). Using Excel for the calculations enabled the use of 'live' formulas into which alternative values could be introduced, rather than one-off calculation of fields in ArcGIS. Layers in ArcGIS also required re-projection from base data after alterations to coordinates or calculation of alternative coordinate fields. The VBA functions and general procedure of GPS location adjustment used are given in *Appendix 4 - Data cleaning and GPS position adjustment* and *Appendix 5 – Functions for calculation of sensor location*.

3.7 Data analysis and mapping

3.7.1 Statistics

Soil Texture

Differences in texture properties between locations, sites, depths and horizon types were determined by analysis of variance (ANOVA) in Microsoft Excel. Because the samples from the three holes at each site were combined for each depth for texture analysis, the site x depth ANOVAs were without replication.

EC of 1:1 soil pastes and extracts

Differences in EC of soil pastes and extracts between locations, sites, depths and horizon types were determined by ANOVA analysis in Excel, either single factor or two-factor with replication, e.g. site vs depth, for which the three holes sampled at each site provided the replicates.

Soil moisture

Tests for the effects of site and sampling date on soil moisture at soil sample sites were by two-factor ANOVA analysis (site and date) without replication in Excel for each location. All measurements used in these analyses were by TDR to 45cm. The first soil moisture measurement date for each location was at initial sampling of the soil sample sites; this was regarded as one date even though the sites were sampled on separate days within a two week period at each location. For these occasions moisture data is a mean of the three replicates at each site. Soil moisture measurements on all other dates were by a single measurement at each site.

Correlations of soil moisture with soil texture parameters at soil sample sites were by linear regression in Excel using data from the soil replicate sampling. As described in section *3.5.4 – Laboratory analyses – Soil texture*, samples from the three replicates at each site were bulked by depth for texture analysis. To obtain corresponding moisture data for regressions, results of gravimetric analyses from the three replicates at each site were averaged by depth.

Tests for the effects of location and survey date on soil moisture during kinematic surveys were by single-factor ANOVA in Excel. For the effect of survey date, separate analyses were done for each location using the two survey dates at each; for the location effect, data from both survey dates was combined for each location.

Comparisons of EC_a data between instruments, modes, surveys and locations

Comparisons were made between means of all EC_a data for different instruments or modes on the same date at the same location (i.e. the same survey), between means of all data for different surveys (i.e. for the same instrument and mode on different dates at the same location), and between means of all data (from all surveys) for the same instrument and mode at each location. Differences between means were determined using the paired *t*-test function of Excel. Extraction of kinematic data for this procedure is described in section *3.7.2 - Mapping and spatial analysis - Extraction of EC_a data for comparisons.*

3.7.2 Mapping and spatial analysis

Cleaning of survey data

Cleaning of survey data was necessary to correct for interference from the ATV and to remove data within interference range of fences, and other isolated data showing interference, possibly from buried metal objects etc. The data was first corrected for location offsets arising from the movement and geometry of the kinematic system, as precise location was necessary for determining fence distances and for improved qualitative interpretation of interference in the EC_a data.

The sequence of steps followed in cleaning and projecting data from kinematic surveys is given in *Appendix 4 - Data cleaning and GPS position adjustment*. A summary of the method applied to the GIS-displayed data is as follows:

1. Adjustment of GPS locations according to antenna offset and system delay
2. Correction of data for ATV interference
3. Visual inspection for anomalous values, artefact or interference signatures, linear features etc. and deletion of points where necessary

4. Selection of extreme values (± 3 std. dev. or by qualitative assessment – see below in this section), visual inspection of the distribution, whether appearing random and in keeping with broader trends, or whether anomalous and suggestive of interference; deletion of points where necessary (outliers were saved for reference)
5. Removal of values within fence interference range.

For EM38 Mk2 data many of the above steps must be applied separately to measurements from both the 1m and 0.5m coil separations. The surveys in this study were each done on a single day, and with the exception of the reconnaissance survey of Burnside, without changing the EM instrument battery. Further adjustments to align survey results might otherwise have been necessary.

EM38 Mk2 data was adjusted to remove the effect of interference caused by proximity to the ATV: 1 mS/m was subtracted from EC_a data from the 0.5m coil separation, and 2 mS/m from the data from the 1m coil spacing, according to the results of interference tests (see section *3.6.3 – Functional tests - ATV Interference).* For the same reason, 7.12 mS/m was subtracted from the EM31 data, which was subsequently divided by 1.12 to correct for the factory adjustment of the instrument to read ground-level EC_a with the instrument raised to a height of 1m.

Initial procedure for removal of extreme values from EC_a datasets (considered probably due to undetected interference such as buried metal objects) was by removing values >± 3 standard deviations (s.d). from the mean. However, visual inspection of distributions of EC_a values did not support this procedure in all cases.

An example is given in Figure 3.18 in which a resemblance of a normal distribution was accompanied by a spike in values at the lower end. When displayed these anomalous values were not aggregated or distributed in any way which suggested a legitimate cause, e.g. they were not contiguous with other similar values. A cut-off point of -2 s.d. would leave approximately half the anomalous values in the dataset; -3 s.d. would leave them all in. A cut-off point could be selected specific to the dataset, for example 2.5 s.d. in this case, however, this would not represent a standardization of procedure if it could not be generally applied to all datasets.

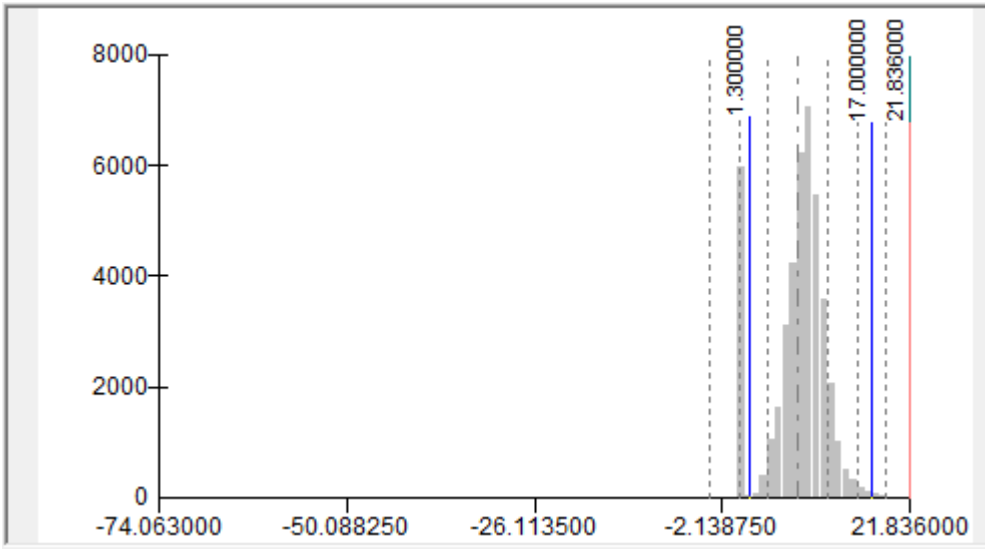

Figure 3.18. Distribution of EC_a from a field survey at Burnside. Mean and standard deviations shown by dashed and dotted lines respectively.

An assumption was therefore made that EC_a from a single survey of one location should show resemblance to a normal distribution or distributions. Values that departed markedly from that pattern at either high or low extremes were selectively displayed, and where no explanation appeared for their retention, they were removed from the dataset. For the data in Figure 3.18 limits of 1.3 and 17 mS/m were chosen.

Interpolation and mapping

Cleaned EC_a data was interpolated to continuous layers ('surfaces') across locations using the 'ordinary kriging' utility of the Geostatistical Analyst group of tools in ArcGIS. Spherical models were used in kriging. Interpolation of elevation data was by the 'topo to raster' utility of ArcGIS.

The interpolated data was displayed in colour bands according to the magnitude of the values. For maps of elevation and for quantitative comparisons of EC_a from different survey dates, colour bands were defined by specified, equal intervals in the data. For relative patterns of EC_a, colour bands were defined in ArcGIS by the Jenks Natural Breaks function which determines intervals between a specified number of bands so as to minimize statistical variance within the bands.

Flow accumulation

Flow accumulation was mapped as a raster surface using the 'flow accumulation' function of the Spatial Analyst group of tools in ArcGIS. This function calculates potential flow accumulation in each cell of a mapped surface using flow direction, the latter mapped from topography data by another function the Spatial Analyst tool group. Values of flow accumulation for point locations, to use for correlations with other data, were extracted from the mapped surfaces in the same manner as described below for kriged EC_a data.

Extraction of EC_a data for comparisons

EC_a from kinematic surveys was compared at each location using kriged values of the EM38 Mk2, 1m and 0.5m and EM31 data for all surveys at that location. These values were extracted from the kriged rasters to the point locations of one dataset e.g. for No.1 Dairy, the EM38 Mk2 data of 8 November provided the points to which were extracted kriged values of EM38 Mk2, 1m and 0.5m and EM31 data from all surveys (including 8 November) at that location using the 'extract multi values to points' feature of ArcGIS. This enabled measurements from each instrument, coil spacing and survey date to be compared at common point locations. Some bias, however, was involved because the kriged values derived from the point data which was also used to determine the points had a more direct relationship to those points than other data.

3.7.3 EC_a depth profile resolution

EMI measurement ratios

The basic principle of the methods developed for EC_a depth profile resolution is that different EMI instruments, measurement modes and or measurement heights are affected differently by uneven distribution of EC_a with depth (EC_a depth profile). The difference between, for example, EM31 and EM38 Mk2 measurements at the same site is dependent on the EC_a depth profile at the site. Only where the EC_a profile is completely even with depth are the two instruments expected to give the same

measurement of EC_a, as should also the vertical and horizontal modes of the EM38 Mk2 in the same situation (Geonics, 1995; 2008; 2012).

For the method used in this study, EC_a depth profile was simulated in simplified form as the EC_a means of two depth ranges: 0-45cm and 45-900cm. In this form the EC_a depth profile is expressed as a single number produced by the ratio of $EC_{a\ 0\text{-}45cm}$ **:** $EC_{a\ 0\text{-}900cm}$. It is recognized that this representation is very much a simplification of the actual EC_a depth profile in most field situations. However, 'raw' EC_a measurements produced by EMI instruments are also subject to unpredictable irregularities as discussed in section

2.1.3 - Geonics EM38 Mk2 and EM31, so any improvement in estimation of EC_a of the upper profile is useful in analysing the relationship of EC_a to soil moisture in that zone.

The difference between EC_a measurements by different instruments or modes at the same site and time can also be represented as the ratio of one measurement to the other, in this case, EM31 (vertical) **:** EM38 Mk2 (1m, vertical). These measurements can be calculated for a known or simulated EC_a depth profile using the known sensitivity profiles of the instruments. The number produced by the EMI measurement ratio therefore expresses the measurement difference as a single number, just as the $EC_{a\ 0\text{-}45cm}$: $EC_{a\ 900cm}$ ratio produces a single number representing the EC_a depth profile.

Numbers produced by the above two ratios according to a range of simulated EC_a depth profiles were correlated by linear regression to produce a linear relationship quantifying the dependence of the EMI measurement ratio on the EC_a depth profile ratio. The relationship of these two ratios is termed the 'depth resolution index' (DRI). The DRI produced in the above manner for the EM31 (vertical) and EM38 Mk2 (1m, vertical) is shown in Figure 3.19. It is assumed in this example of the index that EC_a is evenly distributed with depth within each layer of the profile, while the EC_a of each layer may differ with respect to the other. This is a similar model to the 'two-layered profile' considered in the depth resolution methods of Geonics (1995).

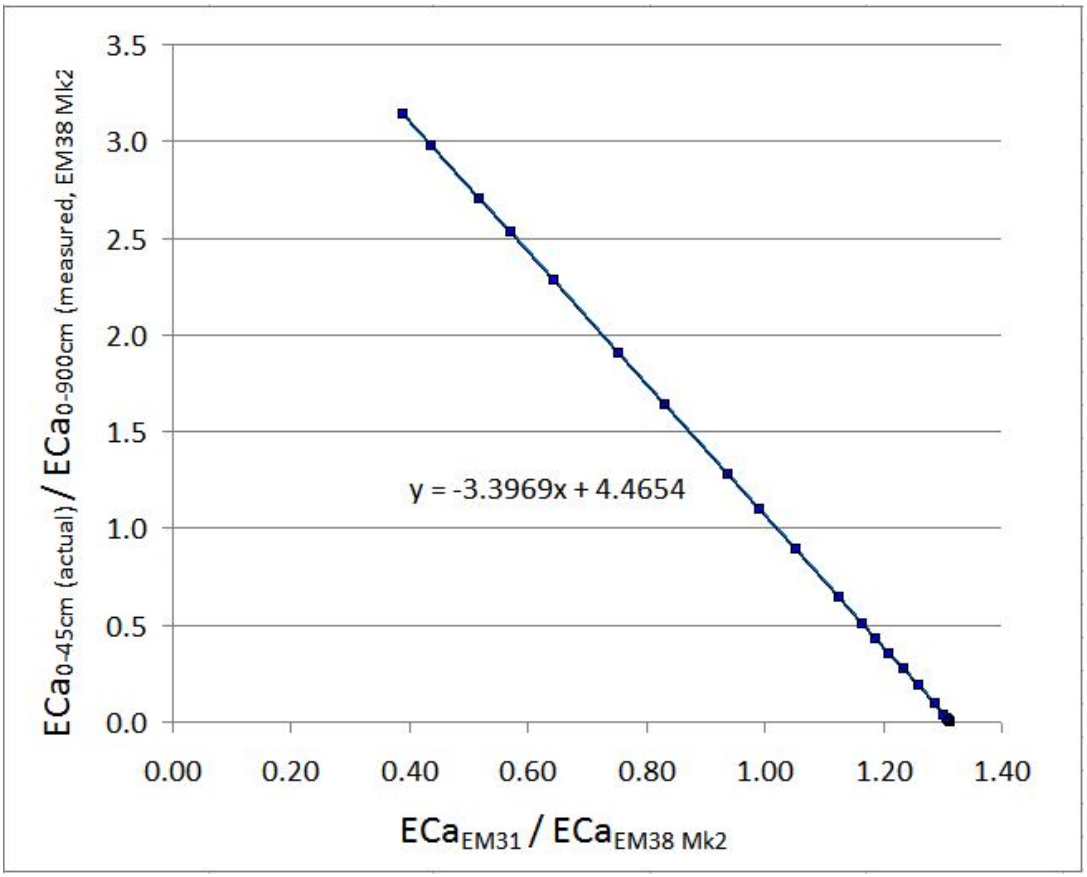

Figure 3.19. Relationship of two EC_a ratios: the 'depth resolution index' (DRI). The DRI in this example assumes even distribution of EC_a within each of the 0-45cm and 45-900cm layers; EM31 is in vertical mode, EM38 Mk2 in vertical mode, 1m coil spacing.

Note that the ratio which provides the *y* variable of the DRI in Figure 3.19 relates EC_a (0-45cm) not to actual (simulated) EC_a (0-900cm), but to the simulated measurement of EC_a (0-900cm) by the EM38 Mk2 (1m, vertical). Also, the DRI is expressed with the EC_a depth profile ratio as the dependent variable, but the physical reality of the relationship is that the EMI measurements and measurement ratios are dependent on the EC_a depth profile.

The correlation expressed by the DRI is linear because both variables contain the same simulated EM38 Mk2 measurement as the divisor, and simulated measurements by the EM31 and EM38 Mk2 are both calculated from the same simulated EC_a profiles which also produce the EC_a depth profile ratio. The DRI is purely theoretical, based on the published specifications of the instruments, and contains no uncertainty, therefore the R^2 value for the above correlation and all such

indices is 1. This does not imply a perfect relationship to any actual EC_a profile in the field; as discussed above, it is only an approximation of a range of EC_a profiles which might be encountered in the field.

The purpose therefore of the EC_a depth resolution method is to quantify the dependence of the EMI measurement ratio on the EC_a depth profile ratio. The coefficient (m) and the constant (c) of the DRI can be applied to ratios of field measurements at the same site and time, so approximating the actual distribution of EC_a between two depth ranges at the site. For the example shown in Figure 3.19, in a survey using EM38 Mk2 and EM31, the actual EC_a of the top 45cm profile is the only component of the model which is not measured, so it can be computed as a proportion of the EC_a (EM38 Mk2) measurement as follows:

$$y = -3.397*x + 4.465 \qquad [11]$$

where: $y = EC_{a\ 0\text{-}45cm\ actual} / EC_{a\ measured\ (EM38\ Mk2)}$

$x = EC_{a\ measured\ (EM31)} / EC_{a\ measured\ (EM38\ Mk2)}$

therefore: $EC_{a\ 0\text{-}45cm\ actual} = EC_{a\ measured\ (EM38\ Mk2)} * y \qquad [12]$

It has subsequently been demonstrated that the above equation can also be presented in the following form:

$$EC_{a\ 0\text{-}45cm\ actual} = -3.397*EC_{a\ measured\ (EM31)} + 4.465*EC_{a\ measured\ (EM38\ Mk2)} \qquad [13]$$

Equation [13] is more elegant and reveals a strong similarity to the methods of Cook and Walker (1992) and Corwin and Rhoades (1982) who combined various EMI measurements of EC_a in linear equations with coefficients to focus the combined measurement profile on a depth range of interest. However, the DRI and associated workings have elsewhere been retained in the forms in which they were used in this study.

As described above, the DRI in Figure 3.19 assumes even EC_a distribution within each profile layer while the mean EC_a of each layer differs with respect to the other. Such a profile is referred to in this study as an 'even-layered profile', and the resulting EC_a depth profile approximation and associated DRI, the 'even-layered model'.

It is thought that the even-layered model is not a close representation of most field EC_a depth profiles; therefore it is not designed to provide accurate estimates of upper profile EC_a, but rather to see if any improvement can be made over raw EMI measurements. To test the assumptions of the even-layered model, other DRI's were calculated assuming various patterns of uneven EC_a distribution within each profile layer, and these were compared with the even-layered model. A more detailed description of method development for EC_a depth profile resolution of both spot measurements of EC_a and kinematic survey data is given in *Appendix 7 – EC_a profiles: method development.*

DRI's produced by two EC_a depth profile approximations were applied to field data: the even-layered model, as described above, and the 'field simulation model' incorporating patterns of unevenness within profile layers anticipated at the field locations from results of soil analyses and observations. In similar fashion to the even-layered model, the field simulation model assumes a constant relative pattern of unevenness within each profile layer while the mean EC_a of each profile layer differs with respect to the other.

Figures 3.20, 3.21 and 3.22 show the modelled responses of the EM31 (vertical) and EM38 Mk2 (1m, vertical) to EC_a depth profiles simulated according to the even-layered and field simulation models. In order to better show the patterns of variation in the simulations, EC_a is plotted on a log scale, and depth is limited to 5m, although the complete simulations are to 9m depth.

Parameters of the above simulations are further summarized in Table 3.03. The simulations assume zero EC_a below 9m depth in every EC_a profile, and the sensitivity of the instruments is assumed to be zero below 1.5x the effective depth range of the instrument and mode: 2.25m for the EM38 Mk2 (vertical) and 9m for the EM31 (vertical). Further details of the simulation of measurements and other aspects of the method are given in *Appendix 7 – EC_a profiles: method development.*

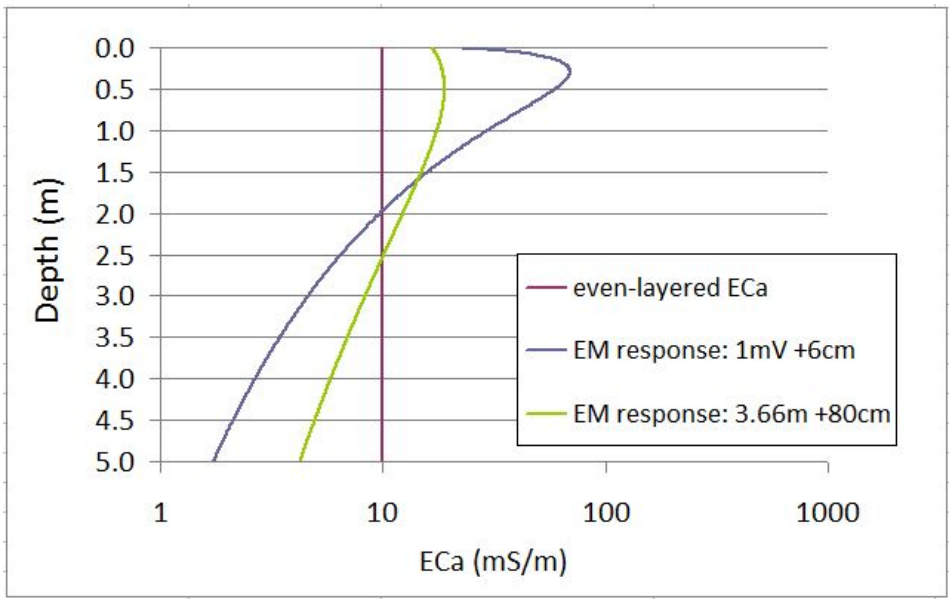

Figure 3.20. Modelled responses of the EM31 and EM38 Mk2 to a simulated even-layered EC_a depth profile with a 1:1 distribution of EC_a between the 0-45cm and 45-900cm profile layers. The response of the EM31 (3.66m coil spacing) is for vertical mode with the instrument raised 80cm above ground; the EM38 Mk2 is 1m coil spacing, vertical mode with the instrument raised 6cm above ground.

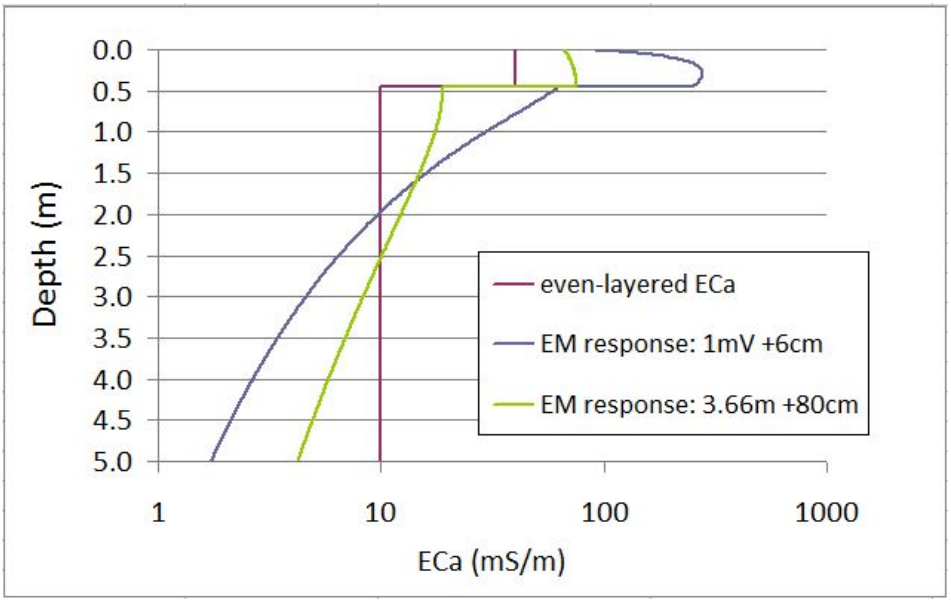

Figure 3.21. Modelled responses of the EM31 and EM38 Mk2 to a simulated even-layered EC_a depth profile with a 4:1 distribution of EC_a between the 0-45cm and 45-900cm profile layers, i.e. EC_a of the 0-45cm layer is 40 mS/m, and of the 45-900cm layer, 10 mS/m. The response of the EM31 (3.66m coil spacing) is for vertical mode with the instrument raised 80cm above ground; the EM38 Mk2 is 1m coil spacing, vertical mode with the instrument raised 6cm above ground.

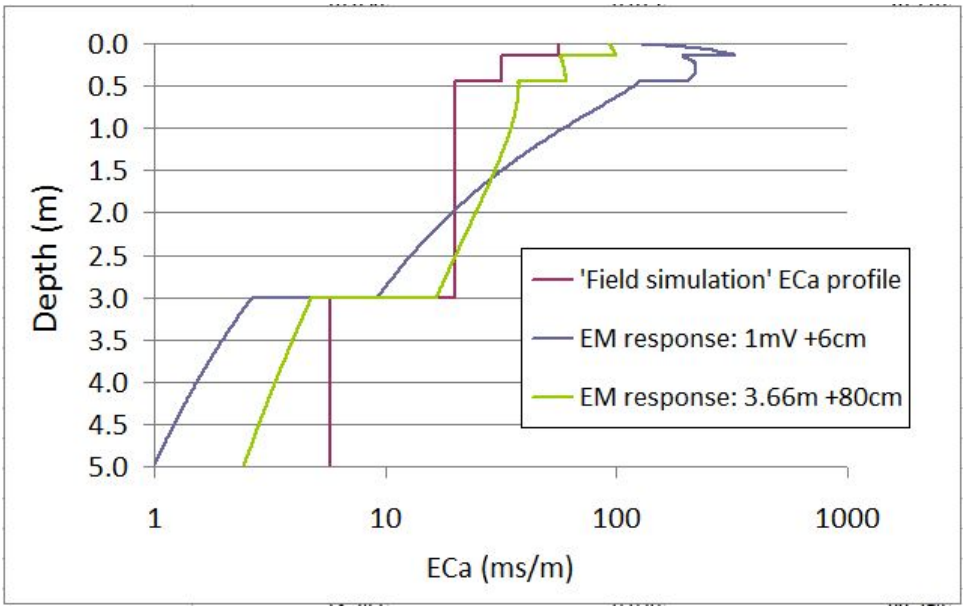

Figure 3.22. Modelled responses of the EM31 and EM38 Mk2 to a 'field simulation' EC_a depth profile with a 4:1 distribution of EC_a between the 0-45cm and 45-900cm profile layers, i.e. mean EC_a of the 0-45cm layer is 40 mS/m, and of the 45-900cm layer, 10 mS/m. The response of the EM31 (3.66m coil spacing) is for vertical mode with the instrument raised 80cm above ground; the EM38 Mk2 is 1m coil spacing, vertical mode with the instrument raised 6cm above ground.

Therefore according to Table 3.03, the simulations in Figures 3.20 and 3.21 each represent one point on the DRI of the even-layered model shown in Figure 3.19 (the points with *x*,*y* coordinates 1.28,0.94 for Figure 3.20, and 2.41,0.605 for Figure 3.21). Figure 3.22 represents one point on the DRI of the field simulation model shown in Figure A7.07 (*Appendix 7*).

According to the method then, if the pattern of variation within each layer of an EC_a profile is known (or approximated), the EC_a of the upper layer can be estimated from whole profile EC_a measurements by different instruments, modes or measurement heights, and the precision of that estimation is limited by the assumptions, approximations and uncertainty of the method, described above and in *Appendix 7 – EC_a profiles: method development*.

Table 3.03. Parameters of modelled EC_a profiles and associated simulated measurements by the EM31 and EM38 Mk2.

Figure	Figure 3.20	Figure 3.21	Figure 3.22
Profile model	Even-layered	Even-layered	Field simulation
DRI coefficient, m	-3.397	-3.397	-5.776
DRI constant, c	4.465	4.465	5.484
EC_a (0-45cm) : EC_a (45-900cm)	1 : 1	4 : 1	4 : 1
Simulated EC_a 0-45cm (mS/m)	10	40	40
Simulated EC_a 45-900cm (mS/m)	10	10	10
Simulated mean EC_a 0-900cm (mS/m)	10	11.5	11.5
EM31 (vertical) simulated measurement (mS/m)	7.33	10.04	12.86
EM38 Mk2 (1m, vertical) simulated measurement (mS/m)	7.81	16.60	20.84
EM31 : EM38 Mk2[a]	0.940	0.605	0.617
EC_a (0-45cm) : $EC_{a\ measured,\ EM38\ Mk2}$[b]	1.280	2.410	1.182
Calculated $EC_{a\ 0\text{-}45cm}$ (mS/m)	10	40	40

a. This field is the *y* coordinate value of the associated depth resolution index.
b. This field is the *x* coordinate value of the associated depth resolution index.

For depth profile resolution of spot measurements of EC_a, the ratio of EM38 Mk2 (1m) measurements in vertical mode to measurements in horizontal mode was used instead of the EM31 : EM38 Mk2 measurement ratio described above. In other respects the method was similar to that described above for use with kinematic data; both versions of the method are described further in *Appendix 7 – EC_a profiles: method development*.

Multi-height measurements

EC_a data from multi-height measurements with the EM38 Mk2 (1m, vertical mode) was also used for qualitative interpretation in terms of EC_a depth profiles. EC_a measured at various heights above ground was plotted against EC_a expected at those heights for an even EC_a profile based on the measurement at ground level (i.e. at 6cm height according to the method in *3.6.1 – EM38 Mk2 – Spot EMI measurements*). These calculations simply multiplied the ground level reading by the remaining fraction of instrument sensitivity profile at the raised height of the instrument (Table 3.04.) These 'expected' measurements were plotted together with the actual EC_a measurements at each height.

Table 3.04. Remaining sensitivity of EM38 Mk2 to ground EC_a in raised positions.

Instrument height (cm)	EM38 (1m, vertical): fraction of sensitivity remaining
0	1.000
6	0.993
44	0.751
87	0.503
194	0.251

Sensitivity of the EM38 Mk2 (1m, vertical mode) at the surface is zero with the instrument at ground level, increasing rapidly to a peak at ~35cm, then decreasing at first rapidly then more gradually with depth. Raising the EM38 Mk2 instrument above the ground therefore reduces the total sensitivity of the instrument while increasing the relative sensitivity to deep EC_a.

Because instrument sensitivity at the surface is zero for a ground level measurement, EC_a at the surface can also be emphasized by raising the instrument. When the instrument is raised ~35cm, peak sensitivity is at the surface and declines with depth throughout the remainder of the sensitivity profile, as it also does with instrument heights greater than 35cm (Figure 3.23).

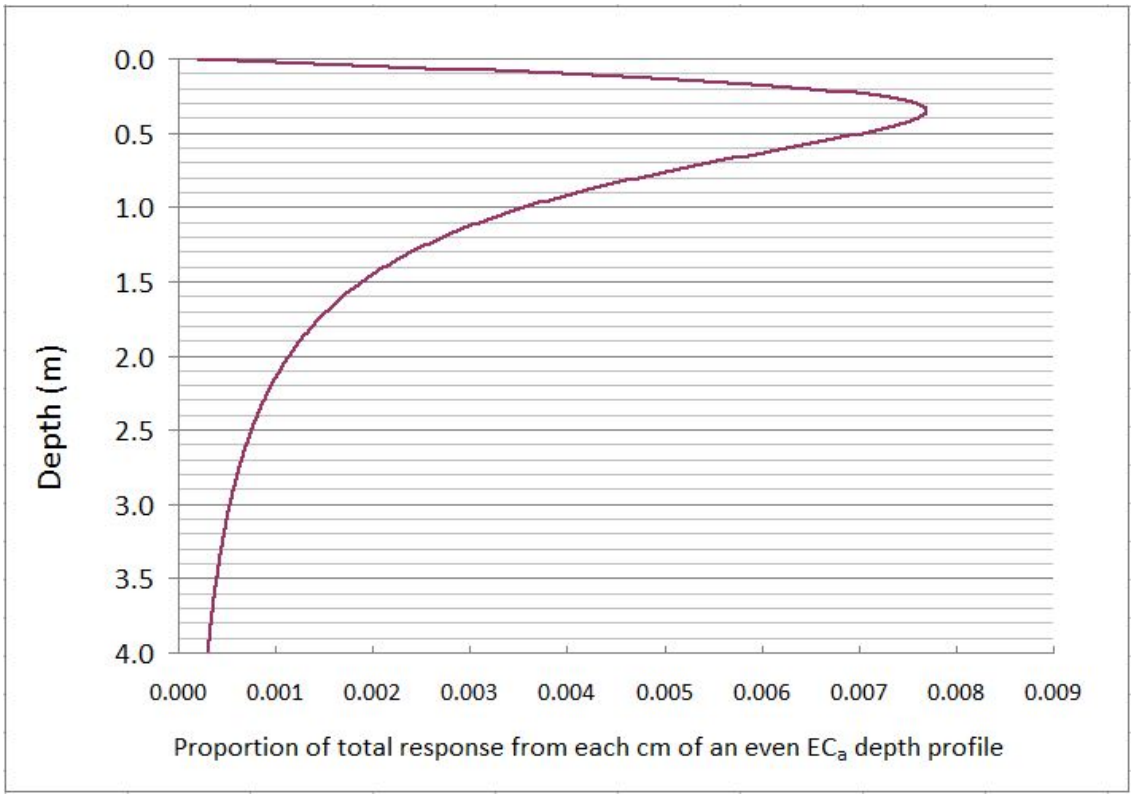

Figure 3.23. Response of the EM38 Mk2 (1m, vertical) to each cm of an even ECa profile, according to the function of Geonics (2008).

Chapter 4

Results and Discussion

This chapter will begin with a brief summary of the results of tests for instrument drift, interference and GPS location error; more detailed descriptions of these results are given in *Appendix 6 – EMI instrument functional tests*. Following this the EC_a of the soil sample sites will be examined and related to soil moisture, texture and electrical conductivity (EC) of soil pastes and extracts, all of which may affect EC_a-soil moisture relationships. Subsequently the EC_a kinematic survey data will be examined and related to soil moisture measurements which accompanied the surveys, and to measurements of depth to sand at No.1 Dairy.
Tables of results data are given in *Appendix 1 –Tables of results*, some of which are also summarized in tables or figures in this chapter. For simplicity in this chapter in relation to EM38 Mk2, '1m' refers to the 1m coil separation, and '0.5m' to the 0.5m coil separation of the instrument.

4.1 EMI instrument functional tests

The results summarized in this section were determined according to the methods in section *3.6.3 – Functional tests* and are presented more fully in *Appendix 6 – EMI instrument functional tests.*

ATV interference

Interference of the ATV with the EMI instruments in kinematic systems was calculated as +7.12 mS/m for the EM31, +2 mS/m for the EM38 Mk2 (1m coil spacing) and +1 mS/m for the EM38 Mk2 (0.5m coil spacing). These amounts were assumed to be constant within the study and were deducted from kinematic measurements of EC_a.

Fence interference

Interference of an electric fence with the EM31 was found to begin at 15m distance i.e. 2.5x the 'effective measurement depth' of the instrument in vertical mode or 5x in horizontal mode. EC_a measurements from kinematic surveys were excluded from datasets where the EM31 was closer than 12m to a fence. (The full 15m exclusion zone, based on the above results of the fence interference test, was reduced to 12m to enable retention of the data between 12-15m from fences, so as not to reduce the survey area over much.) EM38 Mk2 data points recorded within 2m of a fence were excluded from datasets.

Battery and cable effects

EC_a measured by the EM31 was found to be stable over more than 4 hours of stationary operation without battery change in the field, and measurements were similar whether the instrument was powered by Arlec rechargeable or Energizer alkaline batteries. Measurements from the EM38Mk2 (1m) were stable during battery voltage decline within the range recommended by Geonics, but measurements from the EM38 Mk2 (0.5m) were affected slightly by battery voltage decline within that range, and more strongly by changing the battery or by connecting or disconnecting the datalogger cable from the instrument. Recalibration of the instrument corrected these effects.

Calibration of the EM38Mk2 (0.5m) prior to connection of the datalogger may have contributed to inaccurate (negative) EC_a measurements in some kinematic surveys, as observed by Waine (1999). Consequently EM38 Mk2 (0.5m) data was discarded or used only qualitatively in terms of relative patterns.

GPS location error

Using the method described in *Appendix 4* and functions in *Appendix 5*, EM38Mk2 data was corrected for GPS location error according to a tow distance of 2.13m and system delay of 0.2s. EM31 data was corrected according to the distance of the console 0.9m in front and 1.7m to the right of the GPS antenna using the published system delay constant of 1s (Geonics, 1995).

Effects of temperature

Spot measurements of EC_a (EM38Mk2) were not significantly correlated with soil temperature or ambient temperature at either Burnside or No.1 Dairy locations, neither was EC_a affected by ambient temperature in a controlled environment test (see *Appendix 6 – EMI instrument functional tests*).

EC_a for the six kinematic surveys (EM38 Mk2, 1m, vertical mode, means of all readings for each survey) was not significantly correlated with ambient temperature. Correlation with soil temperature was based on means from only four surveys as soil temperature was not measured for the reconnaissance surveys at each location; however, the correlation was negative and significant ($P = 0.01$, $R^2 = 0.98$). This finding is in keeping with the literature on field measurement of EC_a; however, it is the opposite trend than might be expected from theories of EC_a which indicate that EC_a should rise with rise in temperature (see section *2.2.6 - Effect of temperature on EC_a* and *2.3.5 - EC_a and temperature in the field).*

No theory or published method was found to explain a negative effect of increasing soil temperature on EC_a or to correct for that effect. When EC_a data was adjusted by deducting the product of the soil temperature and the coefficient of correlation (which in this case meant adding the product, as the coefficient was negative) correlation of EC_a with soil moisture was weaker. Therefore no correction for soil temperature effects was made with either spot or kinematic measurements of EC_a.

4.2 EC_a and soil moisture at soil sample sites

EC_a measurements examined in this section are single spot measurements, means of three measurements (on soil sampling dates) or point values extracted from interpolated (kriged) raster surfaces of kinematic survey data.

4.2.1 EC_a measurements – Burnside sites

At Burnside, EC_a (EM38 Mk2, 1m, vertical mode) was generally highest at site B1 and lowest at site B3, except in the series of measurements from 22-25.11.11 accompanying soil sampling when site B2 was lowest; that was also the only

occasion on which EC_a was not measured at all sites on the same day, so comparisons between sites may not be valid in that particular case (Figure 4.01).

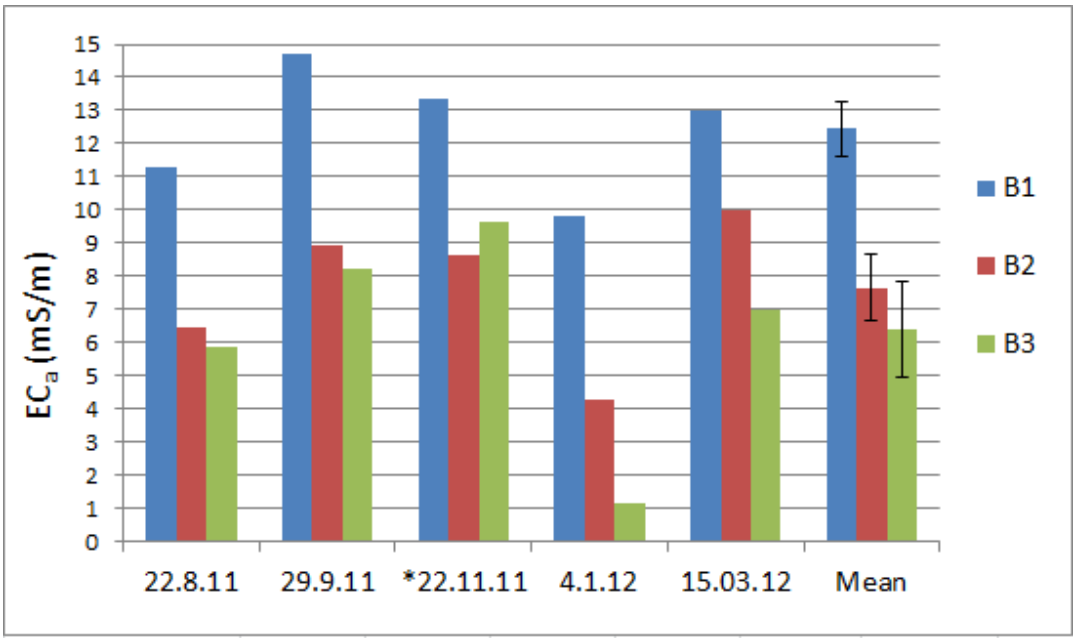

Figure 4.01. EC_a (EM38 Mk2, 1m, vertical) at soil sample sites at Burnside.
* = site measurements across three days: 22.12.11, 23.11.11 and 25.11.11. Error bars are standard error of the mean. EC_a measurements on 22.8.11, 29.9.11 and 4.1.2 were extracted from kinematic survey data. The remainder are spot measurements.

EC_a (EM38 Mk2, 0.5m, vertical) from the two kinematic surveys at Burnside on 29.9.11 and 4.1.12 was not retained as it included many negative values and was therefore inaccurate, possibly due to faulty calibration (see section *4.1 – EMI functional tests - Battery and cable effects* and section *4.4.1 Reconnaissance surveys: topography and EC_a – Negative measurements of EC_a*). The results of spot measurements are shown in Figure 4.02. The EM38 Mk2 (0.5m) measurements are overall lower than the EM38 Mk2 (1m) measurements, and the order of EC_a, highest to lowest between the sites, is similar for both coil spacings only on 15.3.12.

4.2.2 Soil moisture measurements – Burnside sites

As with EC_a (1m, vertical), soil moisture at Burnside was highest at site B1 on the three occasions on which it was measured at the soil sample sites (Figures 4.03 and 4.01).

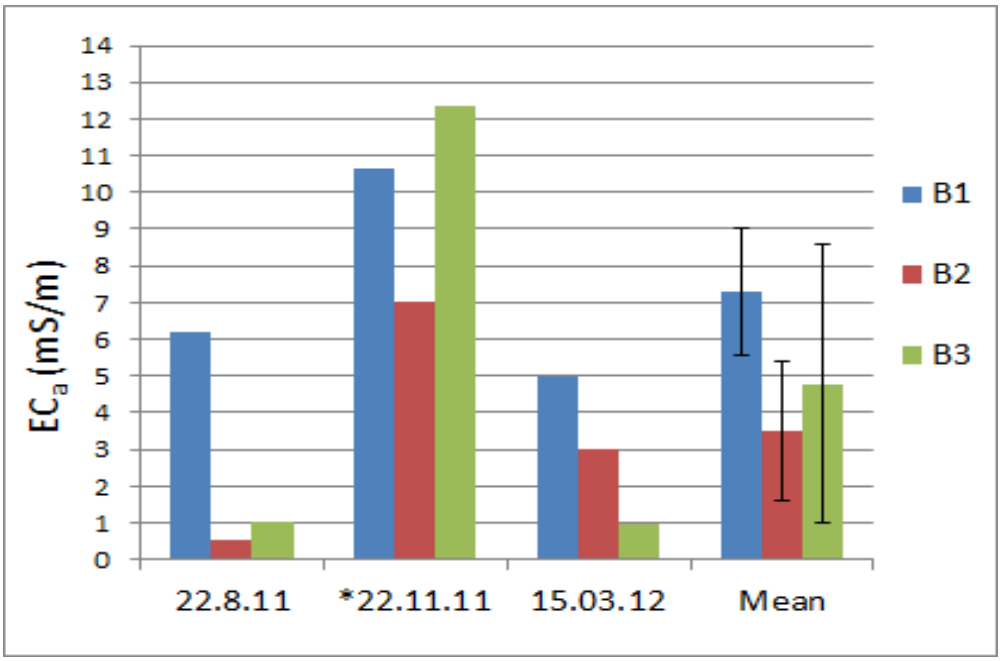

Figure 4.02. EC_a (EM38 Mk2, 0.5m, vertical) at soil sample sites at Burnside.
* = site measurements across three days: 22.12.11, 23.11.11 and 25.11.11. Error bars are standard error of the mean.

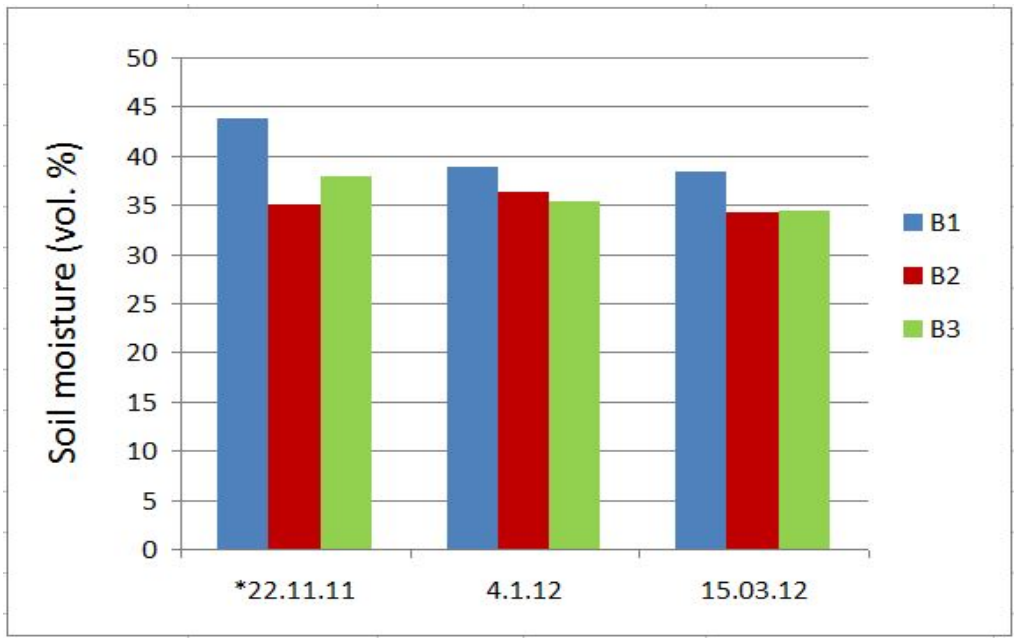

Figure 4.03. Soil volumetric moisture (TDR to 45cm) at soil sample sites at Burnside.
* = site measurements across three days: 22.12.11, 23.11.11 and 25.11.11.

4.2.3 EC_a measurements – No.1 Dairy sites

At No.1 Dairy, EC_a measured by both 1m and 0.5m coil spacings was lowest at site D5 and highest at site D4 on all occasions (Figures 4.04 and 4.05). Data from the 0.5m coil spacing from the kinematic survey on 25.1.12 was not retained as, like the 0.5m data from kinematic surveys at Burnside, it contained many negative values (see section *4.4.1 Reconnaissance surveys: topography and EC_a – Negative measurements of EC_a*).

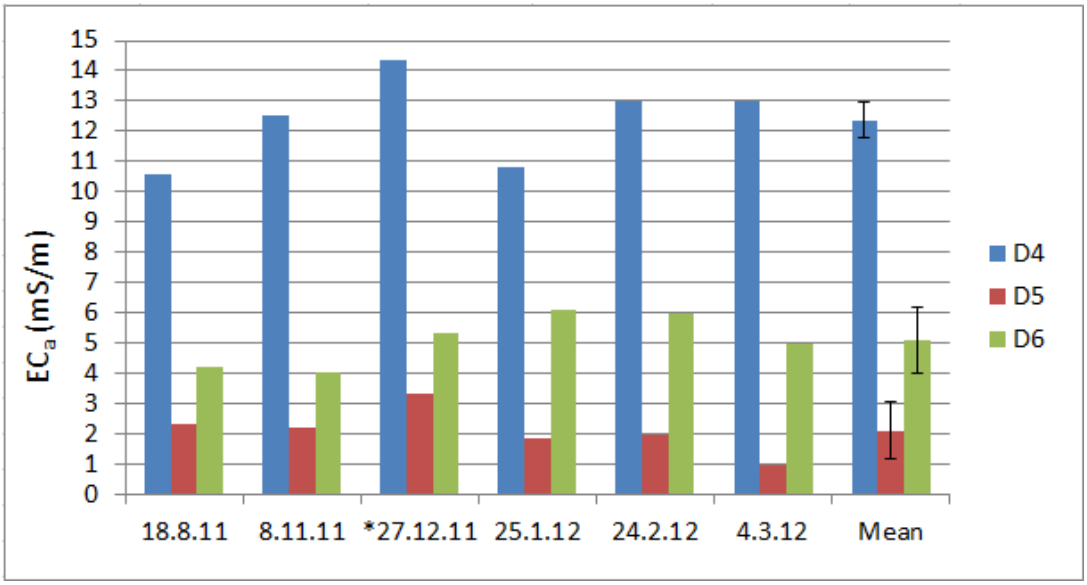

Figure 4.04. EC_a (EM38 Mk2, 1m, vertical) at soil sample sites at No.1 Dairy.
* = site measurements across three days: 27.12.11, 29.12.11 and 6.1.12. Error bars are standard error of the mean.

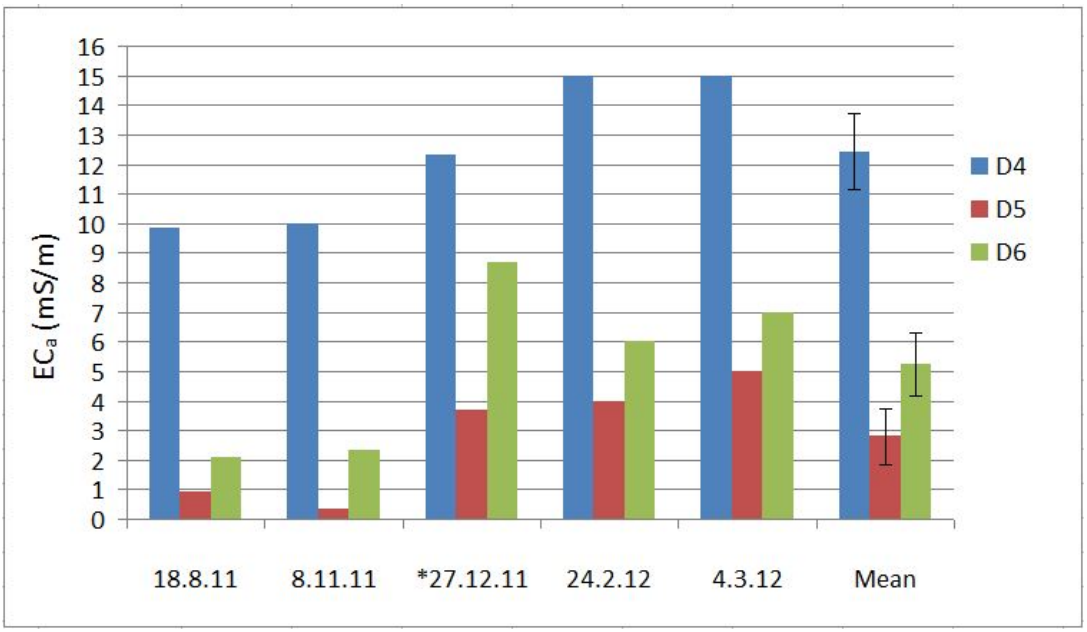

Figure 4.05. EC_a (EM38 Mk2, 0.5m, vertical) at soil sample sites at No.1 Dairy.
* = site measurements across three days: 27.12.11, 29.12.11 and 6.1.12. Error bars are standard error of the mean.

4.2.4 Soil moisture measurements – No.1 Dairy sites

As with EC_a measurements at No.1 Dairy sites, soil moisture was lowest at site D5 and highest at site D4 on all occasions except 27.12.11 when moisture was highest at site D6; that was also the only occasion on which soil moisture was not measured at all sites on the same day (Figure 4.06, 4.04 and 4.05). However, while the taking of moisture measurements at each site on separate days may have affected the relative wetness of the sites in relation to each other, it is not an explanation for the different EC_a-moisture relationship in that instance because at each site EC_a and moisture were measured on the same day.

The patterns of EC_a and of soil moisture were therefore similar between sites at No.1 Dairy. Correlation of EC_a with soil moisture at sample sites is examined in *4.2.6 - Correlation of EC_a with soil moisture at sample sites* where the results of EC_a depth profile resolution are also included.

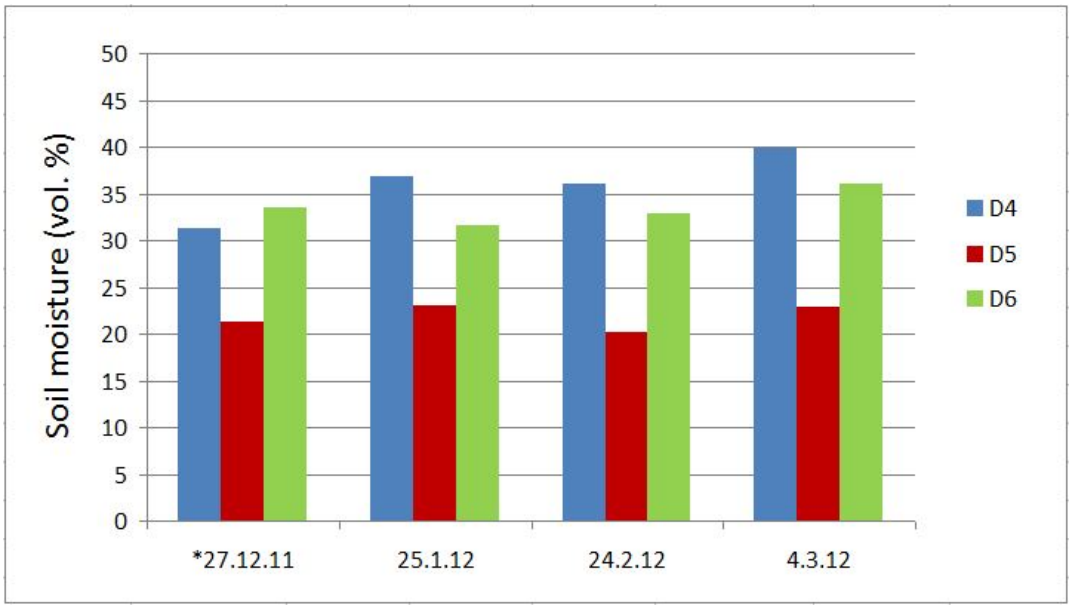

Figure 4.06. Soil volumetric moisture (TDR to 45cm) at soil sample sites at No.1 Dairy. * = site measurements across three days: 27.12.11, 29.12.11 and 6.1.12.

4.2.5 EC_a two-layer models at soil sample sites

Estimates of EC_a in the top 45cm of profile are possible using spot EC_a measurements from two occasions at Burnside and three occasions at No.1 Dairy: the initial sampling of the soil replicate sites at each location, one further occasion of spot sampling at Burnside and two further occasions at No.1 Dairy, according to the methods for spot measurements described in *3.7.3 - EC_a depth profile resolution* and *Appendix 7*.

In all instances estimates of upper profile EC_a are higher than whole profile EC_a except at site B2, Burnside on 15.3.12, where whole profile EC_a is higher (Figure 4.07). The order of EC_a, highest to lowest between sites at each location was the same for upper and whole profile EC_a except at Burnside on 15.3.12 where lowest whole profile EC_a was measured at site B3 but lowest upper profile EC_a at site B2.

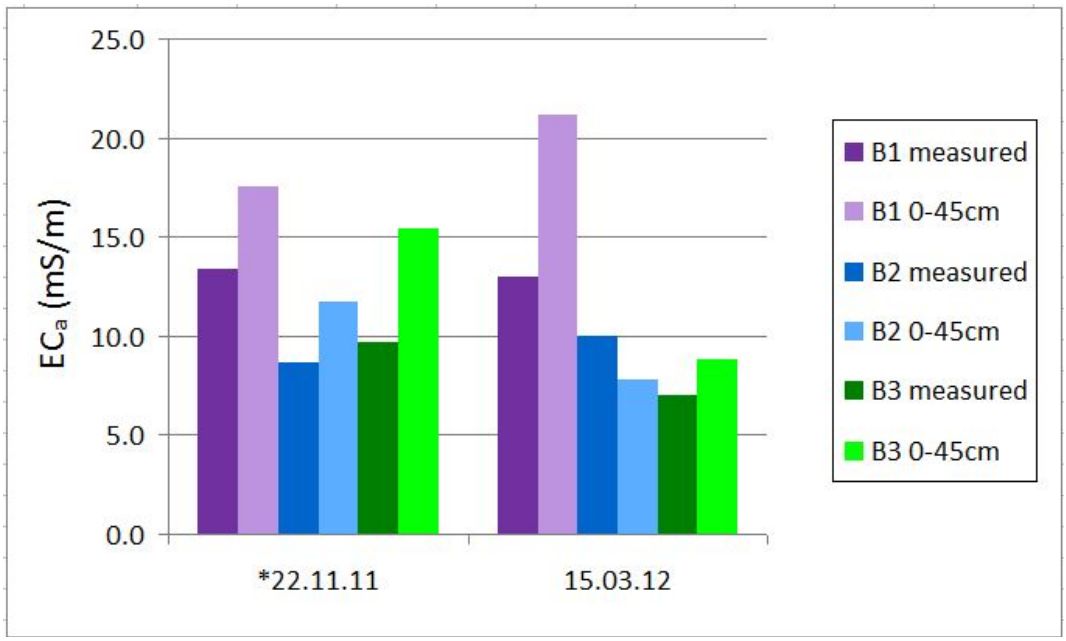

a.

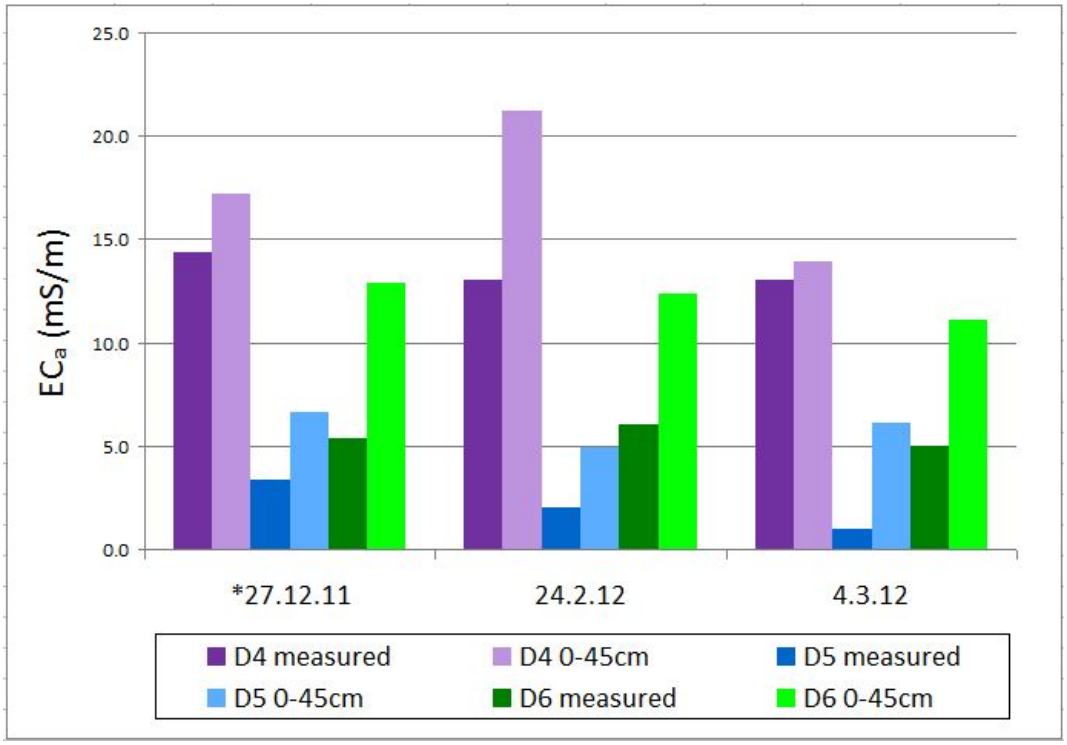

b.

Figure 4.07. EC_a (EM38 Mk2, 1m, vertical) as measured and as calculated for the upper profile (0-45cm) at a) Burnside and b) No.1 Dairy.

4.2.6 Correlation of EC_a with soil moisture at sample sites

Linear correlations of EC_a with soil moisture at sample sites are shown in Table 4.01.

Table 4.01. R^2 values of linear correlations of EC_a with soil volumetric moisture at soil sample sites.

	EM38 1mV +6cm ECa measured (mS/m)	EM38 1mH @grnd ECa measured (mS/m)	ECa 0-45cm calculated (mS/m)
Both locations	0.59	0.60	0.52
Burnside	ns	ns	ns
No.1 Dairy	0.50	0.58	0.60

ns = not significant at the $P = 0.05$ level. Moisture measurements were by TDR to 45cm; regression included all occasions for which EC_a 0-45cm could be calculated i.e. the initial soil sampling at each location for which the 3 replicates at each site were combined as site means, one further occasion at Burnside and two further occasions at No.1 Dairy (i.e. a total of 6 observations at Burnside and 9 at No.1 Dairy.)

Consistent with Figures 4.01-4.07, linear regression shows a positive correlation between EC_a and soil moisture at No.1 Dairy. The best correlation is with EC_a calculated by depth resolution for the upper 45cm of profile, followed by EC_a measured by the EM38 Mk2 in horizontal mode. Both these techniques emphasize EC_a of the upper profile and so might be expected to show better correlations with soil moisture also measured in the upper profile (TDR to 45cm). The modest R^2 values, however, and the absence of significant correlations at Burnside suggest that soil moisture was not the only determinant of EC_a and not necessarily the dominant one.

4.2.7 Multi-height measurements at soil sample sites

Where EC_a is highest at a shallower depth than the peak of instrument sensitivity (35cm depth) the EC_a measurement can be increased by raising the EM38 Mk2 in vertical mode, as described in section *3.7.3 - EC_a depth profile resolution – Multi-height measurements*. A lesser degree of this phenomenon is where EC_a does not

increase with raising of the instrument but decreases less than would be expected for an even EC_a profile.

The above type of result is evident for site B3, Burnside on 15.3.12 and sites D5 and D6, No.1 Dairy on 24.2.12 (Figures 4.08 and 4.09). Lifting the instrument to 44cm height caused a lesser reduction in the EC_a measurement than would be expected for an even EC_a profile, indicating that EC_a was high near the surface (i.e. in the top 35cm of profile; all EC_a below 35cm would be 'de-emphasized' by such raising of the instrument). This is consistent with estimates of EC_a for the top 45cm of profile produced by depth profile resolution using EMI measurement ratios according to the methods in section *3.7.3 - EC_a depth profile resolution* and *Appendix 7* (Figure 4.07.)

It is noted that many of the EC_a values described in this section and depicted in Figures 4.08-4.09 are very low, at the limit of EMI detection, and are in some cases negative. The occurrence of negative EC_a values which by definition cannot be accurate is discussed in section *4.4.1 - Reconnaissance surveys: topography and EC_a – Negative measurements of EC_a*. In keeping with that discussion the analysis of such values in this section is qualitative only. It is supposed that the relative differences between values described here retain some significance because any shortcomings of instrument calibration applied equally to all raised measurements at one site and time.

However, EC_a values calculated for theoretical 'even' EC_a profiles assume a minimum possible EC_a of zero. Therefore the difference between these and the measured values may be exaggerated where the measured values are negative.

Except at site B3, Burnside on 15.3.12, all measurements with the instrument raised to 194cm are lower than predicted for an even EC_a profile. This effect may not be significant in all cases; it is most pronounced for site D5, No.1 Dairy on 4.3.12, indicating that EC_a in that instance was highest in the upper profile, but not at the very surface as there was no increase in the measurement with the initial raising of the instrument to 44cm (Figure 4.10.) Site D5 on that occasion also provided the strongest instance of locally higher EC_a in the top 45cm of profile indicated by EC_a depth profile resolution, so the two methods, depth profile resolution and

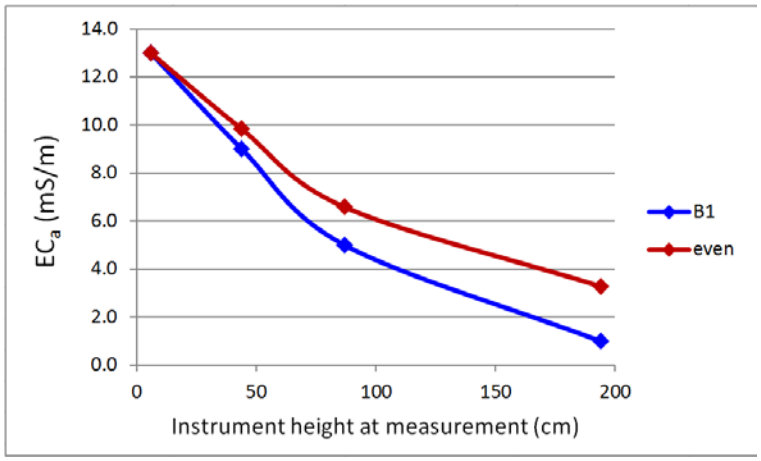

a.

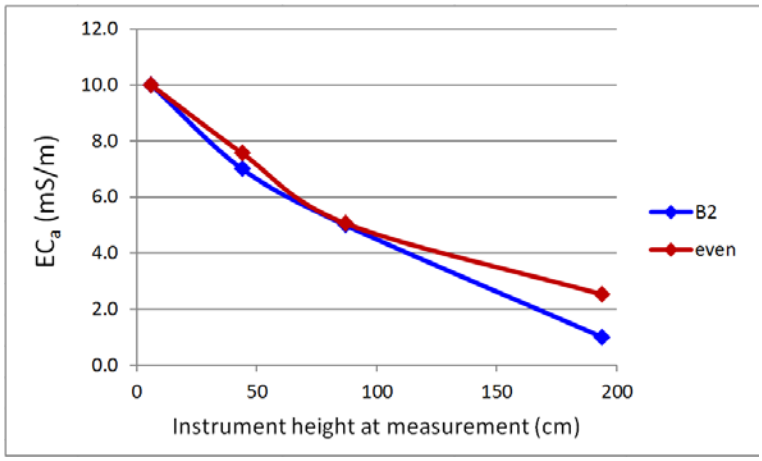

b.

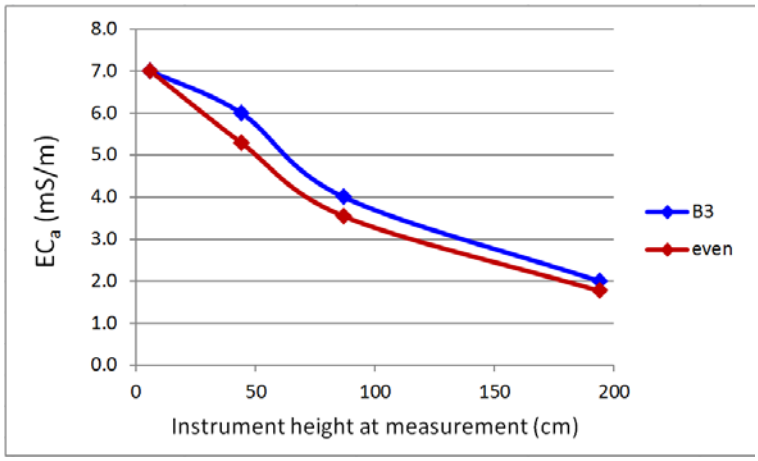

c.

Figure 4.08. Measured and predicted EM38 Mk2 (1m, vertical) EC_a measurements with instrument raised to various heights at Burnside, 15.3.12. Predictions are for an even profile based on the initial measurement at 6cm height.

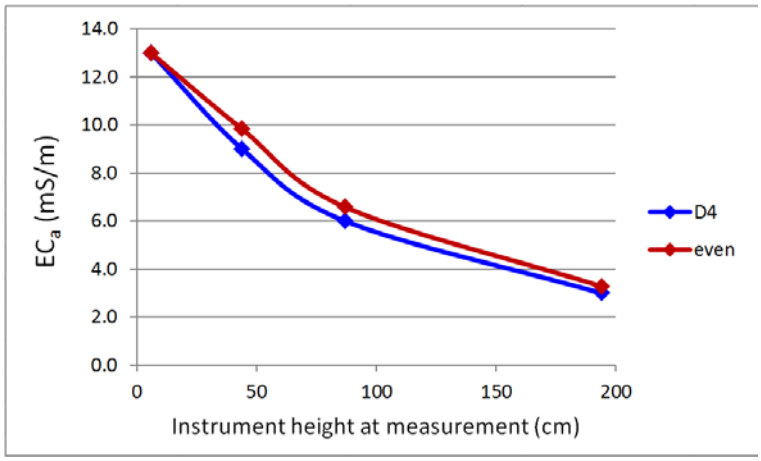

a.

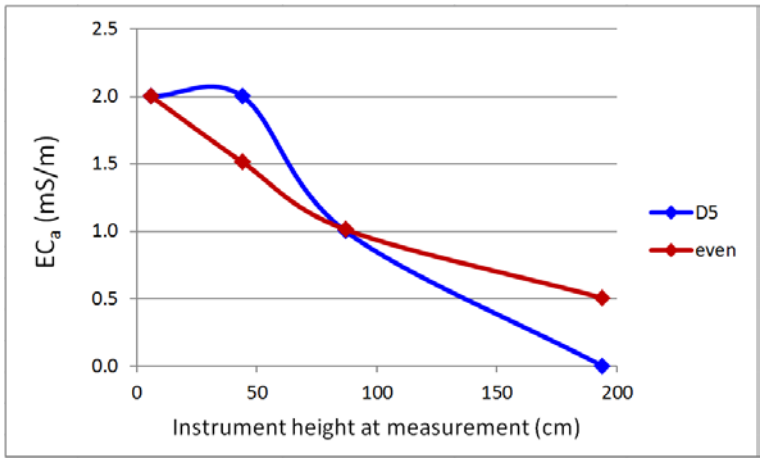

b.

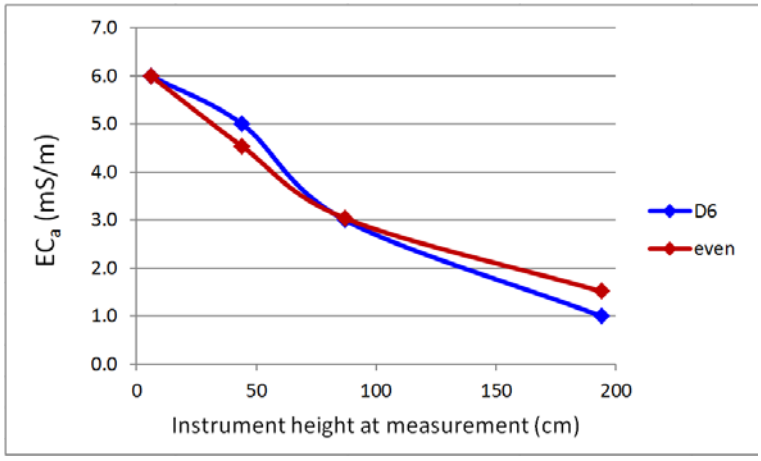

c.

Figure 4.09. Measured and predicted EM38 Mk2 (1m, vertical) EC_a measurements with instrument raised to various heights at No.1 Dairy, 24.2.12. Predictions are for an even profile based on the initial measurement at 6cm height.

prediction from raised height measurements in this case concur (Figures 4.07 and 4.10).

On 24.2.12 at site D5, No.1 Dairy, raising the EM38 Mk2 (1m, vertical) from 6 to 44cm height caused no decrease in measured EC_a indicating that, unlike the situation on 4.3.12 described above, EC_a was high at the surface. One possible explanation for opposite results of EC_a measurement at 44cm height at site D5 on 24.2.12 and 4.3.12 is the presence of a generally wet soil on 4.3.12 which had nonetheless had time to dry at the very surface, compared with wet topsoil from recent rain over dry subsoil on 24.2.12. In that case EC_a measured at ground level (i.e. 6cm) was lower but moisture in the top 45cm higher on 4.3.12 than on 24.2.12 because the effect of moisture on 4.3.12 was mainly above the peak sensitivity of the EM38 Mk2 (1m, vertical) at 35cm depth (Figures 3.23, 4.09 and 4.10). More generally, low EC_a measurements at 194cm height are consistent with the presence of gravels at depth at all sites causing low EC_a at depth.

It was known from installation of piezometers that gravels were present at depths between 2.9 and 3.8m at all three such sites at Burnside and all four at No.1 Dairy, spread over a wide area at each location.

Comparisons of the upper profile estimates with the multi-height data shown in Figures 4.08, 4.09 and 4.10 are difficult because, depending on the distribution of EC_a within the top 45cm, raising the instrument can change the reading either more or less than expected, or even raise instead of lower the reading for the same value or proportion of upper profile EC_a. By coordinating the raised measurement heights with the depths of profile layers for which local EC_a is estimated the two methods could be better integrated.

The above examples, however, serve to illustrate how not only EC_a magnitude but also EC_a depth profile determines measurements by EMI. Because moisture content influences EC_a and also varies with depth, it can potentially cause different EMI measurements of similar EC_a. This may have weakened correlations of EC_a with soil moisture in this study, especially as soil moisture measurements are bulk or 'average' measurements of the top 45cm of profile in which range the EM38 Mk2 (1m, vertical) sensitivity profile shows most variation.

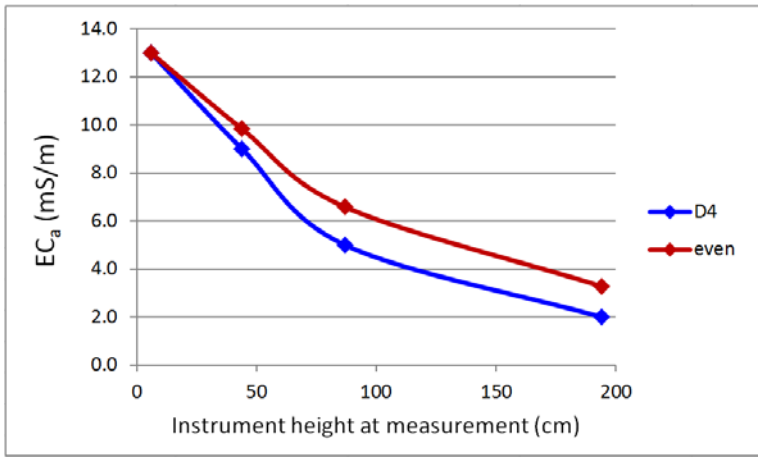

a.

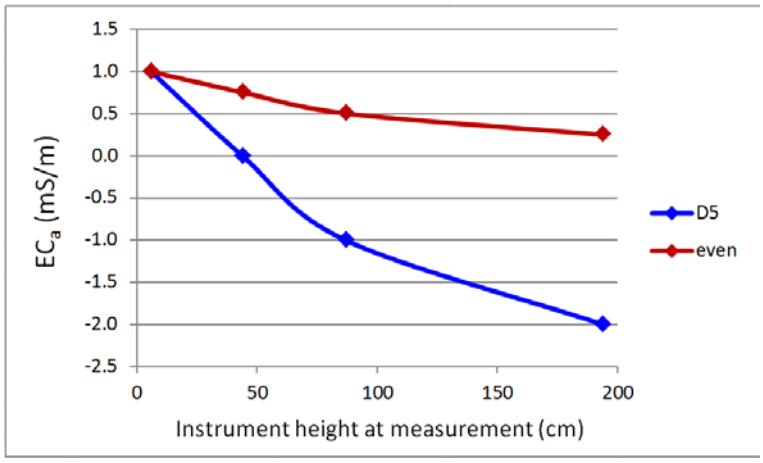

b.

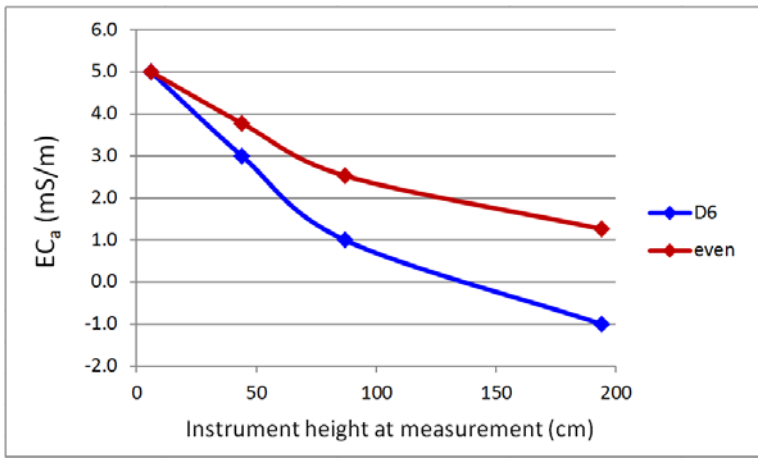

c.

Figure 4.10. Measured and predicted EM38 Mk2 (1m, vertical) EC_a measurements with instrument raised to various heights at No.1 Dairy, 4.3.12. Predictions are for an even profile based on the initial measurement at 6cm height.

Depth resolution of EC_a of soil sample sites does not appear to have corrected for irregular depth profile effects sufficiently to enable strong correlation of EC_a with soil moisture in the upper profile. However, for EC_a depth profile resolution to enable better correlations with soil moisture, a strong and direct relationship between EC_a and soil moisture must first be present. As is discussed below for further results from soil sample sites, it is not certain that such a relationship was present at soil sample sites in this study.

4.2.8 Moisture release characteristics of No.1 Dairy soil samples

Soil moisture measured by TDR at soil sample sites was generally below field capacity (10 kPa) and above or near stress point (100 kPa; Figure 4.11). Moisture in fresh samples from four depths at each site shows that matric potential at the time of soil sampling was mostly a little higher than at field capacity (Figure 4.12). However, at sites D4 and D5 matric potential was noticeably higher close to the surface: higher than stress point (100 kPa) at site D4 and close to permanent wilting point (1500 kPa) at site D5. This illustrates the concept of a soil moisture profile where field capacity is not attained simultaneously or retained equally throughout the soil profile, and also complicates interpretation in terms of EC_a which is thought to respond differently to moisture in different states in the soil (i.e. at different matric potentials; see section *2.2.4 - Limitations and extensions of the dual pathway model*). Variation in soil matric potential may therefore have compounded the effect of simple variation in moisture depth profile in weakening EC_a-soil moisture correlations in this study.

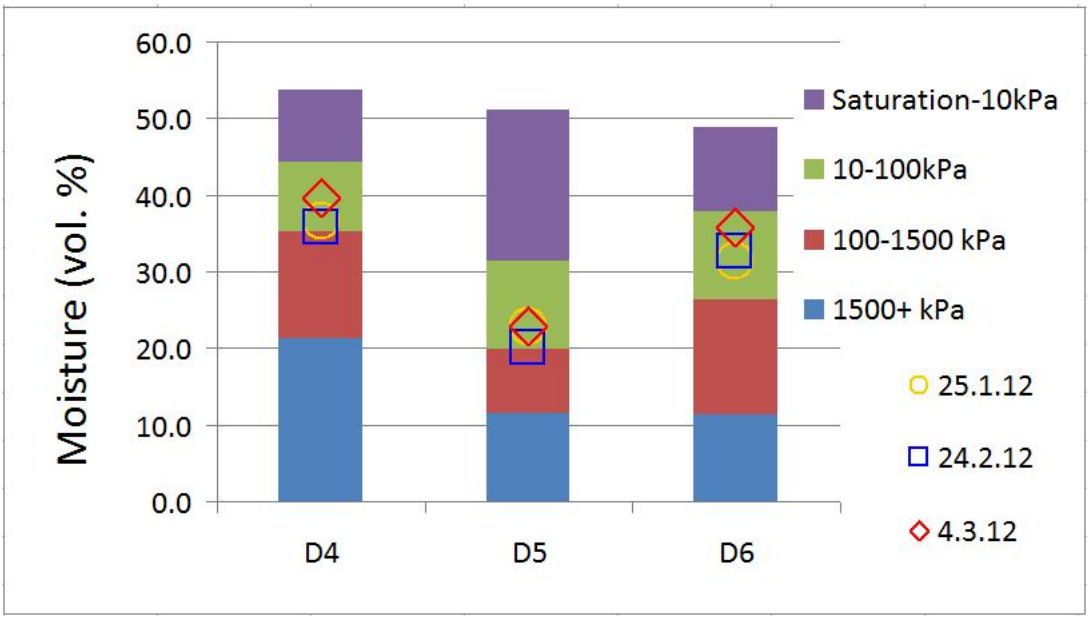

Figure 4.11. Soil volumetric moisture at different matric potentials in samples from three sites at No.1 Dairy, and as measured by TDR at those sites on three occasions. Moisture release characteristics are simple means of values from 4cm, 28cm and 42cm at each site, to show the closest relation to the TDR measurements which are to 45cm.

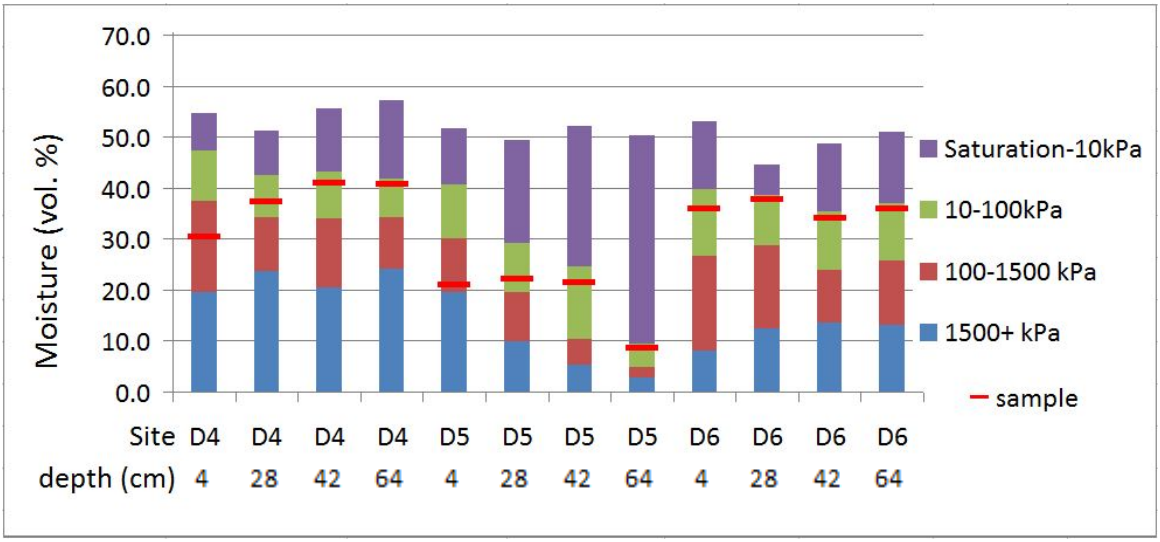

Figure 4.12. Soil volumetric moisture at different matric potentials in samples from three sites at No.1 Dairy, and fresh volumetric moisture at time of sampling. (D4: 27.12.11; D5: 29.12.11; D6: 6.1.12).

4.3 Influences of other soil properties at sample sites

4.3.1 Soil texture

All soils were of silt or loamy silt texture at all sampling depths according to the New Zealand texture classification (Milne et al.,1995) except the 2C sand horizon at No.1 Dairy (Figures 4.13 and 4.14 and Table 4.02). This 2C sand horizon occurred at various depths at all No.1 Dairy sites but was only within sampling depth for the purposes of laboratory analyses at site D5 where it occurred at 54cm depth.

At No.1 Dairy the exceptionally silty site D4 does not show the highest available water capacity as might be expected (Figures 4.11, 4.12 and 4.14). The sandier site D6 shows higher readily available water capacity (10 kPa to 100 kPa soil matric potential) and total available water capacity (10 kPa to 1500 kPa) than site D4. Similarly, sand in the 20-40% range does not appear to limit readily available water capacity at 4, 28 or 42cm depths at the sandiest No.1 Dairy site, D5, but only at 64cm depth where the texture is 90% sand.

No significant differences were found in proportion of clay or in texture fineness between locations, sites, sample depths or horizon types (A vs. B and gley vs. non-gley). Proportions of sand and silt were found to differ significantly between gley and non-gley horizons across both locations and between sites at Burnside, but not between locations, A and B horizons, or sample depths at either location, or between sites at No.1 Dairy (Table 4.03).

Figure 4.13. Particle size distribution of soil samples at four depths from three sites at Burnside. (Sand fractions in blue, silt in green and clay in yellow to red).

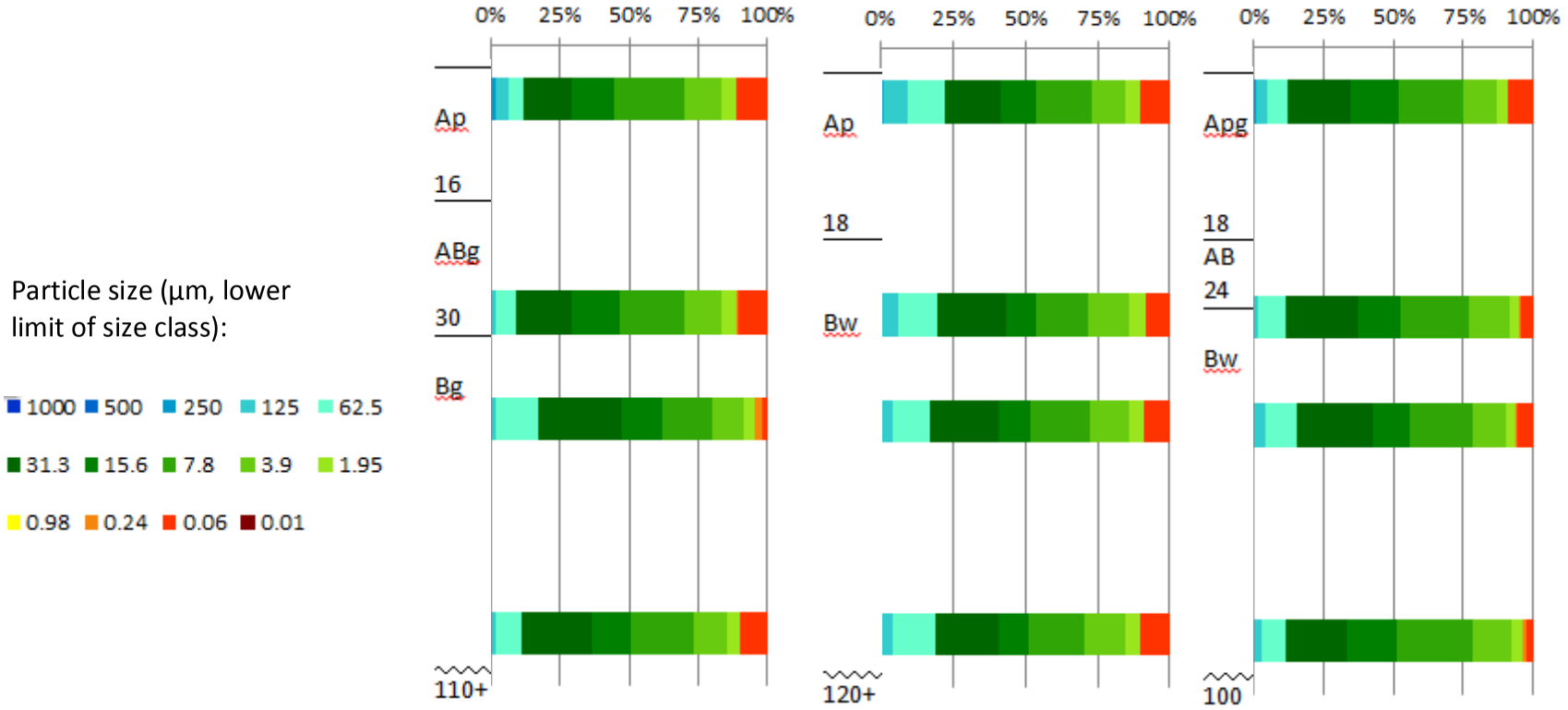

Site B1, Burnside.

Site B2, Burnside.

Site B3, Burnside.

Figure 4.14. Particle size distribution of soil samples at four depths from three sites at No.1 Dairy. (Sand fractions in blue, silt in green and clay in yellow to red).

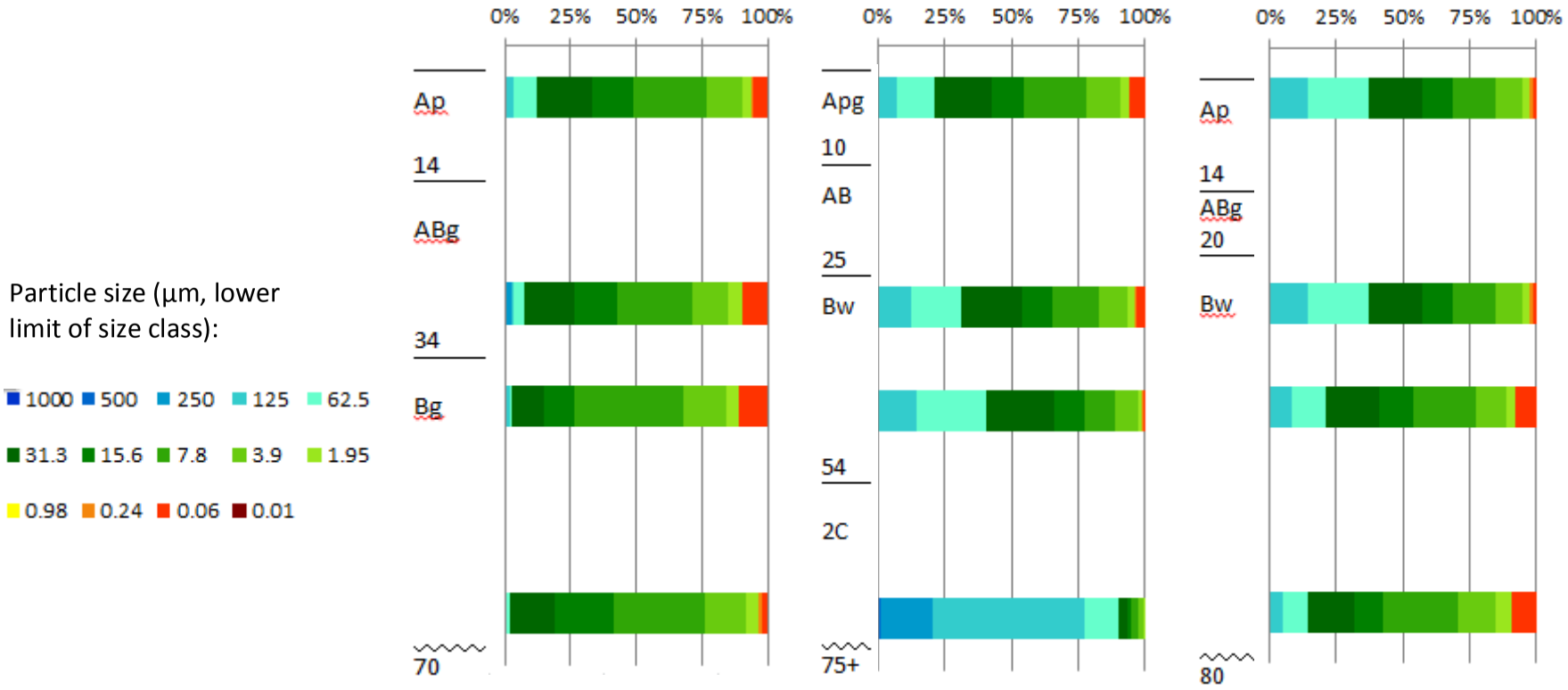

Site D4, No.1 Dairy.

Site D5, No.1 Dairy.

Site D6, No.1 Dairy.

Table 4.02. Texture properties of soil at sample sites. Calculation of soil fineness is described in section *3.5.4 - Laboratory analyses – Soil texture*. All values are simple means of samples from 4, 28 and 42cm depth.

	B1	B2	B3	D4	D5	D6
sand %	12.6	19.8	12.8	7.6	31.0	25.8
silt %	78.2	70.9	80.4	83.5	65.3	68.1
clay %	9.1	9.3	6.8	8.9	3.7	6.1
fineness	2.8	2.7	2.5	2.8	1.9	2.3

Table 4.03. Significant differences in soil texture properties.

	% Sand	% Silt	% Clay	Fineness[a]
Location (Burnside or No.1 Dairy):	no	no	no	no
Horizon type (A or B, both locations):	no	no	no	no
Horizon type (gley or non-gley, both locations, C horizons not included):	yes	yes	no	no
Depth (across both locations):	no	no	no	no
Depth (Burnside):	no	no	no	no
Depth (No.1 Dairy):	no	no	no	no
Site (Burnside):	yes	yes	no	no
Site (No.1 Dairy):	no	no	no	no

a. Calculation of soil fineness is described in section *3.5.4 - Laboratory analyses – Soil texture*.

Sandier horizons had a lower proportion of silt and were less likely to be gleyed. At Burnside, site B2 was sandier and had less silt than sites B1 or B3 which were similar to each other for both properties. Sites at No.1 Dairy showed apparent differences in texture particularly with regard to sand, however, no statistically significant differences were found, possibly due to high variation within and between the small number of sites.

Soil texture, moisture and EC_a

At each location the sandiest site, B2 at Burnside or D5 at No.1 Dairy, was driest on average (Figures 4.03 and 4.06.) This might be expected as sand has better drainage and lower total moisture content at field capacity than silt or clay. Sand, silt, clay and texture fineness are each significantly correlated with soil moisture at sample sites (Table 4.04). None showed evidence of a curvilinear relationship; extending the regressions to a second order polynomial made little improvement to the R^2 values. Of the single parameters, sand is most strongly (and negatively) correlated with soil moisture. A multiple regression of soil moisture against sand and clay showed a correlation only slightly better ($R^2 = 0.70$) than sand alone.

Table 4.04. Correlation by linear regression of individual soil texture variables with soil volumetric moisture at soil sample sites across both locations, Burnside and No.1 Dairy.

	Coefficient	R^2	P
Sand %	-0.36	0.67	1.17×10^{-6}
Silt %	0.38	0.60	8.73×10^{-6}
Clay %	1.52	0.42	6.11×10^{-4}
Texture fineness	10.75	0.64	2.38×10^{-6}

Note: soil samples for texture analysis were bulked replicates for each depth at each site which meant only one mean to 42cm of each texture property was produced for each site, and only three per location – insufficient for separate regressions for each location.

As discussed above and in *4.2.6 - Correlation of EC_a with soil moisture at sample sites*, EC_a is correlated with soil moisture at No.1 Dairy sites but not at Burnside sites while soil texture properties are correlated with soil moisture at sites across both locations (Table 4.04). All soil texture properties are also more strongly correlated with EC_a than soil moisture, suggesting that an effect of soil texture (or some related property) on EC_a, additional to the indirect effect of soil texture via soil moisture, masks any specific relationship of EC_a to soil moisture (Tables 4.01 and 4.05).

Table 4.05. Linear correlations of soil texture properties with variously measured EC_a at sample sites.

	ECa (EM38 Mk2, 1m vertical, mS/m)		ECa (EM38 Mk2, 1m horizontal, mS/m)		ECa 0-45cm (calculated, mS/m)	
	Coefficient	R^2	Coefficient	R^2	Coefficient	R^2
Sand %	-0.47	0.93	-0.40	0.93	-0.042	0.84
Silt %	0.54	0.84	0.46	0.85	0.50	0.73
Clay %	1.65	0.71	1.37	0.68	ns	ns
Fineness	11.52	0.86	9.67	0.84	10.1	0.73

ns = not significant at the $P < 0.05$ level. Texture data is simple means of samples from 4, 28 and 42cm depths at each site.

Such an effect could be that of soil particle surface charge properties (see sections *2.2.3 - 2.2.5*). According to theory based on Archie's Law, sand particles affect EC_a mainly as non-conductors interrupting the flow of electrical current in conductive soil solution; accordingly the coefficients of sand (%) in Table 4.05 are negative. Sandy soils are also likely to be drier, so the negative effect is twofold. A major effect of clay particles on EC_a is thought to be their capacity to conduct electrical current across their extensive surface area, hence the coefficients of clay (%) in Table 4.05 are positive. Clay also increases moisture retention in soil, so while the effects of clay and sand on EC_a are opposite, like sand the effect of clay is twofold.

The effect of soil texture on EC_a over and above its indirect effect through soil moisture may enhance the correlation of EC_a with soil moisture where the texture-moisture relationship is consistent. However, where the texture-moisture relationship is inconsistent, e.g. where moisture varies for reasons unrelated to texture such as rising water table, variable recharge or rates of evapotranspiration due to differences in aspect, slope, topographical position or vegetation cover, soil texture is then another property which may have weakened EC_a-moisture correlations in this study.

Depth resolution of upper profile EC_a did not strengthen correlations with soil texture properties at sample sites (Table 4.05). This may be because of effects on soil moisture in the top 45cm of soil texture deeper in the profile, e.g. by facilitating or inhibiting drainage of the upper profile. The response of EMI to soil texture at depth might therefore strengthen correlations with soil moisture in the upper profile, but is excluded by EC_a depth profile resolution.

4.3.2 Soil type

Burnside

Soils at sample sites B2 and B3 at Burnside were in keeping with their classification in the Manawatu series according to previous mapping. Whilst having loamy silt textures according to the texture classification of Milne et al. (1995), these soils would be considered fine sandy loams according to Cowie (1978), the loamy silt texture class apparently having little currency in soil classification in New Zealand at that time (see section *3.3 – Soils*, Table 4.02, Figure 4.13, *Appendix 8 – Descriptions of soil series* and *Appendix 9 – Soil profiles).* The slightly gleyed Site B3 is considered a Manawatu mottled fine sandy loam.

Site B1 was a loamy silt or fine sandy loam (Cowie, 1978) and clearly gleyed and is identified as a Kairanga fine sandy loam. The absence of a clearly defined topsoil at site B1 which should distinguish the Kairanga from the less mature Parewanui series is attributed to the effects of cultivation, in particular the enhanced oxidation of organic matter in cultivated topsoil. Site B1 was farther from Totara Stream than sites B2 or B3 which is in keeping with the expected positions in relation to sediment source of Manawatu and Kairanga soils.

No.1 Dairy

All soil samples above the underlying 2C sand horizon at No.1 Dairy revealed loamy silt textures, or in the case of site D4, silt. This was despite the position of the location bordering the Manawatu River and Turitea streams where coarser flood sediments might be expected (sand settles more quickly from flood waters as they transgress the floodplain, therefore is often deposited in river levees).

The soil profile at site D4 was gleyed and some gleying was found also at site D6. While these features were only moderate to incipient they are still significant given the apparently young age of the soils; there were clearly impediments to drainage, a feature of Parewanui rather than Rangitikei soils. (The Apg horizon observed at site D4 and at Burnside sites appears more a product of compaction, pugging and manuring of the surface caused by stock in wet conditions).

The indistinct A horizons and somewhat dark B horizons reflecting the acretionary nature of the Rangitikei series were observed as expected at No.1 Dairy. The AB horizons observed were more typical of the Parewanui series. It was concluded that site D4 is best classified as a Parewanui silt due to its texture and obviously impeded drainage. Sites D5 is classified as Rangitikei fine sandy loam and site D6 as Rangitikei mottled fine sandy loam (see section *3.3 – Soils*, Table 4.02, Figure 4.14, *Appendix 8 – Descriptions of soil series* and *Appendix 9 – Soil profiles).*

Soil type, moisture and EC_a

According to the above classifications therefore, differences in soil properties between the Burnside and No.1 Dairy locations are differences between two classes of soil maturity, while differences between sites are differences between soil types.

Analysis of variance reveals no significant differences between locations for EC_a or soil moisture measured at soil sites, but there are significant differences between sites for both properties. (Soil moisture was by TDR to 45cm, EC_a by EM38 Mk2 (1m, vertical); depth resolution of EC_a measurements did not strengthen the results). Sites with the most gleyed soil, B1 and D4, classified as Kairanga fine sandy loam and Parewanui silt respectively, had the highest EC_a and were most often the wettest site at their respective locations. Gleying was also linked to lower sand and higher silt contents (Table 4.03).

It is concluded that differences in drainage characteristics, gleying and texture between soil types contributed to differences in soil moisture and EC_a at sample sites (Table 4.06). It is worth noting that EC_a and moisture measurements at sample sites were not made at both locations on the same dates, and in two cases sites at each location were not measured on the same date (Table 3.01).

Table 4.06. EC_a and soil volumetric moisture at sample sites. Each value is the mean of measurements on two occasions at Burnside and three occasions at No.1 Dairy (i.e. the 'Site measure' dates given in Table 3.01).

	B1	B2	B3	D4	D5	D6
EC_a (EM38 Mk2 1m, vertical, mS/m)	13.2	9.3	8.3	13.4	2.1	5.4
Volumetric moisture (TDR to 45cm, %)	41	35	36	36	18	34

4.3.3 Soil bulk density, particle density and porosity

Sample depth and site show significant effects on soil dry bulk density, particle density and porosity (Table 4.07). Location shows significant effects on bulk density and particle density, but not on porosity. Depth-site interaction and horizon type (A or B) effects are significant for bulk density and porosity, but not for particle density.

Table 4.07. Significance of the effects of various factors on soil dry bulk density, particle density and porosity.

Effect	Bulk Density	Particle Density	Porosity
Location	yes	yes	ns
Depth	yes	yes	yes
Site	yes	yes	yes
Depth-Site interaction	yes	ns	yes
Horizon type: A or B	yes	ns	yes

ns = not significant at the P = 0.05 level

At Burnside, soils at 4cm depth at all sites had lower dry bulk density and higher porosity than at 28, 42 or 64cm depths. At No.1 Dairy the pattern of variation in these properties is complex. Unusually low bulk density at 64cm depth at sites D4 and D6 may have been related to high organic matter based on the appearance of the soil; however, no tests were done for this property (Figure 4.15 and *Appendix 9 – Soil profiles*).

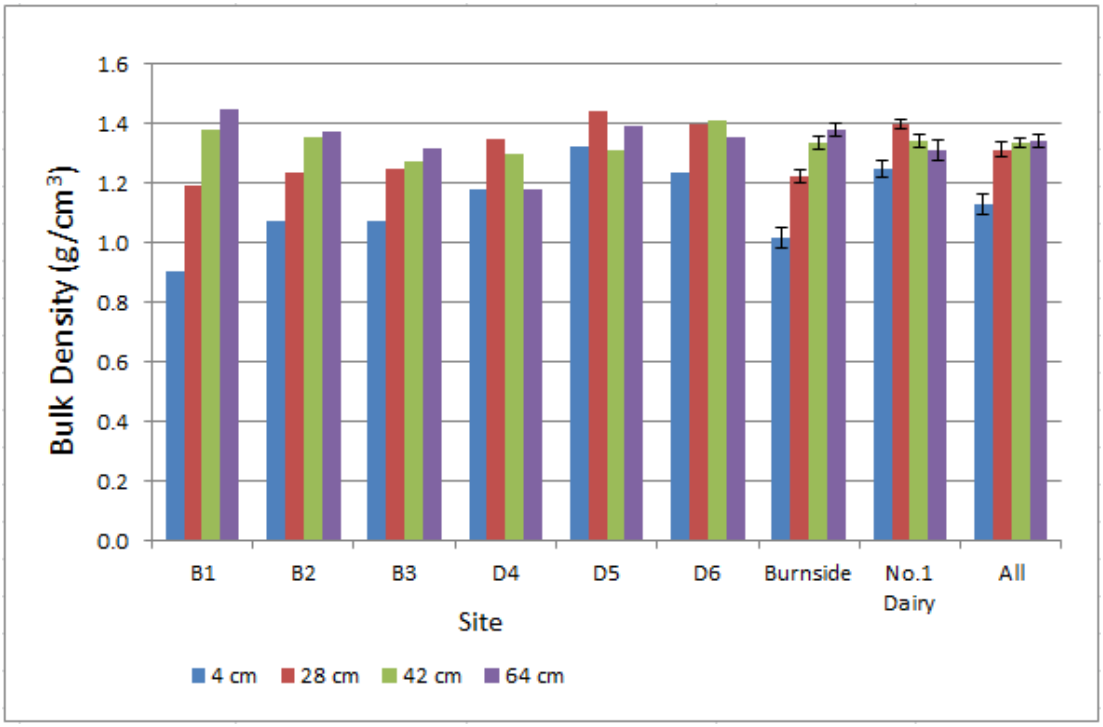

a.

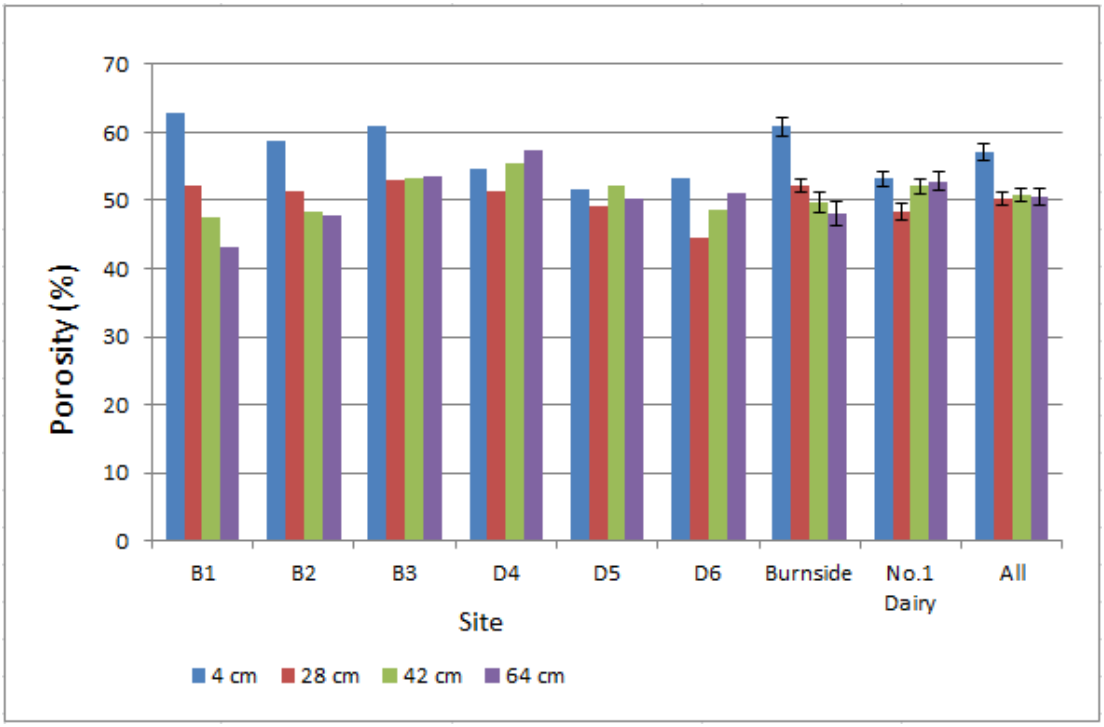

b.

Figure 4.15. a) Bulk density and b) porosity at soil sample sites. Error bars are standard errors of the means.

Bulk density was lower and porosity higher in A horizons (represented by samples from 4cm depth) by comparison with soil at greater depths. This may decrease EC_a near the soil surface in dry conditions, but increase EC_a in saturated conditions by supporting a greater volume of conductive soil solution. Differences in bulk density and porosity also occurred at other depths and between sites and locations. These differences are not expected to have weakened EC_a-moisture correlations in this study as they have their effect on EC_a entirely through moisture. (This finding does not relate to differences in soil texture or pore size distribution related to bulk density and porosity; for those effects see section *4.3.1 - Soil texture* and *4.2.8 - Moisture release characteristics of No.1 Dairy soil samples*).

4.3.4 EC of 1:1 soil pastes and extracts

EC of 1:1 soil pastes and paste extracts was highest close to the soil surface where lower paste:extract EC ratios were also observed at Burnside. This is consistent with deposition of soluble ions at the surface from fertiliser and manure. A similar trend, but less marked, is observed at No.1 Dairy (Figures 4.16, 4.17 and 4.18).

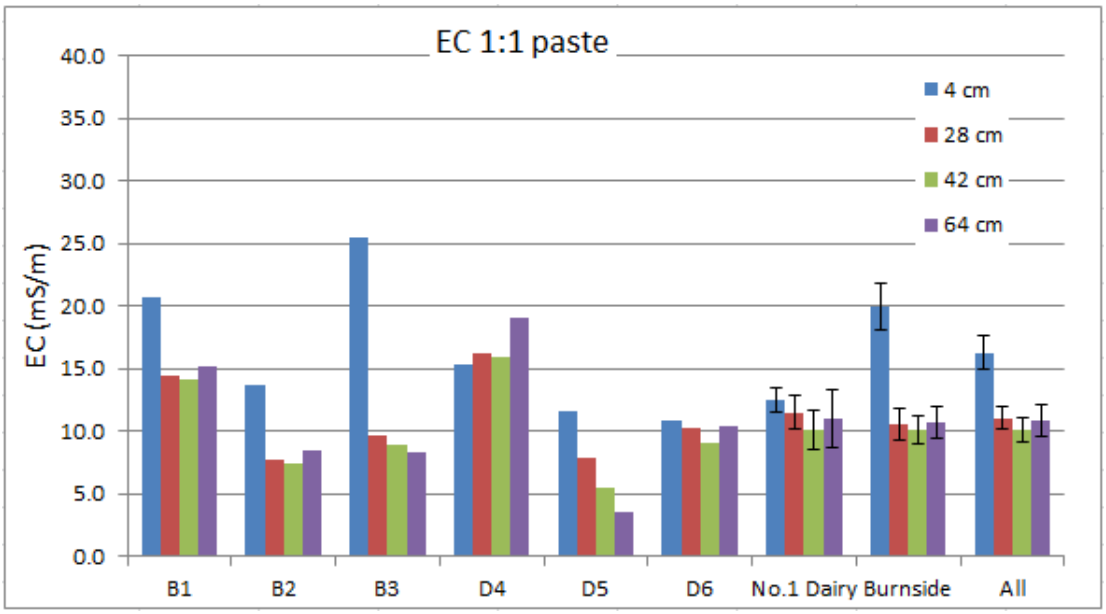

Figure 4.16. EC of 1:1 soil pastes from six sample sites (B1-D6), location means, and overall means. Error bars show standard error of the mean.

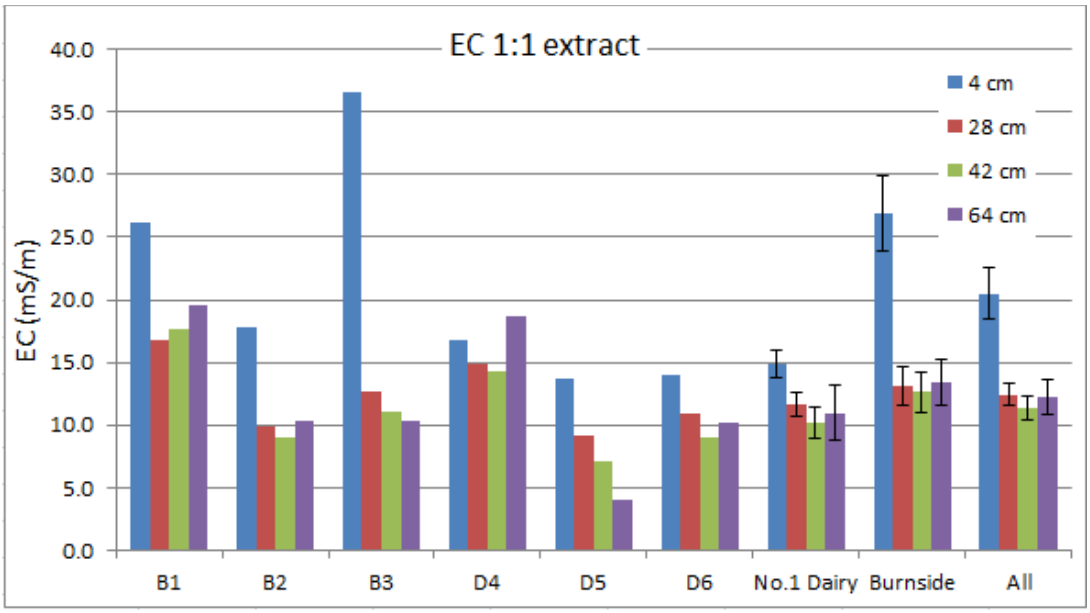

Figure 4.17. EC of 1:1 soil extracts from six sample sites (B1-D6), location means and overall means. Error bars show standard error of the mean.

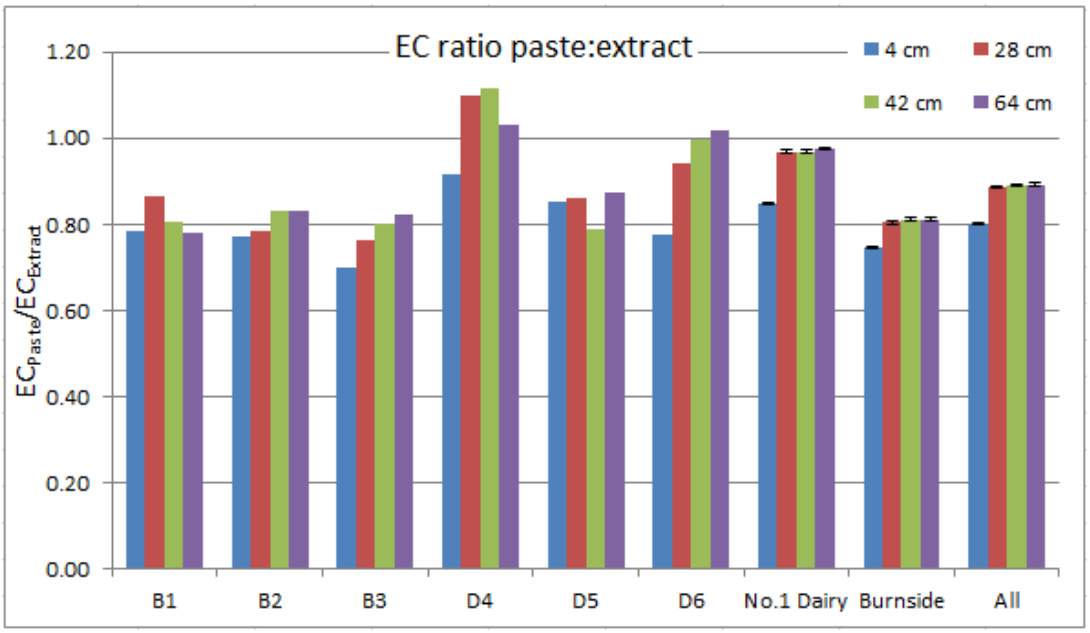

Figure 4.18. Ratios of EC of 1:1 soil pastes to the EC of their extracts from six sample sites (B1-D6), location means and overall means. Error bars show standard error of the mean.

The significance of the effects of various factors on the EC of soil paste, the EC of paste extract, and the paste:extract EC ratio are shown in Table 4.08.

Table 4.08. Significance of differences between measures of sample EC according to various factors.

Factor	EC 1:1 paste	EC 1:1 extract	EC ratio paste:extract
Location (Burnside or No.1 Dairy):	ns	ns	ns
Depth (across both locations):	significant	significant	significant
Site: (across both locations):	significant	significant	significant
Depth/Site interaction:	significant	significant	significant
Horizon type (A or B, both locations):	significant	significant	significant
Horizon type (gley or non-gley, both locations):	significant	significant	ns

ns = not significant at P <0.05 level.

Soil EC, EC_a and moisture

Correlations of EC_a (EM38 Mk2, 1m, vertical mode) with EC of 1:1 soil pastes were stronger than with 1:1 extracts or paste:extract EC ratios, across both locations and at each location (Table 4.09).

Table 4.09. R^2 values of linear correlations of EC_a with EC of 1:1 soil paste at sample sites.

	EC_a (EM38 Mk2, 1m vertical, mS/m)	EC_a (EM38 Mk2, 1m horizontal, mS/m)	EC_a 0-45cm (calculated, mS/m)
Both locations	0.69	0.70	0.52
Burnside	0.47	0.52	ns
No.1 Dairy	0.90	0.86	0.60

ns = not significant at the P < 0.05 level. EC data is simple means to 42cm depth.

It was thought that regressions using EC of soil paste at 4cm, 28cm and 42cm as separate predictors in a multiple regression might improve correlations with EC_a by allowing each variable to be weighted to match the sensitivity profile of the EM38

Mk2; however, no correlations produced by this method were markedly better than correlations with means to 42cm. Neither did depth resolution of upper profile EC_a improve correlations with EC of soil paste.

Resolution of EC_a depth profiles at soil sample sites therefore produced mixed results: correlation with soil moisture appears to be improved slightly at No.1 Dairy but no improvements of correlations with EC of soil paste or with soil texture at either location are observed, despite that these properties are strongly correlated with whole profile EC_a. (The latter was not an objective of this study but could have helped confirm the effectiveness of the depth profile resolution method).

EC of 1:1 soil pastes is more strongly correlated than soil moisture with EC_a (Tables 4.01 and 4.09). Interaction effects on EC_a between soil EC and soil moisture are expressed in the 'dual pathway model' of Rhoades et al. (1976) in which soil volumetric moisture content and solute concentration are multiplied together as components of EC_a (section *2.2.1 - The 'dual pathway' model of EC_a*). Inclusion of EC x soil moisture effects was also found to improve correlation with EC_a by multiple linear regression in this study (Table 4.10).

As EC of soil paste was found to vary between sites, locations, depths and horizon types (Table 4.08) variable soil solute concentration may therefore have weakened EC_a-moisture correlations in this study by causing variation in EC_a-moisture relationships. In particular, correlation by multiple linear regression of EC of soil pastes, soil moisture, and EC x soil moisture at Burnside showed much stronger correlation than EC of soil pastes with EC_a or soil moisture with EC_a, the latter being insignificant. Variation in the EC_a-soil moisture relationship at Burnside caused by interaction between soil moisture and variable soil solute concentrations, both spatially and with depth, is therefore the most probable cause so far identified for the lack of a significant EC_a-soil moisture correlation at soil sample sites at Burnside.

Table 4.10. Correlation by multiple linear regression of EC_a with EC of 1:1 soil paste, soil volumetric moisture and EC x moisture (representing interaction effects) at sample sites at Burnside and No.1 Dairy. EC data is means to 42cm depth; moisture is by TDR to 45cm. EC_a is EM38 Mk2, 1m, vertical mode.

Burnside	**Predictor**	**R^2**	**Significance of *F***
	All	0.87	0.012
		Coefficient	***P***
	Paste EC	-0.29	0.21
	Moisture	-0.56	0.48
	EC*Moisture	0.008	0.20
No.1 Dairy	**Predictor**	**R^2**	**Significance of *F***
	All	0.91	0.005
		Coefficient	***P***
	Paste EC	0.08	0.76
	Moisture	-0.26	0.71
	EC*Moisture	0.002	0.80

4.4 Kinematic surveys

This section examines the general distribution of EC_a from kinematic surveys followed by its relationships to soil moisture and the influence of other soil properties.

4.4.1 Reconnaissance surveys: topography and EC_a

Mapped, kriged data of EC_a (EM38 Mk2, 1m) and elevation for the whole Burnside block from the reconnaissance survey are shown in Figures 4.19 and 4.20 respectively. The study location in the southwest corner of the block shows limited variation in EC_a compared with the block as a whole as it was thought that EC_a-soil

moisture relationships might be more difficult to detect across the full range of EC_a present, incorporating areas of very low EC_a probably caused by near-surface gravels, for example in the northeast corner of the block. The edge of a terrace riser of about 3m height extends onto the southeast corner of the study location. Two other terrace risers are evident at Burnside: across the middle of the block from about 104-106m elevation, and striking northeast across the northern end from about 102-104m elevation.

The No.1 Dairy study location showed a slightly greater range of EC_a than the Burnside study location, more representative of the whole range across the reconnaissance area. It was considered more probable that this variation was strongly influenced by moisture than the variation observed at Burnside as it occurred within an area previously mapped as a single soil type, whereas at Burnside the variation across the block was suggestive of shallow gravels in some areas (information from the farmer supported this interpretation). The terrace riser running along the east side of the No.1 Dairy study location is evident at about 40-42m elevation (Figure 4.21).

Negative measurements of EC_a

The reconnaissance surveys of both Burnside and No.1 Dairy produced some negative measurements of EC_a by the EM38 Mk2 (1m, vertical). While negative electrical conductivity is a theoretical impossibility, the indirect measurement of EC_a as the ratio of secondary to primary magnetic fields in EMI can produce negative measurements. This may indicate interference from metal objects or faulty calibration, but in conditions of low EC_a some negative values which are not the result of interference may be produced even after correct calibration of the EMI instrument. In such instances there is no theoretical basis to guide alteration of the calibration or scaling up of the dataset.

In this study where the data was for qualitative use i.e. only relative differences in EC_a were of interest, and where the negative values were contiguous with other low

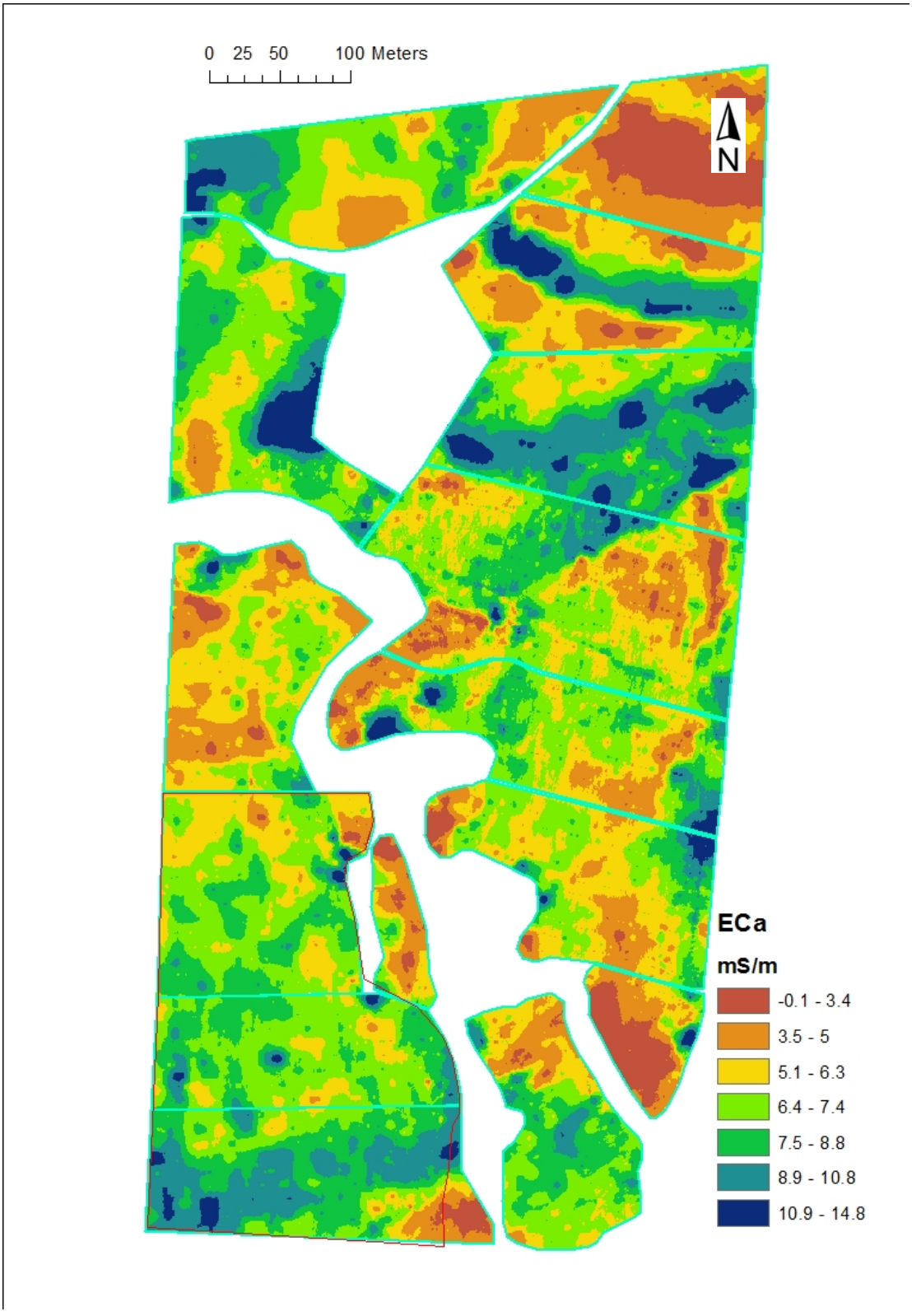

Figure 4.19. EC_a (EM38 Mk2, 1m) in the reconnaissance survey of Burnside Block on 22 August, 2011. The study location is outlined in red in the southwest corner.

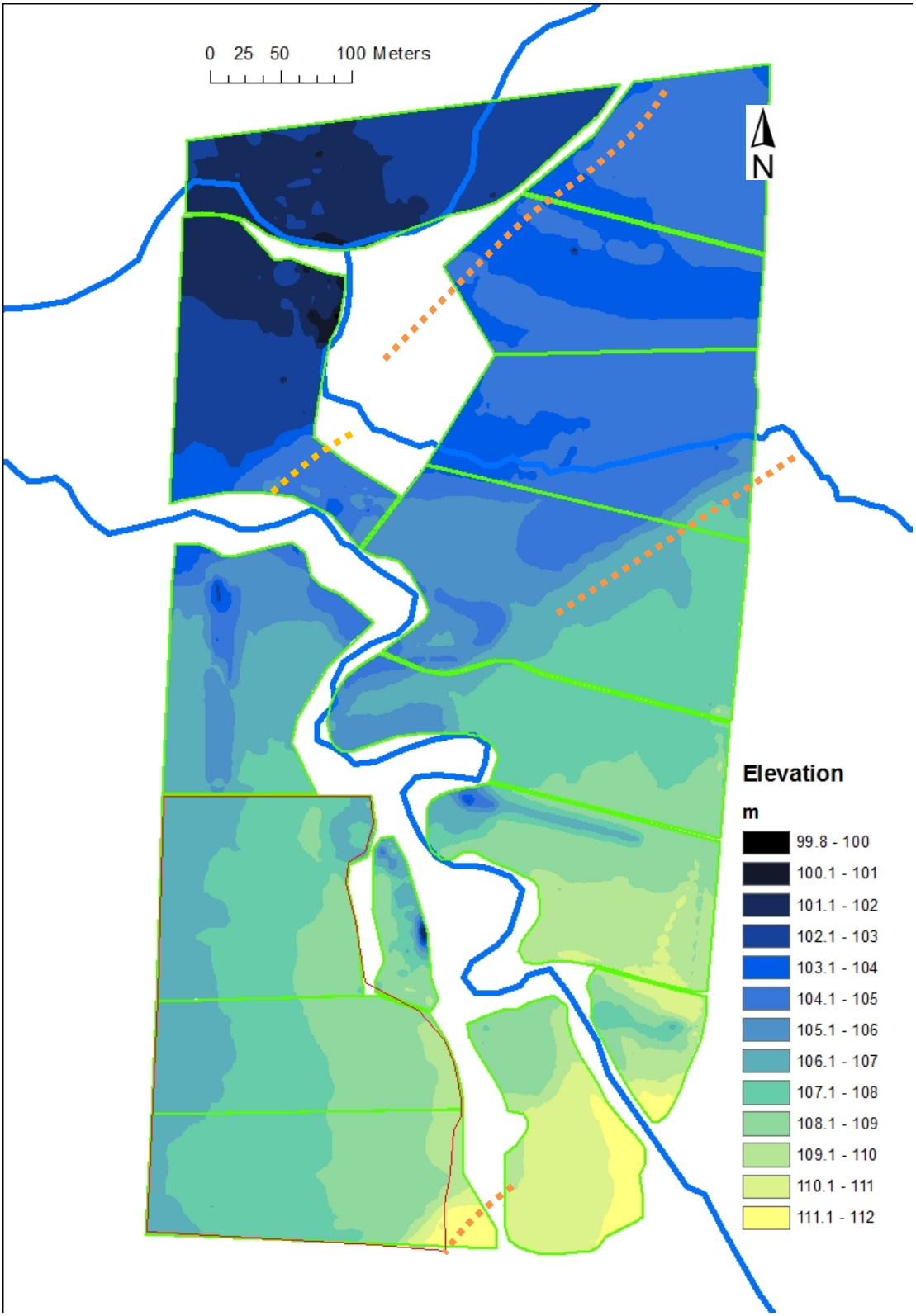

Figure 4.20. Elevation at Burnside Block from RTK GPS data gathered in the reconnaissance survey on 22 August, 2011. Dotted lines show approximate positions of terrace risers. Streams are shown in blue line (Totara Stream enters the block at the high southeast corner).

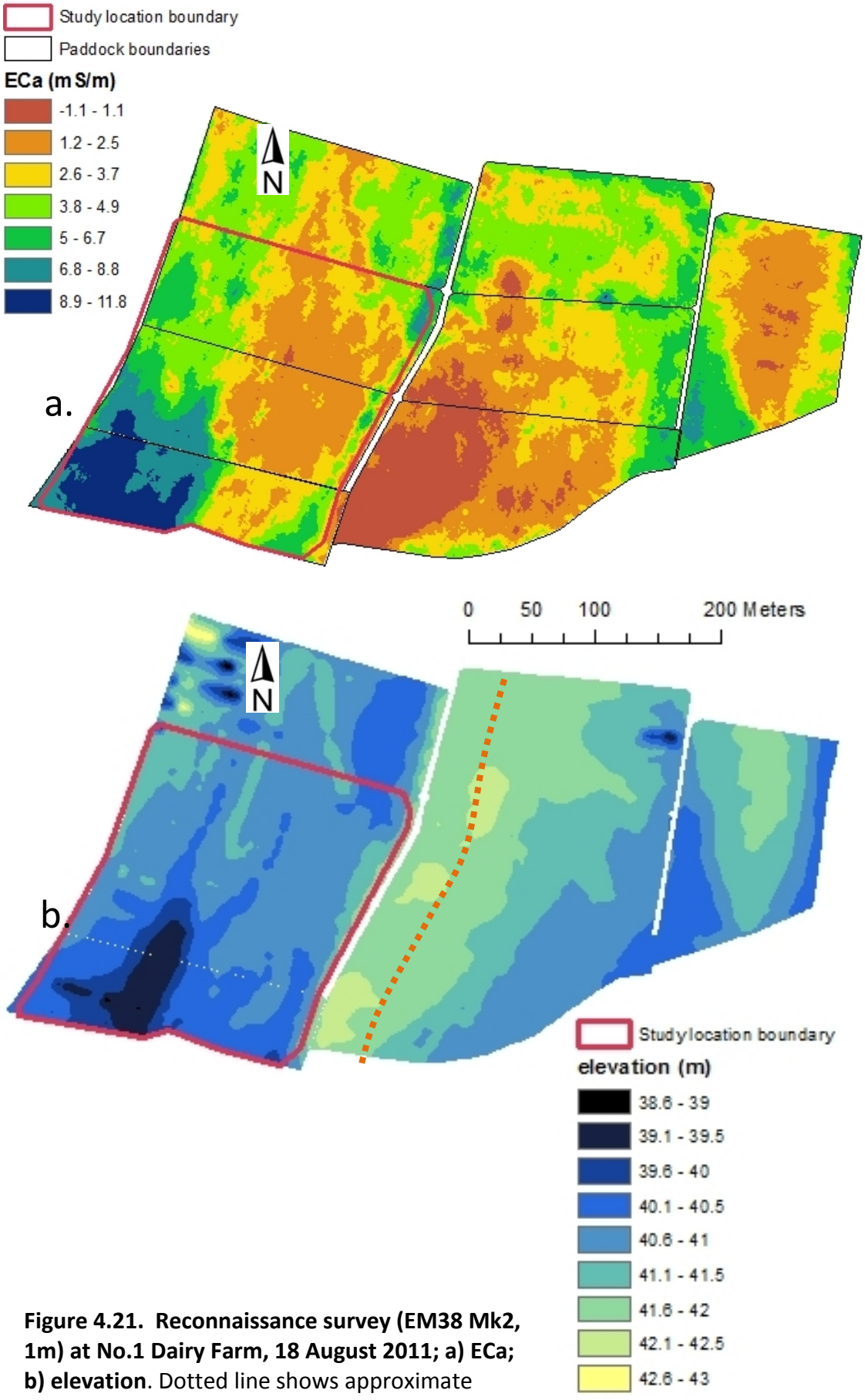

Figure 4.21. Reconnaissance survey (EM38 Mk2, 1m) at No.1 Dairy Farm, 18 August 2011; a) ECa; b) elevation. Dotted line shows approximate position of terrace riser.

values of EC_a, so appearing representative of the landscape and not isolated interference, negative values were retained in datasets. For quantitative use of EC_a data e.g. for EC_a depth profile resolution, negative values which were few in number were excluded from datasets. Large numbers of negative values in EM38 Mk2 (0.5m) data, discussed in *4.4.3 EM38 Mk2 – EM38 Mk2, 0.5m*, were apparently the result of faulty calibration and meant that the data could only be used qualitatively, or not at all.

4.4.2 EM31

The main use of the EM31 data was for comparison with EM38 Mk2 data for EC_a depth profile resolution or for qualitative comparisons. The potential to interpret the EM31 data in terms of soil moisture was limited because no accompanying moisture or soil property data was collected for the full range of the 'effective measurement depth' i.e. to 6m. This was because installation of the piezometers was only successful to 3-4m depth at the maximum, and these depths for the most part remained above the water table at both locations, leading to the abandonment of this element of the programme. The deepest soil samples were from 64cm depth, TDR to 45cm depth, also too shallow to effectively match EM31 measurements of EC_a.

EC_a (EM31) at No.1 Dairy was lower on January 25, 2012 than on 8 November, 2011, and the area of lowest conductivity had increased and spread south (Figure 4.22). EC_a (EM31) at Burnside on 29 September, 2011 and 4 January, 2012 was similar (Figure 4.23). The ranges of EC_a (EM31) at Burnside and No.1 Dairy were similar for the two surveys at each location, showing apparent stability and consistency of EM31 measurements.

Exclusion of EM31 data points within interference range of electric fences according to the results of EMI instrument functional tests resulted in large areas of the study locations without EM31 data; interpolation in these areas was based only on adjacent points. (Interference range was estimated at 15m but points were excluded only within 12m of fences to retain more data; see section *3.6.3 –Functional tests - Fence Interference* and *4.1 – EMI instrument functional tests*). The resulting coverage

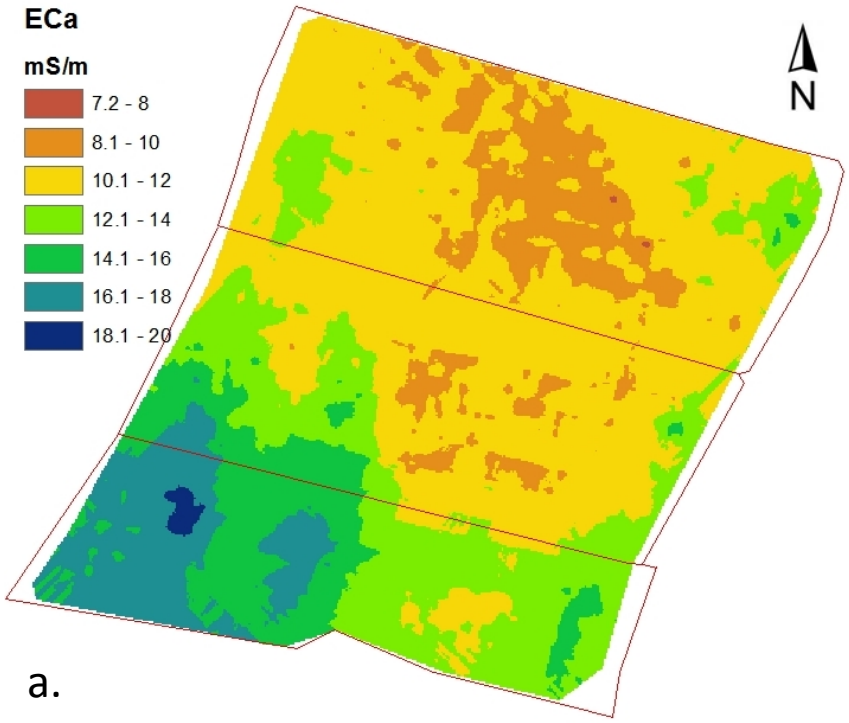

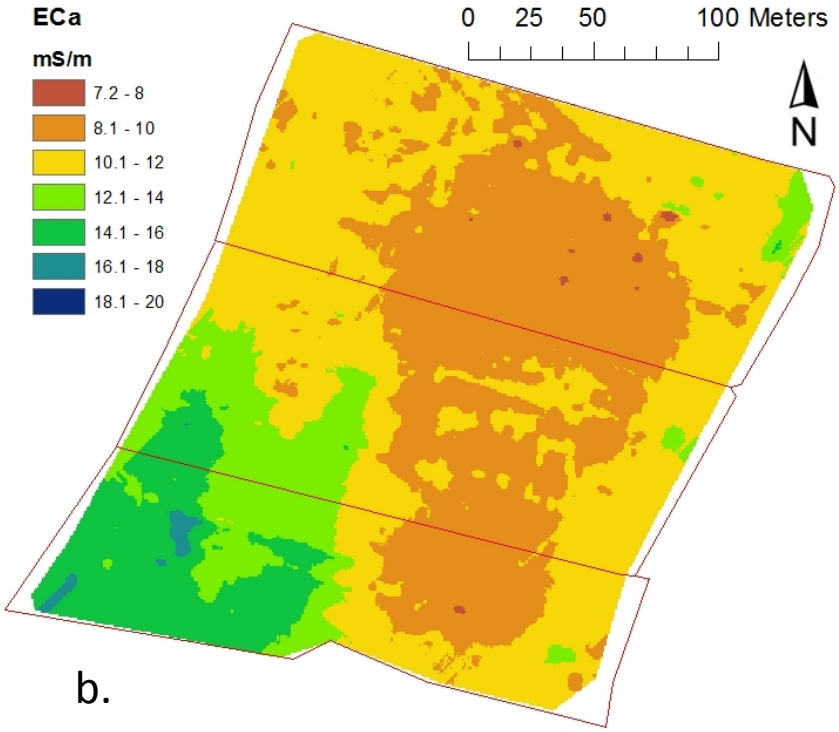

Figure 4.22. EC_a from EM31 kinematic survey of No.1 Dairy location on: a) 8 November 2011; b) 25 January 2012.

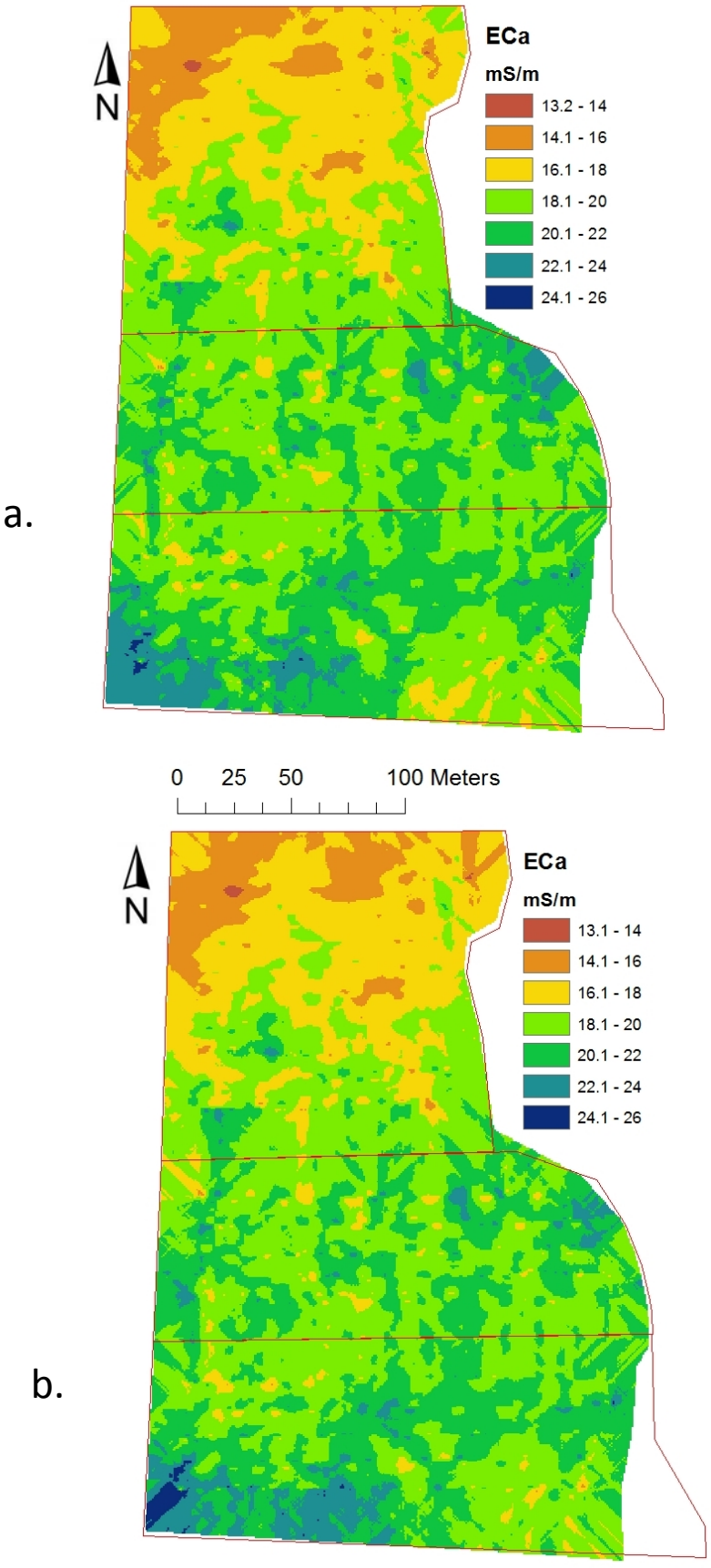

Figure 4.23. EC_a from EM31 kinematic survey of Burnside location on: a) 29 September 2011; b) 4 January 2012.

of EM31 data points at No.1 Dairy on 8 November, 2011 is shown in Figure 4.24. Measurements of soil moisture by TDR in areas without EM31 measurements were removed from datasets for the purpose of correlations with EC_a.

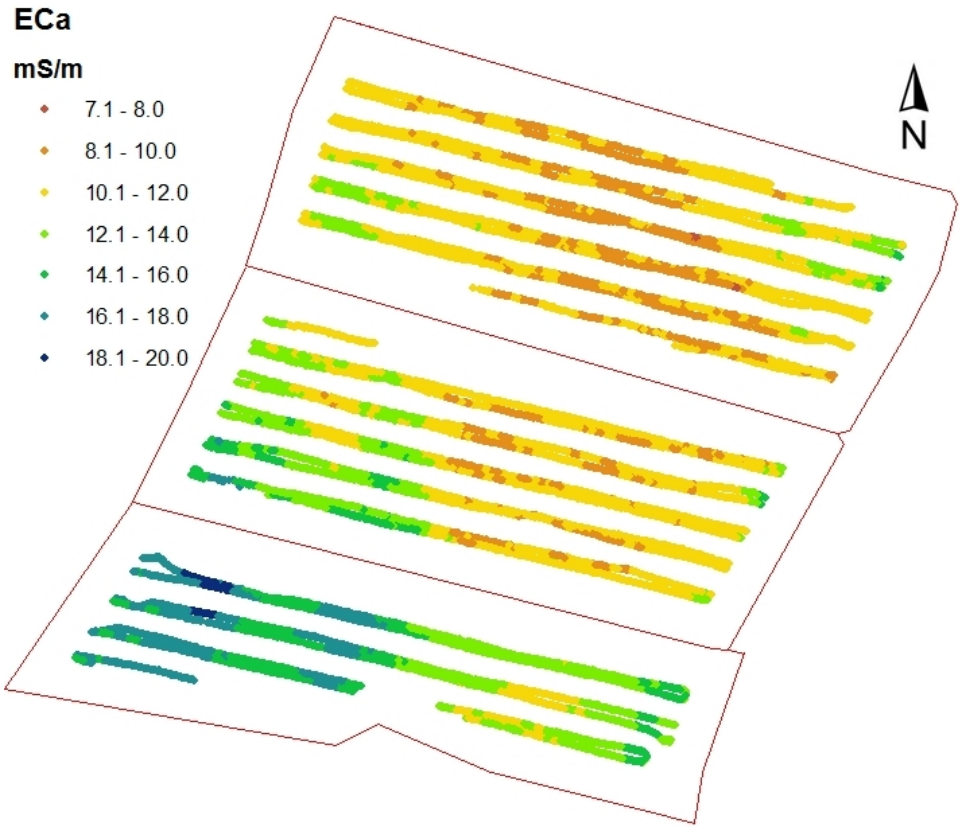

Figure 4.24. EM31 data points at No.1 Dairy, 8 November 2011 (points <12m from fences deleted). Note: Because the EM31 was mounted on a boom to the side of the ATV which was driven in alternate directions across the paddock, guided by the centrally mounted GPS antenna, the swaths (according to the sensor position) were not evenly distributed. This is revealed in the above figure due to correction of the data point locations for GPS offset.

4.4.3 EM38 Mk2

Burnside: EM38 Mk2, 1m

EC_a (EM38 Mk2, 1m) measured at Burnside was higher in the kinematic survey on 29 September, 2011 than on 22 August, 2011, and lowest of all three surveys on 4 January 2012 (Figure 4.25.) The relative pattern of EC_a was similar on the three

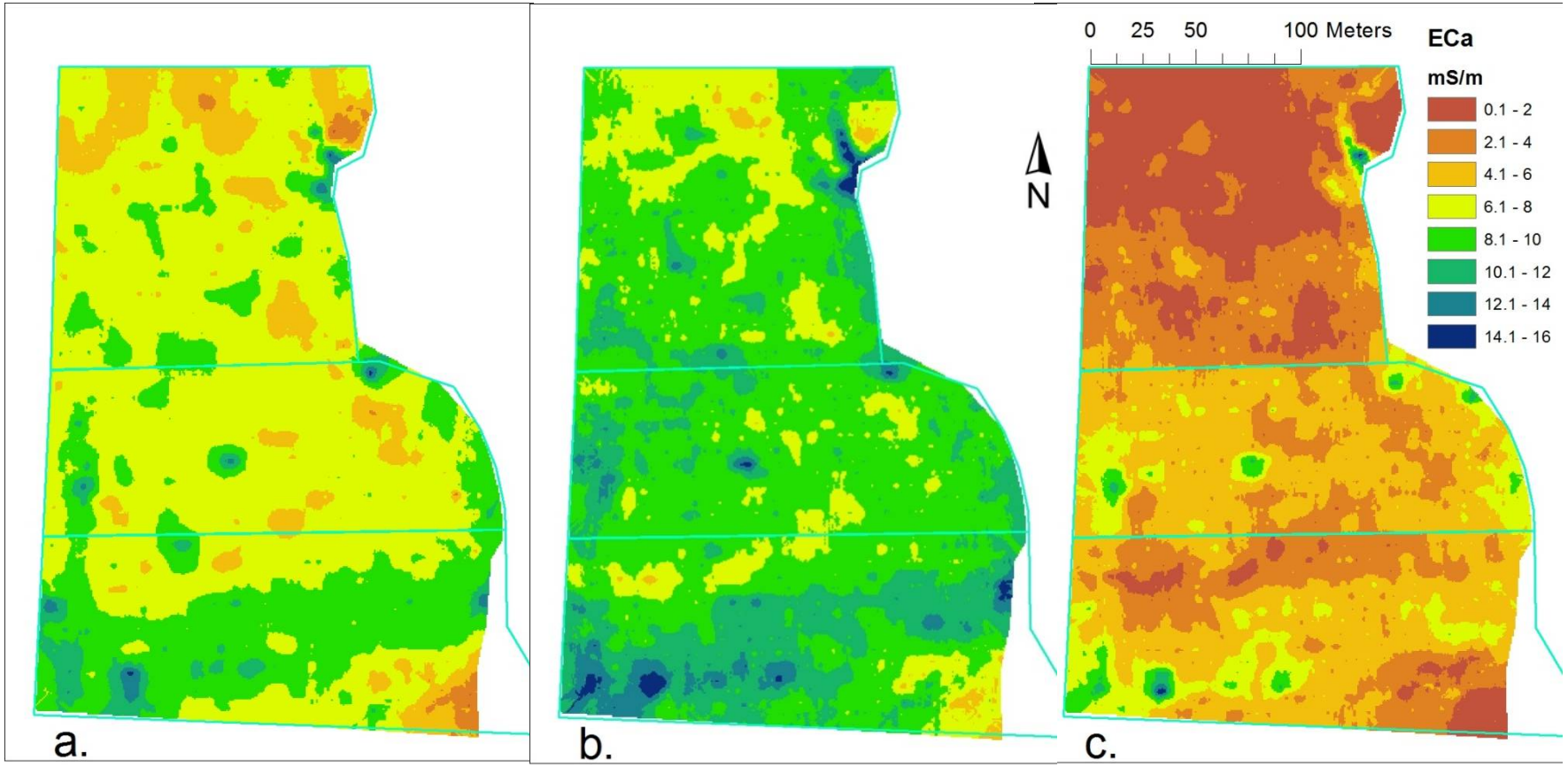

Figure 4.25. EC_a (EM38 Mk2, 1m) at Burnside on: a) 28 August, 2011; b) 29 September, 2011; c) 4 January, 2012.

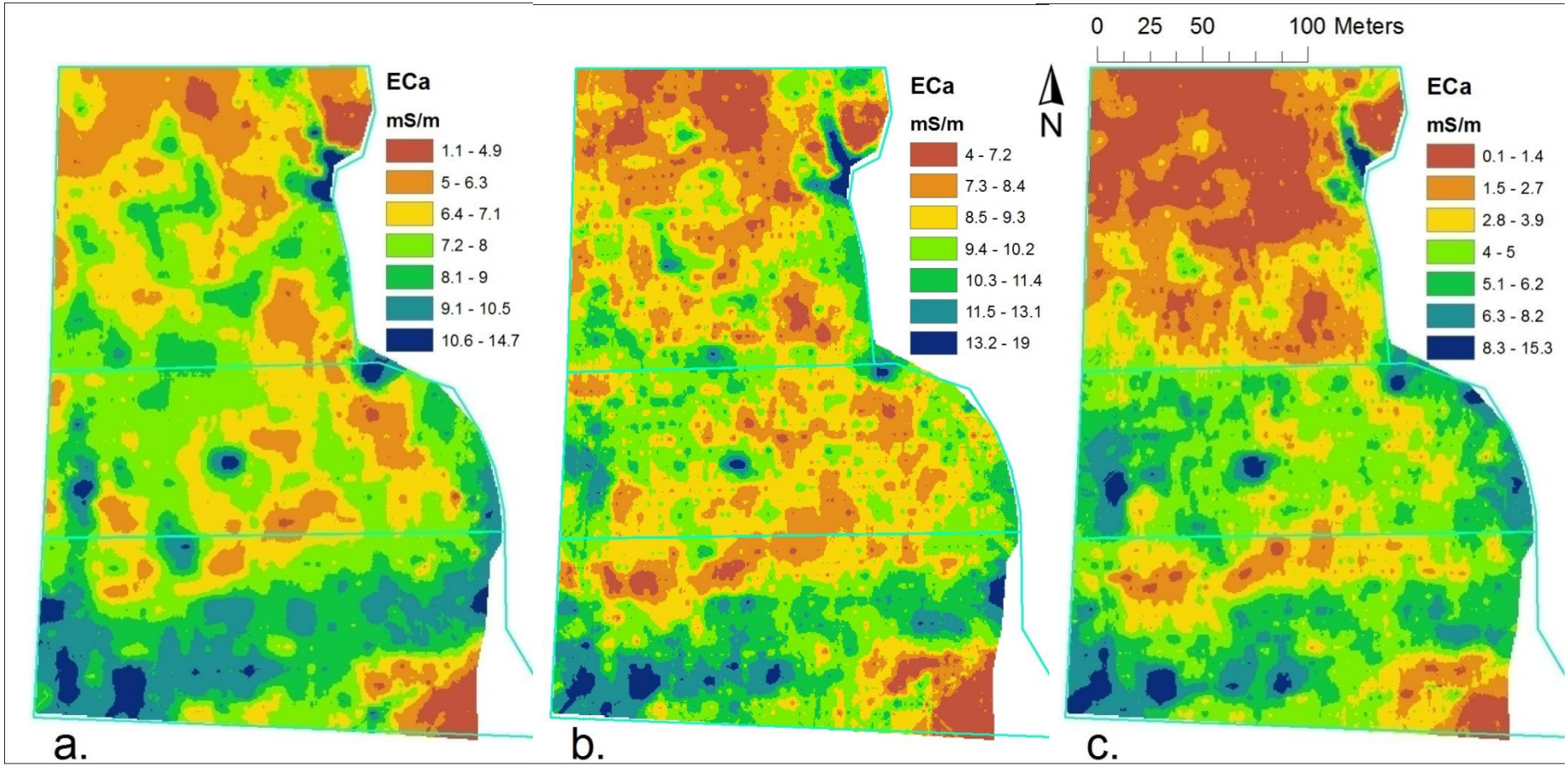

Figure 4.26. EC_a (EM38 Mk2, 1m) relative patterns (Jenks natural breaks) at Burnside on: a) 28 August, 2011; b) 29 September, 2011; c) 4 January, 2012.

survey dates (Figure 4.26.) In the last survey on 4 January 2012 a discontinuity appeared whereby the most northerly paddock showed lower EC_a than the other two paddocks with a noticeable change in EC_a at the fence line. This was not evident in EM31 data for the same date (Figures 4.23 and 4.25).

No.1 Dairy: EM38 Mk2, 1m

EC_a at No.1 Dairy from EM38 Mk2 (1m) data was similar in range and spatial pattern for the three surveys on 18 August 2011 (the reconnaissance survey), 8 November 2011 and 25 January 2012, except that as with the EM31, more high values were measured on 8 November 2011, and low values were concentrated farther south on 25 January 2012 than on 8 November 2011. The 25 January survey also appeared to show less variation in EC_a; the standard deviation of the EM38 Mk2 (1m) data for that date was indeed lower (Figures 4.27 and 4.28).

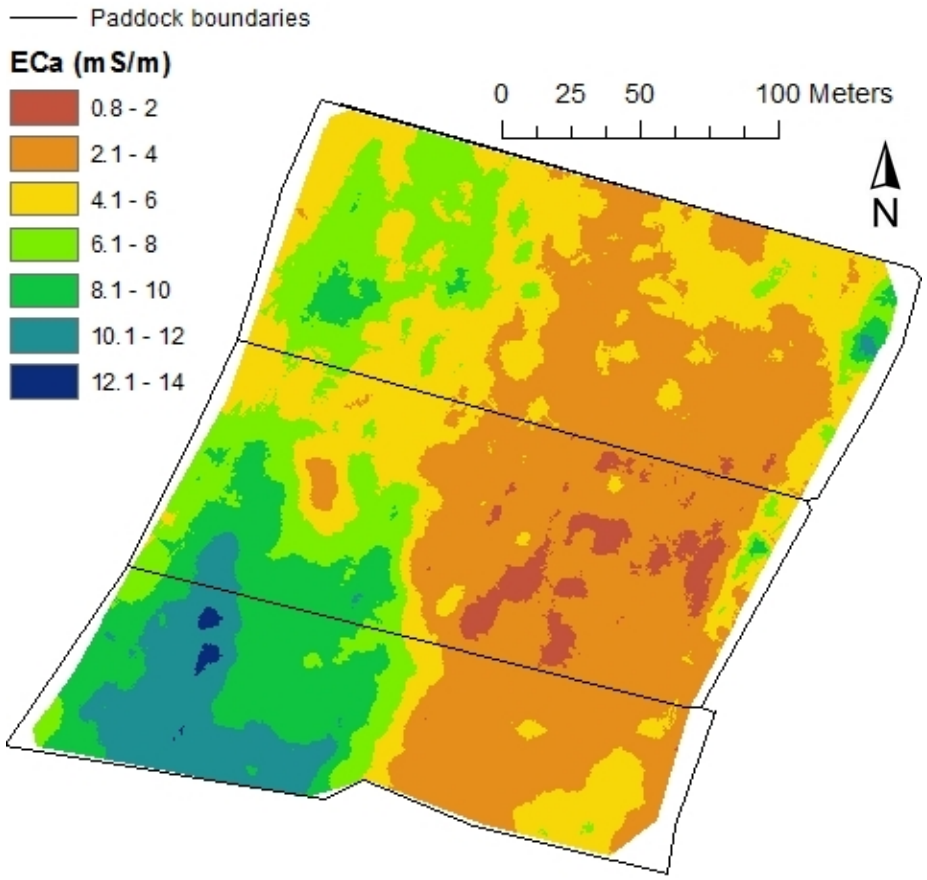

Figure 4.27. EC_a (EM38 Mk2, 1m) kinematic survey of No.1 Dairy location on 25 January 2012.

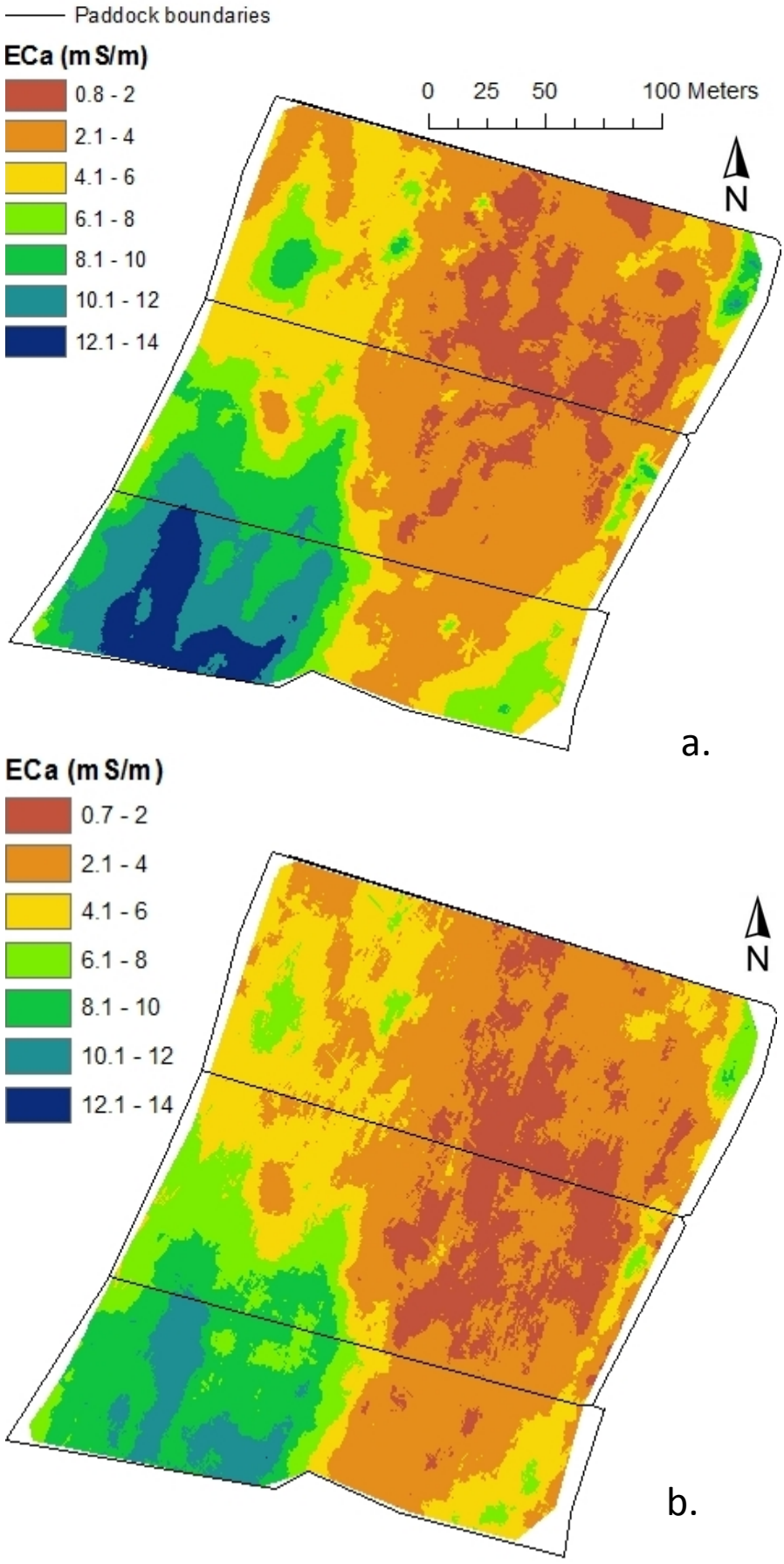

Figure 4.28. EC_a (EM38 Mk2, 1m) kinematic survey of No.1 Dairy location on: a) 8 November 2011; b) 18 August 2011.

EM38 Mk2, 0.5m

Despite the standard calibration procedure, EC_a measurements from the 0.5m coil separation contained many negative values in all surveys. While it may be presumed that these negative values were inaccurate (negative electrical conductivity being impossible) their distribution was contiguous with wider areas of low EC_a measurements from both 0.5m and 1m coil spacings of the EM38 Mk2 and from the EM31; the impression therefore was of faulty calibration requiring correction of the whole 0.5m dataset rather than deletion of anomalous values. Issues with connection or disconnection of the datalogger to the EM38 Mk2 before or after calibration may have been one cause of this error which was not identified until after the kinematic surveys were complete (see section *4.1 – EMI instrument functional tests* and *Appendix 6 - EMI instrument functional tests- Cable and connection effects*).

As no rational basis was found to guide adjustment of the dataset, the 0.5m data could only be used qualitatively. This is unfortunate because the sensitivity of the EM38 Mk2 (0.5m) to near surface EC_a , which is of high relevance to soil moisture and other properties in the agricultural context, complements the deeper sensitivity profiles of the EM38 Mk2 (1m) and EM31, so that absolute values from the 0.5m coil spacing might provide for useful comparisons if they could be obtained.

EM38 Mk2 (0.5m) data from Burnside was discarded because in addition to containing many negative values the data range varied widely between different surveys. EC_a measured by the EM38 Mk2 (0.5m) at No.1 Dairy contained fewer and less negative measurements than at Burnside and the data range was consistent for the three surveys on 18 August and 8 November 2011 and 25 January 2012; therefore the EM38 Mk2 (0.5m) data was retained but for qualitative use only.

As with EC_a measured by the EM38 Mk2 (1m) and EM31, low values were concentrated further south on 25 January and the effect is more marked than in data from the EM38 Mk2 (1m) or the EM31. High temporal change between surveys is indicated in the northwest corner of the study location (Figures 4.29 and 4.30).

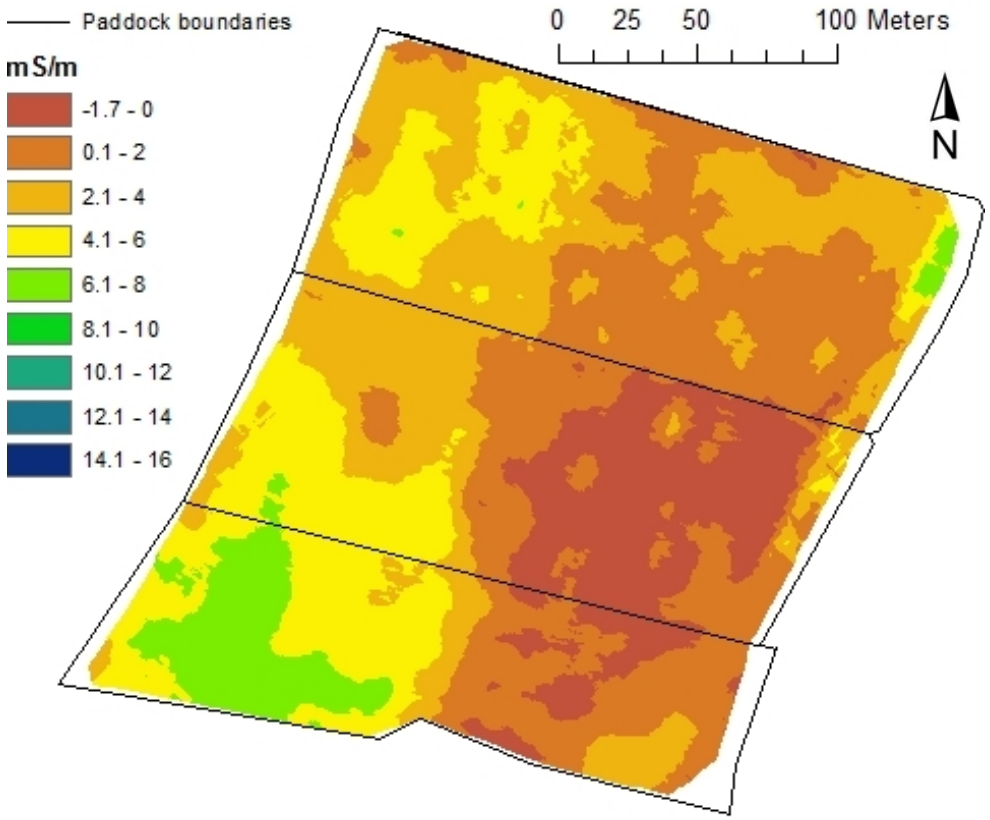

Figure 4.29. EC_a (EM38, 0.5m) kinematic survey of No.1 Dairy location on 25 January 2012.

4.4.4 Kinematic surveys: comparisons between EMI instruments

All EC_a means of all data from each kinematic survey were significantly different (α = 0.05) between instruments, surveys, and locations, except for EM38 Mk2 (0.5m) from the 18 August and 8 November surveys at No.1 Dairy. The overall pattern of the EC_a survey data was that EM38 Mk2 measurements were significantly lower than EM31 measurements interpolated to the same locations, and EM38 Mk2 (0.5m) measurements significantly lower than those from the 1m coil spacing (Figure 4.31).

With regard to the EM31 the above results call into question whether the instrument does indeed give a scaled measurement of similar magnitude but different profile to the EM38 Mk2, or whether the greater and deeper response of the EM31 simply produces a greater measurement of EC_a.

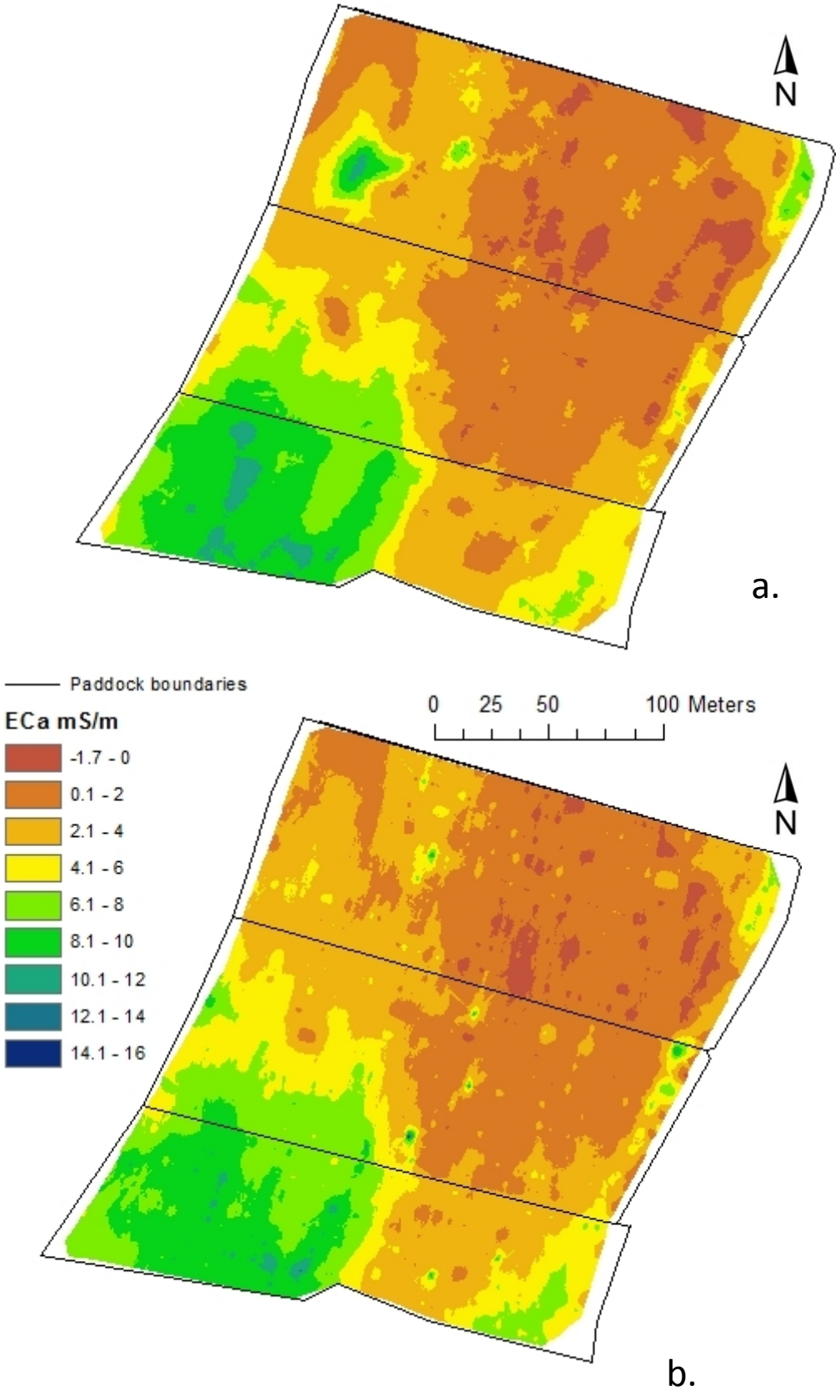

Figure 4.30. EC_a (EM38 Mk2, 0.5m) kinematic survey of No.1 Dairy location on: a) 8 November 2011; b) 18 August 2011.

a.

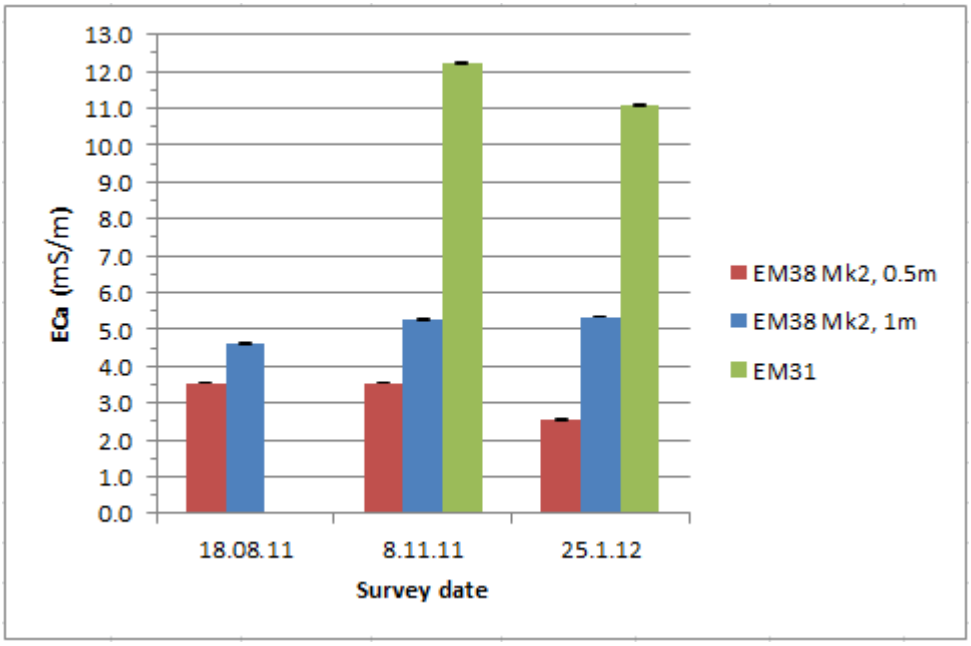

b.

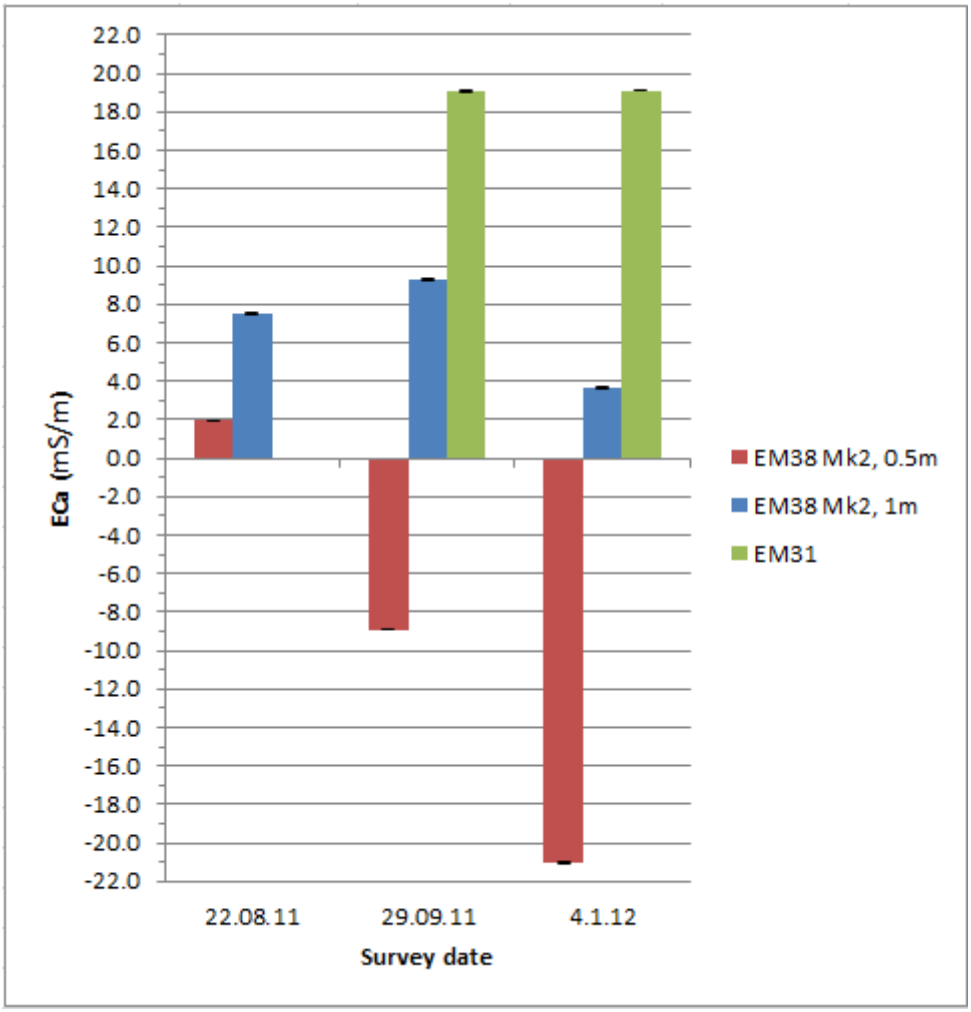

Figure 4.31. EC_a means from a) three surveys at No.1 Dairy; b) three surveys at Burnside. Standard errors of the means are shown but are too small to be easily distinguished.

It was known from coring of piezometer boreholes that gravels were present at depths between 2.9 and 3.8m at 3-4 sites distributed widely across each location. Therefore as the soils at Burnside and No.1 Dairy were overlying gravels, possibly saturated with groundwater but non-saline, and upper profiles were silty, moist, fertilised and manured, EC_a is expected to have been higher in the upper profiles, certainly above gravel depth. Depth resolution of EC_a and analysis of raised height measurements at soil sample sites supports this view. It therefore appears unlikely in this study that the deeper EM31 measurements of EC_a would be greater in magnitude than those of the EM38 Mk2 if the two instruments' responses were scaled to be equivalent for an even profile.

4.4.5 Two-layer models from kinematic surveys

Mean EC_a of the top 45cm of soil profile, calculated from all measurements by the EM31 and EM38 Mk2 (1m) in kinematic surveys according to the methods described in section *3.7.3 – EC_a Depth Profile Resolution* and *Appendix 7 - EC_a depth profiles: method development* is shown in Table 4.11.

Table 4.11. Mean EC_a from kinematic surveys as measured by EM31 and EM38 Mk2 (1m, vertical) and as modeled for the upper 45cm of soil profile.

	EM31 (vertical)	EM38 Mk2 (1m, vertical)	0 – 45cm (even layers)	0 – 45cm ('field profile')
Burnside, 29.9.11	19.1	9.3	-23.41	-20.10
Burnside, 4.1.12	19.1	3.7	-48.55	-20.11
No.1 Dairy, 8.11.11	12.2	5.3	-17.96	-41.66
No.1 Dairy, 25.1.12	11.1	5.3	-13.83	-34.77

Note: 'Even layers' and 'field profile' refer to approximations of variation in EC_a within the modelled depth layers, 0-45cm and 45cm+. In the even-layered model EC_a is considered evenly distributed within each of the two depth layers. A full explanation is given in *3.7.3 EC_a depth profile resolution* and *Appendix 7 – EC_a profiles: method development.*

It is apparent in Table 4.11 that means of calculated EC_a of the top 45cm of profile for the two surveys at each of the two locations show negative and therefore unrealistic values. According to the method and depth resolution indices used in this study, negative values should not be produced as these relate to situations where the contribution of EC_a derived from the top 45cm of profile is less than zero which is not possible. Accordingly, EC_a measured by the EM31 (vertical mode, raised 80cm) should in no case exceed 1.3x that measured by the EM38 Mk2 (1m, vertical mode, raised 6cm) in the even-layered profile model, or in the field simulation model, EM31 should in no case exceed 0.95 x EM38 Mk2 (see *Appendix* 7 and Figure A7.07). In other scenarios, e.g. increasing salinity with depth, EM31 might well exceed EM38 Mk2 by more than these amounts and would not produce negative values according to an appropriate depth resolution index.

As shown in Table 4.11 the EM31 gave measurements of EC_a on average more than twice the magnitude of EM38 Mk2 measurements in every survey in which both instruments were used. The greater measurements of the EM31 appear implausible as high EC_a at depth is not expected in non-saline soils over gravels such as those at Burnside and No.1 Dairy. If, however, EC_a in the layer below 45cm, for which few measurements were available, had EC_a much higher than expected, this would have resulted in calculation by EC_a depth profile resolution of negative EC_a for the top 45cm of profile, as the even-layered and field simulation models used were inappropriate for such a scenario.

Resolution of EC_a depth profiles from kinematic surveys was therefore prevented because the assumption of comparability (not equivalence) between EC_a measurements by the EM31 and EM38 Mk2 was not satisfied, and/or because characterisation of EC_a variation within the two modelled depth layers was inadequate. For whichever reason, EC_a values modelled for the upper profile in kinematic surveys were inaccurate and have not been included in further analyses of the data.

4.4.6 EC_a and soil moisture in kinematic surveys

Moisture measurements accompanying kinematic surveys ranged from 18.5-49.3% volumetric moisture and differed significantly between the two surveys for which moisture was measured at each location (Figure 4.32). As with the individual site measurements, Burnside was on average wetter than No.1 Dairy. The positions of the TDR measurements are shown in Figures 4.33, 4.34 and 4.35.

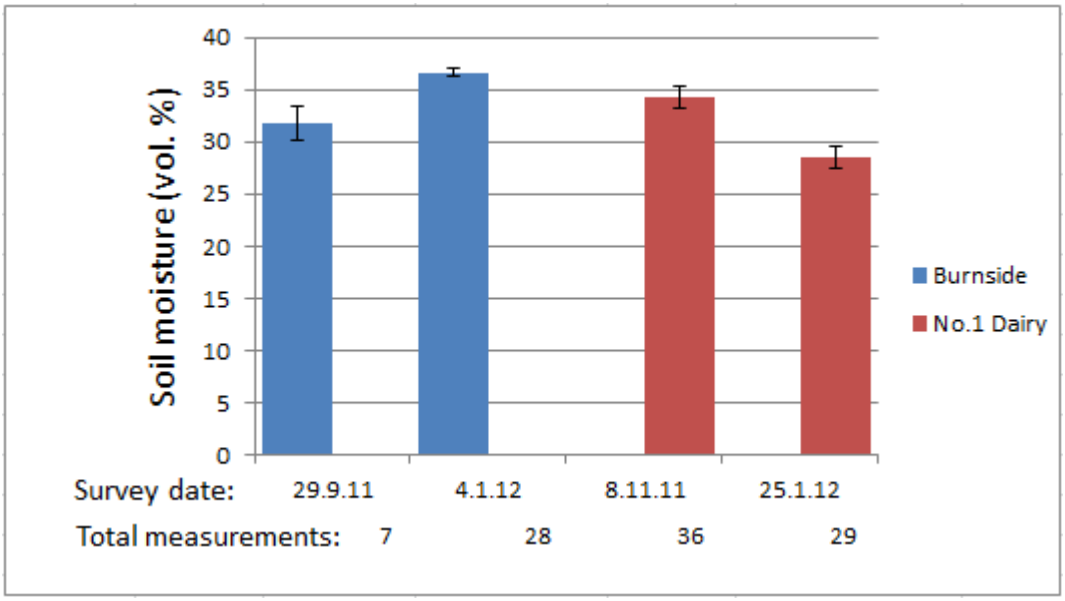

Figure 4.32. Mean soil volumetric moisture accompanying kinematic surveys at two locations on different dates. Error bars are standard error of the mean. The first survey at Burnside (29.9.11) had far fewer measurements as these were from gravimetric analysis of three samples (4, 28 and 64cm depths) taken at each site. TDR proved a quicker method in the field and was adopted for subsequent surveys.

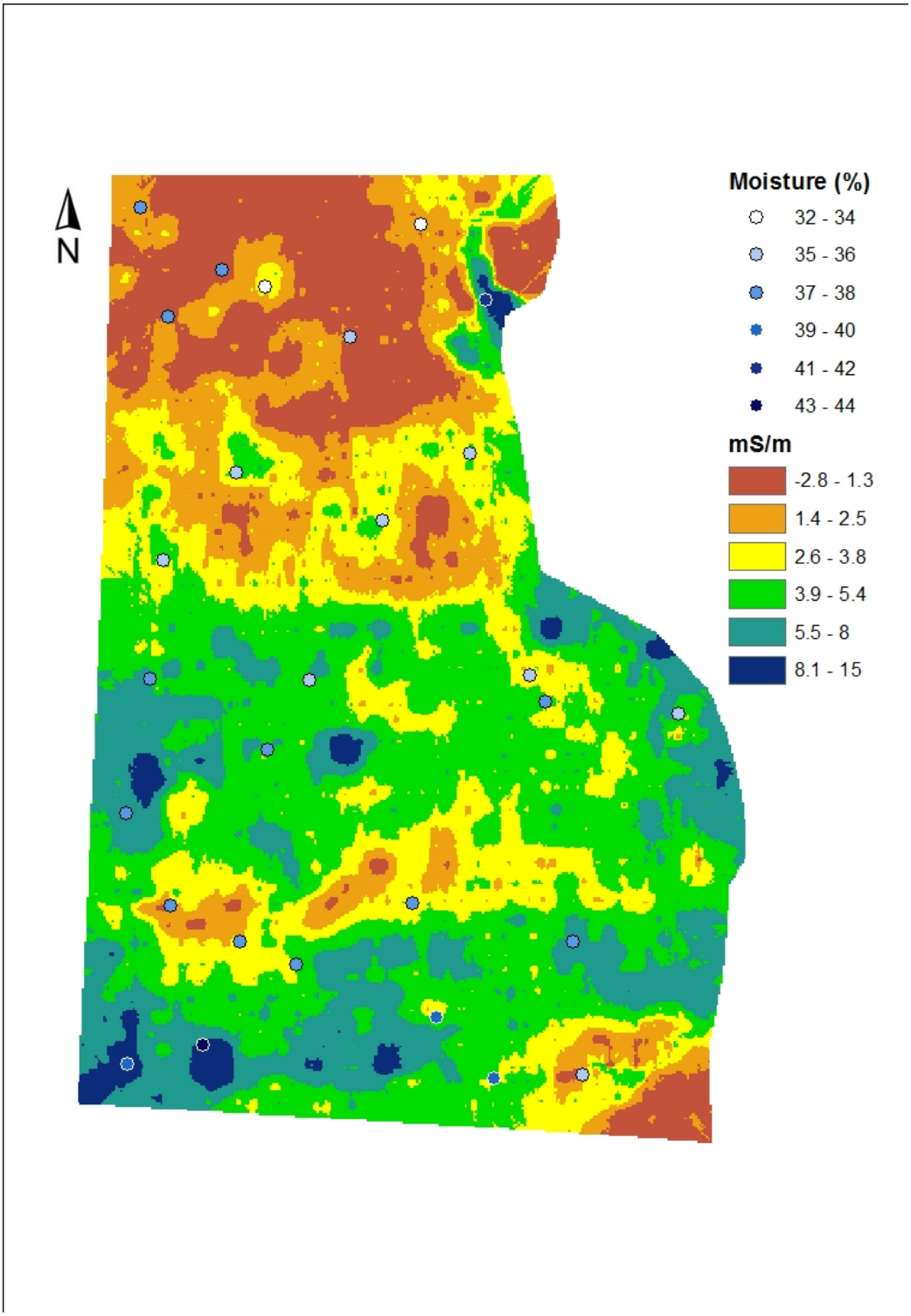

Figure 4.33. Soil moisture and EC_a at Burnside on 4 January 2012. Moisture was measured by TDR to 45cm, EC_a by EM38 Mk2 (1m, vertical mode, kinematic).

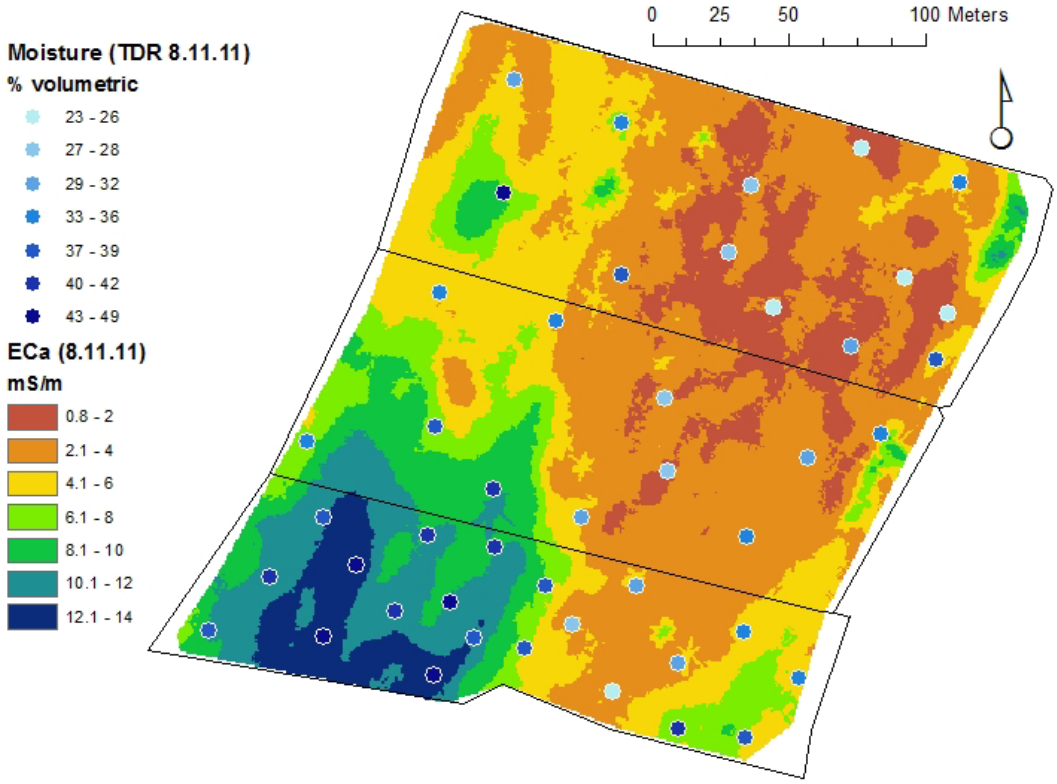

Figure 4.34. Moisture and EC_a at No.1 Diary on 8 November 2011. Moisture was measured by TDR to 45cm, EC_a by EM38 Mk2 (1m, vertical mode, kinematic).

EC_a and soil moisture – EM38 Mk2

EC_a (EM38 Mk2, 1m, vertical mode) was linearly correlated with soil volumetric moisture in all kinematic surveys except on 29.9.11 at Burnside (Table 4.12). On that occasion soil moisture was determined by gravimetric analysis of samples taken over two days (29 and 30.9.11); data was the mean of 3 samples (4, 28 and 64cm) taken at each of 6 sites (not the subsequently established soil sample sites). For the three other kinematic surveys soil moisture was determined by TDR to 45cm at between 28-36 sites on each survey date. The smaller number of moisture measurements taken for the survey at Burnside on 29.9.11 may have weakened statistical analysis and partly explain the lack of correlation between EC_a and soil moisture in that survey.

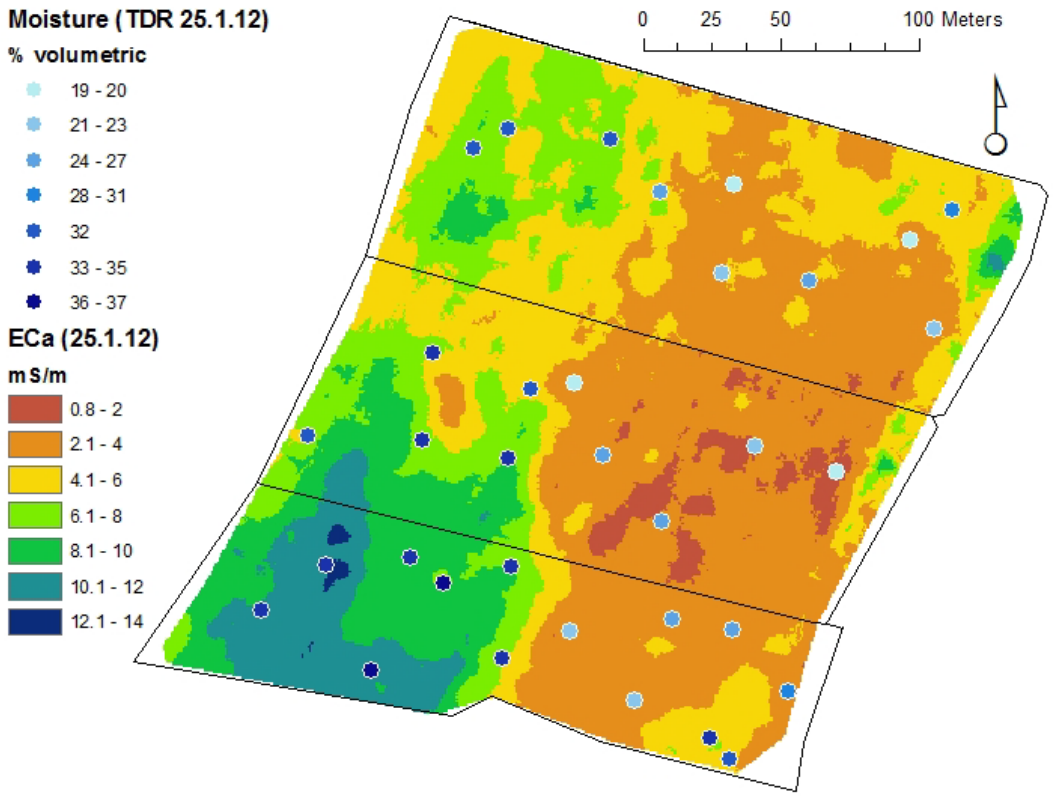

Figure 4.35. Moisture and EC_a at No.1 Diary on 1 January 2012. Moisture was measured by TDR to 45cm, EC_a by EM38 Mk2 (1m, vertical mode, kinematic).

Table 4.12. Correlation by linear regression of EC_a (EM38 Mk2, 1m, vertical) from kinematic surveys with soil volumetric moisture. Moisture = volumetric % by TDR to 45cm or gravimetric analysis (29.9.11 only). The number of measurements for each date are shown in Figure 4.32.

	Coefficient	R^2	Significance
All	0.28	0.30	6.11×10^{-9}
No.1 Dairy all	0.36	0.58	1.22×10^{-13}
No.1 Dairy 8.11.11	0.45	0.67	1.37×10^{-9}
No.1 Dairy 25.1.12	0.39	0.68	3.98×10^{-8}
Burnside all	ns	ns	ns
Burnside 29.9.11	ns	ns	ns
Burnside 4.1.12	0.66	0.37	5.38×10^{-4}

Differences in coefficients of EC_a-soil moisture correlations between locations and surveys, and the modest or low R^2 values, demonstrate that the relationship between EC_a and soil moisture was variable and in no case was EC_a dominated by the effects of soil moisture only. It was shown from soil sample site results that soil solute-soil moisture interaction significantly affected and probably obscured EC_a-soil moisture relationships at Burnside; this is confirmed by the correlation of EC_a with soil moisture at Burnside on 4.1.12, as the effect of soil moisture on EC_a is stronger at higher soil solution concentrations, accounting for the high coefficient value, but variations in soil solution concentration cause variation of the effect, accounting for the low R^2.

Using the natural log of the volumetric moisture data did not improve any of the significant correlations. This result is consistent with the description by Pozdnyakov et al. (2006) of an exponential effect of moisture on EC_a as that effect is thought to be comprised of different linear phases relating to different moisture states, together forming the exponential relationship; moreover the greatest contrasts between linear phases are in dry soils (see section *2.2.4 – Limitations and extensions of the dual pathway model).* As soils in this study were mostly wetter than permanent wilting point, the EC_a-moisture relationship is expected to have been comprised of one or two relatively similar linear phases. Improvements in correlations using a second order polynomial regression were only slight – a change of 0.01-0.02 in the R^2 value – which does not indicate an essentially quadratic relationship.

Attention has also been drawn in the literature to the spatial scale of correlation of EC_a with soil moisture i.e. small scale fluctuations may obscure a correlation of larger spatial extent (e.g. Kachanoski et al. 1990; see section *2.5.2 – Direct interpretation of EC_a as soil moisture proxy).* Small scale fluctuations were apparent in kinematic EC_a data of this study (see *Appendix 6 – EMI instrument functional tests*). It is thought, however, that such an effect is less likely to obscure correlations with EC_a in this study as EC_a data used for regressions was extracted from kriged surfaces, so the points were spatially averaged.

On occasions when replicate moisture measurements were made within a 1m radius of a sample site, variation between the measurements appeared slight. Correlation

of EC_a with flow accumulation modelled from topographic data was significant only at No.1 Dairy with an R^2 of 0.07, an effect far smaller than that of moisture itself, suggesting that moisture was not much controlled by topography. Therefore correlations between EC_a and soil moisture in this study are not thought to be weakened by strong, small scale variation in either variable.

It is evident from correlations of EC_a with soil properties at sample sites that effects of properties other than soil moisture were significant: soil texture and EC of soil paste, the latter representing soluble ion concentration in soil. These properties were not included together with soil moisture in regressions with kinematic EC_a data as they were only determined at a small number of sites; they may, however, have weakened correlations of soil moisture with EC_a in kinematic survey results.

EC_a and soil moisture – EM31

No significant correlations of EC_a (EM31) with soil moisture were found at Burnside. At No.1 Dairy EC_a (EM31) was similarly correlated with soil moisture in both kinematic surveys (Table 4.13). It may be that the similarity of coefficients and R^2 values from the two kinematic surveys with the EM31 at No.1 Dairy arises from the deeper focus of the EM31 sensitivity profile, less influenced by wetting and drying of soil close to the surface, and the associated change in the EC_a-soil moisture relationship caused by different moisture states.

Table 4.13. Correlation by linear regression of ECa (EM31, vertical) from kinematic surveys with soil moisture at No.1 Dairy location. (Moisture = volumetric % by TDR or gravimetric analysis).

	Coefficient	R^2	Significance
No.1 Dairy all	0.24	0.48	1.76×10^{-10}
No.1 Dairy 8.11.11	0.24	0.41	2.97×10^{-5}
No.1 Dairy 25.1.12	0.22	0.47	3.75×10^{-5}

Surface drying at No.1 Dairy was thought to be influenced by soil sandiness causing temporal variation in the spatial EC_a pattern related to soil texture e.g. the

southward movement over time of the zone of lowest EC_a evident in Figures 4.22, 4.27 and 4.28. This effect would have been enhanced where topsoil dried to a different moisture state in sandy areas e.g. close to permanent wilting point as opposed to field capacity in less sandy areas (Figure 4.12). As discussed in section *2.2.4 - Limitations and extensions of the dual pathway model*, different moisture states are thought to exhibit not just different EC_a but different EC_a-moisture relationships; EC_a measured by the EM31 would have been less influenced by such effects, being more focussed on the subsoil which is expected to have remained wetter throughout the study.

While the deeper sensitivity profile of the EM31 appears to have lent stability to the results, the fact that TDR measurement depth was confined to the surface (0-45cm) meant that the relationship between moisture and the deeper EC_a (EM31) measurements was partially indirect, which may be the cause of the lower R^2 values than obtained at No.1 Dairy with the EM38 Mk2. The value of the improved stability of the EC_a-soil moisture correlation using EM31 measurements is therefore lessened by the weakness of correlations with soil moisture in the zone of most interest, the upper profile.

The absence of correlation between EC_a (EM31) and soil moisture at Burnside in both kinematic surveys shows that no consistent EC_a-moisture relationship was found at that location, particularly with the greater measurement depth of the EM31. It is unlikely that this inconsistency was due to effects of soil texture as these are more likely to vary the EC_a-moisture relationship where soil moisture also varies widely, especially where dry conditions occur as discussed above for No.1 Dairy. Texture was less variable at Burnside than at No.1 Dairy; furthermore there was no significant textural discontinuity within the upper few metres at Burnside similar to the underlying sand horizon at No.1 Dairy (this was evident at Burnside from cores extracted from piezometer boreholes to 3 or more metres). Burnside was also more consistently wet across all surveys.

A different factor which might have caused inconsistency in the EC_a-moisture relationship at Burnside is variation in the concentration of soluble ions in soil. In keeping with the dual pathway model of Rhoades et al. (1976) and other research

(e.g. Hanson and Kaita, 1997) inclusion of interaction effects was found to improve correlation of soil moisture and EC of soil paste with EC_a at both Burnside and No.1 Dairy (section *4.3.4 - EC of 1:1 soil pastes and extracts – Soil EC, EC_a and moisture*). However, as with soil moisture and soil texture, EC of 1:1 soil pastes was less variable at Burnside than at No.1 Dairy, except at 4cm depth to which the EM31 is less sensitive (see section *4.3.4 - EC of 1:1 soil pastes and extracts).*

There were suggestions of whole-paddock variations in EC_a at Burnside, perhaps reflecting different fertiliser or grazing histories, which might have disrupted or 'offset' EC_a-moisture relationships across the location (see section *4.4.3 - EM38 Mk2*). This effect, however, was only evident in the EM38 Mk2 data, suggesting a near-surface phenomenon to which the EM31 would have been less susceptible.

The remaining relevant difference between the Burnside and No.1 Dairy locations was the presence of moderately to strongly gleyed soil at Burnside, particularly in deeper horizons. Gleying was mostly only incipient at No.1 Dairy. This gleyed soil indicates periodically reducing conditions of soil chemistry which increase the concentration of soluble ions such as Fe^{2+}. (Analyses showed that gleying was significantly and positively correlated with EC of soil paste and EC of paste extract – Table 4.08). Such ions increase the EC of soil solution and therefore increase the effect of moisture content on EC_a. Patches of more gleyed soil at depth, such as around site B1 at Burnside, may therefore have increased the effect of moisture on EC_a in those areas, causing inconsistency in the EC_a-moisture relationship across the location, particularly with the deeper measurements of the EM31.

Perhaps the most probable reason why a significant EC_a-moisture relationship was found at Burnside with the EM38 Mk2 but not with the EM31 is that, as discussed above, the deeper EM31 measurements were less directly matched to moisture measurements which were to 45cm. The EC_a-moisture relationship detected with the EM38 Mk2 was also weaker at Burnside than at No.1 Dairy as evidenced by the lower R^2 value of the correlation, and significance in only one of the two surveys at Burnside. The relationship with upper profile moisture therefore being weaker than at No.1 Dairy, and the EM31 less directly focussed on it than the EM38 Mk2, meant that the threshold for a significant relationship was not reached in the data.

Moisture mapping with EC_a

Nine points were selected from the dataset of moisture measurements (TDR to 45cm) at No.1 Dairy on 8.11.11. A moisture map was produced by co-kriging these nine points with kinematic EC_a (EM38 Mk2, 1m, vertical) data from the same date using ArcGIS (Figure 4.36). The EC_a data was a raster surface kriged from 19,427 points of EC_a measurement covering the whole location in 6m swaths (Figure 4.34).

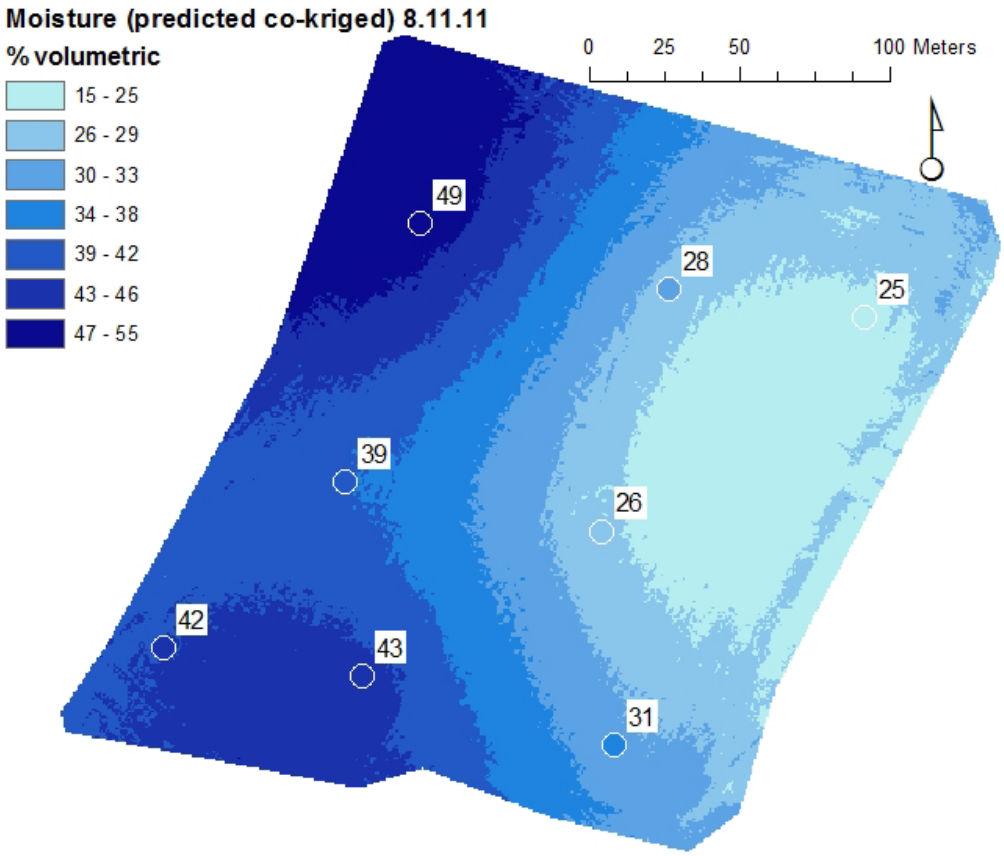

Figure 4.36. Moisture (TDR to 45cm) co-kriged with EC_a (EM38 Mk2, 1m, vertical) at No.1 Dairy, 8.11.11. Moisture measurement point labels show volumetric % moisture (TDR to 45cm) on 8.11.11 (i.e. the points co-kriged to produce the map).

A further moisture map was produced by kriging the same nine points of moisture measurement without EC_a for the same date, 8.11.11. Point values of predicted moisture according to the two maps, kriged and co-kriged, were extracted to 28 points of moisture measurement (TDR to 45cm) on 8.11.11 (these points were not used in kriging). The error (i.e. the difference between the predictions and point measurements) at these points for both maps is shown in Figures 4.37 and 4.38.

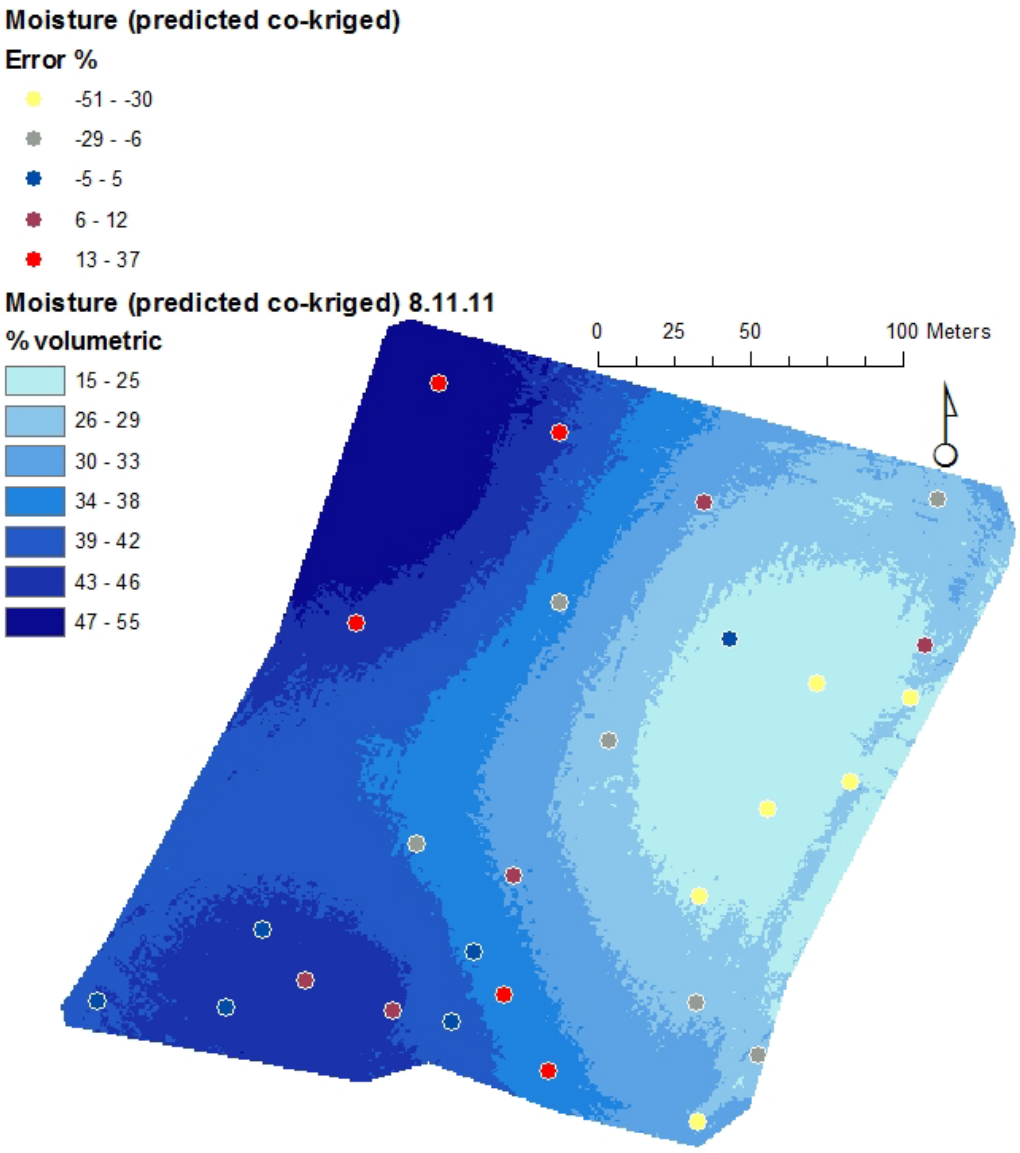

Figure 4.37. Moisture (TDR to 45cm) co-kriged with EC_a (EM38 Mk2, 1m, vertical) at No.1 Dairy, 8.11.11, showing the % error of predictions at points of moisture measurement on 8.11.11. (Moisture measurement points used for the kriging process are not shown.)

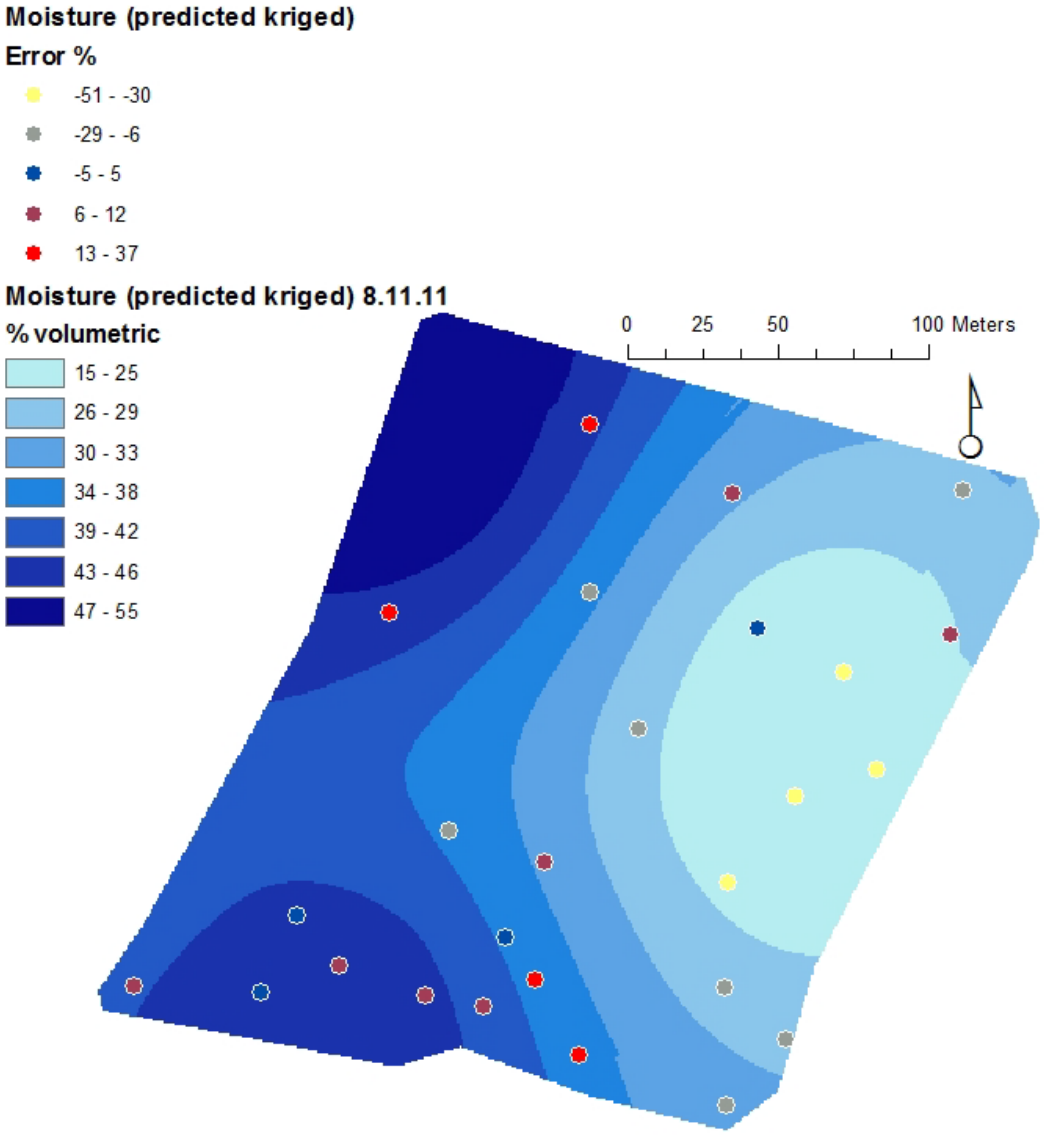

Figure 4.38. Moisture (TDR to 45cm) at No.1 Dairy, 8.11.11, kriged, showing the % error of predictions at points of moisture measurement on 8.11.11. (Moisture measurement points used for the kriging process are not shown.)

It is evident from Figures 4.37 and 4.38 that inclusion of EC_a data together with moisture data in the kriging process made little improvement to the map obtained by kriging the moisture data alone. The mean of moisture measurements at No.1 Dairy on 8.11.11 was 34%; the mean % error of the co-kriged map at the points of moisture measurement was ± 18.4%, and for the map kriged from moisture measurements only, ± 19.3%. It is concluded that the correlation of EC_a (EM38 Mk2, 1m, vertical) with soil volumetric moisture at No.1 Dairy on 8.11.11 was

insufficiently strong (R^2 = 0.67) for the EC_a data to significantly contribute via co-kriging to the map of predicted moisture.

4.4.7 Depth to sand (No.1 Dairy)

Depth to sand was greatest at lower elevations at No.1 Dairy and in areas of higher EC_a. These relationships were not entirely consistent, however, suggesting that depth to sand was not the only factor controlling EC_a. The correlation of EC_a with soil moisture and other soil properties at No.1 Dairy, discussed above, supports this view (Figures 4.39 and 4.40).

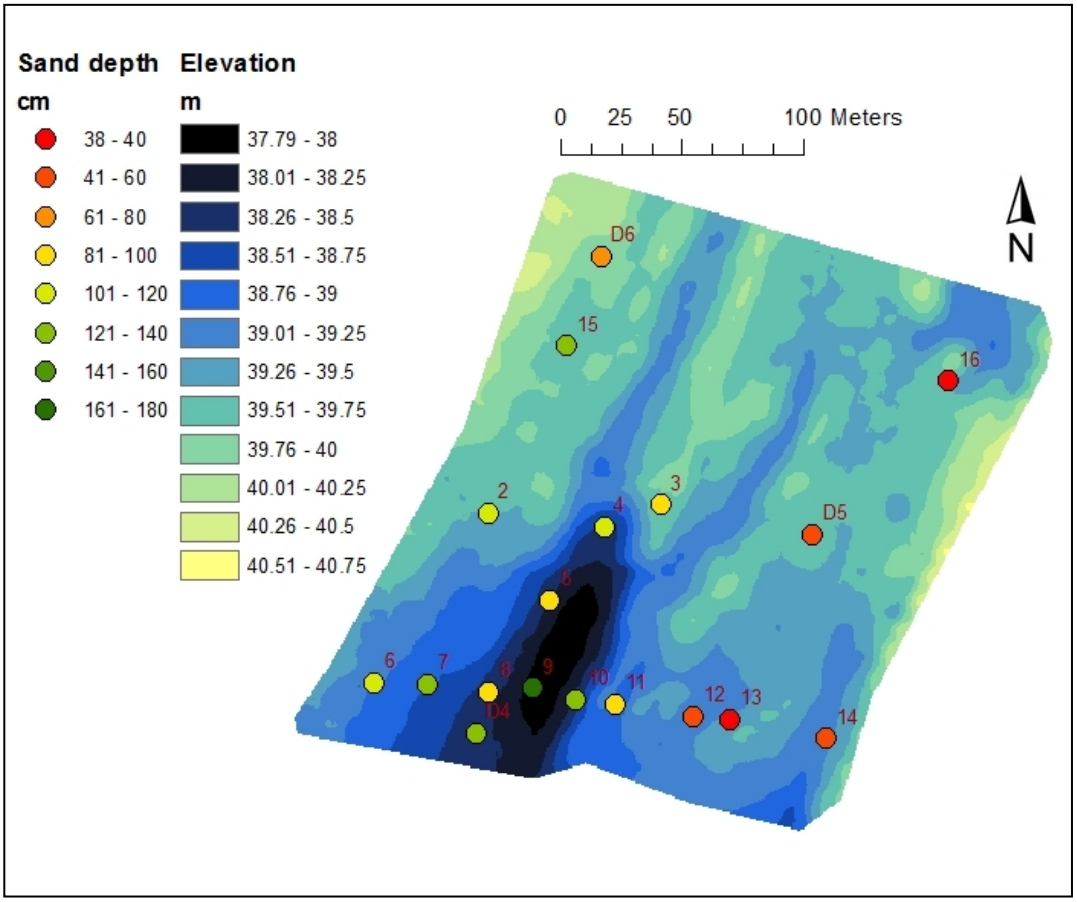

Figure 4.39. Elevation and depth to sand at No.1 Dairy.

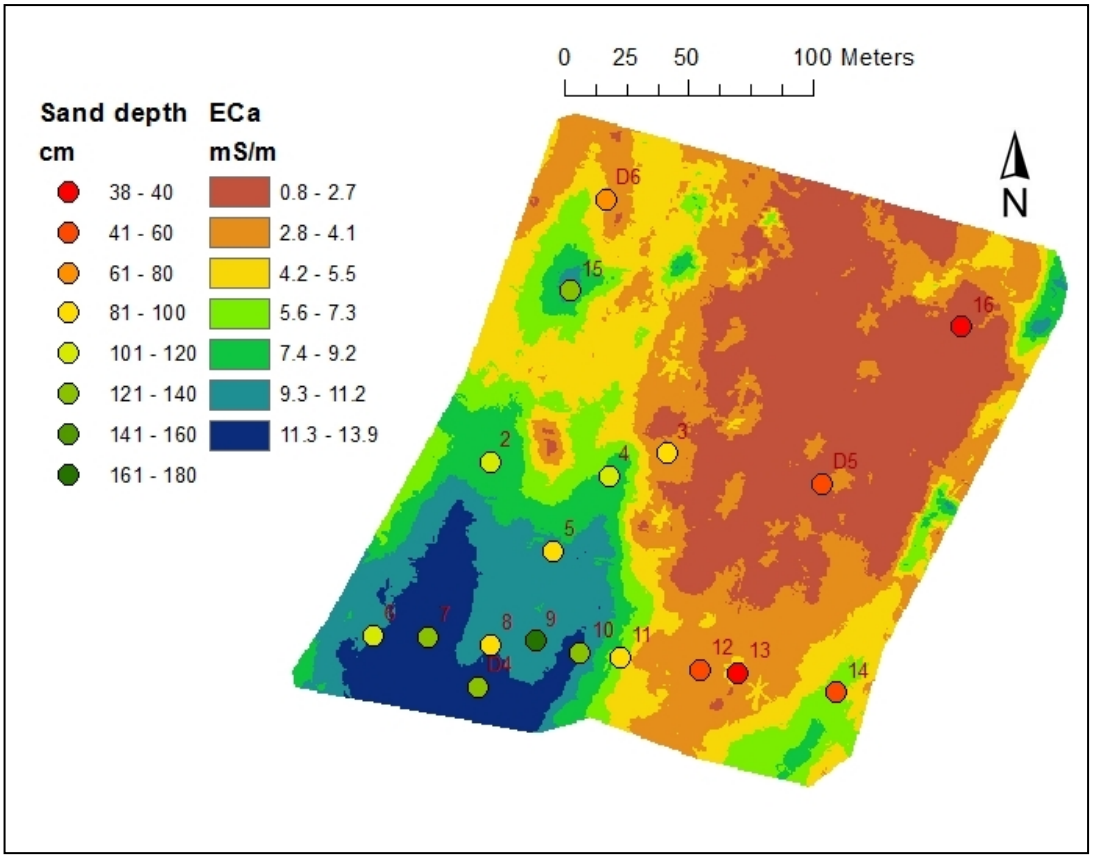

Figure 4.40. EC_a (EM38 Mk2, 1m, vertical, 8.11.11) and depth to sand at No.1 Dairy.

EC_a data is available at the points of sand depth measurement at No.1 Dairy from three kinematic surveys using EM38 Mk2 and two using EM31. EC_a is positively correlated with depth to sand in all instances (Table 4.14).

Table 4.14. R^2 values of significant correlations by linear regression of EC_a (EM38 Mk2, 1m, vertical) and EC_a (EM31, vertical) with depth to sand at No.1 Dairy. EC_a values are extracted from kriged raster surfaces of the kinematic EMI data to the points of sand depth measurement.

Survey date	18.8.11	8.11.11	25.1.12
EM38 Mk2 (1m)	0.56	0.52	0.59
EM31		0.36	0.48

Elevation was negatively correlated with sand depth (R^2 = 0.34). This and the above results confirm the appearance of relationships in Figures 4.39 and 4.40 whereby sand was closest to the surface in areas of higher elevation and lower EC_a.

As the depth of the sand horizon at No.1 Dairy was in every case below the upper 45cm of soil profile, resolution of the upper profile EC_a should therefore have removed this conflicting factor, and therefore may account for improved correlations of EC_a with upper profile moisture at soil sample sites at No.1 Dairy using EC_a modelled for the upper profile (Table 4.01).

However, analysis of soil from sample sites at No.1 Dairy showed that shallower soil overlying sand at site D5 was also sandier than deeper soil over sand at sites D4 and D6. Such variation in texture overlying the sand horizon may have obscured the effect of sand depth in EC_a data, limiting the ability to determine sand depth simply by correlation with EC_a. Depth to sand was generally deeper than pasture rooting depth so would represent an interference in the use of EC_a for assessment of soil moisture or other soil properties in relation to pasture.

Chapter 5

Summary and Conclusions

A range of methods were used with EMI to analyse the relationship of EC_a to soil moisture in alluvial Recent Soils of the Manawatu catchment, lower North Island, New Zealand. The EMI methods included kinematic surveys with two Geonics instruments, the EM38 Mk2 and EM31, and spot measurements at a few selected sites within the survey areas. Spot measurements were made with the EM38 Mk2 in vertical and horizontal modes and at various heights above ground.
A method was developed to estimate EC_a in the upper 45cm of soil profile, to better relate measurements of soil moisture and other soil properties in the upper profile to EC_a. Correlations of EC_a with soil moisture and other soil properties were analysed in the context of EC_a and EMI theory to assess the potential for the use of EC_a to provide quantitative measurements of soil volumetric moisture content. The following conclusions were made.

1. Correlation of EC_a with soil moisture in alluvial Recent soils was variable between times and locations in this study, and was not in every case significant. This is despite that the soils were somewhat similar in texture and parent materials, and moisture contents were close to field capacity in all instances except a few cases of surface drying. EC_a therefore was not controlled in a simple manner by soil moisture.

2. Interaction of the effects of soil moisture with soil texture and solute concentration limited direct correlations of soil moisture with EC_a. It is concluded that strong correlations of EC_a with soil moisture should not be expected across areas with different recent histories of fertilisation, even where other site characteristics and soil properties are similar.

3. A particular feature of moisture-EC_a relationships evident at one location (No.1 Dairy) was the presence of different moisture states – close to field capacity or else permanent wilting point – both spatially across the location and in moisture profiles, whereby different soil horizons were in different moisture states at the same time. A profile in such condition is not expected to show EC_a in keeping with that of an even moisture profile even where average moisture content is the same. This study shows such irregularities can occur even in apparently moist conditions where sandy soils, especially where they are found at the surface, have significance as those most likely to dry to a state giving a different class of EC_a response to EMI.

4. Depth profile resolution of EC_a measurements appeared in one instance to marginally improve EC_a-soil moisture correlation where comparisons between EMI measurements were confined to those made by the same instrument and coil spacing. The method requires characterisation of EC_a variation within each of two depth layers in order to estimate the overall magnitude of EC_a in each of those layers, and additionally depends on comparability (not equivalence) of EC_a measurements made by different EMI instruments or orientations (modes) at the same site and time. Results indicate that characterisation of EC_a variation within soil profile layers, based on soil analyses and profile observations, was inadequate to satisfy this requirement of the method. The assumption of comparability of EMI measurements appears satisfied only for alternative modes of a single instrument and coil spacing. To improve correlations of EC_a with soil moisture using EC_a depth profile resolution, a strong and direct relationship of EC_a with soil moisture is also required. However, in this study correlations of EC_a with EC of soil pastes and with soil texture properties are stronger than with soil moisture, and interaction effects between all these properties are evident. Therefore, without direct, independent measurements of EC_a at different depths, the EC_a depth profile resolution method is not validated even where results seem reasonable.

5. The significant inverse relationship of EC_a with soil temperature, both in this study and reported in the literature, is not expected according to EC_a theory;

methods to correct for this effect therefore lack a sound rationale. Quantitative interpretation of EC_a will require resolution of this uncertainty, and the determination of appropriate methods to correct for it.

6. In addition to the limitations discussed above, EC_a measurement by EMI is at its limit of resolution in non-saline soils; small interferences or calibration errors can rival the magnitude of the measurement. Therefore where the effect of variation in moisture is limited it can easily be obscured by effects of measurement error, solute concentration, horizon depths, or soil texture, where these are either of greater magnitude or simply more variable than the effect of moisture. There was an appearance of the above situation in this study at the Burnside location.

7. In practice it appears likely that most soil moisture assessment by EC_a uses the combined effects of texture and moisture which are stronger than moisture alone. However, while the natural association of moisture and texture lessens the need to differentiate these for qualitative assessment of moisture, the total water content which affects EC_a does not equal plant available water or available water capacity. Sandy soil in this study showed available water capacity equal to or higher than that of silty soil in which total moisture content and related EC_a was significantly higher.

8. Quantitative interpretation of EC_a in terms of soil moisture requires accompanying measurements of soil moisture, soil solution concentration (even in non-saline soils) and soil texture. In fertilised or heavily stocked agricultural land only the latter is relatively stable over time. Some understanding of the depth profiles of these factors in addition to the depth profile of the EC_a measurement (not only the depth profile of instrument sensitivity) will be necessary to invoke the theoretical models of EC_a discussed in Chapter 2, because the soil properties which influence EC_a interact with each other and with EMI where they occur together at the same depth in a soil profile, not according to mean values for the soil profile or site. Simple ‘calibration factors’ relating EC_a to soil moisture cannot be applied accurately across different sites or times.

Chapter 6

Recommendations and Future Work

Despite the weak results of limited exploration of one method of EC_a depth profile resolution in this study, a synthesis of this method with other methods described in the literature, together with greater application of computing power, still offers potential for improving measurements of this vital aspect of EC_a.

For example, whereas EC_a profiles were characterised in the most simple sense in this study as two layers with a boundary of fixed depth between, iterative computation of the method for a sequence of hypothetical boundary depths, and analysis of the differences in results, might provide for more successful EC_a depth profile resolution. Direct independent measurements of EC_a are needed for validation of any such method. However, a preliminary indirect evaluation of the method might be possible in an experimental bed of deep washed sand where conflicting effects of soil texture variation and solute concentration are limited.

The combination of measurements of soil properties at sample sites in this study provided some interesting comparisons but from a limited amount of data. In particular the combination of soil moisture measurements, analysis of soil moisture release characteristics and multi-height EMI measurements relates well to theory of soil moisture-EC_a relationships in different moisture states (Pozdnyakov et al., 2006), and the multi-height measurements are a simple method of identifying basic, qualitative trends in EC_a depth profile. Moisture measurements at various depths would further complement this data. EMI is often used in soil moisture conditions estimated to be at field capacity in order to simplify interpretation of the combined effects of soil moisture and texture. Drier conditions however are a fascinating, complex field to explore, which will provide different information about EC_a-soil moisture relationships, and which has so far been little characterised in the field.

Multiple linear regression of soil moisture and EC of 1:1 soil paste (together with the product of these two factors to represent interaction effects) against EC_a produced much better correlations in this study than simple linear regression of EC_a against either soil moisture or EC of 1:1 soil paste alone. The method of measuring EC of 1:1 soil paste used in this study has potential to be adapted for field use, providing for data collection almost as rapid as for soil moisture with TDR. These measurements together could provide the necessary complementary data needed for interpretation of kinematic EC_a data in terms of soil moisture.

Given the complexities of interpretation of EC_a relationships with specific soil properties such as soil moisture, it is also useful to identify combinations of effects which fortuitously may occur together in consistent ways, so simplifying interpretation of EC_a data. Consistency of soil moisture-texture relationships in field capacity conditions is an example of such a circumstance which has been often exploited in research and agriculture. A further possible such set of conditions was observed in this study in relation to denitrification potential of soil, and is described in Appendix 10.

This thesis will conclude with some guidelines for practical field use of EMI, additional to those which are commonly recognized and described in Geonics (1995, 2008) and in *Appendix 2* and *Appendix 3*:

- Interference of wire fences with the EM31 is first evident at 15m distance; the scope therefore for using the EM31 in small, fenced paddocks is limited.

- The EM38 Mk2, 0.5m coil spacing must be calibrated with any intended cable connections in place and remaining in a live state until the conclusion of measurements. This complicates use in kinematic systems because cable connections may prevent moving the instrument out of interference range of the vehicle for purposes of calibration.

- Precise mapping of EC_a in kinematic surveys requires correction of sensor measurements for GPS antenna offset, or else the positioning of the antenna above the sensor; the latter arrangement may, however, cause interference.

- The broadly consistent relationship of soil moisture with EC_a in field capacity conditions is supported by this study. However, field capacity conditions may be less consistent both spatially and in terms of depth profile than is sometimes thought. Such conditions are best assessed rather than presumed.

- For characterisation of EC_a depth profile in the upper soil profile, the most useful height for measurements by the EM38 Mk2 or EM31 in raised positions is that at which peak sensitivity is at the surface and declines with depth: ~35 cm for the EM38 Mk2 (1m, vertical), and ~1.3m for the EM31 (vertical), as this changes the EMI sensitivity depth profile in the most unambiguous way. Additional raised measurements at lesser heights are also useful.

References

Allred, B. J., M. R. Ehsani and D. Saraswat (2005). "The impact of temperature and shallow hydrologic conditions on the magnitude and spatial pattern consistency of electromagnetic induction measured soil electrical conductivity." Transactions of the ASAE 48(6): 2123-2135.

Auerswald, K., S. Simon and H. Stanjek (2001). "Influence of soil properties on electrical conductivity under humid water regimes." Soil Science 166(6): 382-390.

Blakemore, L. C., P. L. Searle and B. K. Daly (1987). Methods for chemical analysis of soils. Lower Hutt, NZ Soil Bureau, Department of Scientific and Industrial Research.

Bohn, H. L., J. Benasher, H. S. Tabbara and M. Marwan (1982). "Theories and tests of electrical conductivity in soils." Soil Science Society of America Journal 46(6): 1143-1146.

Borchers, B., T. Uram and J. M. H. Hendrickx (1997). "Tikhonov regularization of electrical conductivity depth profiles in field soils." Soil Science Society of America Journal 61(4): 1004-1009.

Brevik, E. C. and T. E. Fenton (2002). "Influence of soil water content, clay, temperature, and carbonate minerals on electrical conductivity readings taken with an EM-38." Soil Survey Horizons 43(1): 9-13.

Brevik, E. C. and T. E. Fenton (2004). "The effect of changes in bulk density on soil electrical conductivity as measured with the geonics EM-38." Soil Survey Horizons 45(3): 96-102.

Brevik, E. C., T. E. Fenton and R. Horton (2004). "Effect of daily soil temperature fluctuations on soil electrical conductivity as measured with the Geonics(R) EM-38." Precision Agriculture 5(2): 145-152.

Brevik, E. C., T. E. Fenton and A. Lazari (2006). "Soil electrical conductivity as a function of soil water content and implications for soil mapping." Precision Agriculture 7: 393-404.

Bronson, K. F., J. D. Booker, S. J. Officer, R. J. Lascano, et al. (2005). "Apparent electrical conductivity, soil properties and spatial covariance in the US southern high plains." Precision Agriculture 6(3): 297-311.

Carroll, Z. L. and M. A. Oliver (2005). "Exploring the spatial relations between soil physical properties and apparent electrical conductivity." Geoderma 128(3-4): 354-374.

Cook, P. G. and G. R. Walker (1992). "Depth profiles of electrical conductivity from linear combinations of electromagnetic induction measurements." Soil Science Society of America Journal 56(4): 1015-1022.

Corwin, D. L. and J. D. Rhoades (1982). "An improved technique for determining soil electrical conductivity depth relations from above-ground electromagnetic measurements." Soil Science Society of America Journal 46(3): 517-520.

Corwin, D. L. and J. D. Rhoades (1990). "Establishing soil electrical conductivity depth relations from electromagnetic induction measurements." Communications in Soil Science and Plant Analysis 21(11-12): 861-901.

Cowie, J. D. (1978). Soils and Agriculture of Kairanga County, North Island, New Zealand. Soil Bureau Bulletin 33. Wellington, NZ, New Zealand Department of Scientific and Industrial Research.

Domsch, H. and A. Giebel (2004). "Estimation of soil textural features from soil electrical conductivity recorded using the EM38." Precision Agriculture 5(4): 389-409.

Eigenberg, R. A., J. A. Nienaber, B. L. Woodbury and R. B. Ferguson (2006). "Soil conductivity as a measure of soil and crop status - A four-year summary." Soil Science Society of America Journal 70(5): 1600-1611.

Ewing, R. P. and A. G. Hunt (2006). "Dependence of the electrical conductivity on saturation in real porous media." Vadose Zone Journal 5(2): 731-741.

Farahani, H. J. and G. W. Buchleiter (2004). "Temporal stability of soil electrical conductivity in irrigated sandy fields in Colorado." Transactions of the ASAE 47(1): 79-90.

Farahani, H. J., G. W. Buchleiter and M. K. Brodahl (2005). "Characterization of apparent soil electrical conductivity variability in irrigated sandy and non-saline fields in Colorado." Transactions of the ASAE 48(1): 155-168.

Friedman, S. P. (2005). "Soil properties influencing apparent electrical conductivity: a review." Computers and Electronics in Agriculture 46(1-3): 45-70.

Friedman, S. P. and N. A. Seaton (1998). "Critical path analysis of the relationship between permeability and electrical conductivity of three-dimensional pore networks." Water Resources Research 34(7): 1703-1710.

Frogbrook, Z. L., M. A. Oliver and K. E. Derricourt (2003). "Exploring the spatial relations between soil properties and electro-magnetic induction (EMI) and the implications for management." Precision Agriculture: 217-222.

Gebbers, R., E. Luck and K. Heil (2007). "Depth sounding with the EM38-detection of soil layering by inversion of apparent electrical conductivity measurements." Precision agriculture '07. Papers presented at the 6th European Conference on Precision Agriculture, Skiathos, Greece, 3-6 June, 2007: 95-102.

Geonics (1995). EM31-Mk2 Operating manual. Ontario, Geonics Ltd.

Geonics (2008). EM38-Mk2 Ground Conductivity Operating Manual. Ontario, Geonics Ltd.

Geonics (2012). Personal communication, 28 February 2012.

Gradwell, M. W. (1971). Methods for physical analysis of soils. New Zealand Soil Bureau Scientific Report. Wellington, NZ, Department of Scientific and Industrial Research.

Hanson, B. R. and K. Kaita (1997). "Response of electromagnetic conductivity meter to soil salinity and soil-water content." Journal of Irrigation and Drainage Engineering-Asce 123(2): 141-143.

Horizons Regional Council. 2008. "Soil properties at Little Rd, Woodville."

Hedley, C. B. (2009). The development of proximal sensing methods for soil mapping and monitoring, and their applicaton to precision irrigation. Palmerston North, NZ, Massey University. PhD.

Hossain, M. B., D. W. Lamb, P. V. Lockwood and P. Frazier (2010). "EM38 for volumetric soil water content estimation in the root-zone of deep vertosol soils." Computers and Electronics in Agriculture 74(1): 100-109.

Huth, N. I. and P. L. Poulton (2007). "An electromagnetic induction method for monitoring variation in soil moisture in agroforestry systems." Australian Journal of Soil Research 45(1): 63-72.

James, I. T., T. W. Waine, R. I. Bradley, J. C. Taylor, et al. (2003). "Determination of soil type boundaries using electromagnetic induction scanning techniques." Biosystems Engineering 86(4): 421-430.

Jaynes, D. B. (1996). "Improved soil mapping using electromagnetic induction surveys." Proceedings of the 3rd International Conference on Precision Agriculture, Minneapolis, Minnesota, USA, 1996. Ed. Robert, P. C.; Rust, R. H.; Larson, W. E. pp 169-179 .

Kachanoski, R. G., E. Dejong and I. J. Vanwesenbeeck (1990). "Field scale patterns of soil water storage from noncontacting measurements of bulk electrical conductivity." Canadian Journal of Soil Science 70(3): 537-542.

Kachanoski, R. G., E. G. Gregorich and I. J. Vanwesenbeeck (1988). "Estimating spatial variations of soil water content using noncontacting

electromagnetic inductive methods." Canadian Journal of Soil Science 68(4): 715-722.

Khakural, B. R., P. C. Robert and D. R. Hugins (1998). "Use of non-contacting electromagnetic inductive method for estimating soil moisture across a landscape." Communications in Soil Science and Plant Analysis 29(11-14): 2055-2065.

Kravchenko, A. N., G. A. Bollero, R. A. Omonode and D. G. Bullock (2002). "Quantitative mapping of soil drainage classes using topographical data and soil electrical conductivity." Soil Science Society of America Journal 66(1): 235-243.

Kuehn, J., A. Brenning, M. Wehrhan, S. Koszinski, et al. (2009). "Interpretation of electrical conductivity patterns by soil properties and geological maps for precision agriculture." Precision Agriculture 10(6, Sp. Iss. SI).

Landcare Research (2013). “NZSC horizon notations and diagnostic characteristics”. http://soils.landcareresearch.co.nz/contents/SoilNames_NZSoilClassification_SoilHorizons.aspx?currentPage=SoilNames_NZSoilClassification_SoilHorizons&menuItem=SoilNames. Accessed 7.3.13.

Lesch, S. M. and D. L. Corwin (2003). "Using the dual-pathway parallel conductance model to determine how different soil properties influence conductivity survey data." Agronomy Journal 95(2): 365-379.

Lesch, S. M., D. L. Corwin and D. A. Robinson (2005). "Apparent soil electrical conductivity mapping as an agricultural management tool in arid zone soils." Computers and Electronics in Agriculture 46(1-3): 351-378.

Luck, E., R. Gebbers, J. Ruehlmann and U. Spangenberg (2009). "Electrical conductivity mapping for precision farming." Near Surface Geophysics 7(1): 15-25.

Lund, E. D., C. D. Christy and P. E. Drummond (1999). "Practical applications of soil electrical conductivity mapping." Precision agriculture '99, Part 1 and Part 2. Papers presented at the 2nd European Conference on Precision Agriculture, Odense, Denmark, 11-15 July 1999: 771-779.

Ma, R. J., A. McBratney, B. Whelan, B. Minasny, et al. (2011). "Comparing temperature correction models for soil electrical conductivity measurement." Precision Agriculture 12(1): 55-66.

Maclaren, R. G. and K. C. Cameron. (1990). Soil Science: An Introduction to the Properties and Management of New Zealand Soils. USA. Oxford University Press.

Mallants, D., Vanclooster, M., Toride, N., Vandergorght, J., et al. (1966). Comparison of three methods to calibrate TDR for monitoring solute movement in undisturbed soil. Soil Science Society of America Journal 60: 747-754.

McBratney, A. B., T. F. A. Bishop and I. S. Teliatnikov (2000). "Two soil profile reconstruction techniques." Geoderma 97(3-4): 209-221.

McBratney, A. B., B. Minasny and B. M. Whelan (2005). "Obtaining 'useful' high-resolution soil data from proximally-sensed electrical conductivity/resistivity (PSEC/R) surveys." Precision Agriculture 05: 503-510.

McCutcheon, M. C., H. J. Farahani, J. D. Stednick, G. W. Buchleiter, et al. (2006). "Effect of soil water on apparent soil electrical conductivity and texture relationships in a dryland field." Biosystems Engineering 94(1): 19-32.

McNeill, J. D. (1980a). Electrical Conductivity of Soils and Rocks. Ontario, Geonics Ltd.

McNeill, J. D. (1980b). Electromagnetic Terrain Conductivity Measurement at Low Induction Numbers. Ontario, Geonics Ltd.

Metservice. (2012). http://www.metservice.com/rural. Accessed 1 April, 2012.

Milne, J. D. G., B. Clayden, P. L. Singleton and A. D. Wilson (1995). Soil Description Handbook. Lincoln, NZ, Manaaki Whenua Press, Landcare Research.

Mojid, M. A. and H. Cho (2008). "Wetting solution and electrical double layer contributions to bulk electrical conductivity of sand-clay mixtures." Vadose Zone Journal 7(3): 972-980.

Mojid, M. A., D. A. Rose and G. C. L. Wyseure (2007). "A model incorporating the diffuse double layer to predict the electrical conductivity of bulk soil." European Journal of Soil Science 58(3): 560-572.

Monteiro Santos, F.A. (2004). 1-D laterally constrained inversion of EM34 profiling data. Journal of Applied Geophysics 56: 123–134.

Mulders, M. A. (1987). Remote sensing in soil science. Amsterdam, Elsevier.

Nadler, A. (1982). "Estimating the soil water dependence of the electrical conductivity soil solution electrical conductivity bulk soil ratio." Soil Science Society of America Journal 46(4): 722-726.

Nadler, A. (2002). "Comments on "Influence of soil properties on electrical conductivity under humid water regimes" by K. Auerswald et al." Soil Science 167(3): 229-230.

Nadler, A. (2005). Methodologies and the practical aspects of the bulkk soil EC (sigma(a)) - Soil solution EC (sigma(w)) relations. Advances in Agronomy, Vol 88. 88: 273-312.

Nadler, A. and H. Frenkel (1980). "Determination of soil solution electrical conductivity from bulk soil electrical conductivity measurements by the 4-electrode method." Soil Science Society of America Journal 44(6): 1216-1221.

National Institute of Water and Atmosphere (NIWA). (2012)." Annual climate summary 2011." http://www.niwa.co.nz/climate/summaries/annual/annual-climate-summary-2011. Accessed 9 January 2013.

New Zealand Centre for Precision Agriculture (2011)." Offset calculation."

New Zealand Centre for Precision Agriculture (2005). "Flood sedimentation pattern 16/2/2004 - Number 1 Dairy Farm - Massey University."

Pollock J, P Nelson, M Richardson, F Lewis, A McDonald (2003). “Massey Soil Map”. Massey University, Palmerston North.

Poulton, M. (2013). Personal communication, 11.1.13.

Pozdnyakov, A. I., L. A. Pozdnyakova and L. O. Karpachevskii (2006). "Relationship between water tension and electrical resistivity in soils." Eurasian Soil Science 39: S78-S83.

Pozdnyakova, L. 1999. Electrical Properties of Soils. PhD Dissertation, University of Wyoming: Laramie, WY, USA.

Reedy, R. C. and B. R. Scanlon (2003). "Soil water content monitoring using electromagnetic induction." Journal of Geotechnical and Geoenvironmental Engineering 129(11): 1028-1039.

Rhoades, J. D. (1981). "Predicting bulk soil electrical conductivity versus saturation paste extract electrical conductivity calibrations from soil properties." Soil Science Society of America Journal 45(1): 42-44.

Rhoades, J. D. (1991). "Soil electrical conductivity and soil salinity - new formulations and calibrations - reply." Soil Science Society of America Journal 55(1): 295-295.

Rhoades, J. D. and D. L. Corwin (1981). "Determining soil electrical conductivity depth relations using an inductive electromagnetic soil conductivity meter." Soil Science Society of America Journal 45(2): 255-260.

Rhoades, J. D. and D. L. Corwin (1990). "Soil electrical conductivity - effects of soil properties and application to soil salinity appraisal." Communications in Soil Science and Plant Analysis 21(11-12): 837-860.

Rhoades, J. D., N. A. Manteghi, P. J. Shouse and W. J. Alves (1989). "Soil electrical conductivity and soil salinity - new formulations and calibrations." Soil Science Society of America Journal 53(2): 433-439.

Rhoades, J. D., P. A. C. Raats and R. J. Prather (1976). "Effects of liquid-phase electrical-conductivity, water-content, and surface conductivity on bulk soil electrical-conductivity." Soil Science Society of America Journal 40(5): 651-655.

Robinson, D. A., I. Lebron, S. M. Lesch and P. Shouse (2004). "Minimizing drift in electrical conductivity measurements in high temperature environments using the EM-38." Soil Science Society of America Journal 68(2): 339-345.

Sauer, M. C., P. F. Southwick, K. S. Spiegler and M. R. J. Wyllie (1955). "Electrical conductance of porous plugs - ion exchange resin solution systems." Industrial and Engineering Chemistry 47(10): 2187-2193.

Shainberg, I., J. D. Rhoades and R. J. Prather (1980). "Effect of exchangeable sodium percentage, cation exchange capacity and soil solution concentration on soil electrical conductivity." Soil Science Society of America Journal 44(3): 469-473.

Sheets, K. R. and J. M. H. Hendrickx (1995). "Noninvasive soil water content measurement using electromagnetic induction." Water Resources Research 31(10): 2401-2409.

Siqueira, G. M., R. V. P. Fontes Junior, A. A. A. Montenegro, Y. L. Barros, E. F. F. Silva (2012). Spatial variability of soil apparent electrical conductivity (ECa) and the water table depth in an alluvial valley under different uses. EGU General Assembly, 22-27 April, 2012 in Vienna, Austria., p.3255.

Slavich, P. G. (1990). "Determining ECa-depth profiles from electromagnetic induction measurements." Australian Journal of Soil Research 28(3): 443-452.

Smith-Rose, R. L. (1934). "Electrical measurements on soil with alternating currents." Proceedings of the IEE 75: 221-237.

Sudduth, K. A., S. T. Drummond and N. R. Kitchen (2001). "Accuracy issues in electromagnetic induction sensing of soil electrical conductivity for precision agriculture." Computers and Electronics in Agriculture 31(3): 239-264.

Sudduth, K.A., Drummond, S.T., Birrell, S.J., Kitchen, N.R., (1996). "Analysis of spatial factors influencing crop yield." In: Robert, P.C., Rust, R.H., Larson, W.E. (Eds)., Proc 3rd Intl. Conf. on Precision Agriculture, Minneapolis, MN, June 23–26 1996. ASA-CSSA-SSSA, Madison, WI, pp.129–140.

Sudduth, K. A., N. R. Kitchen and S. T. Drummond (1999). "Soil conductivity sensing on claypan soils: Comparison of electromagnetic induction and direct methods." Proceedings of the Fourth International Conference on Precision Agriculture, Pts a and B: 979-990.

Swaid, F. A. (2010). Estimating a new approach for describing electrical conductivity parameters in partially saturated sediments. Management of Natural Resources, Sustainable Development and Ecological Hazards Ii. C. A. Brebbia, N. Jovanovic and E. Tiezzi. 127: 363-375.

Triantafilis, J., A. I. Huckel and I. O. A. Odeh (2003). "Field-scale assessment of deep drainage risk." Irrigation Science 21(4): 183-192.

Triantafilis, J. and F. A. M. Santos (2010). "Resolving the spatial distribution of the true electrical conductivity with depth using EM38 and EM31 signal data and a laterally constrained inversion model." Australian Journal of Soil Research 48(5): 434-446.

Tromp-van Meerveld, H. J. and J. J. McDonnell (2009). "Assessment of multi-frequency electromagnetic induction for determining soil moisture patterns at the hillslope scale." Journal of Hydrology (Amsterdam) 368(1/4): 56-67.

US Salinity Laboratory staff. (1954). USDA AGR HBD 60: 90.

Waine, T. W. (1999). Non-Invasive Soil Property Measurement for Precision Farming. Silsoe, Cranfield University. EngD.

Winstead, A. & Fulton, J. (2010). "Getting Started with Precision Agriculture." Better crops with plant food 94(3) 29-30.

Zhadnov, M.S. (2009). Geophysical Electromagnetic Theory and Methods. Methods in Geochemistry and Geophysics: 43. Elsevier.

Zhu, Q., H. Lin and J. Doolittle (2010). "Repeated Electromagnetic Induction Surveys for Determining Subsurface Hydrologic Dynamics in an Agricultural Landscape." Soil Science Society of America Journal 74(5): 1750-1762.

Appendices

Appendix 1. Tables of results.

Table A1.01. Kinematic survey means: EC_a, temperature, moisture.

Date	Location	EC_a (EM38Mk2, 1m, vertical) mean [1]	EC_a (EM31, vertical) mean [1]	Soil temp. ˚C [3]	Ambient temp. ˚C	Moist. % mean [2]
18.8.11	No.1 Dairy	4.51			8.0	
22.8.11	Burnside	7.44			13.0	
8.11.11	No.1 Dairy	5.25	12.22	16.6	17.0	34.32
25.1.12	No.1 Dairy	5.19	11.09	18.4	21.0	28.51
29.9.11	Burnside	9.24	19.08	10.0	16.5	32.59
4.1.12	Burnside	3.87	19.09	20.1	24.0	36.65

1. EC_a is the means of all kinematic measurements from cleaned data of each survey.

2. Moisture is volumetric % measured by TDR to 45cm or in the case of the Burnside survey of 29.9.11, by gravimetric analysis and averaging of samples from 4, 28 and 64cm at each site.

3. Soil temperature is to 15cm depth at the EMI calibration location.

Table A1.02. Measurements of volumetric moisture (%) accompanying kinematic surveys at Burnside.

Date of moisture measurement	Volumetric moisture (%)	Flow accumulation	Elevation (m)	EM38 Mk2 (1m, vertical) 22.8.11	EM38 Mk2 (1m, vertical) 29.9.11	EM31 (vertical) 29.9.11	EM38 Mk2 (1m, vertical) 4.1.12	EM31 (vertical) 4.1.12
4/01/2012	37.50	3	106.79	8.58	10.43	18.58	6.77	20.44
4/01/2012	37.20	12	107.01	7.49	10.44	18.46	4.80	18.45
4/01/2012	34.50	5	109.08	7.74	8.79	20.29	4.64	22.62
4/01/2012	35.90	12	108.46	5.96	8.44	19.57	3.22	19.57
4/01/2012	35.00	83	107.14	7.31	9.19	20.44	4.94	20.44
4/01/2012	37.50	8	106.53	8.39	9.91	21.69	6.03	21.70
4/01/2012	36.30	11	108.37	6.28	7.61	20.89	3.78	20.91
4/01/2012	38.90	15	106.82	11.25	14.33	23.40	10.19	23.42
4/01/2012	36.70	0	107.15	6.99	7.60	16.68	1.64	16.65
4/01/2012	36.40	7	107.42	7.22	8.47	19.85	2.47	19.87
4/01/2012	42.10	3	107.10	12.30	13.51	21.01	8.80	20.99
4/01/2012	37.30	24	107.55	8.23	10.54	19.11	4.33	19.10
4/01/2012	36.10	2	107.86	7.43	9.22	20.93	2.83	20.92
4/01/2012	39.90	90	107.90	7.51	10.11	18.14	3.95	18.09
4/01/2012	38.70	9	108.07	7.96	9.12	18.06	4.01	20.91
4/01/2012	35.20	4	108.36	6.66	8.51	18.16	2.38	18.53
4/01/2012	38.00	8	108.43	9.31	11.22	19.68	5.86	19.67
4/01/2012	35.40	7	107.48	6.03	8.07	17.33	0.93	17.33
4/01/2012	41.50	58	106.84	8.94	14.03	17.88	8.25	17.97
4/01/2012	32.80	1	108.08	7.33	9.12	16.08	1.60	16.12
4/01/2012	32.10	737	106.97	8.55	9.24	17.95	2.88	17.95
4/01/2012	37.50	34	106.60	6.88	8.52	17.71	1.61	16.37
4/01/2012	36.40	45	106.54	5.49	7.72	16.66	0.99	16.67
4/01/2012	35.10	16	107.05	6.87	9.15	20.83	3.83	20.84
4/01/2012	35.20	2	106.73	7.56	10.23	20.51	3.92	20.84
4/01/2012	35.10	21	107.88	8.35	9.46	18.48	3.68	18.49
4/01/2012	35.60	7	108.26	7.57	10.25	17.19	3.77	17.17
4/01/2012	36.40	11	106.87	5.68	8.16	16.35	0.35	16.35
29/09/2011*	32.85	6	106.89	7.99	9.78	19.34	4.58	19.34
29/09/2011*	37.41	0	107.43	9.84	11.31	21.03	5.38	21.02
29/09/2011*	31.40	18	106.86	5.71	8.30	15.99	1.04	16.00
30/09/2011*	26.90	82	108.65	8.72	9.41	21.52	5.60	21.54
30/09/2011*	36.75	116	108.51	6.61	8.39	19.96	4.73	19.98
30/09/2011*	30.21	0	108.20	6.33	8.00	17.29	2.35	17.30

*means of three measurements at 4, 28 and 64cm; all other moisture measurements TDR to 45 or 50cm. EC_a, flow accumulation and elevation data extracted from kriged rasters surface to points of moisture measurement.

Table A1.03. Measurements of volumetric moisture (%) accompanying kinematic surveys at No.1 Dairy.

Date of moisture measurement	Volumetric moisture (%)	Flow accumulation	Elevation (m)	EM38 Mk2 (1m, vertical) 18.8.11	EM38 Mk2 (1m, vertical) 8.11.11	EM31 (vertical) 8.11.11	EM38 Mk2 (1m, vertical) 25.1.12	EM31 (vertical) 25.1.12
25/01/2012	33.50	12	38.91	6.42	7.50	13.51	5.69	11.23
25/01/2012	30.80	3	39.58	4.36	5.23	13.07	3.03	10.62
25/01/2012	21.80	1	39.28	2.65	3.59	11.81	2.63	9.44
25/01/2012	21.10	1	39.25	2.79	4.02	12.75	2.88	10.08
25/01/2012	36.60	7	37.91	8.03	9.44	16.46	8.06	13.83
25/01/2012	36.80	590	38.26	10.32	12.74	15.44	10.64	14.30
25/01/2012	34.80	7	38.97	9.27	11.76	16.32	10.85	15.00
25/01/2012	34.10	4	38.83	11.18	13.24	18.28	11.85	16.38
25/01/2012	33.90	0	38.91	7.01	7.96	13.94	6.10	11.53
25/01/2012	18.70	2	39.77	1.93	1.78	11.10	1.60	9.88
25/01/2012	23.00	2	39.60	1.98	2.14	10.73	1.80	10.35
25/01/2012	27.10	14	39.51	1.62	2.81	9.93	2.45	9.75
25/01/2012	26.40	24	39.04	1.72	2.28	9.82	2.55	9.65
25/01/2012	18.50	0	39.77	3.00	2.52	10.22	2.43	9.87
25/01/2012	33.90	5	38.29	7.62	8.73	14.46	7.66	12.69
25/01/2012	34.00	0	39.39	6.12	6.95	12.17	6.71	12.23
25/01/2012	31.80	1	39.71	6.57	6.75	15.04	6.52	13.42
25/01/2012	34.60	5	39.61	5.68	5.68	12.69	6.14	10.85
25/01/2012	31.50	2	39.22	4.36	5.45	11.87	4.64	10.42
25/01/2012	21.30	10	40.09	1.87	1.74	11.29	2.72	10.01
25/01/2012	30.80	19	39.05	4.31	3.87	11.42	5.05	11.55
25/01/2012	20.40	0	39.82	2.39	1.60	11.87	2.92	10.13
25/01/2012	26.60	8	39.50	2.40	2.17	9.91	3.48	8.53
25/01/2012	21.50	5	39.50	1.68	1.85	10.14	3.60	8.64
25/01/2012	20.00	2	39.54	2.06	1.69	9.96	2.88	9.87
25/01/2012	27.00	0	39.99	3.32	3.54	10.03	4.44	9.72
25/01/2012	32.20	12	39.32	5.22	5.19	10.08	6.38	10.31
25/01/2012	32.40	16	39.87	6.05	6.37	11.18	7.76	11.45
25/01/2012	31.60	6	39.76	4.17	4.20	10.86	6.61	9.75
8/11/2011	25.70	4	39.07	2.79	3.79	12.05	2.87	10.06
8/11/2011	37.60	1	38.84	5.17	6.22	13.84	4.87	11.12
8/11/2011	39.10	16	38.15	9.77	11.72	15.85	9.77	14.50
8/11/2011	42.70	53	38.65	10.98	13.40	16.94	12.01	15.09
8/11/2011	38.40	1	39.18	8.61	10.06	15.91	8.75	16.52
8/11/2011	41.80	82	39.08	8.80	10.53	16.31	9.73	14.46
8/11/2011	43.20	13	38.84	11.53	13.41	17.94	12.05	15.46

Table A1.03 continued

8/11/2011	39.70	17	38.32	8.75	11.19	15.57	9.28	13.53
8/11/2011	43.20	37	37.90	8.24	10.02	17.26	8.70	13.87
8/11/2011	38.90	0	39.05	5.91	6.95	13.59	6.01	10.35
8/11/2011	27.20	2	39.28	2.36	3.90	12.74	2.31	10.12
8/11/2011	31.00	4	39.46	3.23	4.38	11.64	2.69	9.73
8/11/2011	32.90	6	39.33	3.75	4.58	13.07	3.24	10.16
8/11/2011	37.90	14	38.88	5.01	6.29	14.21	5.02	11.09
8/11/2011	33.70	2	39.59	4.05	5.33	13.11	2.96	10.62
8/11/2011	34.10	2	39.78	2.29	4.26	12.35	3.90	11.45
8/11/2011	33.60	4	39.38	2.00	2.66	10.36	2.20	10.13
8/11/2011	26.40	5	39.74	1.41	1.55	10.50	1.83	9.16
8/11/2011	28.40	8	39.18	1.69	2.09	10.48	2.36	9.86
8/11/2011	41.00	20	38.08	8.45	9.53	14.74	8.32	12.95
8/11/2011	38.60	0	39.40	6.15	6.62	12.36	6.48	12.06
8/11/2011	34.10	18	39.68	4.51	4.77	11.86	5.38	10.51
8/11/2011	30.30	0	39.24	4.58	4.10	10.39	4.48	10.50
8/11/2011	30.20	0	39.53	2.03	2.16	10.48	2.02	9.22
8/11/2011	22.80	0	40.10	1.93	1.82	11.12	2.71	10.33
8/11/2011	35.30	237	39.06	4.60	4.44	10.92	5.54	11.44
8/11/2011	26.60	2	39.49	1.50	2.06	9.73	2.92	9.54
8/11/2011	36.00	5	39.34	5.15	7.19	10.28	7.06	10.33
8/11/2011	31.90	0	40.09	4.19	4.13	10.63	6.45	10.76
8/11/2011	49.30	56	39.62	5.60	7.63	11.65	8.42	11.40
8/11/2011	37.90	18	39.74	3.41	3.37	9.80	4.16	9.35
8/11/2011	27.70	1	39.57	2.16	1.57	9.67	3.63	9.04
8/11/2011	25.10	1	39.74	1.91	2.00	9.94	2.71	8.86
8/11/2011	31.20	2	39.59	1.58	1.25	10.25	2.57	9.05
8/11/2011	24.60	6	39.59	2.67	2.17	11.71	3.78	10.82
8/11/2011	37.40	5	40.13	3.14	4.88	9.84	4.53	10.62

Moisture measurements are TDR to 45cm. EC_a, flow accumulation and elevation data extracted from kriged rasters surface to points of moisture measurement.

Table A1.04. Sand depth with elevation and EC_a at No.1 Dairy.
EC_a and elevation data extracted from kriged raster surfaces to points of moisture measurement.

Name	Sand depth (cm)	elevation (m)	EM38 Mk2 (1m, vertical) 25.1.12	EM38 Mk2 (1m, vertical) 8.11.11	EM38 Mk2 (1m, vertical) 18.8.11	EM31 (vertical) 25.1.12	EM31 (vertical) 8.11.11
2	110	39.5	8.5	8.4	6.8	13.1	13.6
3	100	39.6	3.2	3.0	2.6	9.9	9.9
4	116	38.4	7.8	8.0	7.4	13.0	13.5
5	100	38.3	8.8	9.5	8.1	13.1	14.8
6	110	39.0	9.9	10.9	8.8	14.5	16.4
7	125	38.8	11.2	12.9	10.2	15.9	17.4
8	95	38.3	9.1	10.9	8.6	13.2	15.5
9	180	37.9	8.7	9.8	8.3	13.6	17.1
10	140	38.4	9.2	10.8	9.2	13.0	16.1
11	95	38.9	5.5	6.3	6.7	11.0	13.4
12	50	39.1	2.8	3.2	2.8	9.5	12.5
13	38	39.3	4.9	6.2	2.8	9.3	12.7
14	45	39.2	3.7	6.2	5.3	10.5	14.7
15	130	39.7	9.3	9.5	5.6	11.3	13.1
16	38	39.6	3.9	2.5	2.4	11.2	11.5
D4	130	38.3	10.8	12.5	10.6	14.3	15.4
D5	54	39.6	1.9	2.2	2.3	10.3	10.5
D6	80	39.8	6.1	4.1	4.2	10.1	10.4

Table A1.05. Multi-height spot measurements of EC_a. Accompanying moisture measurements shown for reference.

Date	Location	Site	EM38 1mH @grnd ECa measured (mS/m)	EM38 1mV +6cm ECa measured (mS/m)	EM38 1mV +44cm ECa measured (mS/m)	EM38 1mV +44cm ECa calculated (mS/m)	EM38 1mV +87cm ECa measured (mS/m)	EM38 1mV +87cm ECa calculated (mS/m)	EM38 1mV +194cm ECa measured (mS/m)	EM38 1mV +194cm ECa calculated (mS/m)	ECa 0-45cm calculated (mS/m)	Vol. moist. % (TDR to 45cm)
15.03.12	Burnside	B1	15	13	9	9.83	5	6.58	1	3.28	21.2	38.4
15.03.12	Burnside	B2	8	10	7	7.56	5	5.06	1	2.53	7.7	34.3
15.03.12	Burnside	B3	7	7	6	5.29	4	3.54	2	1.77	8.8	34.4
24.2.12	No.1 Dairy	D4	15	13	9	9.83	6	6.58	3	3.28	21.2	36.0
24.2.12	No.1 Dairy	D5	3	2	2	1.51	1	1.01	0	0.51	4.9	20.2
24.2.12	No.1 Dairy	D6	8	6	5	4.54	3	3.04	1	1.52	12.4	32.8
4.3.12	No.1 Dairy	D4	12	13	9	9.83	5	6.58	2	3.28	13.9	39.9
4.3.12	No.1 Dairy	D5	3	1	0	0.76	-1	0.51	-2	0.25	6.1	22.9
4.3.12	No.1 Dairy	D6	7	5	3	3.78	1	2.53	-1	1.26	11.1	36.0

Table A1.06. Single-height spot measurements of EC_a (means of replicate measurements) with data of texture and other analyses (means to 42cm). Accompanying moisture measurements shown for reference.

Date	Location	Site	EM38 1mV +6cm ECa measured (mS/m)	EM38 1mH @grnd ECa measured (mS/m)	ECa 0-45cm calculated even layered (mS/m)	Vol. moist. % (TDR to 45cm)	EC 1:1 paste (mS/m)	fineness	clay %	sand %	silt %
22.11.11	Burnside	B1	13.3	13.7	17.6	43.8	15.1	2.8	9.1	12.6	78.2
23.11.11	Burnside	B2	8.7	9.0	11.7	35.0	8.8	2.7	9.3	19.8	70.9
25.11.11	Burnside	B3	9.7	11.0	15.4	37.9	13.7	2.5	6.8	12.8	80.4
27.12.11	No.1 Dairy	D4	14.3	14.0	17.2	31.2	15.6	2.8	8.9	7.6	83.5
29.12.11	No.1 Dairy	D5	3.3	4.3	6.6	21.2	8.0	1.9	3.7	31.0	65.3
6.1.12	No.1 Dairy	D6	5.3	8.0	12.9	33.4	9.8	2.3	6.1	25.8	68.1

Table A1.07. Single-height replicate spot measurements of EC_a (EM38 Mk2) with data of soil analyses (means to 42cm depth).

Sample Date	Location	Site	Replicate	EM38 1mV +6cm ECa measured (mS/m)	EM38 1mH @grnd ECa measured (mS/m)	ECa 0-45cm calculated even layered (mS/m)	Vol. moist. % (TDR to 45cm)	Vol. moist. % (gravimetric analysis)	Soil particle density ρ (g/cm3)	Dry bulk density (g/cm3)	Total porosity %	Vol. moist. % (TDR to 45cm)	EC 1:1 paste (mS/m)	EC 1:1 extract (mS/m)
22.11.11	Burnside	B1	a	14	13	15.2	43.4	38.04	2.47	1.15	53.72	43.4	16.66	19.13
22.11.11	Burnside	B1	b	13	14	18.8	42.9	37.95	2.49	1.17	52.89	42.9	14.83	17.66
22.11.11	Burnside	B1	c	13	14	18.8	45.2	35.31	2.62	1.16	56.08	45.2	13.68	17.95
23.11.11	Burnside	B2	a	10	10	12.6	34.4	32.06	2.65	1.25	52.28	34.4	9.04	10.60
23.11.11	Burnside	B2	b	9	10	13.7	35.7	33.51	2.44	1.23	49.76	35.7	8.45	10.10
23.11.11	Burnside	B2	c	7	7	8.8	34.9	33.54	2.70	1.18	56.29	34.9	8.79	10.70
25.11.11	Burnside	B3	a	10	13	19.8	38.5	36.50	2.60	1.22	53.19	38.5	16.12	21.70
25.11.11	Burnside	B3	b	9	9	11.3	37.0	33.35	2.71	1.17	57.00	37.0	14.01	18.93
25.11.11	Burnside	B3	c	10	11	15.0	38.3	38.86	2.82	1.21	56.98	38.3	11.03	14.00
27.12.11	No.1 dairy	D4	a	15	13	14.0	31.8	36.75	2.70	1.27	53.02	31.8	16.30	15.48
27.12.11	No.1 dairy	D4	b	15	15	18.9	29.4	34.72	2.84	1.28	54.97	29.4	14.50	13.57
27.12.11	No.1 dairy	D4	c	13	14	18.8	32.5	36.27	2.76	1.29	53.44	32.5	15.97	15.42
29.12.11	No.1 dairy	D5	a	3	4	6.2	22.3	23.60	2.72	1.36	50.21	22.3	9.50	11.80
29.12.11	No.1 dairy	D5	b	3	4	6.2	22.7	21.44	2.80	1.37	51.01	22.7	7.63	8.73
29.12.11	No.1 dairy	D5	c	4	5	7.4	18.7	18.94	2.82	1.36	51.86	18.7	6.93	7.70
6.1.12	No.1 dairy	D6	a	4	8	14.7	33.8	35.19	2.66	1.34	49.79	33.8	9.43	10.78
6.1.12	No.1 dairy	D6	b	5	7	11.1	32.7	36.47	2.66	1.37	48.33	32.7	8.87	9.32
6.1.12	No.1 dairy	D6	c	7	9	13.6	33.8	35.39	2.60	1.34	48.16	33.8	11.00	12.13

Table A1.08. Soil analyses – replicate depth sample results.

Sample Date	Location	Site	Rep.	Sample depth (cm)	Soil series	Horizon type	Soil particle density (g/cm^3)	Dry bulk density (g/cm^3)	Total porosity %	Field vol. moist. %	EC 1:1 paste (mS/m)	EC 1:1 extract (mS/m)
22.11.11	Burnside	B1	a	4	Kairanga	Ap	2.42	0.85	65	42	17.9	21.2
22.11.11	Burnside	B1	a	28	Kairanga	ABg	2.44	1.26	48	40	17.5	19.7
22.11.11	Burnside	B1	a	42	Kairanga	Bg	2.55	1.32	48	33	14.7	16.5
22.11.11	Burnside	B1	a	64	Kairanga	Bg	2.48	1.39	44	34	13.4	18.0
22.11.11	Burnside	B1	b	4	Kairanga	Ap	2.47	0.93	62	45	22.0	28.4
22.11.11	Burnside	B1	b	28	Kairanga	Bg	2.54	1.17	54	34	10.9	11.1
22.11.11	Burnside	B1	b	42	Kairanga	Bg	2.46	1.41	43	35	11.7	13.5
22.11.11	Burnside	B1	b	64	Kairanga	Bg	2.56	1.52	41	39	13.1	15.1
22.11.11	Burnside	B1	c	4	Kairanga	Ap	2.43	0.93	62	44	-	-
22.11.11	Burnside	B1	c	28	Kairanga	ABg	2.52	1.15	54	35	13.5	16.9
22.11.11	Burnside	B1	c	42	Kairanga	Bg	2.91	1.40	52	28	13.9	19.0
22.11.11	Burnside	B1	c	64	Kairanga	Bg	2.59	1.44	45	38	17.2	21.5
23.11.11	Burnside	B2	a	4	Manawatu	Ap	2.80	1.03	63	31	13.9	17.5
23.11.11	Burnside	B2	a	28	Manawatu	Bw	2.53	1.33	48	32	7.7	9.1
23.11.11	Burnside	B2	a	42	Manawatu	Bw	2.61	1.41	46	33	5.6	5.2
23.11.11	Burnside	B2	a	64	Manawatu	Bw	2.59	1.37	47	31	7.4	7.1
23.11.11	Burnside	B2	b	4	Manawatu	Ap	2.44	1.16	53	39	13.4	16.1
23.11.11	Burnside	B2	b	28	Manawatu	Bw	2.36	1.13	52	28	5.6	6.0
23.11.11	Burnside	B2	b	42	Manawatu	Bw	2.51	1.39	45	33	6.4	8.2
23.11.11	Burnside	B2	b	64	Manawatu	Bw	2.55	1.43	44	34	6.6	8.6
23.11.11	Burnside	B2	c	4	Manawatu	Ap	2.62	1.03	61	39	11.9	15.2
23.11.11	Burnside	B2	c	28	Manawatu	Bw	2.73	1.24	54	32	7.2	9.0

Table A1.08 continued

23.11.11	Burnside	B2	c	42	Manawatu	Bw	2.76	1.27	54	30	7.3	7.9
23.11.11	Burnside	B2	c	64	Manawatu	Bw	2.79	1.32	53	33	9.2	11.1
25.11.11	Burnside	B3	a	4	Manawatu	Apg	2.63	1.14	57	40	26.5	39.0
25.11.11	Burnside	B3	a	28	Manawatu	Bw	2.52	1.20	52	33	11.2	14.6
25.11.11	Burnside	B3	a	42	Manawatu	Bw	2.66	1.32	51	36	10.7	11.5
25.11.11	Burnside	B3	a	64	Manawatu	Bw	2.98	1.33	55	34	6.8	7.0
25.11.11	Burnside	B3	b	4	Manawatu	Apg	2.65	1.03	61	35	25.6	35.9
25.11.11	Burnside	B3	b	28	Manawatu	Bw	2.73	1.28	53	34	9.3	11.1
25.11.11	Burnside	B3	b	42	Manawatu	Bw	2.76	1.19	57	31	7.2	9.8
25.11.11	Burnside	B3	b	64	Manawatu	Bw	2.78	1.28	54	32	8.4	10.2
25.11.11	Burnside	B3	c	4	Manawatu	Ap	2.96	1.05	64	44	21.6	29.0
25.11.11	Burnside	B3	c	28	Manawatu	Bw	2.73	1.26	54	34	5.5	6.6
25.11.11	Burnside	B3	c	42	Manawatu	Bw	2.77	1.32	53	39	6.0	6.4
25.11.11	Burnside	B3	c	64	Manawatu	Bw	2.76	1.34	51	36	6.3	6.4
27.12.11	No.1 dairy	D4	a	4	Parewanui	Ap	2.42	1.16	52	34	14.7	14.3
27.12.11	No.1 dairy	D4	a	28	Parewanui	AB	2.73	1.33	51	37	17.3	16.5
27.12.11	No.1 dairy	D4	a	42	Parewanui	Bg	2.95	1.31	56	39	16.9	15.7
27.12.11	No.1 dairy	D4	a	64	Parewanui	Bg	3.04	1.18	61	41	21.2	20.7
27.12.11	No.1 dairy	D4	b	4	Parewanui	Ap	2.71	1.10	59	27	15.8	17.9
27.12.11	No.1 dairy	D4	b	28	Parewanui	ABg	2.79	1.39	50	37	14.9	12.4
27.12.11	No.1 dairy	D4	b	42	Parewanui	Bg	3.01	1.35	55	39	12.8	10.5
27.12.11	No.1 dairy	D4	b	64	Parewanui	Bg	2.77	1.17	58	41	15.2	13.5
27.12.11	No.1 dairy	D4	c	4	Parewanui	Ap	2.71	1.29	53	29	14.8	16.9
27.12.11	No.1 dairy	D4	c	28	Parewanui	ABg	2.77	1.33	52	36	15.7	13.9
27.12.11	No.1 dairy	D4	c	42	Parewanui	Bg	2.81	1.24	56	44	17.4	15.5
27.12.11	No.1 dairy	D4	c	64	Parewanui	Bg	2.51	1.19	53	40	20.0	20.3

Table A1.08 continued

29.12.11	No.1 dairy	D5	a	4	Rangitikei	Apg	2.69	1.34	50	26	14.3	17.7
29.12.11	No.1 dairy	D5	a	28	Rangitikei	AB	2.75	1.40	49	25	8.7	9.5
29.12.11	No.1 dairy	D5	a	42	Rangitikei	C	2.72	1.33	51	21	5.5	8.3
29.12.11	No.1 dairy	D5	a	64	Rangitikei	C	2.80	1.34	52	7	3.8	4.3
29.12.11	No.1 dairy	D5	b	4	Rangitikei	Apg	2.65	1.35	49	21	10.0	11.5
29.12.11	No.1 dairy	D5	b	28	Rangitikei	AB	2.98	1.47	51	24	7.7	8.9
29.12.11	No.1 dairy	D5	b	42	Rangitikei	C	2.76	1.29	53	20	5.2	5.9
29.12.11	No.1 dairy	D5	b	64	Rangitikei	C	2.81	1.44	49	8	2.9	3.1
29.12.11	No.1 dairy	D5	c	4	Rangitikei	Apg	2.88	1.28	56	16	9.3	10.0
29.12.11	No.1 dairy	D5	c	28	Rangitikei	AB	2.82	1.47	48	17	6.6	7.7
29.12.11	No.1 dairy	D5	c	42	Rangitikei	C	2.76	1.32	52	23	4.9	5.5
29.12.11	No.1 dairy	D5	c	64	Rangitikei	C	2.79	1.41	50	11	3.0	3.0
6.1.12	No.1 dairy	D6	a	4	Rangitikei	Ap	2.52	1.22	52	37	10.3	14.1
6.1.12	No.1 dairy	D6	a	28	Rangitikei	Bw	2.72	1.40	48	36	10.0	10.7
6.1.12	No.1 dairy	D6	a	42	Rangitikei	Bw	2.75	1.39	49	33	8.0	7.6
6.1.12	No.1 dairy	D6	a	64	Rangitikei	Bw	2.80	1.31	53	36	10.5	9.8
6.1.12	No.1 dairy	D6	b	4	Rangitikei	Ap	2.67	1.25	53	36	7.8	9.7
6.1.12	No.1 dairy	D6	b	28	Rangitikei	Bw	2.55	1.42	44	39	9.5	9.5
6.1.12	No.1 dairy	D6	b	42	Rangitikei	Bw	2.75	1.44	48	35	9.3	8.9
6.1.12	No.1 dairy	D6	b	64	Rangitikei	Bw	2.74	1.39	49	35	10.2	10.3
6.1.12	No.1 dairy	D6	c	4	Rangitikei	Ap	2.72	1.24	54	34	13.5	16.4
6.1.12	No.1 dairy	D6	c	28	Rangitikei	Bw	2.33	1.37	41	38	10.6	11.1
6.1.12	No.1 dairy	D6	c	42	Rangitikei	Bw	2.74	1.40	49	34	8.9	8.9
6.1.12	No.1 dairy	D6	c	64	Rangitikei	Bw	2.77	1.37	51	36	9.5	8.6

Table A1.09. Calculation of EC_a (0-45cm) at soil sample sites.
Depth resolution index (even-layered profile): y = 2.413x - 1.156
Accompanying moisture measurements shown for reference.

Date	Location	Site	EM38 1mH @grnd ECa measured (mS/m)	EM38 1mV +6cm ECa measured (mS/m)	EM38 1mH / EM38 1mV +6cm	Depth resolution factor (even layered profile)	ECa 0-45cm calculated (mS/m)	Vol. moist. % (TDR to 45cm)
15.03.12	Burnside	B1	15	13	1.15	1.63	21	38.4
15.03.12	Burnside	B2	8	10	0.80	0.77	8	34.3
15.03.12	Burnside	B3	7	7	1.00	1.26	9	34.4
24.2.12	No.1 Dairy	D4	15	13	1.15	1.63	21	36.0
24.2.12	No.1 Dairy	D5	3	2	1.50	2.46	5	20.2
24.2.12	No.1 Dairy	D6	8	6	1.33	2.06	12	32.8
4.3.12	No.1 Dairy	D4	12	13	0.92	1.07	14	39.9
4.3.12	No.1 Dairy	D5	3	1	3.00	6.08	6	22.9
4.3.12	No.1 Dairy	D6	7	5	1.40	2.22	11	36.0
22.11.11	Burnside	B1a	13	14	0.93	1.08	15	43.4
22.11.11	Burnside	B1b	14	13	1.08	1.44	19	42.9
22.11.11	Burnside	B1c	14	13	1.08	1.44	19	45.2
23.11.11	Burnside	B2a	10	10	1.00	1.26	13	34.4
23.11.11	Burnside	B2b	10	9	1.11	1.53	14	35.7
23.11.11	Burnside	B2c	7	7	1.00	1.26	9	34.9
25.11.11	Burnside	B3a	13	10	1.30	1.98	20	38.5
25.11.11	Burnside	B3b	9	9	1.00	1.26	11	37.0
25.11.11	Burnside	B3c	11	10	1.10	1.50	15	38.3
27.12.11	No.1 dairy	D4a	13	15	0.87	0.94	14	31.8
27.12.11	No.1 dairy	D4b	15	15	1.00	1.26	19	29.4
27.12.11	No.1 dairy	D4c	14	13	1.08	1.44	19	32.5
29.12.11	No.1 dairy	D5a	4	3	1.33	2.06	6	22.3
29.12.11	No.1 dairy	D5b	4	3	1.33	2.06	6	22.7
29.12.11	No.1 dairy	D5c	5	4	1.25	1.86	7	18.7
6.1.12	No.1 dairy	D6a	8	4	2.00	3.67	15	33.8
6.1.12	No.1 dairy	D6b	7	5	1.40	2.22	11	32.7
6.1.12	No.1 dairy	D6c	9	7	1.29	1.95	14	33.8

Table A1.10. Soil moisture retention results.

Sample date	Site	Rep.	Sample depth (cm)	Vol. moisture (%) fresh	Vol. moisture (%) @10kPa	Vol. moisture (%) @100 kPa	Vol. moisture (%) @1500 kPa
27.12.11	D4	a	4	34	49	39	19
27.12.11	D4	a	28	37	43	34	21
27.12.11	D4	a	42	39	41	33	15
27.12.11	D4	a	64	41	42	35	18
27.12.11	D4	b	4	27	47	35	22
27.12.11	D4	b	28	37	42	34	25
27.12.11	D4	b	42	39	42	34	20
27.12.11	D4	b	64	41	42	35	25
27.12.11	D4	c	4	29	47	38	17
27.12.11	D4	c	28	36	43	34	25
27.12.11	D4	c	42	44	46	36	26
27.12.11	D4	c	64	40	41	33	29
29.12.11	D5	a	4	26	43	35	14
29.12.11	D5	a	28	25	31	22	10
29.12.11	D5	a	42	21	24	10	5
29.12.11	D5	a	64	7	8	4	2
29.12.11	D5	b	4	21	40	28	20
29.12.11	D5	b	28	24	30	20	10
29.12.11	D5	b	42	20	23	9	5
29.12.11	D5	b	64	8	10	4	3
29.12.11	D5	c	4	16	38	27	24
29.12.11	D5	c	28	17	26	17	9
29.12.11	D5	c	42	23	27	11	6
29.12.11	D5	c	64	11	11	6	3
6.1.12	D6	a	4	37	41	29	8
6.1.12	D6	a	28	36	37	27	12
6.1.12	D6	a	42	33	35	23	12
6.1.12	D6	a	64	36	37	26	14
6.1.12	D6	b	4	36	39	26	7
6.1.12	D6	b	28	39	40	30	13
6.1.12	D6	b	42	35	36	24	16
6.1.12	D6	b	64	35	36	24	11
6.1.12	D6	c	4	34	39	25	8
6.1.12	D6	c	28	38	40	30	12
6.1.12	D6	c	42	34	35	24	13
6.1.12	D6	c	64	36	38	26	14

Table A1.11. Soil texture results (Particle Size Distribution Analyser).
Particle size class definitions (µm): sand = 2000-62.5; silt = 62.5-1.95; clay = <1.95.
Fineness calculation:
Fineness = $3.8*T - 0.91*T^2 + 1.9686$; $T = 0.03*\text{clay}(\%) - 0.004*\text{sand}(\%)$

Particle size	Sample depth	B1	B2	B3	D4	D5	D6
sand	4cm	12.0	22.1	11.9	12.3	21.0	37.0
sand	28cm	8.6	20.0	11.1	7.5	31.3	19.6
sand	42cm	17.3	17.3	15.3	2.9	40.6	20.9
sand	64cm	11.1	19.1	11.6	1.8	90.3	14.5
silt	4cm	76.4	67.5	79.0	81.4	72.7	60.2
silt	28cm	80.1	71.6	83.8	82.7	64.9	72.6
silt	42cm	78.3	73.5	78.5	86.3	58.3	71.5
silt	64cm	79.1	70.8	84.8	94.6	9.7	75.9
clay	4cm	11.6	10.3	9.2	6.3	6.3	2.8
clay	28cm	11.3	8.4	5.0	9.8	3.7	7.8
clay	42cm	4.5	9.2	6.3	10.7	1.1	7.6
clay	64cm	9.8	10.1	3.7	3.6	0.0	9.6
fineness	4cm	3.0	2.8	2.8	2.5	2.4	1.7
fineness	28cm	3.0	2.6	2.4	2.9	1.9	2.5
fineness	42cm	2.2	2.7	2.4	3.1	1.5	2.5
fineness	64cm	2.9	2.8	2.2	2.3	0.5	2.8

Appendix 2. EM38 Mk2 calibration method.

1. Allow instrument to equilibrate with ambient temperature.

2. Check battery: set mode switch to BAT, reading should be higher than 720. (Initial energizer readings are >1200 and need re-checking after 2 hours operation).

3. Set mode switch to QP, observe readings around the immediate calibration site (~1.5m radius) to make sure there are no large fluctuations indicating interference from buried metal or any other source.

4. Instrument at 1.5m height, horizontal mode, mode switch = 1m. Set IP and QP to zero using 1m controls.

5. Instrument position as above, set QP (1m) to 50 mS/m (='H'). If 50 mS/m is not within range, any clearly defined value of a reasonable magnitude is OK.

6. Instrument still at 1.5m height, pivot around long axis to vertical mode. Note QP reading ('V').

7. Return instrument to horizontal mode, set QP to V-H. (E.g. if the reading in horizontal mode was 50, and in vertical mode 52, return to horizontal mode and set QP to 2).

8. Repeat for the above procedure for 0.5m coil spacing, mode switch =0.5m, using 0.5m controls.

9. The instrument is considered calibrated when, at 1.5m height, V=2H for both coil spacings.

10. With the instrument in survey position, set the IP to zero.

Sensitivity check: instrument at 1.5m height, horizontal mode, mode switch = 1m. Rotate QP (1m) zero knob clockwise one turn. Meter should change between 20 and 28 mS/m. Return zero knob to previous position.

For 0.5m application, change should be between 28 and 30 mS/m.

For EM38, QP at 1000 mS/m range, rotate IP coarse knob 1 step clockwise, then return to original position. If QP reading changes, adjust phase control screw. Repeat until no change.

Adapted from Geonics (2008).

Appendix 3. EM31 setup method.

The EM31 is factory calibrated. The following procedures however, are required when preparing for use.

1. Attach the transmitter tube to the main console.
2. Set mode switch to OPER, range switch to 1000.
3. Check that conductivity ('C') reading is zero ±1. If necessary it can be adjusted with a small flat screwdriver through a small hole on the console (see diagram in *EM31 Mk2 – Operating Manual*).
4. Set mode switch to OFF, attach the receiver tube.
5. Set the range switch to 100, mode switch to OPER.
6. Set the inphase ('I') reading to zero ± 0.1 using the coarse and fine COMPENSATION controls.
7. Set the mode switch to PHASE. Note the conductivity reading.
8. Rotate the COARSE control one step clockwise. Conductivity reading should be unchanged (±0.2). Return COARSE control to original position.
9. If in the above procedure the conductivity reading was changed, the phase should be adjusted using the screw on the main panel. An decrease in conductivity is corrected by a clockwise adjustment of the screw, and vice versa. Return COARSE control to original position.
10. With the instrument in survey position, set the IP to zero.
11. Sensitivity check: mode switch in COMP position. Rotate COARSE control one step clockwise. Conductivity should change between 22 and 26 mS/m. Return COARSE control to original position.
12. Mode switch to OPER to begin use.

Adapted from Geonics (1995).

Appendix 4. Data cleaning and GPS position adjustment.

EM31 files:

- open Excel, import .xyz file, save as .xlsx
- format time field with custom format: hh:mm:ss.000
- create 'seconds' field (number format) = above field *24*60*60
- convert all fields to number format

EM31 and EM38mkII files:

- display data in ArcMap
    - project in NZ Map Grid
    - add x,y coordinate fields
    - close ArcMap
- in Excel:
    - open .dbf; save as .xlsx (2007) or .xlsm (2010 macro-enabled workbook)
        - note: Excel 2010 attaches user-defined functions to specific worksheets – it is easiest then to open a previous worksheet containing the functions, save it under a new name, and transfer the data into it
    - calculate a 'point_gap_s' field
    - if EM towed on mat (e.g. 38mkII):
        - if data logged at 1hz, point gap = time in seconds since reading before last (accounts for 'lag' in mat aligning with direction of travel)
        - if 5hz, point gap = time in seconds since 10th reading back
    - if EM on boom (e.g. EM31), point gap = time in seconds since last reading
    - don't worry about bad values in first cell or cells – will be deleted later
    - copy and paste 'point gap' field as values

- create ‘last_X’ and ‘last_Y’ columns (for each point, the coordinates of the point the same number back as for ‘point gap’ above) to enable calculation of Theta (degrees past N, E, S or W of direction of travel) and DirTrav (NE, SE, SW or NW) if there is no ‘direction of travel’ field, e.g. ‘Course’, and to calculate travel for system delay calculations
    - copy and paste as values
- delete first data rows
- calculate TravelDir (NE, SE, SW or NW)
    - copy and paste as values
- calculate Theta
    - some cells won’t compute because the bike was stationary so had no detectable orientation; these will be deleted anyway in the steps below
    - copy and paste as values (so formulas won’t crash when rows are deleted)
- calculate Speed in m/s from distance travelled and seconds between points (will use this with system delay in offset calculations)
    - copy and paste as values
- remove duplicates using rounded x,y coordinate fields (1 d.p. = 0.1m distance in a metre-based grid)
- delete values with point gap values significantly larger or smaller than the expected measurement gap (sort by point gap)
- delete values with very high or low m/s speeds
- add and calculate offset x,y fields
    - m_back = m back ± system delay (s) * m/s
    - depends on whether gps location precedes or follows data point in order of logging; should be determined experimentally
    - EM31 on old ATV: m_back = -0.9, m_left = -1.7
    - EM38 Mk2 on old ATV: m_back = 2.13 + 0.2s * speed (m/s), m_left = 0

        - there is a 0.25m difference between the 0.5m and 1m coils on the EM38 Mk2; alternative positions can be calculated for these if desired (to display in ArcMap these will need separate shapefiles for each, but initially the alternative coordinates can be calculated in the same Excel file)

        - copying and pasting the offset X and Y fields as values will make the spreadsheet easier to handle

- display .xlsx in ArcMap using offset coordinate fields; export to shapefile

    - if working in Excel 2010, the file must have been saved as a workbook (not a macro-enabled workbook) in order to add to ArcMap

    - display EM in 'quantity' colour bands

    - delete points close to fences:

        - (assuming there is a polygon shapefile of paddock boundaries) make a polyline shapefile of paddock boundaries (fences)

        - in ArcCatalog, right click in folder, select 'New' – 'Shapefile' – 'Polyline'; name the file, select projection (NZMG)

        - drag and drop polyline file into ArcMap table of contents (list of layers at side)

        - start editing, set polyline file as target

        - right click file of boundary polygons, 'select all'

        - 'copy' in ArcMap Edit menu, then 'paste' in same

        - save edits (polyline file should now be populated with boundary lines)

        - set point shapefile as target

        - select by location and delete points which intersect polyline file; use a buffer of 12m for EM31, 3m for EM38mkII

        - save edits

- examine for further 'artifacts' – linear features from pipes or overhead wires etc.

- check visual continuity between blocks (times) of survey, battery change points etc.

- using the above .xlsx file in Excel, calculate high and low cutoff points (+- 3 s.d). in CV1m and CV05m data

- in ArcMap highlight high and low cut points ('select by attribute') – examine whether clumped, random, or associated with areas of less extreme highs and lows

    - make files (layers) of cut points, remove from main data set.

Appendix 5. Functions for calculation of sensor location.

The following functions in VBA were used to offset sensor log point locations in Excel by set distances back and to the side of GPS position. Needed are the x,y coordinates of the log points in a metre-based grid, and the coordinates of previously logged points.

1. Function to identify a direction (NE, SE, SW, or NW) for every course bearing (FromX and FromY are the coordinates of the preceding point):

```
Function Direction(X, Y, FromX, FromY)
  If X >= FromX And Y > FromY Then
    Direction = "NE"
  ElseIf X >= FromX And Y <= FromY Then
    Direction = "SE"
  ElseIf X <= FromX And Y < FromY Then
    Direction = "SW"
  Else
    Direction = "NW"
  End If
End Function
```

2. Function to calculate an angle in radians for trig-based GPS sensor offset calculations:

```
Function Angle(Direction, X, Y, FromX, FromY)
  If Direction = "NE" Or Direction = "SW" Then
    Angle = Atn(Abs(Y - FromY) / Abs(X - FromX))
  Else
    Angle = Atn(Abs(X - FromX) / Abs(Y - FromY))
  End If
End Function
```

3. Function to calculate an offset ‘x’ coordinate of the sensor log point (M_Left and M_Back are the distances of the sensor behind and to the left of the GPS antenna):

```
Function X_Off(Dir, X, Angle, M_Back, M_Left)
  If Dir = "NE" Then
    X_Off = X - (M_Back * Cos(Angle)) - (M_Left * Sin(Angle))
  ElseIf Dir = "SE" Then
    X_Off = X - (M_Back * Sin(Angle)) + (M_Left * Cos(Angle))
  ElseIf Dir = "SW" Then
    X_Off = X + (M_Back * Cos(Angle)) + (M_Left * Sin(Angle))
  Else
    X_Off = X + (M_Back * Sin(Angle)) - (M_Left * Cos(Angle))
  End If
End Function
```

4. Function to calculate an offset ‘y’ coordinate of a sensor log point:

```
Function Y_Off(Dir, Y, Angle, M_Back, M_Left)
  If Dir = "NE" Then
    Y_Off = Y - (M_Back * Sin(Angle)) + (M_Left * Cos(Angle))
  ElseIf Dir = "SE" Then
    Y_Off = Y + (M_Back * Cos(Angle)) + (M_Left * Sin(Angle))
  ElseIf Dir = "SW" Then
    Y_Off = Y + (M_Back * Sin(Angle)) - (M_Left * Cos(Angle))
  Else
    Y_Off = Y - (M_Back * Cos(Angle)) - (M_Left * Sin(Angle))
  End If
End Function
```

5. Function to calculate speed of travel:

```
Function Speed(Dir, X, Y, FromX, FromY, Seconds, Angle)
   If Dir = "NE" Or Dir = "SW" Then
      Speed = (Abs(X - FromX) / Cos(Angle)) / Seconds
   Else
      Speed = (Abs(Y - FromY) / Cos(Angle)) / Seconds
   End If
End Function
```

Appendix 6. EMI instrument functional tests.

Explanation of terminology in this Appendix: quad-phase (QP) is the measurement which represents EC_a on Geonics instruments. Both QP and in-phase (IP) are measured in millisiemens per metre (mS/m).

Effect of temperature: EM38 Mk2.

When temperature was artificially raised in a nylon tent, IP and QP readings from the EM38 Mk2 (1m, vertical mode, stationary) showed limited drift. IP from the EM38 Mk2 (0.5m, vertical mode, stationary) was inversely related to ambient temperature while QP fell with drop in temperature (the QP trend was limited; Figures A6.01 and A6.02).

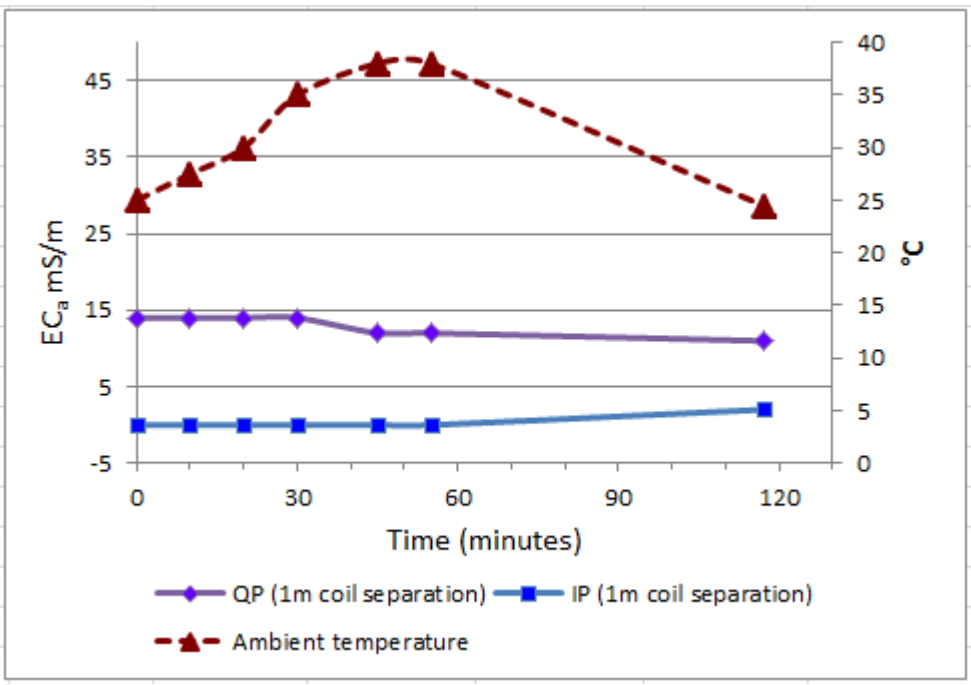

Figure A6.01. EM38 Mk2 (vertical mode, 1m) IP and QP readings with ambient temperature change.

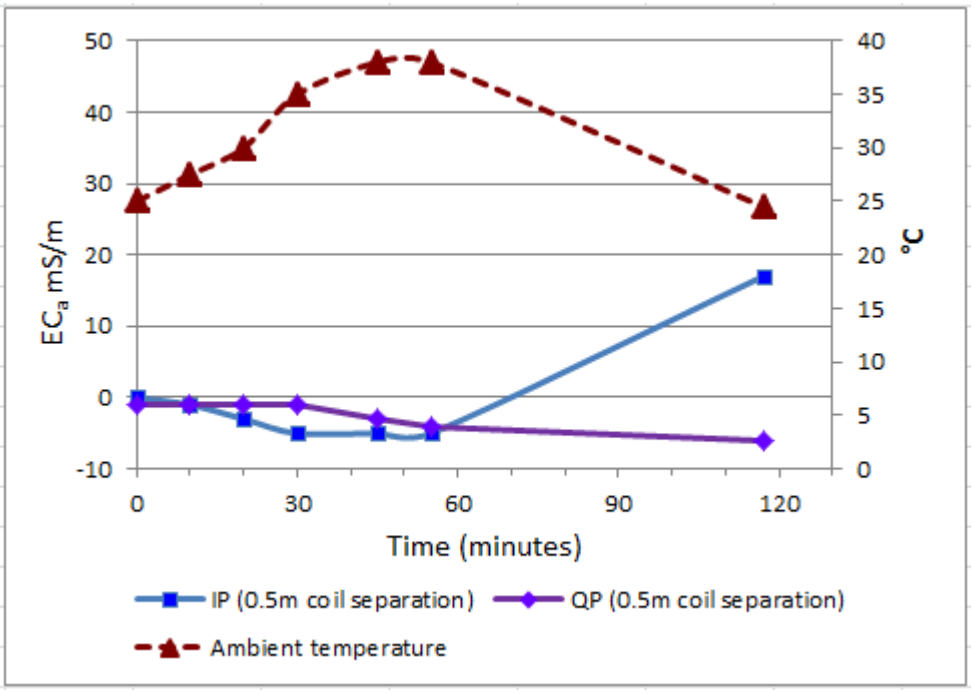

Figure A6.02. EM38 Mk2 (vertical mode, 0.5m) IP and QP readings with ambient temperature change.

From the above results it is concluded that change in ambient temperature may affect EM38 Mk2 IP readings in ways unrelated to soil temperature (variation in soil temperature was < 0.5°C). In the temperature range considered (20-38°C) that effect appeared confined to the 0.5m coil spacing. It is not clear how effects on IP and QP were related, or how the effects were related to internal temperature correction mechanisms which the EM38 Mk2 does possess (Geonics, 2012).

Battery effects: EM38 Mk2

An apparent effect on EC_a measurement of changing the EM38 Mk2 instrument battery was noticed in data from the Burnside reconnaissance survey of 22.8.11. While data from the 1m coil spacing appeared continuous across the survey area, data from the 0.5m spacing showed an apparent discontinuity which corresponded to the location of a battery change. The instrument was not recalibrated at replacement of the battery (Figure A.6.03).

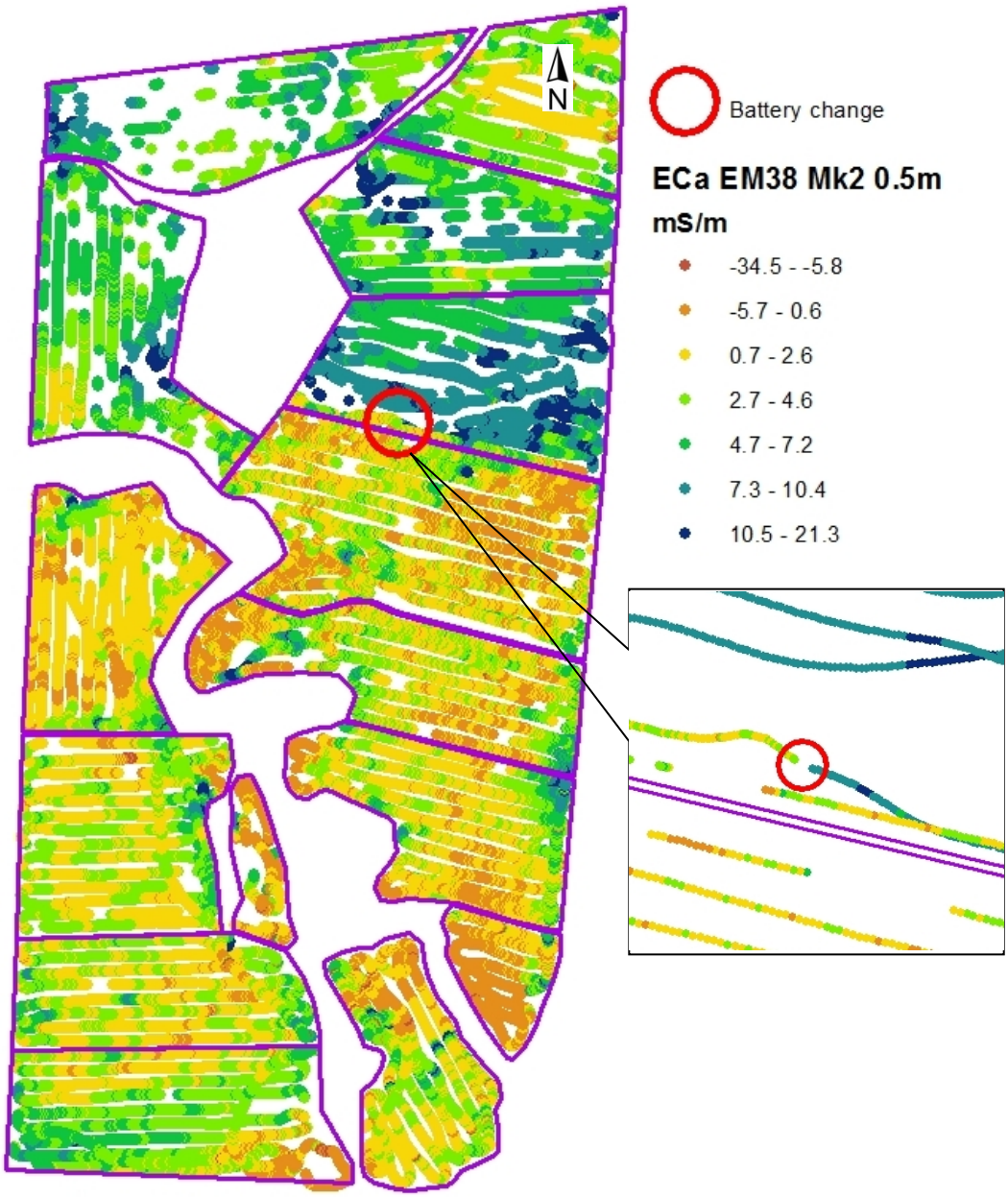

Figure A6.03. EC_a measured by EM38 Mk2 (vertical mode, 0.5m coil spacing) at Burnside, 22.8.11, showing discontinuity at battery change.

During a stationary field test, EC_a measured by both the 1m and 0.5m coil spacings of the EM38 Mk2 declined significantly over a four hour period during which battery voltage declined from 8.99 to 8.01V (1188 and 791 respectively on the EM38 Mk2 battery gauge; Geonics (2008) indicate battery replacement when or before the battery gauge drops to 760). The decline related to the 0.5m coil spacing was greater.

Following replacement of the battery with a new battery having a voltage of 8.68V, EC_a measured by the 1m coil spacing remained stable while EC_a measured by the 0.5m spacing more than doubled, from 8 mS/m to 17 mS/m. The instrument was then recalibrated, at which EC_a measured by the 1m coil spacing again remained stable while EC_a measured by the 0.5m spacing reduced to 13 mS/m – close to the initial reading of 12 mS/m (Figure A6.04).

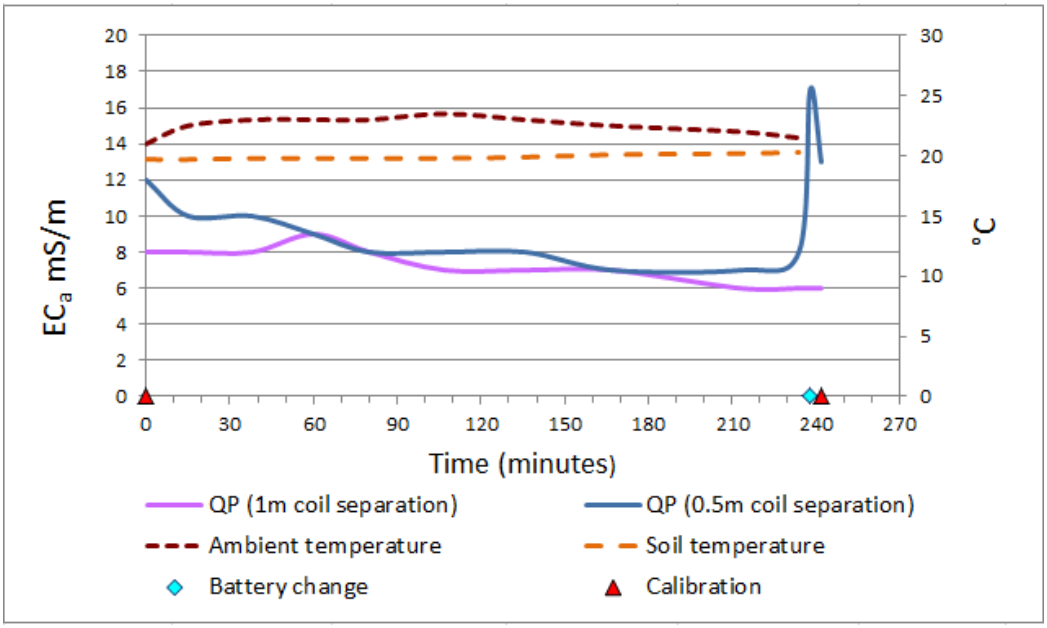

Figure A6.04. Stability of EC_a measured by EM38 Mk2 during decline of instrument battery voltage and replacement of battery.

The above results suggest that EC_a measured by the 1m coil spacing of the EM38 Mk2 is relatively stable across the recommended range of battery voltage, but that EC_a measured by the 0.5m spacing may be affected by decline in battery voltage within the recommended range and also requires instrument recalibration when the battery is replaced.

In view of the above findings it would seem that best practice for field surveys is to conduct the survey using a single battery, and for consistent results from the 0.5m spacing to limit the survey extent to a range of battery voltage well within the recommended limit, or else to recalibrate the instrument at battery changes, preferably at the initial calibration site to confirm parity of measurement throughout

the survey. (The above experiments did not confirm whether correction of battery effects was consistent across different calibration sites).

Battery effects: EM31

EC_a measured by EM31 remained relatively stable over 4½ hours of stationary operation during which voltage from the battery pack declined from 5.48 to 5.02 V. The battery pack was loaded with Arlec rechargeable 'C' cell batteries, the individual voltages of which were 1.34-1.41 V at the beginning of the test, declining to 1.22-1.27 V by the end of the test. Following this the rechargeable batteries were replaced with Energizer 'C' cell batteries having individual voltages of 1.50-1.60 V. The voltage of the battery pack loaded with the Energizers was 6.38 V. With the EM31 powered by the Energizer batteries, measured EC_a was unchanged. EC_a measurements by the EM31 therefore showed good stability with declining battery voltage and battery change (Figure A6.05).

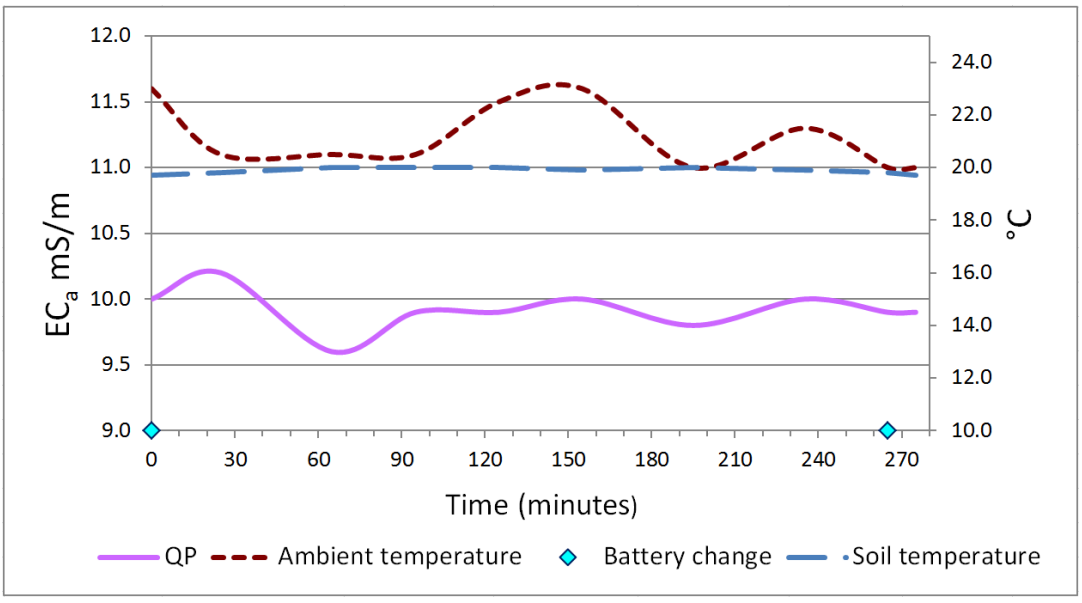

Figure A6.05. EM31 stationary test for effects of battery depletion.

Cable and connection effects

The position of the data cable connecting the Allegro field computer to the EM38 Mk2 was found to affect IP and QP readings. At a field test site the readings for the 1m and 0.5m coil spacings following calibration were:

QP: 2 and 4 mS/m respectively; IP: 0 mS/m for both coil spacings.

For the 1m coil spacing (vertical mode) moving the cable caused IP to vary between 1-9 mS/m and QP between 8-9 mS/m from the original readings. For the 0.5 coil spacing IP varied between 4-39 mS/m and QP between 1-9 mS/m from the original readings.

QP values shown on the EM38 Mk2 instrument panel were similar to those on the Allegro; IP however, differed on the Allegro. When IP on the instrument showed 2 and 6 mS/m for the 1m and 0.5m coil spacings respectively, IP on the Allegro showed 0.06 for both coil spacings. Variation in QP and IP caused by cable movement was observed on the Allegro as well as the instrument panel, IP on the Allegro in keeping with its smaller magnitude.

As described by Waine (1999) it was found that attaching the Allegro field computer with the EM38 Mk2 switched on following calibration caused an offset, particularly in the QP (0.5m) reading which on the occasion of the test increased from 9 to 24 mS/m. The effect was not reversed when the Allegro was disconnected; a further offset occurred, from 24 to 37 mS/m. Switching off the EM38 Mk2 and disconnecting the battery before the Allegro was attached did not prevent the effect.

Calibration of the EM38 Mk2 with and without the Allegro attached produced similar values as displayed on the instrument panel. However, in this instance the Allegro displayed a different value for QP (0.5m) than the instrument panel for the same parameter: 28 mS/m on the Allegro versus 8 mS/m on the EM38 Mk2.

Best field practice appears to be calibration of the instrument with the field computer attached. Further work is needed to determine whether the presence of different readings on the Allegro and the EM38 Mk2 instrument is a regular

phenomenon and if so, which if either are correct, and which of these appear in logged data.

ATV interference: EM31

Interference of the ATV with EMI instruments was expected due to the considerable bulk of conductive metals of the ATV and their proximity to the instruments. Data from the test for ATV interference with the EM31 was dominated by random effects, presumably error. EC_a fluctuated ±25% or more in quick succession, sometimes appearing to alternate between high and low values. This did not appear due to ATV interference as the shoulder-carried data showed a similar effect. No metal or interfering objects were worn or carried by the surveyor other than the handheld GPS, datalogger and associated cables, all of which were positioned away from the EM31. Values from the kriged ATV data extracted to the shoulder carried data points did not show the characteristic fluctuation due to the smoothing effect of the kriging process.

EC_a measured using the ATV was higher than that measured while shoulder-carrying; for the most part there was no overlap between the datasets. Linear regression of kriged ATV vs. shoulder-carried EC_a showed no significant relationship. It is assumed that the expected relationship was obscured by the large random fluctuations in EC_a measurements.

ATV interference was estimated as the mean of differences between kinematic and shoulder-carried EC_a at common points: + 7.12 mS/m. In making this estimate it was assumed that the spatial patterns of kriged EC_a were genuine despite that they were obscured in the raw data by random fluctuation (Figure A6.06).

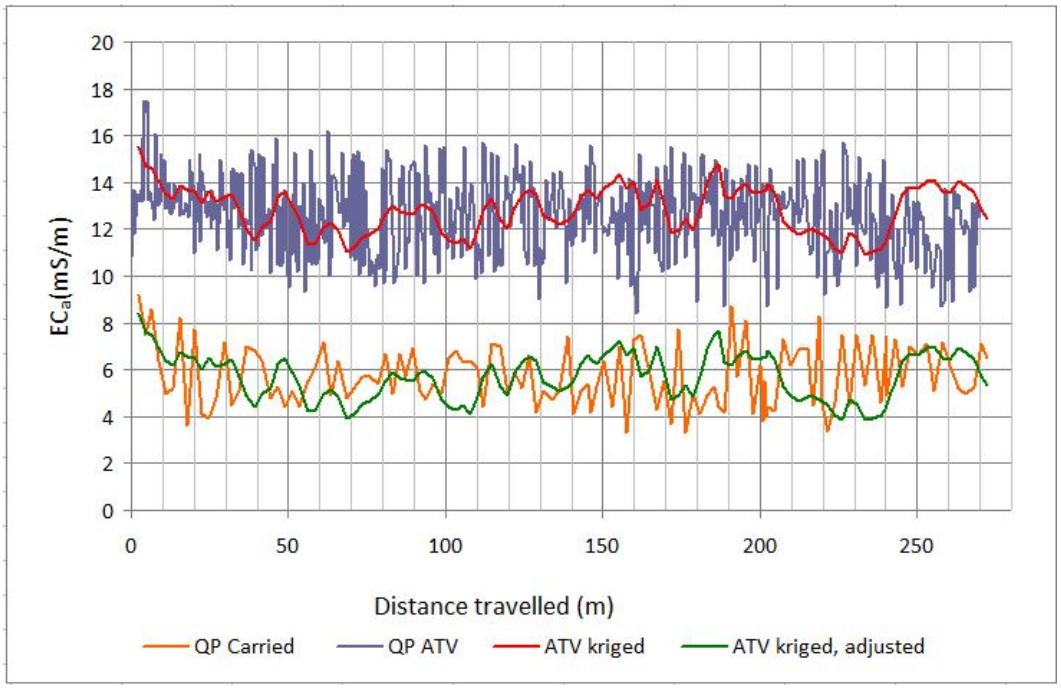

Figure A6.06. EC_a from shoulder-carried and kinematic EM31 at common points.

Regarding the random fluctuation itself, this emerges as a potentially significant obstacle to quantitative interpretation of EC_a data as it appears to represent error of ±20% or more in many readings. EC_a was not observed to fluctuate to any significant extent in stationary tests. The fluctuation therefore may have been related to flexing and tilting of the EM31 instrument caused by movement; still it is hard to reconcile this degree of error with the effect of raising and lowering the instrument by the amounts involved. It may be that motion has some other additional effect on the instrument.

ATV interference: EM38 Mk2

Interference of the ATV with EC_a measured by the EM38 Mk2 in the sled was suggested at distances less than 3m. The towing distance of the kinematic rig used for this research was 1.63m. From the data obtained, interference at towing distance was estimated at + 2mS/m for the 1m coil spacing and + 1mS/m for the 0.5m coil spacing. This was also consistent with the shorter effective depth range of the 0.5m spacing (Figures A6.07 and A6.08).

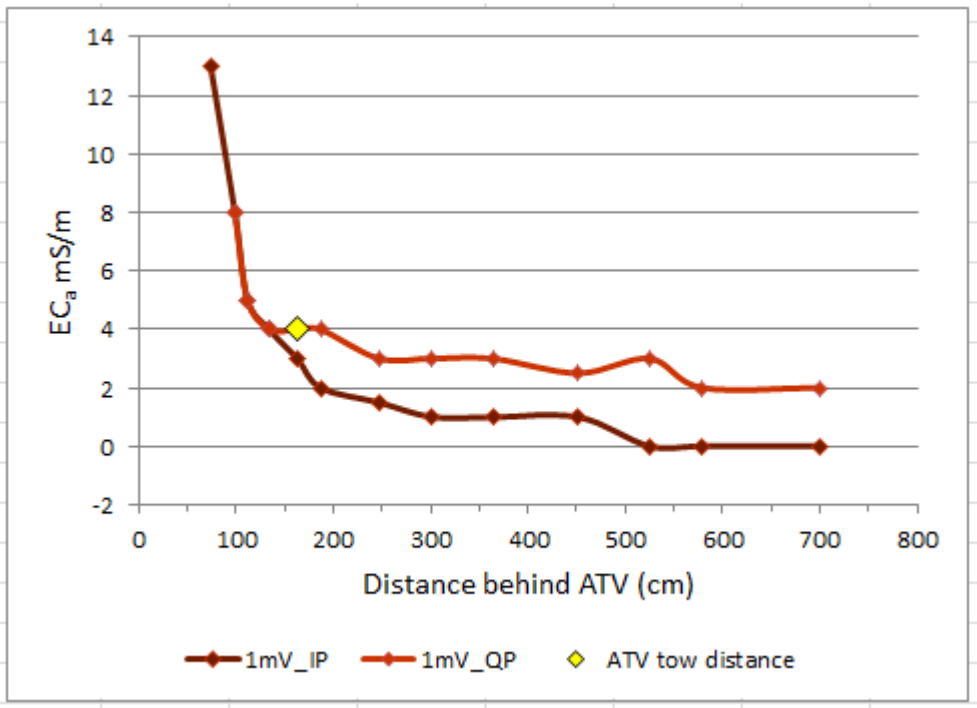

Figure A6.07. Effect of ATV proximity on EC_a measured by EM38 Mk2 (1m, vertical).

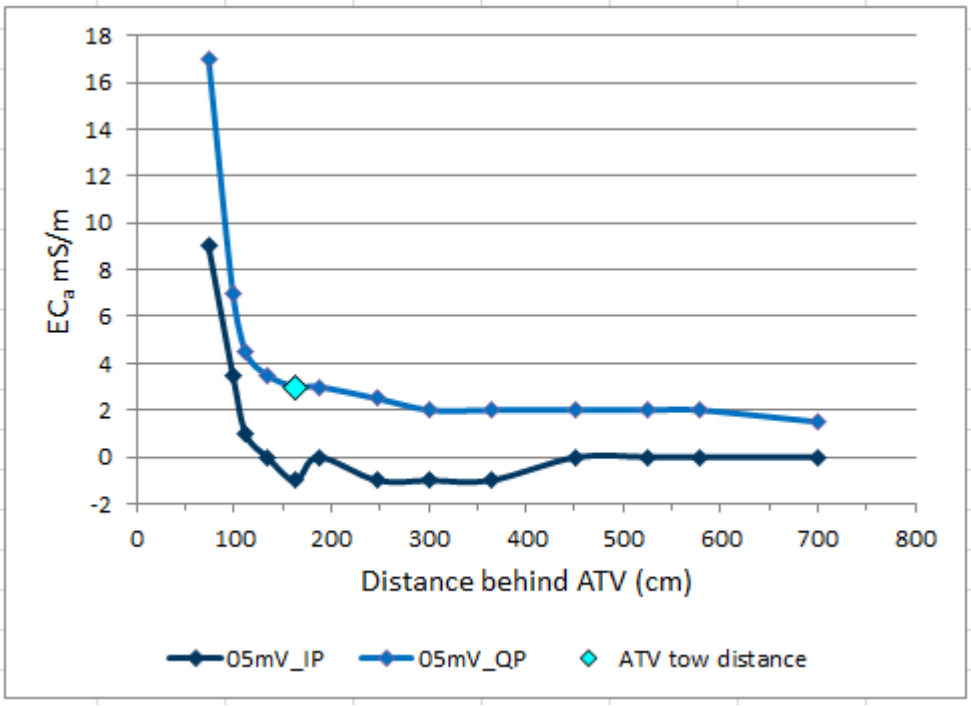

Figure A6.08. Effect of ATV proximity on EC_a measured by EM38 Mk2 (0.5m, vertical).

Fence interference

Two factors are expected to have obscured the effect of fence interference on the EM31: variation in ground EC_a and the pulsing of electrical current in the fence. However, an increase in EC_a was significantly correlated to fence proximity by linear regression ($R^2 = 0.49$, $P = 3.2 \times 10^{-188}$).

The EM31 was presented mostly side-on i.e. horizontal mode with respect to the fence, but close to the fence in the raised position on the outriggers the instrument was increasingly presented above the lower fence wires but still beside the uppermost wire.

The above factors are evident in Figures A6.09 and A6.10. An increase in EC_a with proximity to the fence is accompanied by many other low and mid-range values at all distances. The influence of the fence appears to reflect the horizontal mode sensitivity of the instrument except at very close proximity where aspects of the vertical mode sensitivity are suggested, in particular the relative insensitivity at proximity < 1m. It appears that interference was limited at distances >15m from the fence, which is 2.5 x the 'effective depth range' of the EM31 in vertical mode, or 5 x in horizontal mode.

GPS offsets

The characteristic EC_a signature of buried metal objects is described by Geonics (1995) as a zone of low EC_a between two adjacent zones of high EC_a. Such an EC_a signature of a buried metal pipe was used to estimate tow distance and system delay for kinematic surveys with the EM38 Mk2, Allegro data logger and serial cable connection. Figure A6.11a shows EC_a logged while towing the EM38 Mk2 at various speeds in both directions perpendicular to a buried pipe. Figure A6.11b shows the same data corrected according to a tow distance of 2.13m and system delay of 0.2s. This was the closest aggregation (~1.5m) of low EC_a points that could be obtained using various postulated values for tow distance and system delay in VBA functions used to calculate the offset (see *Appendix 5 - Functions for calculation of sensor location*). The EC_a values of the EM38 Mk2 (0.5m) appear unrealistic, probably due to calibration issues discussed in *4.1 – EMI instrument functional tests*, but are used

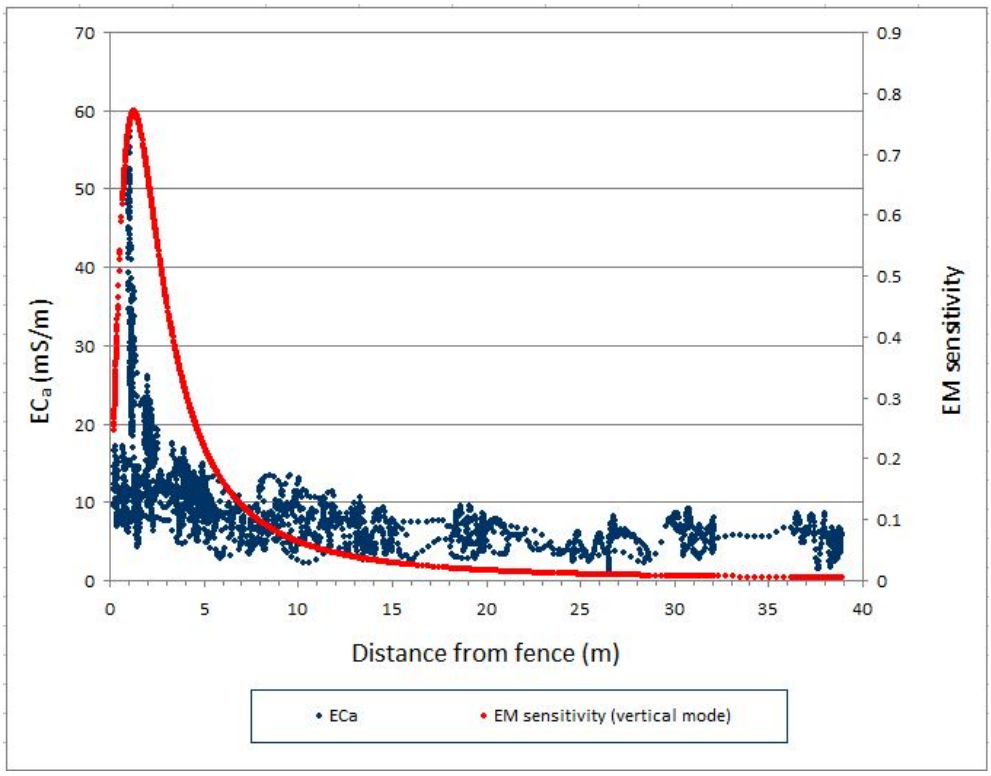

Figure A6.09. EM31 sensitivity (vertical mode) and measured EC_a in proximity to an electric fence.

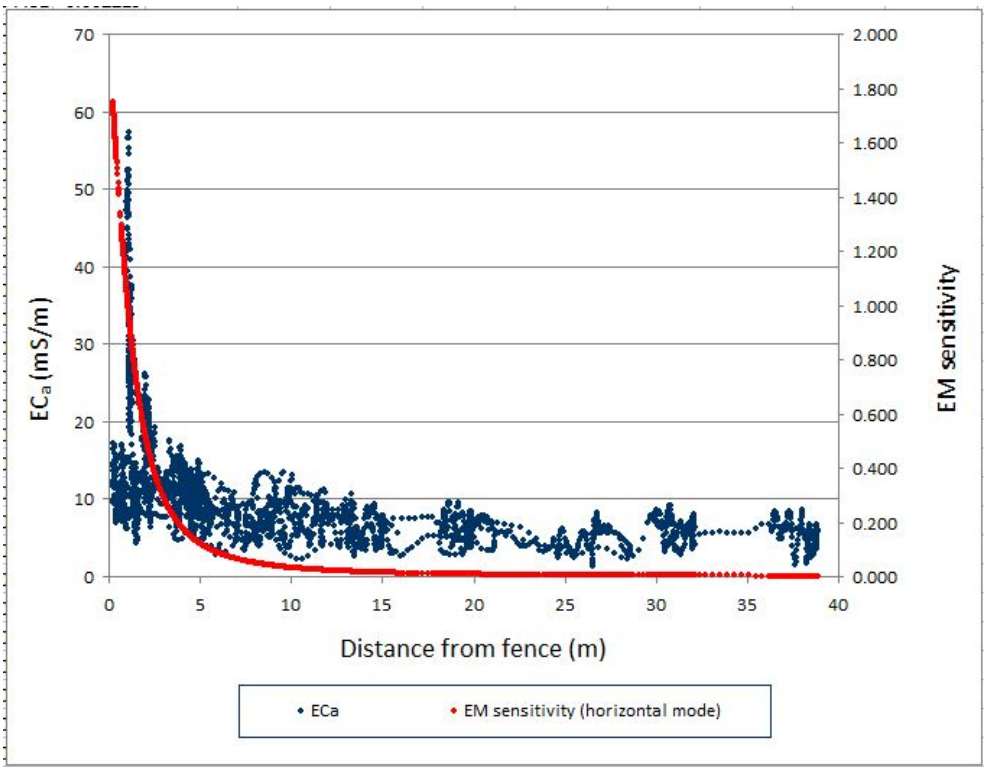

Figure A6.10. EM31 sensitivity (horizontal mode) and measured EC_a in proximity to an electric fence.

here as they more clearly depict the pipe signature. The EC_a signature of the pipe used in this instance extended approximately 7.5m on either side of the pipe according to the corrected data.

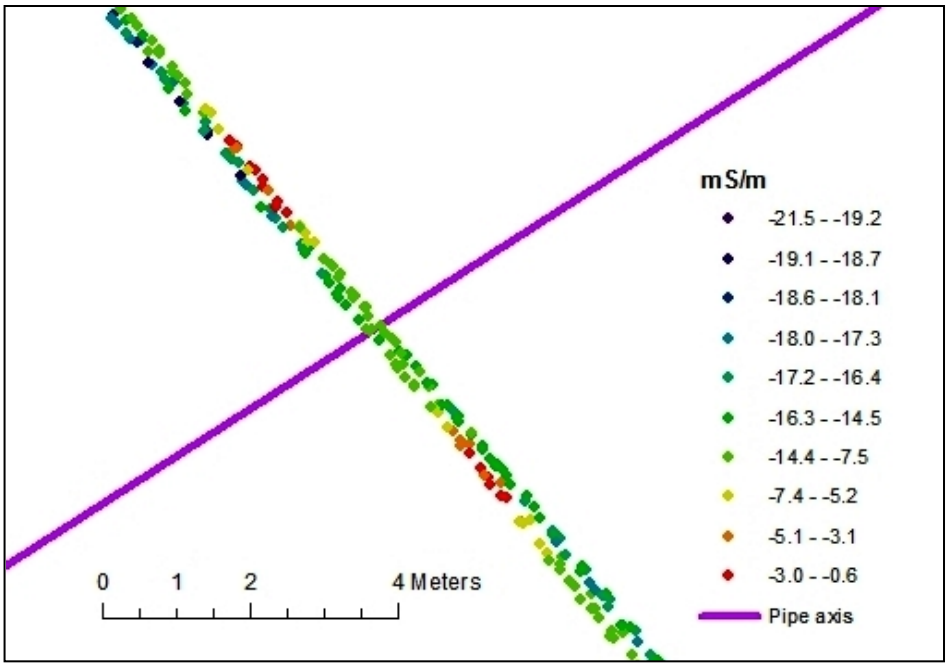

a.

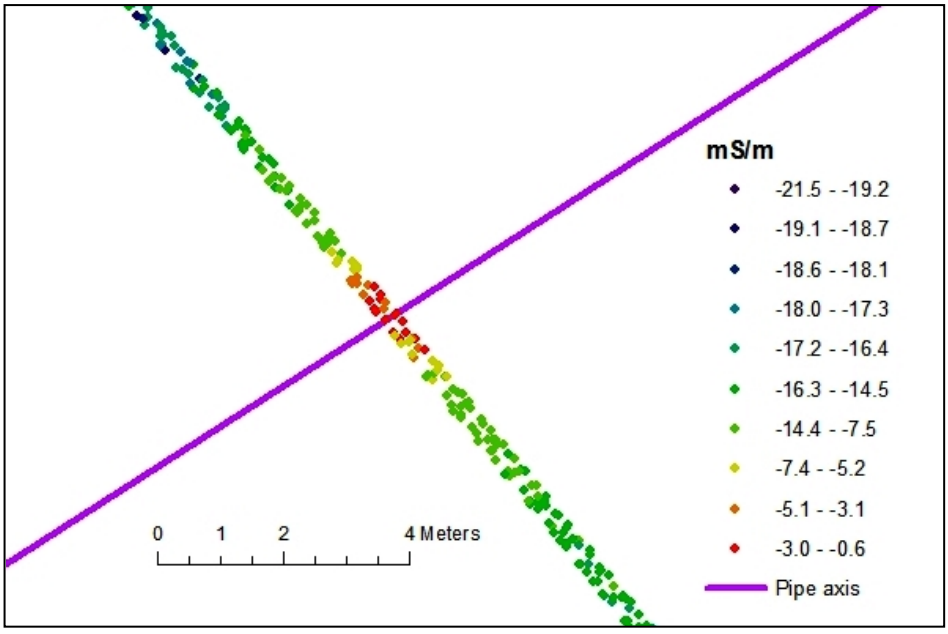

b.

Figure A6.11. EC_a measured by EM38 Mk2 (0.5m, vertical) towed at various speeds perpendicular to a buried pipe.
a) data uncorrected for GPS location offset; b) data corrected for GPS location offset.

Appendix 7. EC_a depth profiles: method development

EC_a depth profile resolution with kinematic data

A method was developed, as described in *3.7.3 – EC_a depth profile resolution*, using simulated EC_a data and the sensitivity profiles of the EM31 and EM38 Mk2 determined by the functions given by Geonics (1995, 2008). The method has some similarity to the methods of Slavich (1990), Cook and Walker (1992) and Geonics (1995). However, for kinematic surveys data was only available from vertical modes of the EM31 and EM38 Mk2, not horizontal modes as used by Slavich (1990) and Cook and Walker (1992), as no kinematic surveys were done with either instrument in horizontal mode. Furthermore the EM38 Mk2 (0.5m) data could only be used qualitatively due to apparent calibration error as described in *4.4.3 - EM38 Mk2 – EM38 Mk2, 0.5m*. It was therefore decided to develop a method for use with kinematic data based on a comparison of EM31 and EM38 Mk2 (1m) measurements at common points. (Values were extracted to these common points from kriged raster surfaces of the survey data using ArcGIS).

Rather than use the expected responses of the EM31 and EM38 Mk2 as two predictors in a multiple regression as did Slavich (1990) with EM38 vertical and horizontal modes, instead a ratio of EM31 to EM38 Mk2 measurements is used as a single predictor. The method is designed this way so that it applies equally to a wide range of measured EC_a values. The method therefore quantifies the relative difference between EC_a measurements by different instruments for a given EC_a profile. Such differences between EC_a measurements are caused by differences between the sensitivity depth profiles of the instruments.

It was decided to model EC_a depth profiles as two layers: 0-45cm and 45-900cm. This was for simplicity and because TDR moisture measurements concurrent with kinematic surveys were made to 45cm depth. The methods of Geonics (1995) also use EMI measurement ratios, hypothetical two-layered profiles and in some instances address the issue of EC_a depth profile separately from EC_a magnitude, as does this method (see section *2.4.4 - Simulation methods*). Geonics (1995) describes a method for a two-layered EC_a profile to determine the thickness of the upper

profile layer when the EC_a of that layer is known; the method developed here determines the EC_a of that layer when its thickness is known i.e. specified.

The depth limit of 9m for modelled EC_a depth profiles was introduced because the theoretical sensitivity profile of EMI instruments is to infinite depth which is more complex to model, and because it is likely in practice that substrates below 9m made negligible contributions to measured EC_a in this study, both because of their nature, being gravels, rock or consolidated material of low conductivity, and because the sensitivity of EMI instruments to material below 9m is small (18.4% of the total sensitivity profile of the EM31 raised 80cm, 5.5% for the EM38 Mk2, 1m, raised 6cm; however, those proportions assume an infinite and even profile of EC_a; response to a limited conductive layer below 9m is only a fraction of those amounts).

However, so as to make an equitable comparison between measurements by different instruments, each instrument and mode was considered insensitive below a depth equal to 1.5x its 'effective measurement depth'. That depth is 9m for the EM31 (vertical mode) and 2.25m for the EM38 Mk2 (1m, vertical mode).

Peak sensitivity of the EM38 Mk2, 1m in vertical mode is at about 35cm depth, and for the EM31 (vertical mode) it is at about 1.3m with the instruments at ground level (Geonics, 1998, 2008.) According to Geonics (2012) both instruments should give similar readings of an even EC_a profile of infinite depth, with the proviso that the EM31 is factory set to read correctly in this way from a measurement height of 1m above ground (Geonics, 1995) as discussed in *2.1.3 - Geonics EM38 Mk2 and EM31*. The manufacturer's adjustment of the EM31 to read correctly at 1m height, however, does not change the shape but only the magnitude of its sensitivity profile. As EM31 measurements in this study are corrected for this adjustment, it is disregarded in modelling the sensitivity profile of the instrument.

The depths then to which each instrument is more sensitive compensate for those to which it is relatively insensitive, and the total response of each instrument is adjusted by the manufacturer to equal the EC_a of an even EC_a profile (Geonics 1995). The apparently larger total sensitivity of the EM31 produced by the EMI response functions of Geonics (2008) in Figure 2.01 in this case does not reflect the actual

total sensitivity of the instrument. Given these considerations, and the measurement heights of the instruments as used in kinematic surveys in this study, the sensitivity profiles are better represented as calculated from the 'relative cumulative response' functions of Geonics (2008) as shown in Figure A7.01.

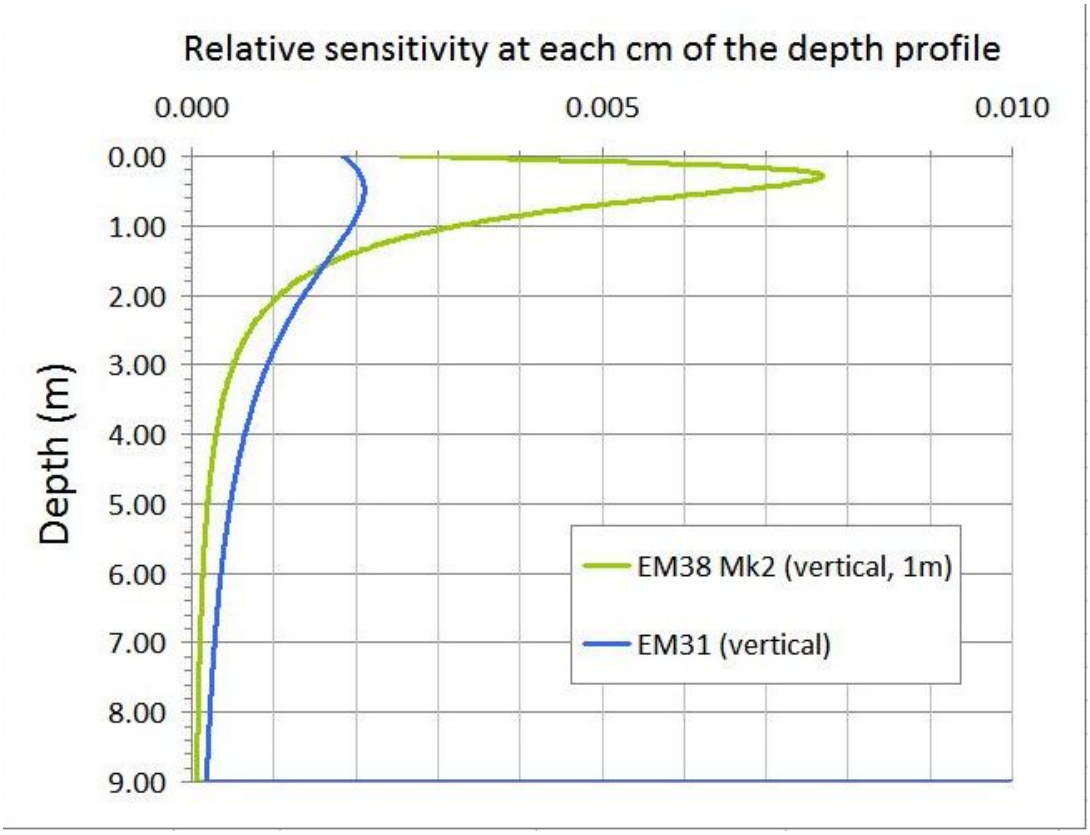

Figure A7.01. Responses to an even EC_a profile of the EM31 and EM38 Mk2 (1m) in raised measurement positions. (Assuming equal total sensitivity profiles of the EM31 and EM38 Mk2 with both instruments at ground level).

As can be seen in Figure A7.01 there are still appreciable differences between the sensitivity profiles of the instruments providing for comparisons which are diagnostic of EC_a depth profile. The total response of each instrument in this case does not sum to 1 x EC_a of an even EC_a profile because part of the instrument sensitivity is lost in the space above ground. This affected the EM31 more as it was raised higher, losing about 8.4% of its total sensitivity, or 10.3% of the sensitivity to 9m depth.

The proportion of EC_a in the top 45cm of profile is quantified as the ratio $EC_{a\ 0\text{-}45cm}$ **:** $EC_{a\ 0\text{-}900cm}$ where $EC_{a\ 0\text{-}45cm}$ is taken to be the actual (i.e. simulated) EC_a of the top 45cm of profile, while $EC_{a\ 0\text{-}900cm}$ is taken to be the EC_a measurement (simulated) of the EM38 Mk2 (1m, vertical). This is done so that the resulting model can be applied directly to EM38 Mk2 field measurements, yet indicate the actual (not measured) EC_a of the upper profile.

The second simulated ratio used in the method is the EMI measurement ratio, EM31 **:** EM38 Mk2 (both instruments in vertical mode) for each simulated EC_a profile. This ratio is found by statistical regression to have a linear relationship to the $EC_{a\ 0\text{-}45cm}$ **:** $EC_{a\ 0\text{-}900cm}$ ratio. The relationship of these two ratios is termed the 'depth resolution index' (DRI) as described in *3.7.3 - EC_a depth profile resolution - EMI measurement ratios* and depicted in Figure 3.19.

Two-layer EC_a profiles were simulated with various values of EC_a in the 0-45cm and 45-900cm layers. In the first instance, EC_a within each layer was assumed evenly distributed: the 'even-layered' model described in section *3.7.3 - EC_a depth profile resolution - EMI measurement ratios*. The responses of the EM31 and EM38 Mk2 (1m) to these profiles were modelled according to the instrument sensitivity profiles shown in Figure A7.01.

As the DRI in Figure 3.19 assumes even distribution of EC_a within each of the 0-45cm and 45-900cm layers, further profiles were simulated containing uneven distribution of EC_a within layers (but the same mean EC_a values as even layers) to see what effect this would have on the DRI. These simulated profiles are shown in Figures A7.02, A7.03 and A7.04, in which mean EC_a of the 0-45cm and 45-900cm profile layers and of each whole profile (0-900cm) is in every case 10mS/m.

Among the simulated profiles are two 'truncated' profiles of limited depth (Figure A7.04). These also retain the same mean EC_a as other simulated profiles but the EC_a of the 45-900cm layer is concentrated entirely in the 45-450cm or 45-150cm depth range; in other respects EC_a of both profile layers is even.

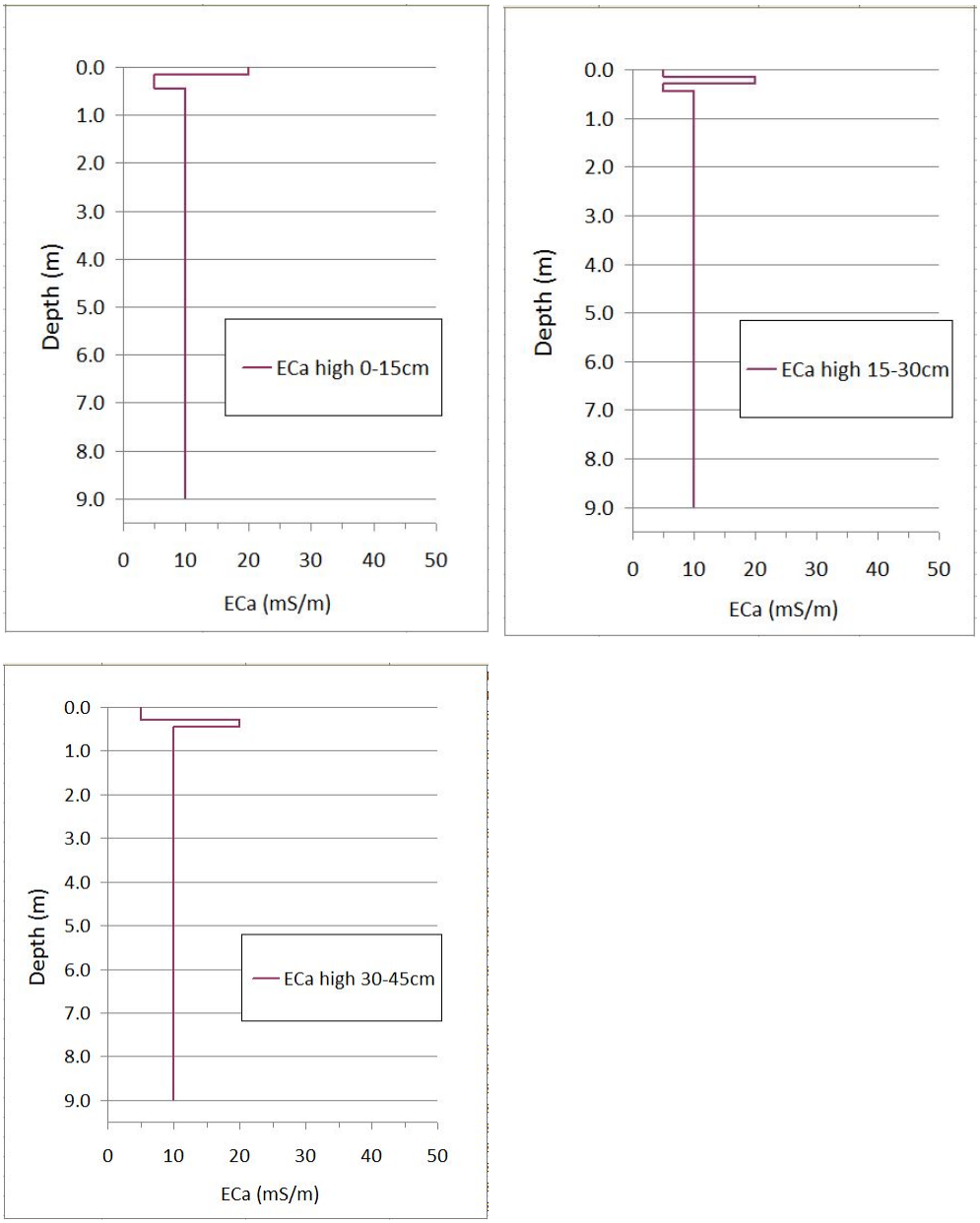

Figure A7.02. Simulated EC_a profiles with uneven upper (0-45cm) layers.

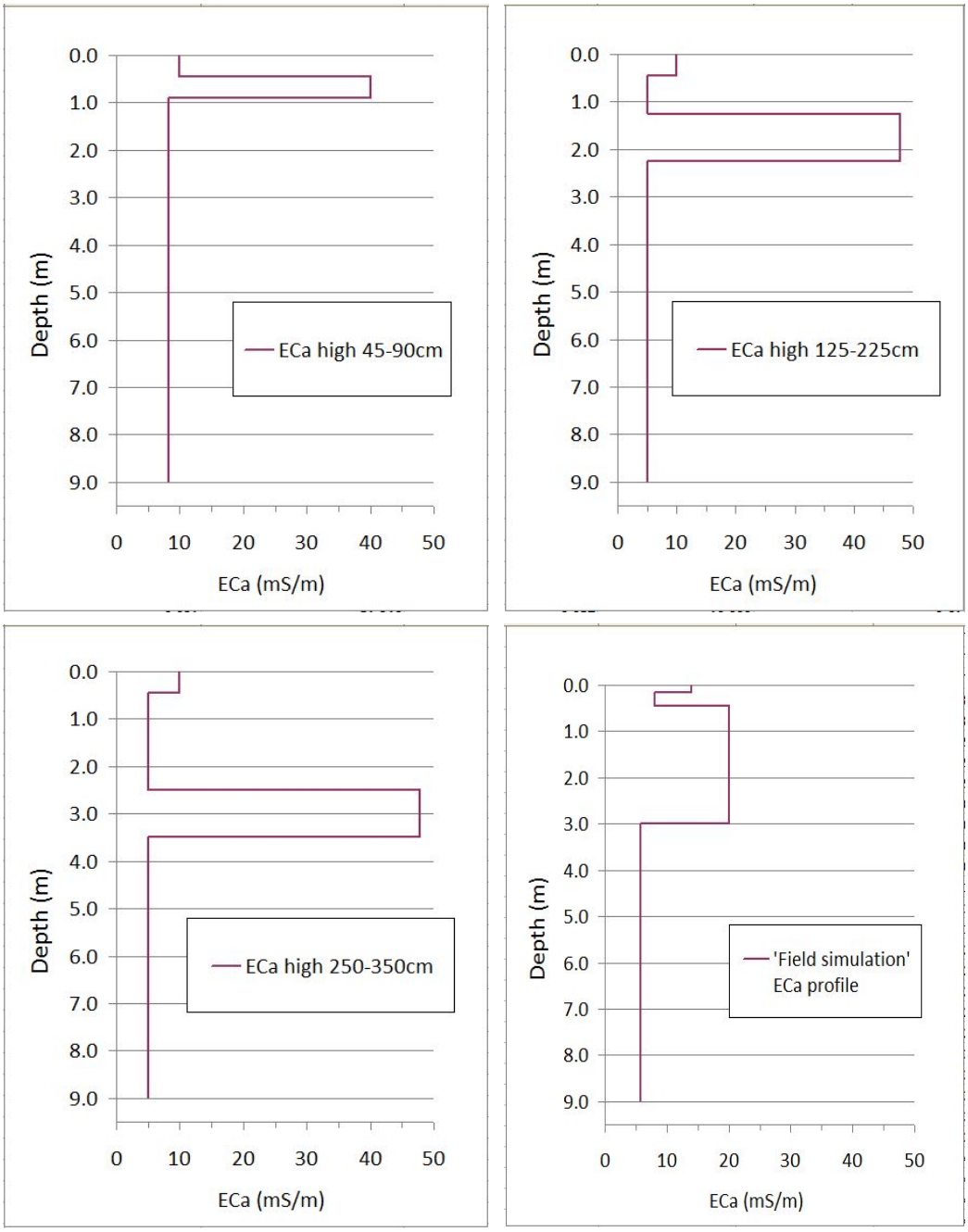

Figure A7.03. Simulated EC_a profiles with uneven lower (45-900cm) layers, and the 'field simulation' profile.

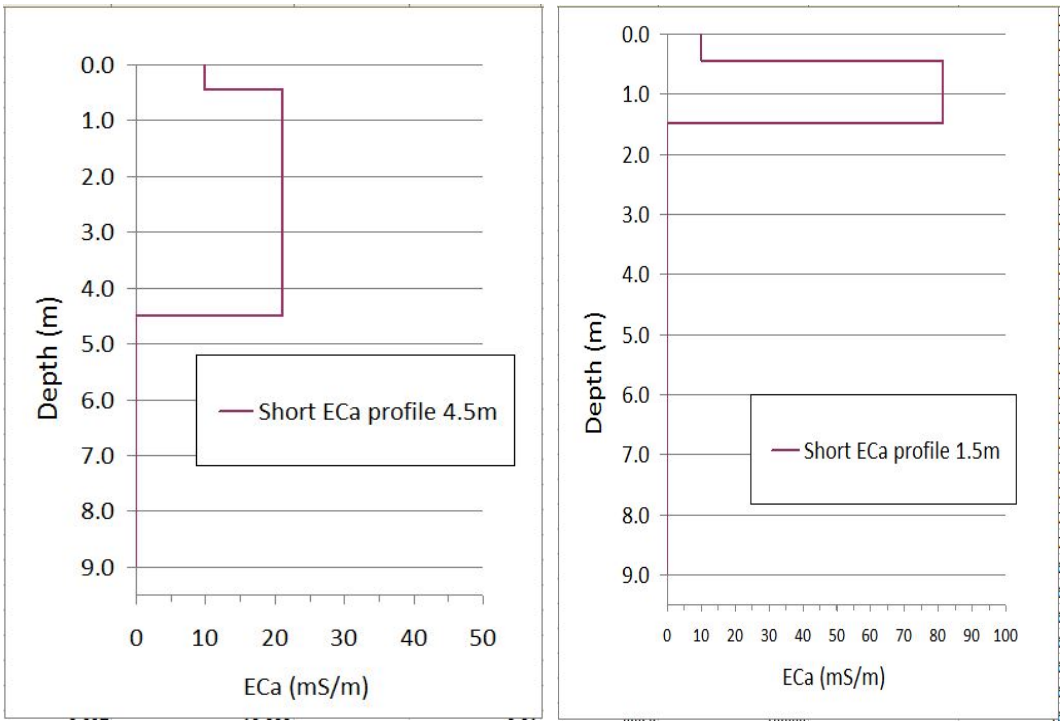

Figure A7.04. Templates for simulated EC_a profiles with limited depth.

Simulated EMI measurements of the profiles in Figures A7.02, A7.03 and A7.04 then quantify the effects of the different patterns of EC_a depth profile on different types of EMI measurements (different instruments, modes and measurement heights), as the true EC_a of each layer and of each whole profile is the same. The simulated EC_a measurement of each layer is divided by the simulated EC_a of the layer (in every case 10 mS/m) to produce a modified 'instrument sensitivity' for each instrument and mode to each layer of each simulated profile. The derived 'cumulative relative sensitivity' of each instrument and mode to each layer of each profile type is shown in Table A7.01. It is found that the modified instrument sensitivities calculated for each layer of the even profile are identical to those initially produced by the 'cumulative relative response' functions of Geonics (2008), thus somewhat confirming this aspect of the calculations for the method, which is further described below.

Table A7.01. Sensitivity of EMI instruments to simulated two-layered EC_a depth profiles.

	EM38 Mk2 (1m, V, +6cm)		EM38 Mk2 (1m, H, +0cm)		EM31 (3.66m, V, +80cm)	
Profile model	Sensitivity 0-44cm	Sensitivity 45-225cm	Sensitivity 0-44cm	Sensitivity 45-113cm	Sensitivity 0-44cm	Sensitivity 45-900cm
Even-layered	0.293	0.489	0.555	0.234	0.091	0.642
0-15cm high	0.253	0.489	0.661	0.234	0.088	0.642
15-30cm high	0.312	0.489	0.544	0.234	0.091	0.642
30-45cm high	0.314	0.489	0.459	0.234	0.092	0.642
45-90cm high	0.293	1.161	0.555	0.785	0.091	0.830
125-225cm high	0.293	0.864	0.555	0.117	0.091	0.969
250-350cm high	0.586	0.251	1.109	0.120	0.181	0.739
Depth limit 450cm	0.293	1.541	0.555	1.378	0.091	1.145
Depth limit 150cm	0.293	3.508	0.555	2.860	0.091	1.745
Field simulation	0.277	1.447	0.597	1.370	0.090	1.123

To simulate EC_a measurements of the various profiles in Figures A7.02, A7.03 and A7.04, and so calculate the sensitivity fractions shown in Table A7.01, the 'cumulative relative sensitivity' of each cm of the sensitivity profile of each different instrument and mode was calculated using the functions of Geonics (2008). These factors were then multiplied by the EC_a of the corresponding cm of the simulated EC_a depth profile, and the products totalled to give mean EC_a for the profile and for each of the layers. (The sum of the response gives mean EC_a because the total 'relative cumulative sensitivity' of every instrument and mode for an even profile equals 1, therefore for an even profile: total sensitivity x total profile EC_a = total profile EC_a).

The modified instrument sensitivity factors were then applied to further simulated even-layered EC_a profiles with various values of EC_a in the 0-45cm and 45-900cm layers. These profiles did not have similar EC_a in the 0-45cm and 45-900cm layers, but as with the earlier simulated profiles, mean EC_a of each whole profile (0-900cm) was 10 mS/m. This second phase of simulated measurements quantified the effect on measurement of uneven EC_a distribution between the 0-45cm and 45-900cm layers, and incorporated the effects of uneven EC_a distribution within the layers via the modified instrument sensitivity factors. Note: it can be shown that although the modified sensitivity factors were calculated for profiles with mean EC_a of 10 mS/m for each profile layer and for the whole profile, the same sensitivity factors are produced for each profile shape regardless of the mean EC_a of each layer and of the

whole profile, provided the relative unevenness or 'shape' of the EC_a depth profile within each layer is preserved.

Effect of uneven EC_a distribution within layers

Unevenly distributed EC_a within the 0-45cm layer of simulated profiles had limited effect on DRI's (Figure A7.05). Two explanations are suggested for this effect: firstly, the EM38 Mk2 in vertical mode has low sensitivity to EC_a very close to the surface, not greatly different from that of the EM31 (Figure A7.01). Secondly, the area of high sensitivity of the EM38 Mk2 (vertical) in the upper profile is very narrow, and the sensitivity of the EM31 to the whole 0-45cm layer is only approximately 12% of total instrument sensitivity to 9m (with the instrument raised 80cm). Therefore there is limited potential for uneven EC_a distribution in the 0-45cm layer to affect differences between measurements by the EM31 and EM38 Mk2 which in turn determine the DRI.

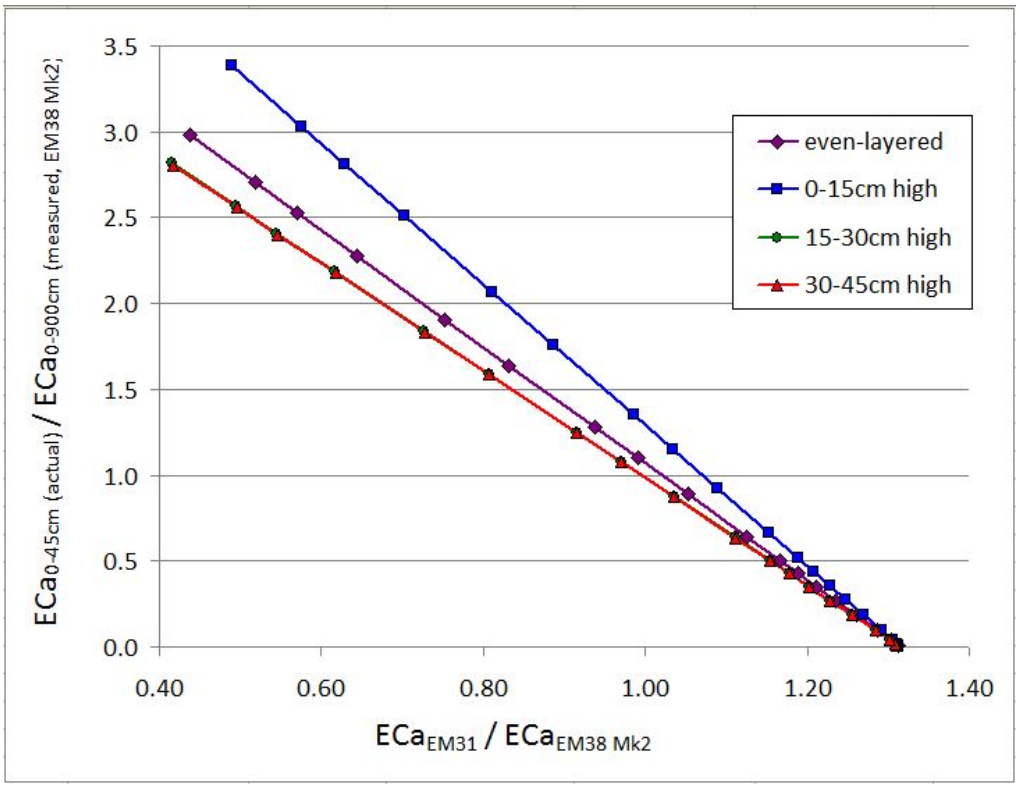

Figure A7.05. Depth resolution indices for simulated EC_a profiles with unevenly distributed EC_a in the 0-45cm layer.

The most noticeable effect on the DRI of unevenly distributed EC_a within the 0-45cm layer is where EC_a is higher in the upper 15cm of the 0-45cm layer, in which case EM31 : EM38 Mk2 measurement ratio is higher in relation to the $EC_{a\ 0\text{-}45cm}$: $EC_{a\ 0\text{-}900cm}$ ratio.

Unevenly distributed EC_a in the 45-900cm profile layer showed greater effects on the DRI than unevenly distributed EC_a in the 0-45cm layer (Figure A7.06). Truncated profiles with no EC_a below 150 or 450cm, and profiles with EC_a highest in the top of the lower layer i.e. 45-90cm showed lower ratios of expected EM31 : EM38 Mk2(1m) measurements than profiles with even lower layer. This is because the sensitivity of the EM31 is spread over an extensive, deep profile, while EC_a in the above simulations was concentrated in a relatively short depth range to which the EM38 Mk2(1m) was also sensitive (Figures A7.01 and A7.06).

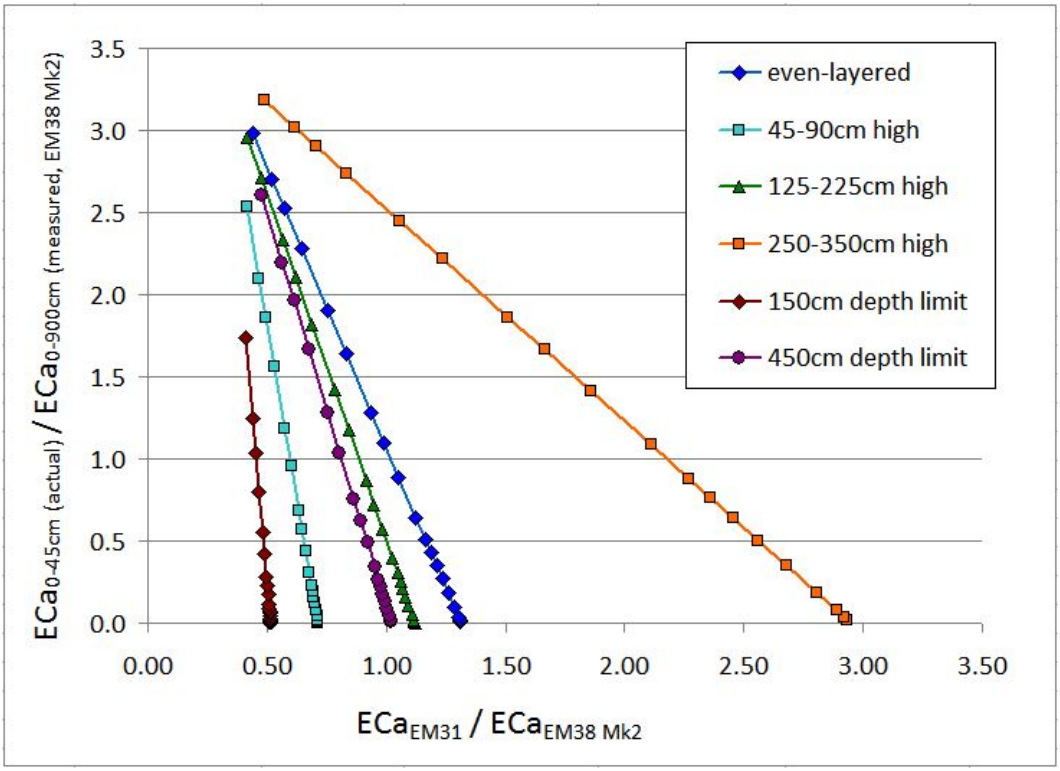

Figure A7.06. Depth resolution indices for simulated EC_a profiles with unevenly distributed EC_a in the 45-900cm layer.

Profiles with lower layer EC_a concentrated in the 250-350cm range showed higher EM31 : EM38 Mk2 (1m) measurement ratios than profiles with even layers,

especially where EC_a in the 0-45cm layer was low. These were the only profiles where EC_a was concentrated in a depth range to which the EM31 was more sensitive than the EM38 Mk2, and accordingly produced the only DRI appreciably higher than the DRI for even-layered profiles.

It was concluded that DRI's for two-layer EC_a profiles are significantly affected by uneven EC_a distribution within layers, especially within the lower layer (45-900cm). It was therefore decided to estimate probable unevenness of EC_a in the upper and lower layers at the study locations to produce a 'field simulation profile' from which could be modelled a DRI for use with field data, to compare with the even-layered model.

EC of 1:1 soil pastes and paste extracts was higher in samples from 4cm depth than from 28cm, 42cm or 64cm depths at most sample sites at Burnside and No.1 Dairy (*see section 4.3.4 – EC of 1:1 soil pastes and extracts*). It was also known from piezometer installation that gravels were present at depths between 2.9 and 3.8m at all three piezometer sites at Burnside and all four at No.1 Dairy, spread over a wide area at each location. It was therefore hypothesized that EC_a in the 0-45cm layer of most profiles would be highest in the 0-15cm depth range, reflecting the high EC of soil pastes from 4cm depth soil samples, while EC_a of the lower layer would be limited at depths greater than 3m due to the presence of gravels.

A field simulation EC_a profile was estimated incorporating the above patterns of uneven EC_a distribution within layers, with the upper portion highest in each profile layer. As with other EC_a profiles simulating uneven EC_a distribution within layers, EC_a of each layer and of the whole profile was 10 mS/m. An example of the responses of the EM38 Mk2 (1m, vertical) and EM31 (vertical) to the field simulation profile is shown in Figure 3.20. The DRI's of the even-layered and field simulation models are shown in Figure A7.07.

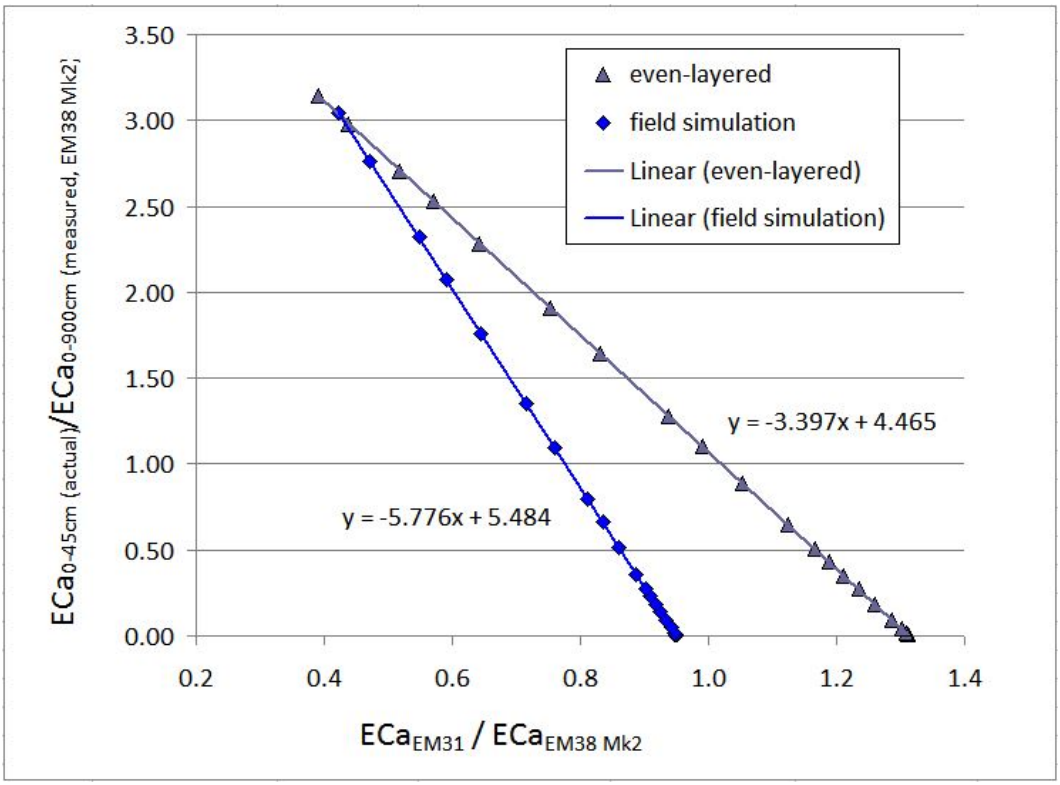

Figure A7.07. Depth resolution indices for even-layered and field simulation models used with kinematic survey data.

An example of EC_a depth resolution using the above method for an even-layered profile using data from Table A7.02 is shown below. Note: although measurements of EC_a by each instrument and mode were simulated as the sum of EMI response x EC_a for each cm of profile to 1.5x the effective measurement depth of the instrument, for the even-layered model the simulation can be simplified as the sum of EMI response x EC_a for the whole of each of the profile layers, 0-45cm and 45cm to 1.5x the effective measurement depth, as shown in Table A7.02.

EM38 Mk2		Modelled measurement of EC_a of profile (to 1.5x effective measurement depth; (mS/m)):	6.35			
1.0m		Actual EC_a of profile to 9m depth (mS/m):	9.75			
0.06m		Actual EC_a of profile to 0.45m depth (mS/m):	5.00			
1/POWER(4*A *A +1,1/2)		$ECa_{actual\ 0\text{-}45cm}$ / $ECa_{measured\ (EM38\ Mk2)}$	0.7875			
EM38 Mk2 sensitivity profile depth (m)	Depth/coil spacing (A)	Cumulative response at upper boundary depth: EM38 Mk2 (1m, vertical mode)	Sensitivity to profile layer	Modelled sensitivity to profile layer	EC_a of profile layer (mS/m)	Modelled measurement from profile layer
0.06	0.06	0.993	0.293	0.293	5	1.46
0.51	0.51	0.700	0.489	0.489	10	4.89
2.31	2.31	0.212	0.212	0.000	10	0.00
EM31		Measured EC_a of profile to 1.5x effective measurement depth (mS/m):	6.87			
3.66m		Actual EC_a of profile to 9m depth (mS/m):	9.75			
0.80m		Actual EC_a of profile to 0.45m depth (mS/m):	5.00			
1/POWER(4*A *A +1,1/2)		$EC_{a\ measured\ (EM31)}$ / $EC_{a\ measured\ (EM38\ Mk2)}$	1.0827			
EM31 sensitivity profile depth (m)	Depth/coil spacing (A)	Cumulative response at upper boundary depth: EM31 (vertical mode)	Sensitivity to profile layer	Modelled sensitivity to profile layer	EC_a of profile layer (mS/m)	Modelled measurement from profile layer
0.80	0.219	0.916	0.091	0.091	5	0.4526
1.25	0.342	0.826	0.642	0.642	10	6.4219
9.80	2.678	0.184	0.184	0.000	10	0.0000

Table A7.02. EM31 Mk2 (vertical, raised 80cm) data for generation of a depth resolution curve.

Calculation of $EC_{a\ 0\text{-}45cm}$ for the example in Table A7.02 is as follows:

Depth resolution index: $Y = mX + c$

where: $Y = EC_{a\ 0\text{-}45cm\ (actual)} / EC_{a\ 0\text{-}900cm\ (EM38\ Mk2)}$

$X = EC_{a\ measured\ (EM31)} / EC_{a\ measured\ (EM38\ Mk2)}$

and for an even profile: m = -3.397

c = 4.465

and for the example in Table A7.02:

$EC_{a\ measured\ (EM31)}$ = 6.87 mS/m

$EC_{a\ measured\ (EM38\ Mk2)}$ = 6.35 mS/m

X = 6.87/6.35 = 1.0819

Y = -3.397*1.0819 + 4.465 = 0.7898

6.35 mS/m*0.7898 = 5.0 mS/m = $EC_{a\ 0\text{-}45cm\ (actual)}$

In the above example and in Table A7.02 the simulated EC_a profile is even-layered with a mean EC_a of 9.75 mS/m to 9m depth and no EC_a below 9m. Mean EC_a to 45cm depth is 5 mS/m; the remainder of the profile to 9m depth is 10 mS/m, giving the whole profile mean EC_a of 9.75 mS/m. The predicted EM31 (vertical) measurement is less than 9.75 mS/m because the instrument is raised 80cm above ground, so losing the uppermost part of its sensitivity profile, and it is assumed in the simulation to have zero response below 1.5x its effective depth range i.e. 9m (the simulated EC_a profile also in any case having zero EC_a below that depth) so losing also the deepest part of its sensitivity profile. (The EM31 is factory adjusted to read correctly when raised 1m above ground, however, in this study EM31 data was corrected for this adjustment so that it would read correctly at ground level, so the adjustment is disregarded.)

The EM38 Mk2 (1m, vertical) measurement in the above example is less than 9.75 mS/m because the instrument is raised 6cm, so losing a small portion at the top of its sensitivity profile, and because it is assumed in the simulation to have zero response below 1.5x the effective measurement depth i.e. 2.25m.

EC_a depth resolution from spot measurements

From spot EC_a measurements at soil replicate sites, data was available for EM38 Mk2 (vertical mode) measurements at various heights and EM38 Mk2 (horizontal mode) measurements at ground level. No EM31 measurements were made at soil sample sites.

Following the method developed for kinematic survey data, ratios of $EC_{a\ 0\text{-}45cm}$: $EC_{a\ measured\ (EM38\ Mk2)}$ of simulated profiles were plotted against ratios of various raised or horizontal mode simulated measurements to those of the EM38 Mk2 (1m, vertical mode, +6cm; Figure A7.08).

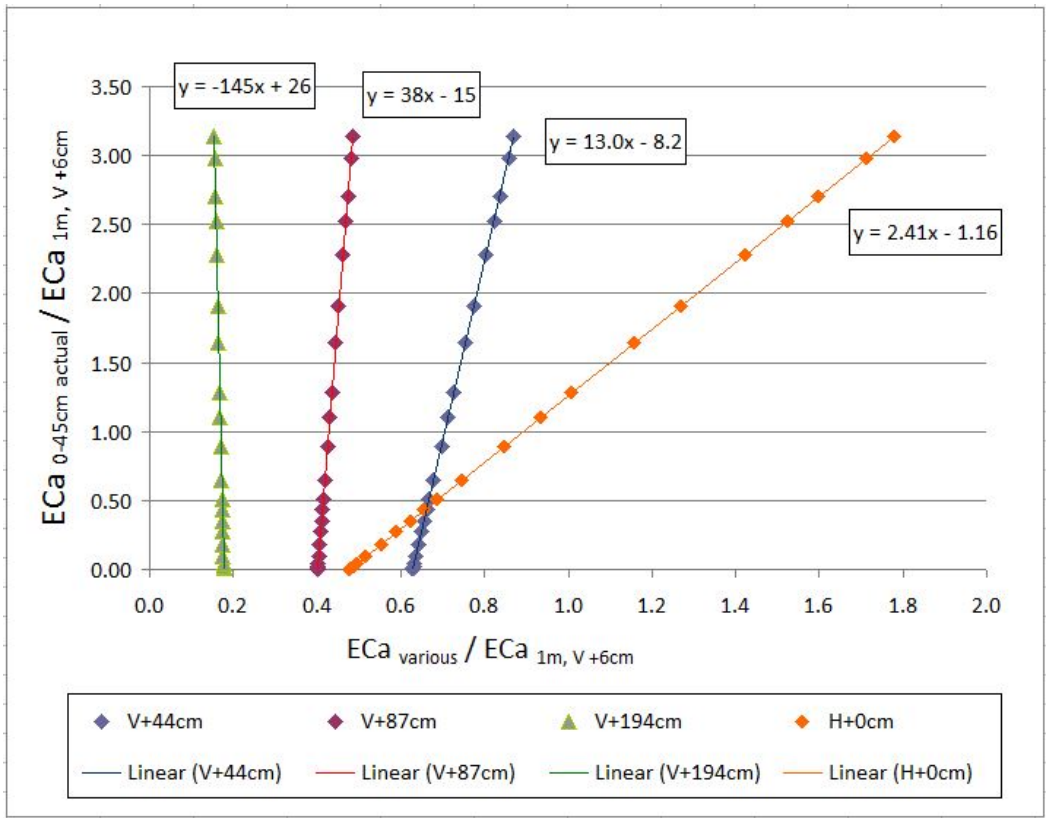

Figure A7.08. Depth resolution indices for EC_a spot measurements (EM38 Mk2, 1m). Even-layered model. V = vertical mode; H = horizontal mode; +cm = instrument height above ground.

Ratios with raised height measurements were not strongly affected by the distribution of EC_a between upper and lower profiles. However, ratios of horizontal mode to vertical mode measurements responded with good resolution to changes in EC_a distribution between upper and lower profiles.

It was decided to use the EM38 Mk2 horizontal and vertical mode measurements for depth resolution of EC_a at soil replicate sites. As to variation within the upper and lower profile zones, the 'field simulation profile' described in *EC_a depth profile resolution with kinematic data* was initially used to estimate this. However, results

with depth resolution of kinematic data suggested no advantage of the field simulation model over the even-layered model, so it was abandoned in favour of the even-layered model which is the one shown in Figure A7.08, producing a DRI with values for *m* and *c* of 2.41 and -1.16 respectively.

Appendix 8. Descriptions of soil series.

Rangitikei series

The youngest of the alluvial soils associated with the Manawatu River, the Rangitikei series are well to excessively drained, rapidly accumulating soils with no distinct topsoil, low organic matter and weak structure. Textures vary from fine sandy loam to loamy sand, with flood layering and (indistinct) buried topsoils common. Previous surveying at No.1 Dairy also identified a silt loam member of this series which is mapped across the whole study location. Rangitikei soils have been considered mostly too flood prone to be good for agriculture (Cowie, 1978).

The Rangitikei fine sandy loam is less frequently flooded than other Rangitikei soils and subject to some melanisation and worm-mixing of the upper profile; for these reasons it is identified as transitional to the more mature Manawatu series. Fresh sediment deposits in this soil are not deep. (Neither is the soil deep as a whole – underlying sand occurring more than 60cm from surface is considered deep for this soil (Cowie, 1978)).

As the No.1 Dairy soils mapped as Rangitikei silt loam over sand (Pollock, 2003) are finer again than the Rangitikei fine sandy loam described above, yet more of the above features – melanisation, worm-mixing, and associated structural development - might be expected, though not generally typical of the Rangitikei series. It is also noted that the soils of No.1 Dairy , though subject to flooding, appear sufficiently stable to sustain agriculture in contrast to the description above by Cowie (1978). Melanisation and gleying of the profiles also bears witness to some history of stability (see *Appendix 9 – Soil profiles*).

Parewanui series

These soils are of similar maturity to the Rangitikei series but are imperfectly to poorly drained, sometimes occurring in recently abandoned meanders of the Manawatu River (Cowie, 1978). Poor drainage suggests a lower sand content than the Rangitikei soils; indeed Parewanui soils are generally finer-textured and further from the river sediment source. Topsoils are indistinct (as with the Rangitikei series), subsoils greyish with yellowish or brown mottles (‘gleying’ associated with periodic

waterlogging). A fine sandy loam, silt loam and 'heavy silt loam' are described in the Parewanui series, each with increasingly poor drainage (Cowie, 1978). The silt loam is described as having a deep, dark greyish brown topsoil over a heavier, dark grey heavy silt loam with brown and red mottles and coarse blocky and medium and fine nutty structure, and medium contents of well-humified organic matter (Cowie, 1978).

Manawatu Series

Older and higher in the landscape than the Rangitikei soils, Manawatu soils are slower accumulating, contain more organic matter (still fairly low), more worm-mixing and less flood layering. Topsoils are deep and dark brown, subsoils yellowy or olive brown, but topsoil-subsoil differences are still not strongly marked. The silt loam member is described as having a friable brown topsoil (23cm) and a light olive brown subsoil, the latter firm, blocky silt loam, over a sandy loam with some grey mottles. The sandy loam and fine sandy loam members have sand underlying within a metre depth (Cowie, 1978).

Kairanga Series

The imperfectly to poorly drained companion to the Manawatu series, of similar age, infrequently flooded, these soils are also worm-mixed and show no flood layering. Kairanga soils often border rivers and streams and are distinguished from Parewanui soils by distinct, dark greyish brown topsoils and blocky subsoils. The silt loam has a grey, clay loam subsoil with yellowish red or brown mottles. The fine sandy loam has yellowish brown mottles. These members grade into one another. A 'heavy silt loam' is also described with a clay loam to clay subsoil, almost structureless below 48cm (Cowie, 1978).

Appendix 9. Soil profiles

Profile descriptions made at soil sample sites, B1, B2 and B3 at Burnside and D4, D5 and D6 at No.1 Dairy are shown in Figures A9.01-A9.06.

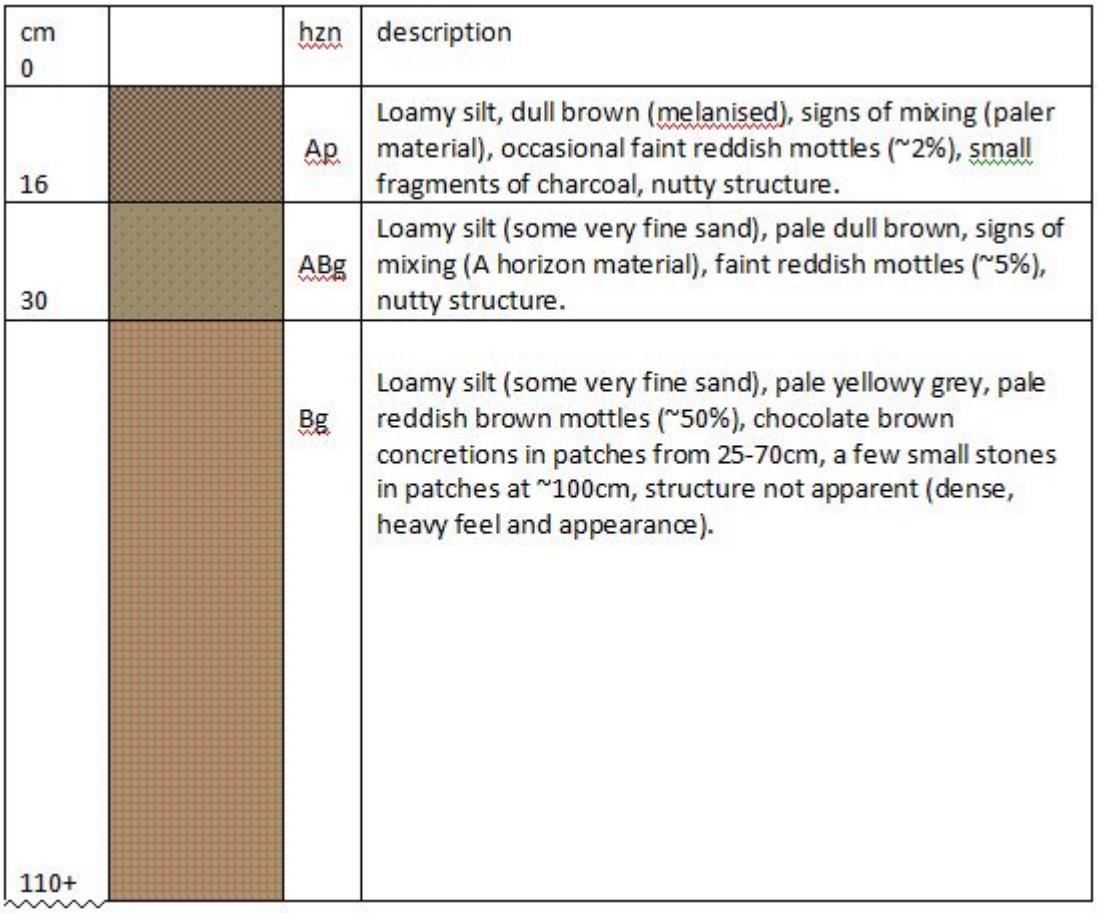

Figure A9.01. Soil profile at sample site B1, Burnside.
Generalized profile description from 3 holes made with a Dutch auger on 22.11.11.

cm 0		hzn	description
18		Ap	Loamy silt, appearing mixed, some slightly browner (melanised) material with paler dull yellowy brown (B horizon?) material, overall pale for an A horizon, nutty structure.
120+		Bw	Loamy silt (with some sand and clay), finer with increasing depth then sandier again at >100cm, yellowy brown, very faint pale and reddish brown mottles at 50-100cm, nutty structure.

Figure A9.02. Soil profile at sample site B2, Burnside.
Generalized profile description from 3 holes made with a Dutch auger on 23.11.11.

cm 0		hzn	description
18		Apg	Silt to loamy silt (some sand and clay), appearing mixed, some slightly browner (melanised) material with paler brown patches and reddish brown mottles (~5%), overall pale for an A horizon, nutty structure.
24		AB	As above but no reddish mottles, less melanised material.
100		Bw	Silt to loamy silt (some fine sand and clay incorporated), dull yellowy brown, nutty structure.
120+		Bg	Moist, silt to loamy silt (incorporating some sand and clay), yellowy grey with faint reddish brown mottles (~50%), nutty structure.

Figure A9.03. Soil profile at sample site B3, Burnside.
Generalized profile description from 3 holes made with a Dutch auger on 23.11.11.

cm 0		hzn	description
14		Ap	Silt (some fine sand), mixed appearance: pale brown, pale reddish brown and darker brown (melanised) peds, overall pale for an A horizon, firm nutty structure.
34		ABg	Silt (some fine sand), dull greyish brown (humified), faint reddish mottles, firm nutty structure.
70		Bg	Silt, dull greyish brown, reddish brown mottles, crumbly, nutty structure.
105		Bg2	Silt (no sand felt), small amount clay, dull greyish brown, reddish brown mottles but less gleyed than Bg, wet, soft, smooth.
130		Bg3	As for Bg.
140+		2C	Fine sand, loose, dark olive; many red brown mottles at upper boundary.

Figure A9.04. Soil profile at sample site D4, No.1 Dairy.
Profile is a generalisation from 3 holes dug with spade on 27.12.11.

cm 0		hzn	description
10		Apg	Loamy silt (some fine sand), pale greyish brown, very pale for an A horizon, red-brown mottles, firm nutty structure.
25		AB	Loamy silt (much fine sand), medium brown with paler brown inclusions, nutty structure.
54		Bw	Loamy silt (much fine sand), dull yellowish brown, weak nutty structure.
75+		2C	Fine sand, dull yellowish brown, loose, unstructured.

Figure A9.05. Soil profile at sample site D5, No.1 Dairy.
Profile is a generalisation from 3 holes dug with a spade on 29.12.11.

cm 0		hzn	description
14		Ap	Loamy silt (much fine sand), dull brown (melanised) with some paler ped faces, pale for an A horizon, nutty structure (5-10cm peds).
20		ABg	Loamy silt (much fine sand), dull greyish brown (melanised), some ped faces paler, firm nutty structure.
80		Bw	Loamy silt (much fine sand), dull brown (melanised), nutty structure.
90+		2C	Loamy fine sand, dull yellowish brown, unstructured.

Figure A9.06. Soil profile at sample site D6, No.1 Dairy.
Profile is a generalisation from 3 holes dug with a spade on 6.1.12.

Appendix 10. EC_a for indicating denitrification potential of soil

A particular composite regime of influences on EC_a was identified as having interpretive potential for indicating denitrification potential of soil. Alluvial silt and clay tend to be deposited in lower lying areas farther from source, which tend to be wetter both because of topography and the lesser drainage capacity of the fine soil materials. These soils are more likely therefore to be gleyed or reduced due to waterlogging. Each of these factors – fine texture, wet conditions and gleying – cause higher EC_a in their own capacity, i.e. the higher surface area of fine soil particles, particularly clay, the greater saturation by conductive soil solution in wet soils, and the solubilisation of ions by reduction. In addition these factors all have interaction effects which increase EC_a: the retention of moisture in fine textured soils, the multiplicative effect of water and ions in increasing soil solution conductivity, and the attraction of cations to clays, tending to their retention in soil. The natural tendency of the above factors to occur together may give a strong signal of reducing conditions in soil indicated by higher EC_a, especially as measured by the deeper sensitivity profile of the EM31 which is better focused on the depth where gleying is likely to occur and less influenced by surface processes which could obscure that signal: wetting, drying, fertilising and manuring, heating and cooling. This finding suggests a possible use for EC_a in identifying and locating the denitrification potential of soils which was possibly observed in this study at Burnside.
